Under the surface: Disentangling climate effects on *Calanus finmarchicus* dynamics in a high latitude system

Kristina Øie Kvile

Dissertation presented for the degree of
Philosophiae Doctor (PhD)
2015

Centre for Ecological and Evolutionary Synthesis
Department of Biosciences
Faculty of Mathematics and Natural Sciences
University of Oslo

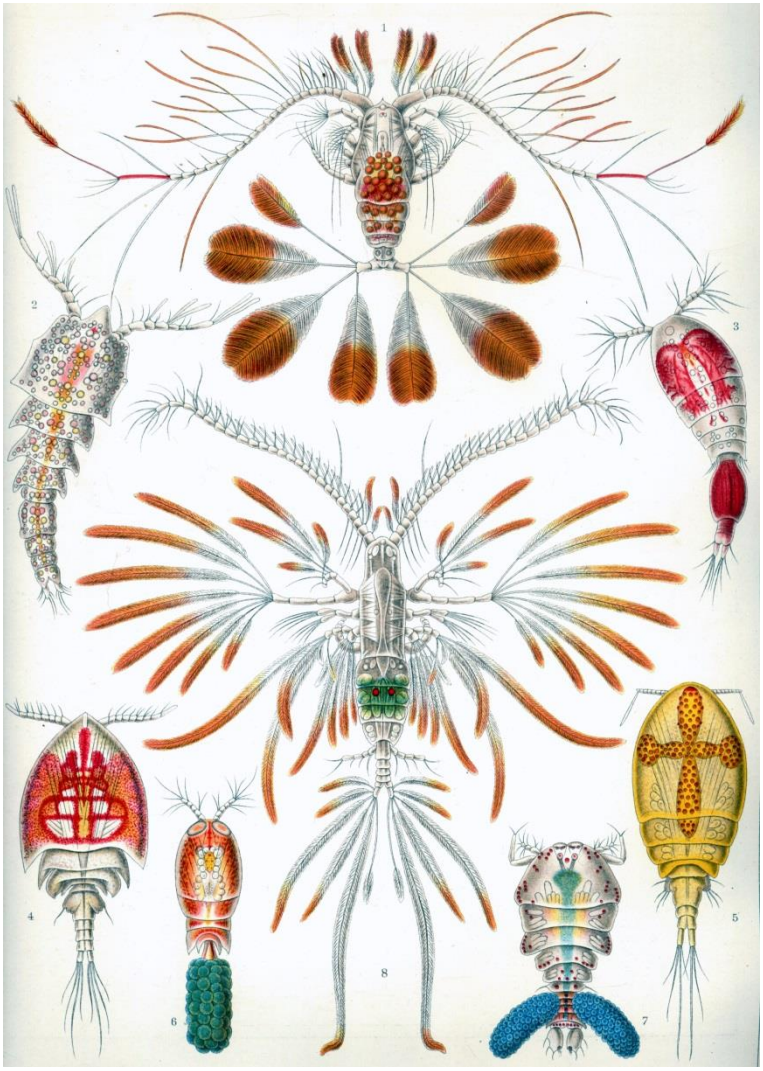

Ernst Haeckel, *Kunstformen der Natur* (1904)

Man skulde ikke tro, at saa smaa Dyreformer skulde være af saa stor Betydning for et Lands Økonomi

Norwegian fisheries biologist Axel Boeck describing the prey of the herring (1871)

Preface

August 2012 I started as a PhD student at the University of Oslo. I was a little concerned; my plan had been to work with cold-water corals, could zooplankton be any fun? And would I sit in front of a computer for three years? The three years have passed, and I must admit I have become proud to call myself a zooplankton/statistics/modelling person. I am very privileged to work with something as exciting as science, and zooplankton are actually really fun!

Zooplankton aside, doing a PhD would not have been the same without the people. Especially, I want to thank my main supervisor, Leif Christian. I could not have asked for a better mentor. You always have time, excellent ideas, patience, constructive comments and humour! To Øystein, thank you for stepping in as co-supervisor and being so generous with your time for discussions and questions. I also thank Padmini – for sharing your insight on zooplankton and helping me get hands-on experience on board, and Nils Christian – for always encouraging me to aim high.

It has been great to be part of such a diverse and dynamic centre as CEES, and of the best group of all, the Marine Group. Marine lunches are the best lunches! To those who have been my office mates during (parts of) these three last years: Gio, Anna, Mats, Elisabeth, Maja, Emmi, Alex, Sofia, Fred, Chloé and Leana, thanks for all the good laughs! I have also benefited from being part of the Nordic Research Centre NorMER. Our annual meetings across the Nordic capitals were among the highlights of my time as a PhD student. NorMER also opened doors to other research nodes. I would like to thank Øyvind and Anders for making my stay in the Theoretical Ecology Group in Bergen both inspiring and fun. I hope we can continue to collaborate (and go skiing!) in the future. And to the guys in DTU Aqua's wonderful castle (Martin, Alex, Uffe, Kasper, Sofia and others), thanks for your hospitality in Copenhagen and for making state space modelling (a little) less of a black box.

This project has benefited from a fruitful collaboration with the marine research institute PINRO in Murmansk. The articles in this dissertation would not have been possible without the countless hours spent by the PINRO scientists who collected, sorted, identified, counted, and finally, digitised the data. I would especially like to thank Irina Prokopchuk for your collaboration with the articles, immense effort digitising and inspecting the data, and warm welcome in Murmansk in 2013. I also had the privilege to meet Emma Orlova, who contributed with her expert knowledge to the first paper of this

thesis. We will fondly remember her as an authority within the field of zooplankton research.

Finally, I would like to thank my friends who dragged me out of the PhD bubble during the past three years, you are the best! To my family, thank you for always supporting me, even when it meant living in the middle of the ocean. I will try to come home more often. Kristian, you make every day happier and any problem smaller, thank you for being there.

Kristina Oie Kvile

University of Oslo, 2015

List of papers

Paper I

Kvile, KØ, Dalpadado, P, Orlova, E, Stenseth, NC, Stige, LC (2014) Temperature effects on *Calanus finmarchicus* vary in space, time and between developmental stages. *Marine Ecology Progress Series*, 517, 85–104.

Paper II

Kvile, KØ, Langangen, Ø, Prokopchuk, I, Stenseth, NC, Stige, LC. Disentangling the mechanisms behind climate effects on zooplankton. Submitted to *Proceedings of the National Academy of Sciences of the United States of America*.

Paper III

Kvile, KØ, Fiksen, Ø, Prokopchuk, I, Opdal, AF. Coupling a hydrodynamic model with biological survey data gives new insight into long-term variation in *Calanus finmarchicus* spawning areas. Manuscript.

Paper IV

Kvile, KØ, Stige, LC, Prokopchuk, I, Langangen, Ø. A statistical regression approach to estimate copepod mortality from spatiotemporal survey data. Submitted to *Journal of Plankton Research*.

Summary

Zooplankton form the link between primary production and higher trophic levels in pelagic ecosystems. In the Atlantic waters of the Norwegian and Barents Seas, the copepod *Calanus finmarchicus* is an important food source for a range of animals, including pelagic fish and early life stages of demersal fish. The aim of this PhD dissertation is to improve our knowledge of the dynamics of this key zooplankton species in the north-eastern Norwegian Sea and south-western Barents Sea. We combine long-term spatiotemporal survey data, state-of-the-art statistical methods and oceanographic particle tracking to disentangle how climate variation influences *C. finmarchicus* abundance, distribution and seasonality. We also shed light on two elusive aspects of zooplankton dynamics in the open ocean, namely the spatiotemporal distribution of egg production and the level of mortality.

In **Paper I**, we show that abundances of *C. finmarchicus* in different developmental stages correlate differently to changes in ambient temperature, and that earlier peak abundance of the younger copepodite stages in spring relates to increased temperatures. In **Paper II**, we use particle tracking to map the environmental variation experienced by *C. finmarchicus* from spring to summer. We find indications of a positive effect of the combination of shallow mixed-layer-depth and increased wind on food availability (chlorophyll biomass) in spring, and in turn on *C. finmarchicus* biomass in summer. In **Paper III**, we use particle tracking to back-calculate potential spawning areas from observed *C. finmarchicus* copepodites in spring. Depending on ocean current dynamics, *C. finmarchicus* in the Norwegian Sea-Barents Sea system can be transported vast distances from egg to copepodite. However, copepodites sampled within the Barents Sea appear to have a more local origin than commonly assumed. **Paper IV** explores a statistical regression approach to estimate mortality rates for zooplankton developmental stages. Compared to previous studies, the estimated mortality rates for *C. finmarchicus* copepodites are relatively low, but possibly elevated for the older stage-pair (CIV-CV). The statistical regression approach is shown to be robust to both advection and trends in recruitment.

With the works compiled in this dissertation, I aim to improve our general knowledge of *C. finmarchicus*' life-history in a high-latitude marine ecosystem, and our understanding of potential responses of the species to climate change.

Content

Introduction

Climate effects on zooplankton, why bother?

For a marine biologist, highlighting the importance of the oceans seems unnecessary. Besides the facts, the simple joy of being at sea and experiencing life under the surface is reason enough. But for many people, oceans are distant, inaccessible areas with seemingly little impact on their lives. Many studies have aimed to quantify the value of nature, and although such assessments are controversial (Seppelt *et al.*, 2011), they provide interesting perspectives on why we should bother to understand the changes occurring in nature. For example, the oceans are important for climate regulation, nutrient cycling and oxygen production (Costanza *et al.*, 1997; Field *et al.*, 1998). Their most obvious value is for food; almost 3 billion people receive 20 percent of their daily animal protein from fish, and fisheries and aquaculture provide around 55 million jobs (FAO, 2014).

Oceans absorb atmospheric heat, and during the past 40 years, temperatures in the upper oceans have on average increased by more than 0.1°C per decade (Pörtner *et al.*, 2014). The strongest warming has occurred at high latitudes, a trend predicted to continue during the 21st century (IPCC, 2014). Rising temperatures are further predicted to increase thermal stratification and Arctic sea ice retreat (IPCC, 2014), which in turn will influence biological production in high-latitude regions.

Most climate effects studies in the Arctic have focused on fish and marine mammals, while few studies target zooplankton (Wassmann *et al.*, 2011). One reason might be the lack of commercial interest; zooplankton are generally not harvested for human consumption. Nonetheless, zooplankton play a critical role in marine ecosystems. By preying on phytoplankton and in turn being the dominant food source for a range of organisms, including fish, seabirds and marine mammals, they channel energy from primary production to higher trophic levels. Of particular relevance are copepods, the crustacean subclass containing the most abundant multicellular organisms on the planet (Schminke, 2006). Zooplankton also contribute to the carbon cycle through the 'biological pump'; a large portion of the carbon that is fixed by phytoplankton and subsequently eaten by zooplankton sinks to the sea floor as faecal pellets or zooplankton carcasses, and is potentially buried and removed from the carbon cycle (Richardson, 2008).

Previous studies have indicated that climate change influences zooplankton biomass, geographical distribution, phenology (seasonality) and species composition (Richardson, 2008). Due to their central role as secondary producers, disentangling the complex web of different and interacting climate effects on zooplankton is critical to understand the potential future of marine ecosystems.

Bottom-up versus top-down control

Climate variation can affect zooplankton physiology directly (Hirst & Bunker, 2003), but may also influence zooplankton in a more indirect fashion, through alterations in ocean currents (Heath *et al.*, 1999), primary production (Richardson & Schoeman, 2004) or the abundance of predators (Frank *et al.*, 2005). However, the relative importance of such bottom-up (food availability, physical environment) and top-down (predation) mechanisms is debated (Frank *et al.*, 2013; Greene, 2013).

Typically, marine zooplankton dynamics are explained by bottom-up effects of food availability, which in turn reflects variation in physical factors such as temperature, light and stratification (Atkinson *et al.*, 2004; Ware & Thomson, 2005). In the north-eastern North Atlantic, regional warming apparently triggered a northward shift in phytoplankton abundance and thereby calanoid zooplankton, ultimately affecting fish abundance (Beaugrand *et al.*, 2002, 2003; Richardson & Schoeman, 2004). On the other hand, examples of top-down control by planktivorous fish exist from the Baltic (Casini *et al.*, 2009), Black Sea (Llope *et al.*, 2011) and several upwelling regions worldwide (Verheye & Richardson, 1998; Cury *et al.*, 2000; Ayón *et al.*, 2008). Observations from the Northwest Atlantic indicate that top-down control might be stronger in cold, species-poor regions than in warmer, more species-diverse counterparts (Worm & Myers, 2003; Frank *et al.*, 2005, 2006; Petrie *et al.*, 2009). Supporting this notion, several recent studies from the cold and relatively species-poor Barents Sea suggest that zooplankton biomass in the area is primarily top-down controlled (Stige *et al.*, 2009, 2014a; Dalpadado *et al.*, 2012, 2014; Johannesen *et al.*, 2012).

The hidden world of zooplankton

Investigating both bottom-up and top-down effects, or even marine zooplankton dynamics in general, is challenging due to the influence of advection (Aksnes *et al.*, 1997). Sampling zooplankton in the ocean gives a snapshot of the plankton community in a specific location and moment. But ocean currents can transport zooplankton hundreds of kilometres in less than a month (**Paper III**), and the samples alone do not reveal the observed specimens' past drift trajectories. It may be unclear how much zooplankton dynamics in one area is driven by influx from neighbouring areas as compared to local production. Further, to investigate effects of environmental variation, we should ideally know the environment in the sampled zooplankton's past drift trajectories, not only at the survey location. Scientists may study zooplankton in real time by following water patches in the ocean (Irigoien *et al.*, 2000), but to cover large areas or long periods is impractical. And when working with historical survey data, going back in time to sample more is obviously impossible.

Advection also challenges the estimation of zooplankton mortality rates. In fact, mortality is considered a 'black box' in marine zooplankton population dynamics (Runge *et al.*, 2004), much due to the difficulty in separating recruitment and mortality from transport (emigration and immigration). The vertical life table (VLT) approach (Aksnes & Ohman, 1996) is commonly used to estimate mortality in zooplankton populations influenced by advection. However, the method is known to be susceptible to trends in recruitment (Aksnes & Ohman, 1996) and has recently been criticised for its sensitivity to advection (Gentleman *et al.*, 2012). Several authors have emphasised that improved knowledge about variation in mortality is needed in order to understand the sensitivity and potential responses of zooplankton populations to climate change (Ohman *et al.*, 2004; Plourde *et al.*, 2009; Gentleman *et al.*, 2012).

Aim

The scope of this dissertation is to investigate how zooplankton dynamics respond to climatic variation, focusing on *Calanus finmarchicus* in the Atlantic waters of the north-eastern Norwegian Sea and the south-western Barents Sea. We assess associations between climate variation and *C. finmarchicus* biomass, stage-specific abundance, distribution and phenology. In addition, we explore two central topics in zooplankton research: the

influence of advection on the spatial distribution of populations and the estimation of mortality rates. Both topics require knowledge of the transport patterns and zooplankton dynamics in the region investigated, but the methods applied are transferable to other regions and populations.

Specifically, the aim of **Paper I** is to quantify temperature effects on *C. finmarchicus* abundance on various spatial, temporal and developmental scales. In **Paper II**, we further explore potential bottom-up effects on *C. finmarchicus*, assessing how temperature, mixed-layer-depth and wind in spring influence biomass in summer. To improve our understanding of the controlling mechanisms, we use particle tracking to map the physical environment likely experienced by the sampled zooplankton in spring, and investigate the relationship between these physical variables and food availability (chlorophyll biomass). In **Paper III,** we couple survey data with drift modelling to back-calculate spawning areas of copepodites later sampled in different survey transects in the Norwegian and Barents Seas, thereby describing the connectivity between the areas. The goal of **Paper IV** is to improve our knowledge of *C. finmarchicus* mortality rates by exploring a statistical regression approach for mortality estimation. Below, I first present the study area, organism and methods used in the works compiled in this dissertation. Thereafter, I discuss the main findings along with relevant literature to establish a broader context.

Setting the stage

The scene

The Barents Sea is an Arctic shelf sea bordering Norway and the Kola peninsula in the south, Novaya Zemlya in the east, the Arctic Ocean in the north and the Norwegian Sea in the west (Fig. 1) (Sakshaug *et al.*, 2009a). Being a shelf sea, the average depth of the Barents Sea is only 230 m. The Norwegian Sea consists of two deep basins (the Norwegian and Lofoten basins) exceeding 3000 meters, and forms together with the Greenland and Iceland Seas the collective Nordic Seas (Blindheim, 2004). Circulation in the Norwegian Sea is dominated by Atlantic waters from the North Atlantic Ocean (Blindheim, 2004). In the eastern Norwegian Sea, the Norwegian Atlantic Current flows northward close to the Norwegian continental shelf, and one branch of this current enters the Barents Sea. On the Norwegian continental shelf, the Norwegian Coastal current flows northward and enters

the southern Barents Sea. These northbound 'highways' connect the Norwegian and Barents Seas, and climate variation in the Barents Sea is to a large degree controlled by the inflow of Atlantic water (Ingvaldsen & Loeng, 2009). Temperatures in the Barents Sea fluctuated between cold and warm periods during the second half of the 20th century, but have predominantly increased during the past decades (Johannesen *et al.*, 2012).

The south-western Barents Sea connected to the Norwegian Sea is a highly productive area, hosting what is probably the world's largest stocks of cod and capelin (Gjøsæter, 2009). The largest herring stock in world, the Norwegian spring spawning herring, periodically enters the Barents Sea from the Norwegian Sea (Stenevik *et al.*, 2015). These waters also support a rich fauna of marine mammals and seabirds. Nevertheless, the bulk of animal biomass is represented by zooplankton, in particular, different species of calanoid copepods and krill (Sakshaug *et al.*, 2009a).

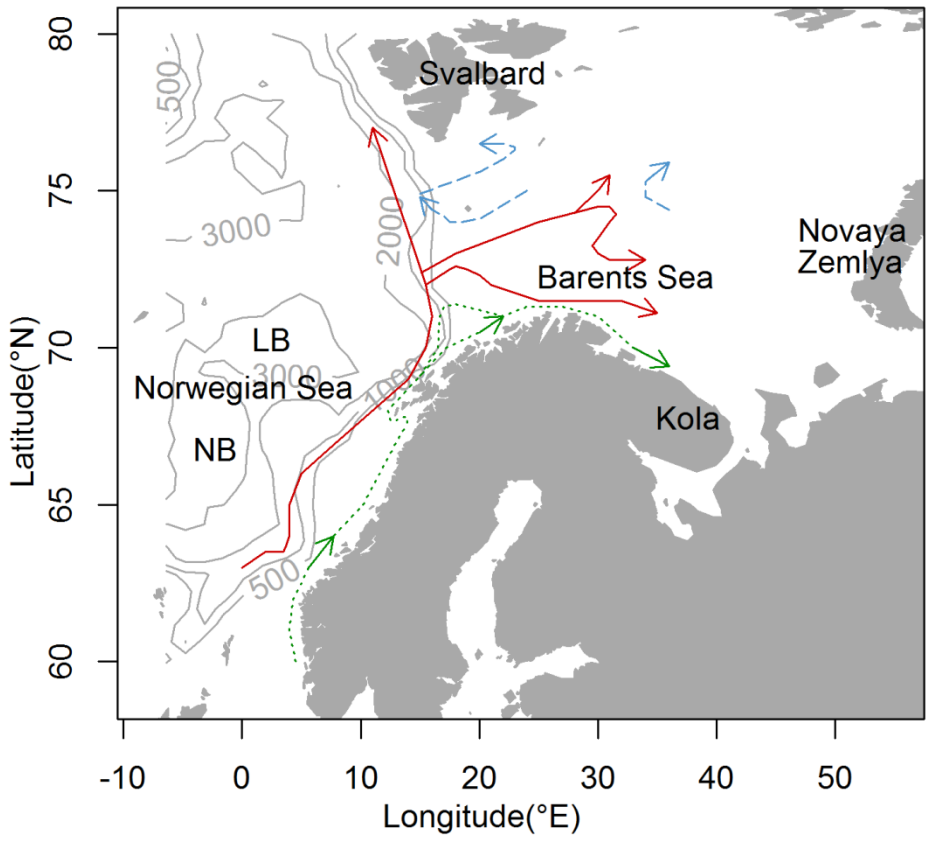

Fig. 1. Map of the Norwegian Sea and Barents Sea with depth contours (>500 m, grey lines) and the main surface currents connecting the two seas: the Norwegian Atlantic Current (solid red arrows), the Norwegian Coastal Current (dotted green arrows) and Arctic water currents (dashed blue arrows). The two deep sea basins in the Norwegian Sea are the Norwegian Basin (NB) and the Lofoten Basin (LB).

The actor

The copepod *Calanus finmarchicus* (Fig. 2) is the dominant mesozooplankton[1] species in terms of biomass in the North Atlantic (Melle *et al.*, 2014), including in the Atlantic waters of the Norwegian and Barents Seas (Orlova *et al.*, 2010). Its congeners *C. glacialis* and *C. hyperboreus* are primarily associated with Arctic water masses (Eiane & Tande 2009; Broms *et al.* 2009). *C. finmarchicus* is an important food source for several pelagic fish species (e.g. herring and capelin), and larvae and juveniles of demersal fish (e.g. cod and haddock) (Melle *et al.*, 2004, 2014). Total zooplankton biomass in the Barents Sea area varies throughout the year (Eiane & Tande, 2009), both linked to advection (i.e. Atlantic water inflow) and local production regimes (Wassmann *et al.*, 2006). *C. finmarchicus* dominates in spring and summer, while other species might be more important in autumn (Eiane & Tande, 2009).

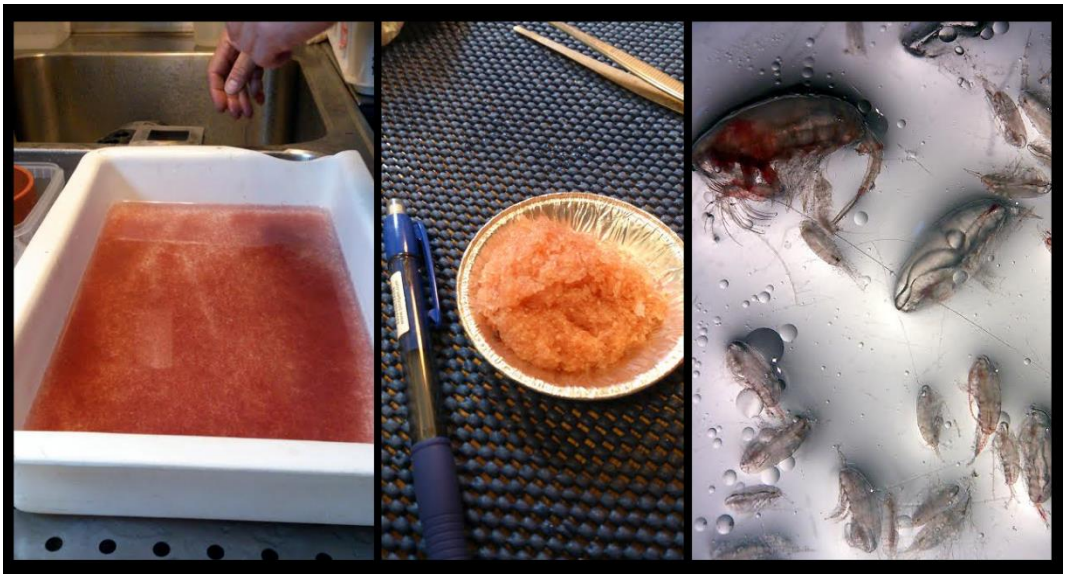

Fig. 2. The Norwegian name raudåte ("red bait") appropriately describes the copepod *Calanus finmarchicus*. Left: A sample from a vertical haul coloured red by *C. finmarchicus*. Middle: A dish of mesozooplankton (mainly *C. finmarchicus*) prepared for weighing. Right: Microscope view of three copepod species commonly found in the Barents Sea: The carnivore *Paraeuchaeta* sp. (upper left), the larger herbivore *C. hyperboreus* (middle right), and various stages of *C. finmarchicus*. All pictures are taken by K. Ø. Kvile on the research vessel Johan Hjort in the Barents Sea.

[1] Multicellular heterotrophic organisms between 0.2 and 20 mm.

The phenology of herbivorous zooplankton at high latitudes is tightly coupled to the spring phytoplankton bloom, a strategy to maximise growth in the temporally limited food window. *C. finmarchicus* primarily feeds on phytoplankton, but microzooplankton can be a supplementary food source (Irigoien *et al.*, 1998; Mayor *et al.*, 2006). Internal lipid reserves can be utilised for growth and egg production when phytoplankton availability is low (Mayor *et al.*, 2006; Falk-Petersen *et al.*, 2009), but feeding on high quality phytoplankton seems to benefit egg production (Jónasdóttir *et al.*, 2002).

In the Atlantic waters of the northern Norwegian Sea and the Barents Sea, *C. finmarchicus* typically has a one-year life cycle (Fig. 3), including an overwintering phase in deep waters (Eiane & Tande, 2009). The overwintering population mainly consists of stage CV, but also some CIV and adults (Melle *et al.*, 2004; Slagstad & Tande, 2007). The core overwintering areas are the Norwegian and Lofoten Basins (Melle *et al.*, 2014), but *C. finmarchicus* might also overwinter in fjords (Hirche, 1983; Kaartvedt, 1996). It is debated to which degree the Barents Sea is a successful overwintering area (see 'Results and Discussion' below). The adults ascend to spawn early in spring, before or during the onset of the spring bloom (Hirche *et al.*, 2001). Peak egg production typically takes place in April-May in the Norwegian Sea (Melle *et al.*, 2004; Broms & Melle, 2007), and in May-June in the Atlantic waters of the Barents Sea (Melle & Skjoldal, 1998; Eiane & Tande, 2009).

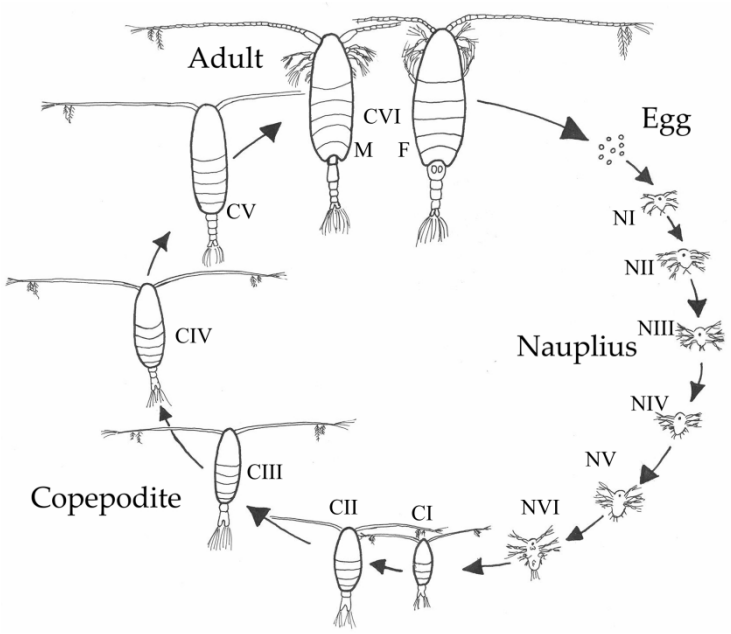

Fig. 3. The copepod life cycle. The copepod develops from eggs, through six naupliar stages (NI-NVI) and five copepodite stages (CI-CV) to adults (CVI males or females). Source: NERC ZIMNES project.

Approach

Field data

Long-term monitoring of zooplankton is considered a key to identify climate change impacts on marine ecosystems (Hays *et al.*, 2005). An extensive dataset in both space and time was collected by the Knipovich Polar Research Institute of Marine Fisheries and Oceanography (PINRO, Murmansk, Russia) between 1959 and 1993 (Fig. 4) (Nesterova, 1990). Surveys were conducted in the north-eastern Norwegian Sea and Norwegian continental shelf and the south-western Barents Sea (hereafter termed the NS-BS) in spring (April-May) and summer (June-July). The surveys thus covered most of the active, surface-dwelling period of *C. finmarchicus*' life-cycle. The complete dataset was digitised shortly before the initiation of this PhD project, and contains information from about 5000 samples on both *C. finmarchicus* stage-specific abundances (ind. m^{-3}) and total biomass (mg wet weight m^{-3}) estimated from stage-specific individual weights (Kanaeva, 1962).

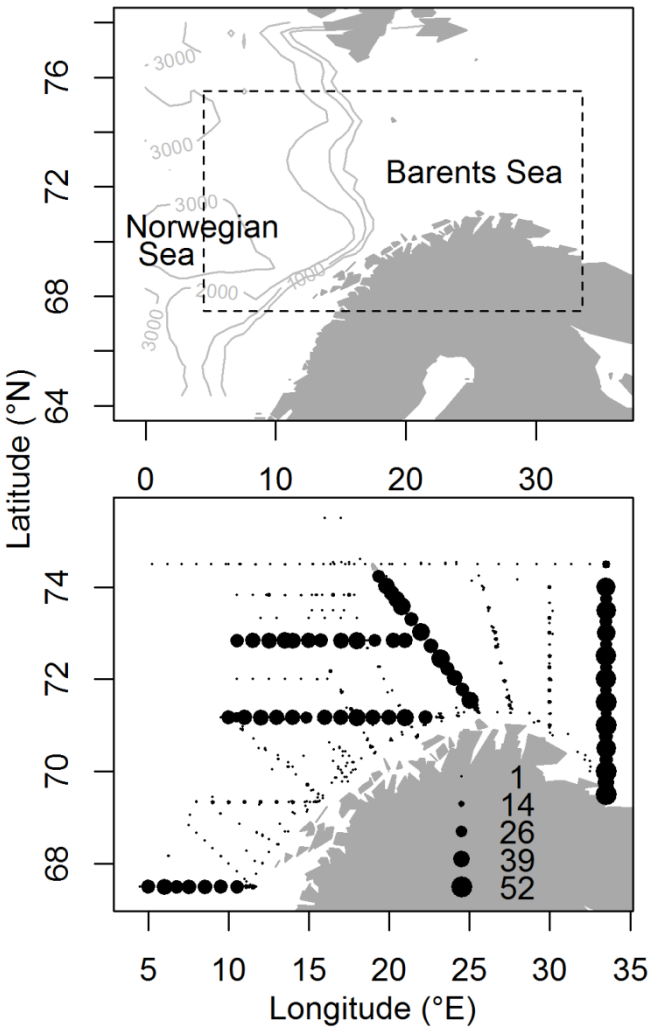

Fig. 4. Position of the survey area (dashed box, upper panel) and the distribution of survey stations with data on *C. finmarchicus* (lower panel). The size of the dots reflects the total number of times a station was sampled during the period 1959-1993.

The latter includes all naupliar (NI-NVI) and copepodite (CI-CV) stages and adult males and females (CVI). The stage-specific abundance data are used in **Paper I**, **III** and **IV**, where we aim to estimate (**I**) temperature-effects on stage-specific abundances, (**III**) areas where the new generation copepodites (CI-CIV) were recruited as eggs in spring, and (**IV**) stage-specific mortality rates. In **Paper II**, we use the total biomass data to quantify environmental effects on *C. finmarchicus* biomass from spring to summer on local and regional scales.

Drift modelling

As described above, the role of advection should be considered when investigating both zooplankton mortality rates (Aksnes & Ohman, 1996) and environmental effects on zooplankton dynamics (Pedersen *et al.*, 2001). As a solution, we apply oceanographic drift modelling in **Paper II-IV** to take into account the horizontal transport of *C. finmarchicus*. With this approach, a set of virtual particles representing zooplankton are released within the area of interest in the ocean model domain. We can then track both their drift trajectories and the ambient environment experienced by the particles. The ocean model simulates flow fields (currents) and hydrography (e.g. temperature and salinity) based on climatological data. In **Paper II-IV**, we use an ocean model hindcast archive which reproduces flow fields and hydrography in the NS-BS and adjacent areas back to 1959 (Lien *et al.*, 2013).

In the Norwegian and Barents Sea areas, drift modelling has been applied in numerous studies to track the movement of early life stages of fish (e.g. Ådlandsvik & Sundby, 1994; Vikebø *et al.*, 2005; Opdal *et al.*, 2011), but also of *C. finmarchicus* (e.g. Bryant *et al.*, 1998; Speirs *et al.*, 2005; Torgersen & Huse, 2005; Samuelsen *et al.*, 2009). However, the output of such models is rarely directly used in statistical analyses of observation data (but see Baumann *et al.*, 2006; Hidalgo *et al.*, 2012; Stige *et al.*, 2014a). In **Paper II**, the drift model results are implemented in a statistical analysis to quantify the importance of both (1) advection from spring to summer and (2) environmental variation likely experienced in spring on spatial variation in *C. finmarchicus* summer biomass.

In **Paper III**, we use drift modelling to map potential spawning areas where *C. finmarchicus* copepodites sampled in the NS-BS were likely to have originated as eggs. A similar approach was previously used by Speirs *et al.* (2004) for *C. finmarchicus* in the Norwegian Sea. But while these authors estimated spawning areas based on observations

from a limited area in one year, we could investigate variation both between years and areas.

Lastly, the oceanographic drift model is in **Paper IV** coupled to a simple population model of *C. finmarchicus*. We use the model to create synthetic datasets resembling the actual survey data, with known mortality rates. In that way, we can assess the performance of different mortality estimation methods on data influenced by both horizontal drift and variation in temperature and recruitment.

Statistical analyses

In biological systems, the shape of the relationship between the predictor and the response variable is often unknown, and it might be more sober to 'let the data speak' than to assume a (e.g. linear) relationship. Generalized additive models (GAMs) are flexible nonparametric statistical regression models where the relationship between variables are modelled as smooth functions and not specified *a priori* (Hastie & Tibshirani, 1990; Wood, 2006). The regression analyses in **Paper I** and **II** are performed using GAMs, and we use a GAM to estimate mortality of *C. finmarchicus* stage-pairs in **Paper IV**.

When working with spatial data, neighbouring observations are often more similar than distant observations. In other words, spatial autocorrelation is likely to occur. This can lead to overestimation of the statistical significance of model effects (too low p-values). To account for possible spatial autocorrelation, we use a bootstrap approach (resampling years with replacement) to calculate confidence intervals of the model effects in **Paper I**, **II** and **IV**.

Results and Discussion

Several environmental factors might influence *C. finmarchicus* dynamics. Below, I will discuss how findings from this dissertation, along with previous literature, shed light on the effects of (1) temperature, (2) food availability and (3) advection. Thereafter, I will highlight some general lessons learned from this work.

Temperature

The warming of the oceans during the past decades has led to observed impacts on marine life, and marine organisms generally show stronger responses to climate change than terrestrial organisms (Poloczanska *et al.*, 2013). As many other marine animals, zooplankton are poikilothermic[2], and temperature variation therefore directly influences physiological processes. For *C. finmarchicus*, lab studies have shown that egg production increases and development time decreases with increased ambient temperature (Corkett *et al.*, 1986; Hirche *et al.*, 1997; Campbell *et al.*, 2001). It is more difficult to infer temperature effects in the field, where the influence of other factors, such as food availability and advection, can be confounded with the effect of temperature (see the following sections). Still, Neuheimer *et al.*, (2010) found that temperature to a large degree explained observed temporal variability in both development rates and egg production in *C. finmarchicus* in the Northwest Atlantic, even when food availability and female abundance was accounted for. A recent meta-analysis showed a clear link between temperature and the species' distribution, with maximum abundances occurring at 12-13°C (Melle *et al.*, 2014). The ecological niche[3] of the species has previously been described as within a lower temperature range (6-10°C, Helaouët & Beaugrand, 2007). In either way, considering the temperatures commonly observed in the NS-BS – typically below 6°C in spring and 8°C in summer (Fig. 2, **Paper I**) – we would expect a positive effect of increased temperatures on *C. finmarchicus* abundance in this region.

In **Paper I**, we indeed observe a positive relationship between ambient temperature and abundance of *C. finmarchicus* stage CV and adult females, but for the younger stages (CI-CIV), the temperature association is positive in spring and negative in summer. We interpret this as a temperature effect on the timing of the new generation in spring. The abundances of the young copepodite stages typically peak in late spring/early summer in the NS-BS (Fig. 4, **Paper I**). With increased temperatures, egg production may start earlier and/or the development of the new generation may happen faster, leading to increased abundances in spring relative to summer. In **Paper II**, we find that mean *C. finmarchicus* biomass in spring is positively related to temperature in spring, but the mean change in biomass from spring to summer is lower after a warm spring than a cold spring. Together, the results from **Paper I** and **II** indicate that increased temperatures, as predicted in future

[2] An organism whose body temperature varies with the surroundings
[3] The range of environmental factors (e.g. temperature) tolerated by a species

climate scenarios, might increase the *C. finmarchicus* biomass available for predators in spring, but not in summer. On the other hand, the negative association between temperature in spring and biomass growth until summer might result from increased predation pressure removing additional biomass in warm years (see Discussion in **Paper II**).

A number of studies from other regions have found that zooplankton phenology shifts to 'earlier when warmer' (reviewed in Richardson, 2008; Mackas *et al.*, 2012). This could be a physiological effect (e.g. faster development), an effect of temperature on the timing of food availability or predator abundance, or temperature functioning as a cue (Mackas *et al.*, 2012). In high latitude areas with a temporally restricted food window, environmental cues are likely important for the timing of events such as reproduction and seasonal vertical migration. It has been reported that *C. finmarchicus* occurs earlier in the NS-BS in warm years, possibly due to earlier spawning (Ellertsen *et al.*, 1989; Orlova *et al.*, 2010). Such a mechanism could potentially explain the temperature associations described in **Paper I** and **II**.

The seasonal development of different organisms respond differently to climate variation (Poloczanska *et al.*, 2013), which can, according to the match/mismatch hypothesis, have ecological implications (Hjort, 1914; Cushing, 1990; Beaugrand *et al.*, 2003; Durant *et al.*, 2007). For example, the peak day of spawning of Northeast Arctic cod in the Lofoten area is believed to be relatively fixed and invariant of temperature, and as the larvae feed mainly on *C. finmarchicus* nauplii, the timing of peak nauplii abundance is likely important for cod recruitment (Ellertsen *et al.*, 1987, 1989). In **Paper I**, we find that the abundance of observed *C. finmarchicus* developmental stages in some areas appear to peak before or after the survey period. But for areas where the peaks of stages CI-CIII occur within the survey period, these are found to shift earlier by one to two weeks with a temperature increase of 2°C (from 1°C below to 1°C above the mean) (Fig. 8, **Paper I**). This is a relatively small change compared to previous observations of zooplankton phenology, including for copepods in the North Sea (11 days change per °C) (Edwards & Richardson, 2004; Richardson, 2008).

Finally, different field studies have found contrasting associations between temperature and *C. finmarchicus* mortality (Tande, 1988; Plourde *et al.*, 2009). It seems unlikely that temperature would directly cause mortality, except in the extreme cases with temperatures outside *C. finmarchicus*' thermal range (e.g. close to 0°C as in the study by

Tande (1988)). Temperature is more likely a proxy for other factors influencing mortality and survival (e.g. food availability or predation). It is also important to note that with the commonly used vertical life table (VLT) approach (Aksnes & Ohman, 1996) and the statistical regression approach (SRA) we present in **Paper IV**, temperature is included in the calculation of stage duration and therefore influences the estimated mortality rates (higher temperature → shorter development time → higher estimated mortality). In general, mortality estimations are subject to much uncertainty. Further development and evaluation of the statistical regression approach (**Paper IV)** might improve our baseline estimates, and allow us to investigate possible environmental effects on mortality.

Food availability

Although it has been emphasised that a combination of top-down and bottom-up forces controls zooplankton biomass in the NS-BS (Mueter *et al.*, 2009; Dalpadado *et al.*, 2014), consistent bottom-up effects of climate or food availability have rarely been demonstrated. Reported relationships with temperature or other climate indices are often conflicting (Tande *et al.*, 2000; Dalpadado *et al.*, 2003; Stige *et al.*, 2009, 2014a). The season-dependent temperature associations described in this dissertation (**Paper I** and **II**) shed new light on potential climate effects on *C. finmarchicus* in this region.

The positive association between temperature and *C. finmarchicus* abundance in spring (**Paper I)** might be related to temperature effects on spring bloom timing and magnitude. Earlier spring bloom timing in subarctic areas has been associated with ocean warming (Harrison *et al.*, 2013), and chlorophyll (Chl) concentration has been shown to correlate positively with temperature in several North Atlantic regions (Feng *et al.*, 2014). Food availability could influence *C. finmarchicus* abundance through several mechanisms. First, field observations from several areas, including the Norwegian and Barents Seas, have indicated that *C. finmarchicus* egg production increases with food availability (Niehoff *et al.*, 1999; Head *et al.*, 2000, 2013; Stenevik *et al.*, 2007; Melle *et al.*, 2014). Secondly, increased food availability may decrease development time (Head et al. 2000, Campbell et al. 2001), which could both decrease mortality (leaving less time to be eaten) (Lopez, 1996), and increase abundances in spring relative to summer by shifting the abundance peak. Finally, food limitation may directly cause mortality due to starvation

(Lopez, 1996; Heath *et al.*, 2008) or increased cannibalism by adults and older copepodite stages on eggs and nauplii (Ohman *et al.*, 2008; Plourde *et al.*, 2009)[4].

Increased zooplankton abundance has been linked to elevated phytoplankton production in the Northwest Atlantic (Greene & Pershing, 2007; Greene, 2013), but few field studies from the NS-BS have directly linked variation in *C. finmarchicus* abundance to food availability. In a recent study, inter-annual variability in Chl and mesozooplankton biomass was positively correlated in only one of five Barents Sea regions (Dalpadado *et al.*, 2014).

In **Paper II**, we look more closely at potential links between temperature, food availability and *C. finmarchicus* biomass, using satellite data of Chl as a proxy for phytoplankton biomass. As the satellite data are unavailable at a regular scale prior to 1998 and the PINRO dataset ends in 1993, we cannot directly investigate effects of Chl on *C. finmarchicus* biomass. Instead, we relate Chl biomass in spring to the physical covariates used in the analysis of zooplankton biomass.

In the period investigated in May, the mixed-layer-depth (MLD) is generally stabilised, and the spring bloom likely already initiated. Although the relative importance of different mechanisms driving spring bloom initiation has been subject to much debate recently (Huisman *et al.*, 1999; Behrenfeld, 2013; Sathyendranath *et al.*, 2015 and references therein), observations indicate that in the NS-BS, large blooms take place mainly when the MLD is shallower than 40-60 m (Sakshaug *et al.*, 2009b; Bagøien *et al.*, 2012). Ambient temperature does not appear to influence Chl biomass during the surveyed period in spring (**Paper II**). On the other hand, Chl biomass is positively related to ambient wind speed when MLD is shallow. This indicates that wind-induced mixing increases phytoplankton biomass after the spring bloom initiation, possibly due to nutrient renewal. *C. finmarchicus* biomass in summer is in the same manner positively related to the combination of increased wind and shallow MLD at back-calculated positions in spring. These results indicate that bottom-up effects of food availability in spring influence *C. finmarchicus* biomass in the NS-BS in summer.

The positive effect of wind on Chl biomass in **Paper II** contrasts the generally negative wind-Chl correlations in high-latitude regions (Kahru *et al.*, 2010). The study by Kahru *et al.* (2010) was, however, based on yearly means. And while the typically strong winds and deep MLD in winter/early spring at high latitudes removes phytoplankton from

[4] Note however that Bonnet *et al.* (2004) found that egg ingestion by *C. helgolandicus* females was independent of the degree of starvation.

the euphotic zone (Huisman *et al.*, 1999), wind-induced mixing when the MLD is stabilised likely has a positive effect on phytoplankton production in the NS-BS (Sakshaug *et al.*, 2009b). Stratification is predicted to increase globally with ocean warming, thereby increasing primary production in high-latitude areas (Chust *et al.*, 2014). Our results suggest that the interaction between MLD and wind will be important in projecting both phytoplankton and zooplankton biomass in spring and summer at high latitudes.

Advection

The Norwegian Atlantic current brings both warm water and zooplankton into the Barents Sea. Advection can therefore be a confounding factor when assessing temperature-effects on zooplankton dynamics in the NS-BS. Elevated zooplankton biomass in the Barents Sea during warm periods has been linked both to higher local growth rates and increased influx from the Norwegian Sea (Dalpadado *et al.*, 2003), but it is not clear which mechanism dominates. In order to disentangle the effects of temperature and advection, we specifically include drift as a covariate in the statistical model in **Paper II**. We find that influx of particles representing *C. finmarchicus* biomass explains 5-6% of the spatiotemporal variation in summer biomass. Accounting for advection, we find that spatially resolved biomass in summer relates positively to temperature at back-calculated positions in spring. This could indicate a positive effect of temperature on egg production and growth in spring reflected in observed biomass in summer. However, mean biomass in summer is not higher after a warm than a cold spring (**Paper II**). It therefore seems likely that the locally positive temperature effect results from more biomass originating from south-western areas closer to core overwintering areas in the Norwegian Sea, where temperatures generally are higher than in the north-eastern parts of our survey area.

It is commonly claimed that advection from the Norwegian Sea is the dominant source of *C. finmarchicus* biomass in the Atlantic waters in the Barents Sea (Skjoldal & Rey, 1989; Helle, 2000; Edvardsen *et al.*, 2003a; Torgersen & Huse, 2005). The bulk of this transport happens when zooplankton in the Norwegian Sea reside in surface waters, from about March to August (Edvardsen *et al.*, 2003b). However, changes in zooplankton biomass in the eastern Norwegian Sea do not seem to affect the amount advected into the Barents Sea, and it has been estimated that 67-77% of zooplankton production in the Barents Sea is local (Dalpadado *et al.*, 2012; Skaret *et al.*, 2014).

In **Paper III**, we back-calculate potential areas where copepodites sampled in the NS-BS in spring were spawned as eggs. We find that copepodites sampled in the Barents Sea entrance may originate from both local and distant spawning areas to the south along the Norwegian shelf edge. Zooplankton production in this area will clearly be influenced by the dynamics of the Norwegian Atlantic Current. On the other hand, copepodites sampled farther east in the Barents Sea (the Kola transect at 33.5°E) likely originate from spawning areas within the Barents Sea proper. We cannot determine if females ascending from overwintering in the Norwegian Sea typically drift into the Barents Sea before spawning, or if these results reflect spawning by individuals overwintering in the Barents Sea. *C. finmarchicus* has been observed in the Barents Sea in winter (Manteifel, 1941; Pedersen, 1995), and at equally shallow overwintering depths in other regions (Dale *et al.*, 1999; Head & Pepin, 2007). However, due to the risk of the offspring being transported out to the north of the area, a local Barents Sea population would likely die off within few years without influx from the Norwegian Sea (Aksnes & Blindheim, 1996; Skaret *et al.*, 2014). Still, as ambient food availability and temperature likely are important for *C. finmarchicus* egg production and development, the results from **Paper III** indicate that environmental conditions within the Barents Sea likely influence the *C. finmarchicus* biomass available for higher trophic levels in the area.

In summary, **Paper II** and **III** confirm that influx from the Norwegian Sea is important in explaining spatial distribution of *C. finmarchicus* in the NS-BS, but farther east on the Barents Sea shelf, local production seems to dominate.

In **Paper IV,** we simulate a *C. finmarchicus* population in the NS-BS influenced by realistic drift patterns and being subject to fixed mortality rates. We find that as long as egg production is constant, the commonly used vertical life table (VLT) approach for mortality estimation (Aksnes & Ohman, 1996) performs well. If spatiotemporally varying recruitment is introduced, the mortality estimates from the VLT are biased. This confirms the findings of Gentleman *et al.* (2012), who highlighted the sensitivity of the VLT to spatial gradients in production. We describe a statistical regression approach (SRA) which incorporates the effects of both temporal and spatial trends in production. Applying this method to simulated data gives promising results, suggesting that the SRA could be a useful tool for mortality estimation in advective open ocean systems.

The importance of scale

Previous climate effect studies on zooplankton in the NS-BS have typically focused on total biomass of species or size groups, and/or data aggregated over years or areas (e.g. Tande *et al.*, 2000; Dalpadado *et al.*, 2003; Stige *et al.*, 2014b). The results in this dissertation indicate that zooplankton dynamics are associated with temperature variation with complex spatiotemporal and developmental interactions (**Paper I)**. Studies overlooking these interactions might fail to detect effects of climate variation. In **Paper II**, we follow a population of *C. finmarchicus* from spring to summer, and therefore look at total biomass instead of stage-specific abundances with quick temporal turnover. Investigating environmental effects on both local and regional scales reveals temperature associations that might seem contradictory, but highlights different aspects of *C. finmarchicus* dynamics in the NS-BS: (1) Inflow of biomass from warmer, south-western areas, and (2) overall increased biomass in warm springs not necessarily persisting until summer.

The high spatial resolution and long time span of the survey data allow us in **Paper III** to describe the year-to-year variation in potential spawning areas and drift trajectories to on-shelf and off-shelf survey transects. A take-home message from this paper is that making generalisations about the source areas for *C. finmarchicus* in the NS-BS is difficult, and that links between large-scale climatic phenomena (e.g. the NAO[5]) and connectivity within the NS-BS are not clear-cut. Small-scale variation, such as local wind fields, is likely important in determining the distribution of *C. finmarchicus* eggs and copepodites in the area.

Finally, limited knowledge of stage-specific mortality is believed to be an important drawback in models of zooplankton population dynamics, where mortality rates usually are taken from a few studies and tuned *a posteriori* to give reasonable results (Runge *et al.*, 2004). Our estimations indicate that *C. finmarchicus* mortality rates in the NS-BS are relatively similar across copepodite stages, but possibly higher for the older stage-pair (**Paper IV**). Due to uncertainty in the data, we did not investigate mortality rates for eggs and nauplii, which are likely higher than for copepodites (e.g. Eiane & Ohman, 2004; Ohman *et al.*, 2004). Mortality rates are also likely to vary over both time and space (Eiane

[5] The North Atlantic Oscillation, a climate phenomenon driven by differences in sea pressure between the Icelandic low and the Azores high. The NAO influences air circulation in the North Atlantic, and thereby ocean circulation and weather.

et al., 2002; Ohman *et al.*, 2008; Plourde *et al.*, 2009). Mapping spatiotemporal variation in zooplankton mortality should be a continued priority in future studies.

The way forward

In the studies collated in this dissertation, we combine past zooplankton observations with estimates from an ocean model hindcast. Although the emerged picture is retrospective, the results can inform us about the potential future of *C. finmarchicus* in the NS-BS. **Paper I** and **II** indicate that increased temperatures might accelerate *C. finmarchicus* production, increasing biomass in spring but not necessarily in summer. It is particularly the timing of the young stages in spring which is influenced by temperature variation. Successful growth of predators on zooplankton does not only depend on the total biomass available, but on the structure of the zooplankton community (e.g. size distribution and seasonality) (van Deurs *et al.*, 2015). Climate impacts on the seasonality of key zooplankton species such as *C. finmarchicus* can therefore influence the growth of its predators in the NS-BS, including commercially important fish species such as the Northeast Arctic cod.

We show in **Paper II** that the combination of shallow MLD and strong wind in spring can trigger favourable conditions for the growth of *C. finmarchicus* biomass until summer. Thermal stratification is predicted to increase globally (IPCC, 2014), which could benefit biological production at high latitudes (Chust *et al.*, 2014). Increased stratification might increase food availability for *C. finmarchicus* early in spring, but according to the results in **Paper II**, the positive effect of shallow MLD on Chl biomass in May, and *C. finmarchicus* biomass in summer, is only present when the interacting effect of wind is accounted for. Future climate projections suggest increased mean wind speed in Northern Europe, but these are highly uncertain (McInnes *et al.*, 2011; Pryor *et al.*, 2012). Climate change can also influence the relative importance of top-down and bottom-up control, with possibly nonlinear and unexpected responses (Litzow & Ciannelli, 2007). I would claim that to predict the future of *C. finmarchicus* in the NS-BS, or indeed other marine populations under climate change, and expecting it to hold true under realised future climate scenarios, is to move on thin ice.

This dissertation also describes the effects of water circulation on the distribution of *C. finmarchicus*' early developmental stages (**Paper III**) and how we might improve the estimation of zooplankton mortality rates in advective systems (**Paper IV**). On these topics,

several questions remain to be answered, such as (*i*) the main source of *C. finmarchicus* females spawning in the Barents Sea, and (*ii*) how spatiotemporal variation in mortality relates to both bottom-up and top-down effects. Improved knowledge of both natural mortality rates and the connectivity between populations are important steps on the way to disentangle the web of climate effects on zooplankton populations.

Several studies have highlighted the apparent dominance of top-down control of zooplankton in the Barents Sea (Stige *et al.*, 2009, 2014a; Dalpadado *et al.*, 2012, 2014; Johannesen *et al.*, 2012). However, top-down control seems to be weaker in the south-western compared to north-eastern Barents Sea, and also weaker in spring compared to summer and autumn (Stige *et al.*, 2009, 2014a). Through this dissertation, I demonstrate how effects of temperature, advection and water-column properties, through its effects on food availability, can influence the dynamics of *C. finmarchicus* in the NS-BS, and discuss how this in turn may affect the feeding conditions for its predators. While bottom-up forcing is the focus here, I do not claim that top-down effects should be neglected. In fact, a large fraction of the variation in the data remains unexplained (**Paper I** and **II)**. The combined effects of bottom-up and top-down forcing in explaining the spatiotemporal dynamics of *C. finmarchicus* in the NS-BS, both within and between years, should be further investigated. With the works compiled in this dissertation, we might be a few steps closer to solving the puzzle.

Acknowledgements

I thank Leif Chr. Stige, Øystein Langangen, Guri Sogn Andersen and Kristian Seierstad for helpful comments on this introduction.

References

Aksnes DL, Blindheim J (1996) Circulation patterns in the North Atlantic and possible impact on population dynamics of *Calanus finmarchicus*. *Ophelia*, **44**, 7–28.

Aksnes DL, Ohman MD (1996) A vertical life table approach to zooplankton mortality estimation. *Limnology and oceanography*, **41**, 1461–1469.

Aksnes D, Miller C, Ohman M, Wood S (1997) Estimation techniques used in studies of copepod population dynamics—a review of underlying assumptions. *Sarsia*, **82**, 279–296.

Atkinson A, Siegel V, Pakhomov E, Rothery P (2004) Long-term decline in krill stock and increase in salps within the Southern Ocean. *Nature*, **432**, 100–103.

Ayón P, Swartzman G, Bertrand A, Gutiérrez M, Bertrand S (2008) Zooplankton and forage fish species off Peru: Large-scale bottom-up forcing and local-scale depletion. *Progress In Oceanography*, **79**, 208–214.

Bagøien E, Melle W, Kaartvedt S (2012) Seasonal development of mixed layer depths, nutrients, chlorophyll and *Calanus finmarchicus* in the Norwegian Sea – A basin-scale habitat comparison. *Progress in Oceanography*, **103**, 58–79.

Baumann H, Hinrichsen H-H, Möllmann C, Köster FW, Malzahn AM, Temming A (2006) Recruitment variability in Baltic Sea sprat (*Sprattus sprattus*) is tightly coupled to temperature and transport patterns affecting the larval and early juvenile stages. *Canadian Journal of Fisheries and Aquatic Sciences*, **63**, 2191–2201.

Beaugrand G, Reid PC, Ibañez F, Lindley JA, Edwards M (2002) Reorganization of North Atlantic marine copepod biodiversity and climate. *Science (New York, N.Y.)*, **296**, 1692–4.

Beaugrand G, Brander KM, Alistair Lindley J, Souissi S, Reid PC (2003) Plankton effect on cod recruitment in the North Sea. *Nature*, **426**, 661–4.

Behrenfeld MJ (2013) Abandoning Sverdrup's Critical Depth Hypothesis on phytoplankton blooms. *Ecology*, **91**, 977–989.

Blindheim J (2004) Oceanography and climate. In: *The Norwegian Sea Ecosystem* (ed Skjoldal HR), pp. 65–96. Tapir Academic Press, Trondheim.

Bonnet D, Titelman J, Harris R (2004) *Calanus* the cannibal. *Journal of Plankton Research*, **26**, 937–948.

Broms C, Melle W (2007) Seasonal development of *Calanus finmarchicus* in relation to phytoplankton bloom dynamics in the Norwegian Sea. *Deep Sea Research Part II: Topical Studies in Oceanography*, **54**, 2760–2775.

Broms C, Melle W, Kaartvedt S (2009) Oceanic distribution and life cycle of Calanus species in the Norwegian Sea and adjacent waters. *Deep Sea Research Part II: Topical Studies in Oceanography*, **56**, 1910–1921.

Bryant AD, Hainbucher D, Heath M (1998) Basin-scale advection and population persistence of *Calanus finmarchicus*. *Fisheries Oceanography*, **7**, 235–244.

Campbell RG, Wagner MM, Teegarden GJ, Boudreau CA, Durbin EG (2001) Growth and development rates of the copepod *Calanus finmarchics* reared in the laboratory. *Marine Ecology Progress Series*, **221**, 161–183.

Casini M, Hjelm J, Molinero J-C et al. (2009) Trophic cascades promote threshold-like shifts in pelagic marine ecosystems. *Proceedings of the National Academy of Sciences of the United States of America*, **106**, 197–202.

Chust G, Allen JI, Bopp L et al. (2014) Biomass changes and trophic amplification of plankton in a warmer ocean. *Global Change Biology*, **20**, 2124–2139.

Corkett CJ, McLaren IA, Sevigny J-M (1986) The rearing of the marine calanoid copepods *Calanus finmarchicus* (Gunnerus), *C. glacialis* (Jaschnov) and *C. hyperboreus* (Kroyer) with comment on the equiproportional rule. *Syllogeus*, **58**, 539–546.

Costanza R, Arge R, Groot R De et al. (1997) The value of the world ' s ecosystem services and natural capital. *Nature*, **387**, 253–260.

Cury P, Bakun A, Crawford R, Jarre A, Quiñones R, Shannon L, Verheye H (2000) Small pelagics in upwelling systems: patterns of interaction and structural changes in "wasp-waist" ecosystems. *ICES Journal of Marine Science*, **57**, 603–618.

Cushing DH (1990) Plankton production and year-class strength in fish populations: an update of the match/mismatch hypothesis. *Advances in Marine Biology*, **26**, 249–293.

Dale T, Bagøien E, Melle W, Kaartvedt S (1999) Can predator avoidance explain varying overwintering depth of *Calanus* in different oceanic water masses? *Marine Ecology Progress Series*, **179**, 113–121.

Dalpadado P, Ingvaldsen R, Hassel A (2003) Zooplankton biomass variation in relation to climatic conditions in the Barents Sea. *Polar Biology*, **26**, 233–241.

Dalpadado P, Ingvaldsen RB, Stige LC, Bogstad B, Knutsen T, Ottersen G, Ellertsen B (2012) Climate effects on Barents Sea ecosystem dynamics. *ICES Journal of Marine Science*, **69**, 1303–1316.

Dalpadado P, Arrigo KR, Hjøllo SS et al. (2014) Productivity in the Barents Sea - response to recent climate variability. *PloS one*, **9**, e95273.

Van Deurs M, Jørgensen C, Fiksen Ø (2015) Effects of copepod size on fish growth: a model based on data for North Sea sandeel. *Marine Ecology Progress Series*, **520**, 235–243.

Durant JM, Hjermann DØ, Ottersen G, Stenseth NC (2007) Climate and the match or mismatch between predator requirements and resource availability. *Climate Research*, **33**, 271–283.

Edvardsen A, Tande KS, Slagstad D (2003a) The importance of advection on production of *Calanus finmarchicus* in the Atlantic part of the Barents Sea. *Sarsia*, **88**, 261–273.

Edvardsen A, Slagstad D, Tande KS, Jaccard P (2003b) Assessing zooplankton advection in the Barents Sea using underway measurements and modelling. *Fisheries Oceanography*, **12**, 61–74.

Edwards M, Richardson AJ (2004) Impact of climate change on marine pelagic phenology and trophic mismatch. *Nature*, **430**, 881–884.

Eiane K, Ohman MD (2004) Stage-specific mortality of *Calanus finmarchicus*, *Pseudocalanus elongatus* and *Oithona similis* on Fladen Ground, North Sea, during a spring bloom. *Marine Ecology Progress Series*, **268**, 183–193.

Eiane K, Tande KS (2009) Meso and macrozooplankton. In: *Ecosystem Barents Sea* (eds Sakshaug E, Johnsen G, Kovacs K), pp. 209–234. Tapir Academic Press, Trondheim.

Eiane K, Aksnes DL, Ohman MD, Wood S, Martinussen MB (2002) Stage-specific mortality of *Calanus* spp. under different predation regimes. *Limnology and Oceanography*, **47**, 636–645.

Ellertsen B, Fossum P, Solemdal P, Sundby S, Tilseth S (1987) The effect of biological and physical factors on the survival of Arcto-Norwegian cod and the influence on recruitment variability. In: *The effect of oceanographic conditions on distribution and population dynamics of commercial fish in the Barents Sea. Proceedings of the third Soviet-Norwegian Symposium, Murmansk, 26-28 May 1986* (ed Loeng H), pp. 101–126. Institute of Marine Research, Bergen.

Ellertsen B, Fossum P, Solemdal P, Sundby S (1989) Relation between temperature and survival of eggs and first-feeding larvae of northeast Arctic cod (*Gadus morhua* L.). *Rapports et Proces-Verbaux des Reunions du Conseil Inter- national pour l'Exploration de la Mer*, **191**, 209–219.

Falk-Petersen S, Mayzaud P, Kattner G, Sargent JR (2009) Lipids and life strategy of Arctic *Calanus*. *Marine Biology Research*, **5**, 18–39.

FAO (2014) *The State of World Fisheries and Aquaculture*. 223 pp.

Feng J, Stige L, Durant J et al. (2014) Large-scale season-dependent effects of temperature and zooplankton on phytoplankton in the North Atlantic. *Marine Ecology Progress Series*, **502**, 25–37.

Field CB, Behrenfeld MJ, Randerson JT, Falkowski P (1998) Primary production of the biosphere: integrating terrestrial and oceanic components. *Science*, **281**, 237–240.

Frank KT, Petrie B, Choi JS, Leggett WC (2005) Trophic cascades in a formerly cod-dominated ecosystem. *Science (New York, N.Y.)*, **308**, 1621–1623.

Frank KT, Petrie B, Shackell NL, Choi JS (2006) Reconciling differences in trophic control in mid-latitude marine ecosystems. *Ecology Letters*, **9**, 1096–1105.

Frank KT, Petrie B, Fisher J a D, Leggett WC (2013) Setting the record straight on drivers of changing ecosystem states. *Fisheries Oceanography*, **22**, 143–146.

Gentleman WC, Pepin P, Doucette S (2012) Estimating mortality: Clarifying assumptions and sources of uncertainty in vertical methods. *Journal of Marine Systems*, **105-108**, 1–19.

Gjøsæter H (2009) Commercial fisheries (fish, seafood and marine mammals). In: *Ecosystem Barents Sea* (eds Sakshaug E, Johnsen G, Kovacs K), pp. 373–414. Tapir Academic Press, Trondheim, Norway.

Greene CH (2013) Towards a more balanced view of marine ecosystems. *Fisheries Oceanography*, **22**, 140–142.

Greene CH, Pershing AJ (2007) Climate drives sea change. *Science (New York, N.Y.)*, **315**, 1084–1085.

Harrison WG, Børsheim KY, Li WKW et al. (2013) Phytoplankton production and growth regulation in the Subarctic North Atlantic: A comparative study of the Labrador Sea-Labrador/Newfoundland shelves and Barents/Norwegian/Greenland seas and shelves. *Progress in Oceanography*, **114**, 26–45.

Hastie T, Tibshirani R (1990) *Generalized Additive Models*. Chapman and Hall, London UK., 335 pp.

Hays GC, Richardson AJ, Robinson C (2005) Climate change and marine plankton. *Trends in ecology & evolution*, **20**, 337–44.

Head E, Pepin P (2007) Variations in overwintering depth distributions of *Calanus finmarchicus* in the slope waters of the NW Atlantic continental shelf and the Labrador Sea. *Journal of Northwest Atlantic Fishery Science*, **39**, 49–69.

Head EJH, Harris LR, Campbell RW (2000) Investigations on the ecology of *Calanus* spp. in the Labrador Sea. I. Relationship between the phytoplankton bloom and reproduction and development of *Calanus finmarchicus* in spring. *Marine Ecology Progress Series*, **193**, 53–73.

Head EJH, Harris LR, Ringuette M, Campbell RW (2013) Characteristics of egg production of the planktonic copepod, *Calanus finmarchicus*, in the Labrador Sea: 1997-2010. *Journal of Plankton Research*, **35**, 281–298.

Heath MR, Backhaus JANO, Richardson K, Slagstad DAG, Dunn J, Fraser JG, Gallego A (1999) Climate fluctuations and the spring invasion of the North Sea by *Calanus finmarchicus*. *Fisheries Oceanography*, **8**, 163–176.

Heath MR, Rasmussen J, Ahmed Y et al. (2008) Spatial demography of *Calanus finmarchicus* in the Irminger Sea. *Progress in Oceanography*, **76**, 39–88.

Helaouët P, Beaugrand G (2007) Macroecology of *Calanus finmarchicus* and *C. helgolandicus* in the North Atlantic Ocean and adjacent seas. *Marine Ecology Progress Series*, **345**, 147–165.

Helle K (2000) Distribution of the copepodite stages of *Calanus finmarchicus* from Lofoten to the Barents Sea in July 1989. *ICES Journal of Marine Science*, **57**, 1636–1644.

Hidalgo M, Gusdal Y, Dingsor GE et al. (2012) A combination of hydrodynamical and statistical modelling reveals non-stationary climate effects on fish larvae distributions. *Proceedings of the Royal Society B: Biological Sciences*, **279**, 275–283.

Hirche H-J (1983) Overwintering of *Calanus finmarchicus* and *Calanus helgolandicus*. *Marine Ecology Progress Series*, **11**, 281–290.

Hirche H-J, Meyer U, Niehoff B (1997) Egg production of *Calanus finmarchicus*: effect of temperature, food and season. *Marine Biology*, **127**, 609–620.

Hirche H-J, Brey T, Niehoff B (2001) A high-frequency time series at Ocean Weather Ship Station M (Norwegian Sea): population dynamics of *Calanus finmarchicus*. *Marine Ecology Progress Series*, **219**, 205–219.

Hirst AG, Bunker AJ (2003) Growth of marine planktonic copepods: global rates and patterns in relation to chlorophyll a, temperature, and body weight. *Limonology And Oceanography*, **48**, 1988–2010.

Hjort J (1914) Fluctuations in the great fisheries of northern Europe viewed in the light of biological research. *Rapports et Proces-Verbaux des Reunions du Conseil International pour l'Exploration de la Mer*, **20**, 1–228.

Huisman J, Oostveen P van, Weissing FJ (1999) Critical depth and critical turbulence: Two different mechanisms for the development of phytoplankton blooms. *Limnology and Oceanography*, **44**, 1781–1787.

Ingvaldsen RB, Loeng H (2009) Physical oceanography. In: *Ecosystem Barents Sea* (eds Sakshaug E, Johnsen G, Kovacs K), pp. 33–64. Tapir Academic Press, Trondheim.

IPCC (2014) *Climate Change 2014: Synthesis Report. Contribution of Working Groups I, II and III to the Fifth Assessment Report of the Intergovernmental Panel on Climate Change* (eds Team CW, Pachauri RK, Meyer LA). Geneva, 151 pp.

Irigoien X, Head R, Klenke U et al. (1998) A high frequency time series at weathership M , Norwegian Sea , during the 1997 spring bloom : feeding of adult female Calanus finmarchicus. *Marine Ecology Progress Series*, **172**, 127–137.

Irigoien X, Harris RP, Head RN, Lindley JA, Harbour D (2000) Physiology and population structure of *Calanus finmarchicus* (Copepoda: Calanoida) during a Lagrangian tracer release experiment in the North Atlantic. *Journal of Plankton Research*, **22**, 205–221.

Johannesen E, Ingvaldsen RB, Bogstad B et al. (2012) Changes in Barents Sea ecosystem state, 1970-2009: climate fluctuations, human impact, and trophic interactions. *ICES Journal of Marine Science*, **69**, 880–889.

Jónasdóttir SH, Gudfinnsson H., Gislason A, Astthorsson OS (2002) Diet composition and quality for *Calanus finmarchicus* egg production and hatching success off south-west Iceland. *Marine Biology*, **140**, 1195–1206.

Kaartvedt S (1996) Habitat preference during overwintering and timing of seasonal vertical migration of *Calanus finmarchicus*. *Ophelia*, **44**, 145–156.

Kahru M, Gille ST, Murtugudde R, Strutton PG, Manzano-Sarabia M, Wang H, Mitchell BG (2010) Global correlations between winds and ocean chlorophyll. *Journal of Geophysical Research*, **115**, C12040.

Kanaeva IP (1962) Mean weight of copepods of Central and Northern Atlantic, the Norwegian and Greenland Seas. *M. Pishchepromizdat*, **46**, 253–266 (in Russian).

Lien VS, Gusdal Y, Albretsen J, Melsom A, Vikebø F (2013) Evaluation of a Nordic Seas 4 km numerical ocean model hindcast archive (SVIM), 1960-2011. *Fisken og Havet*, **7**, 1–80.

Litzow MA, Ciannelli L (2007) Oscillating trophic control induces community reorganization in a marine ecosystem. *Ecology Letters*, **10**, 1124–1134.

Llope M, Daskalov GM, Rouyer TA, Mihneva V, Chan KS, Grishin AN, Stenseth NCHR (2011) Overfishing of top predators eroded the resilience of the Black Sea system regardless of the climate and anthropogenic conditions. *Global Change Biology*, **17**, 1251–1265.

Lopez MDG (1996) Effect of starvation on development and survivorship of naupliar *Calanus pacificus* (Brodsky). *Journal of Experimental Marine Biology and Ecology*, **203**, 133–146.

Mackas DL, Greve W, Edwards M et al. (2012) Changing zooplankton seasonality in a changing ocean: Comparing time series of zooplankton phenology. *Progress In Oceanography*, **97-100**, 31–62.

Manteifel BP (1941) Plankton and herring in the Barents Sea. *Trudy PINRO. Transactions of the Knipovich Polar Scientific Institute of Sea-Fisheries and Oceanography Murmansk*, **7**, 125–218 (in Russian).

Mayor DJ, Anderson TR, Irigoien X, Harris R (2006) Feeding and reproduction of *Calanus finmarchicus* during non-bloom conditions in the Irminger Sea. *Journal of Plankton Research*, **28**, 1167–1179.

McInnes KL, Erwin TA, Bathols JM (2011) Global Climate Model projected changes in 10 m wind speed and direction due to anthropogenic climate change. *Atmospheric Science Letters*, **12**, 325–333.

Melle W, Skjoldal H (1998) Reproduction and development of *Calanus finmarchicus*, *C. glacialis* and *C. hyperboreus* in the Barents Sea. *Marine Ecology Progress Series*, **169**, 211–228.

Melle W, Ellertsen B, Skjoldal HR (2004) Zooplankton: The link to higher trophic levels. In: *The Norwegian Sea Ecosystem* (ed Skjoldal HR), pp. 137–202. Tapir Academic Press, Trondheim.

Melle W, Runge J, Head E et al. (2014) The North Atlantic Ocean as habitat for *Calanus finmarchicus*: Environmental factors and life history traits. *Progress in Oceanography*, **129**, 244–284.

Mueter FJ, Broms C, Drinkwater KF et al. (2009) Ecosystem responses to recent oceanographic variability in high-latitude Northern Hemisphere ecosystems. *Progress in Oceanography*, **81**, 93–110.

Nesterova VN (1990) *Plankton biomass along the drift route of cod larvae (reference material)*. PINRO, Murmansk (in Russian), 64 pp.

Neuheimer AB, Gentleman WC, Pepin P, Head EJH (2010) Explaining regional variability in copepod recruitment: Implications for a changing climate. *Progress in Oceanography*, **87**, 94–105.

Niehoff B, Klenke U, Hirche H, Irigoien X, Head R, Harris R (1999) A high frequency time series at Weathership M, Norwegian Sea, during the 1997 spring bloom:the reproductive biology of *Calanus finmarchicus*. *Marine Ecology Progress Series*, **176**, 81–92.

Ohman M, Eiane K, Durbin E, Runge J, Hirche H (2004) A comparative study of *Calanus finmarchicus* mortality patterns at five localities in the North Atlantic. *ICES Journal of Marine Science*, **61**, 687–697.

Ohman MD, Durbin EG, Runge JA, Sullivan BK, Field DB (2008) Relationship of predation potential to mortality of Calanus finmarchicus on Georges Bank, northwest Atlantic. *Limnology and Oceanography*, **53**, 1643–1655.

Opdal AF, Vikebø F, Fiksen Ø (2011) Parental migration, climate and thermal exposure of larvae: spawning in southern regions gives Northeast Arctic cod a warm start. *Marine Ecology Progress Series*, **439**, 255–262.

Orlova EL, Boitsov VD, Nesterova VN (2010) *The influence of hydrographic conditions on the structure and functioning of the trophic complex plankton - pelagic fishes – cod*. Knipovich's Polar Research Institute of Marine Fisheries and Oceanography (PINRO), Murmansk, 190 pp.

Pedersen G (1995) Why does a component of *Calanus finmarchicus* stay in the surface waters during the overwintering period in high latitudes? *ICES Journal of Marine Science*, **52**, 523–531.

Pedersen OP, Tande KS, Slagstad D (2001) A model study of demography and spatial distribution of *Calanus finmarchicus* at the Norwegian coast. *Deep Sea Research Part II: Topical Studies in Oceanography*, **48**, 567–587.

Petrie B, Frank KT, Shackell NL, Leggett WC (2009) Structure and stability in exploited marine fish communities: Quantifying critical transitions. *Fisheries Oceanography*, **18**, 83–101.

Plourde S, Pepin P, Head EJH (2009) Long-term seasonal and spatial patterns in mortality and survival of *Calanus finmarchicus* across the Atlantic Zone Monitoring Programme region, Northwest Atlantic. *ICES Journal of Marine Science*, **66**, 1942–1958.

Poloczanska ES, Brown CJ, Sydeman WJ et al. (2013) Global imprint of climate change on marine life. *Nature Climate Change*, **3**, 919–925.

Pryor SC, Barthelmie RJ, Clausen NE, Drews M, MacKellar N, Kjellström E (2012) Analyses of possible changes in intense and extreme wind speeds over northern Europe under climate change scenarios. *Climate Dynamics*, **38**, 189–208.

Pörtner H-O, Karl D, Boyd PW et al. (2014) Ocean systems. In: *Climate Change 2014: Impacts, Adaptation, and Vulnerability. Part A: Global and Sectoral Aspects. Contribution of Working Group II to the Fifth Assessment Report of the*

Intergovernmental Panel on Climate Change (eds Field CB, Barros VR, Dokken DJ, Mach KJ, Mastrandrea MD, Bilir TE, Chatterjee M, Ebi KL, Estrada YO, Genova RC, Girma B, Kissel ES, Levy AN, MacCracken S, Mastrandrea PR, White LL), pp. 411–484. Cambridge University Press, Cambridge and New York, NY.

Richardson AJ (2008) In hot water: zooplankton and climate change. *ICES Journal of Marine Science*, **65**, 279–295.

Richardson AJ, Schoeman DS (2004) Climate impact on plankton ecosystems in the Northeast Atlantic. *Science (New York, N.Y.)*, **305**, 1609–12.

Runge JA, Franks PS, Gentleman WC, Megrey BA, Rose KA, Werner FE, Zakardijan B (2004) Diagnosis and prediction of variability in secondary production and fish recruitment processes: developments in physical-biological modeling. *The Sea: The Global Coastal Ocean: Multiscale Interdisciplinary Processes*, **13**, 413–473.

Sakshaug E, Johnsen G, Kovacs K (eds.) (2009a) *Ecosystem Barents Sea*. Tapir Academic Press, Trondheim.

Sakshaug E, Johnsen G, Kristiansen S, Quillfeldt C von, Rey F, Slagstad D, Thingstad F (2009b) Phytoplankton and primary production. In: *Ecosystem Barents Sea* (eds Sakshaug E, Johnsen G, Kovacs K), pp. 167–207. Tapir Academic Press, Trondheim, Norway.

Samuelsen A, Huse G, Hansen C (2009) Shelf recruitment of *Calanus finmarchicus* off the west coast of Norway: role of physical processes and timing of diapause termination. *Marine Ecology Progress Series*, **386**, 163–180.

Sathyendranath S, Ji R, Browman HI (2015) Revisiting Sverdrup's critical depth hypothesis. *ICES Journal of Marine Science: Journal du Conseil*, **72**, 1892–1896.

Schminke HK (2006) Entomology for the copepodologist. *Journal of Plankton Research*, **29**, i149–i162.

Seppelt R, Dormann CF, Eppink FV, Lautenbach S, Schmidt S (2011) A quantitative review of ecosystem service studies: approaches, shortcomings and the road ahead. *Journal of Applied Ecology*, **48**, 630–636.

Skaret G, Dalpadado P, Hjøllo SS, Skogen MD, Strand E (2014) *Calanus finmarchicus* abundance, production and population dynamics in the Barents Sea in a future climate. *Progress in Oceanography*, **125**, 26–39.

Skjoldal HR, Rey F (1989) Pelagic production and variability of the Barents Sea ecosystem. In: *Biomass Yields and Geography of Large Marine Ecosystems* (eds Sherman K,

Alexander LM), pp. 241–286. American Association for the Advancement of Science. Selected Symposia.

Slagstad D, Tande KS (2007) Structure and resilience of overwintering habitats of *Calanus finmarchicus* in the Eastern Norwegian Sea. *Deep Sea Research Part II: Topical Studies in Oceanography*, **54**, 2702–2715.

Speirs DC, Gurney WSC, Holmes SJ et al. (2004) Understanding demography in an advective environment: modelling *Calanus finmarchicus* in the Norwegian Sea. *Journal of Animal Ecology*, **73**, 897–910.

Speirs DC, Gurney WSC, Heath MR, Wood SN (2005) Modelling the basin-scale demography of *Calanus finmarchicu*s in the north-east Atlantic. *Fisheries Oceanography*, **14**, 333–358.

Stenevik EK, Melle W, Gaard E, Gislason A, Broms CTÅ, Prokopchuk I, Ellertsen B (2007) Egg production of *Calanus finmarchicus* — A basin-scale study. *Deep Sea Research Part II: Topical Studies in Oceanography*, **54**, 2672–2685.

Stenevik EK, Vølstad JH, Høines Å, Aanes S, Óskarsson GJ, Jacobsen JA, Tangen Ø (2015) Precision in estimates of density and biomass of Norwegian spring-spawning herring based on acoustic surveys. *Marine Biology Research*, **11**, 449–461.

Stige LC, Lajus DL, Chan K-S, Dalpadado P, Basedow S, Berchenko I, Stenseth NC (2009) Climatic forcing of zooplankton dynamics is stronger during low densities of planktivorous fish. *Limnology and Oceanography*, **54**, 1025–1036.

Stige LC, Dalpadado P, Orlova E, Boulay A-C, Durant JM, Ottersen G, Stenseth NC (2014a) Spatiotemporal statistical analyses reveal predator-driven zooplankton fluctuations in the Barents Sea. *Progress in Oceanography*, **120**, 243–253.

Stige LC, Langangen Ø, Yaragina NA et al. (2014b) Combined statistical and mechanistic modelling suggests food and temperature effects on survival of early life stages of Northeast Arctic cod (*Gadus morhua*). *Progress in Oceanography*, **134**, 138–151.

Tande KS (1988) Aspects of developmental and mortality rates in *Calanus finmarchicus* related to equiproportional development. *Marine Ecology Progress Series*, **44**, 51–58.

Tande K, Drobysheva S, Nesterova V, Nilssen EM, Edvardsen A, Tereschenko V (2000) Patterns in the variations of copepod spring and summer abundance in the northeastern Norwegian Sea and the Barents Sea in cold and warm years during the 1980s and 1990s. *ICES Journal of Marine Science*, **57**, 1581–1591.

Torgersen T, Huse G (2005) Variability in retention of *Calanus finmarchicus* in the Nordic Seas. *ICES Journal of Marine Science*, **62**, 1301–1309.

Verheye HM, Richardson AJ (1998) Long-term increase in crustacean zooplankton abundance in the southern Benguela upwelling region (1951-1996): bottom-up or top-down control? *ICES Journal of Marine Science*, **55**, 803–807.

Vikebø F, Sundby S, Adlandsvik B, Fiksen O (2005) The combined effect of transport and temperature on distribution and growth of larvae and pelagic juveniles of Arcto-Norwegian cod. *ICES Journal of Marine Science*, **62**, 1375–1386.

Ware DM, Thomson RE (2005) Bottom-up ecosystem trophic dynamics determine fish production in the Northeast Pacific. *Science (New York, N.Y.)*, **308**, 1280–1284.

Wassmann P, Reigstad M, Haug T et al. (2006) Food webs and carbon flux in the Barents Sea. *Progress In Oceanography*, **71**, 232–287.

Wassmann P, Duarte CM, Agustí S, Sejr MK (2011) Footprints of climate change in the Arctic marine ecosystem. *Global Change Biology*, **17**, 1235–1249.

Wood SN (2006) *Generalized additive models: an introduction with R*. Chapman and Hall/CRC, Boca Raton, Florida.

Worm B, Myers RA (2003) Meta-analysis of cod-shrimp interactions reveals top-down control in oceanic food webs. *Ecology*, **84**, 162–173.

Ådlandsvik B, Sundby S (1994) Modelling the transport of cod larvae from the Lofoten area. *ICES Mar Sci. Symp.*, **198**, 379–392.

Vol. 517: 85–104, 2014
doi: 10.3354/meps11024

MARINE ECOLOGY PROGRESS SERIES
Mar Ecol Prog Ser

Published December 15

Temperature effects on *Calanus finmarchicus* vary in space, time and between developmental stages

Kristina Øie Kvile[1,*], Padmini Dalpadado[2], Emma Orlova[3,‡], Nils C. Stenseth[1], Leif C. Stige[1]

[1]Centre for Ecological and Evolutionary Synthesis (CEES), Department of Biosciences, University of Oslo, PO Box 1066 Blindern, 0316 Oslo, Norway

[2]Institute of Marine Research, PO Box 1870 Nordnes, 5817 Bergen, Norway

[3]Knipovich Polar Research Institute of Marine Fisheries and Oceanography, Knipovich-St. 6, 183763 Murmansk, Russia

ABSTRACT: Temperature is considered one of the major factors shaping marine zooplankton distribution, abundance and phenology. During the past decades, the Barents Sea experienced strong temperature fluctuations, but previous studies have not identified a clear link between temperature and the dynamics of the key copepod species *Calanus finmarchicus*. We investigated associations between regional and local water temperature and *C. finmarchicus* abundance in Atlantic waters of the Norwegian and Barents Seas between 1959 and 1992. Results differed depending on the developmental stage, season and area, emphasising the value of detailed data series in climate effect studies. Abundances of copepodite stage CV and adult females showed no strong correlations with regional temperature indices, but were positively linked to local temperature in both spring and summer. For nauplii and young copepodite stages (CI–CIV), associations with both regional and local temperature estimates were positive in spring, but negative in summer. The results indicate that the phenology of young copepodites may be particularly responsive to climate change, which in turn may influence predators feeding on these life stages.

KEY WORDS: Barents Sea · Copepod · Climate change · Generalised additive models · Norwegian Sea · Seasonality · Temperature · Zooplankton

INTRODUCTION

Temperature is believed to be the most important factor structuring marine ecosystems (e.g. Richardson 2008, Hoegh-Guldberg & Bruno 2010), and warming of the oceans due to climate change is currently altering a wide range of marine ecosystem properties (e.g. production, species composition and seasonal timing; Pörtner et al. 2014). By virtue of a combination of factors, zooplankton are thought to be ideal climate indicators (Richardson 2008). For example, as zooplankton are poikilothermic, physiological processes such as growth and reproduction are tightly coupled to temperature variation. The short life span of most zooplankton (often less than 1 yr) allows a quick response in population dynamics to climatic variation. Furthermore, since few zooplankton species are to date commercially harvested, effects of climate variation are less likely to be confounded with effects of fishing than in many other marine groups.

Effects of temperature variability have been reported on zooplankton distribution, species composition, abundance and phenology (seasonal development) (Edwards & Richardson 2004, Richardson 2008). Zooplankton populations typically display pronounced seasonality correlated with variation in temperature or other external factors (e.g. photoperiod, phytoplankton production), particularly in high-latitude areas where food availability is re-

*Corresponding author: k.o.kvile@ibv.uio.no
‡Deceased

stricted to a short time window (Eiane & Tande 2009, Mackas et al. 2012). Observed alterations in phenology have often been correlated with temperature, typically with seasonal processes occurring earlier during warmer years (Orlova et al. 2010, McGinty et al. 2011, Mackas et al. 2012). Climate change can affect marine plankton phenology differently across functional groups and trophic levels (Edwards & Richardson 2004). In this study, we demonstrate how temperature variation might affect a zooplankton species differently depending on the geographical area, season and developmental stage.

The Barents Sea is a highly productive subarctic shelf sea, in particular in southwestern areas adjacent to the Norwegian Sea, and plankton represent the bulk of animal production (Sakshaug et al. 2009). *Calanus finmarchicus* is the dominant copepod species in the Atlantic water masses in the Norwegian and Barents Seas (Melle et al. 2004, Eiane & Tande 2009, Orlova et al. 2010). In the Norwegian Sea, north of 68°N, *C. finmarchicus* usually has a 1 yr life cycle, during which it develops through 6 nauplii stages (NI–NVI) and 5 copepodite stages (CI–CV) to the adult stage (CVI) (Eiane & Tande 2009). By the end of the growth season (late summer), older stages (mainly CV, but also CIV and CVI; Melle et al. 2004) descend to deeper waters to over-winter. When adults return to the surface in spring to feed on phytoplankton and spawn, the life cycle is completed. *C. finmarchicus* is the primary food source for many fish species, including Northeast Arctic cod larvae that prey on nauplii and young copepodite stages (Ellertsen et al. 1987, 1989, Karamushko & Karamushko 1995).

The Barents Sea experienced alternating cold and warm periods during the second half of the 20th century, with a warming trend dominating since the 1980s (Johannesen et al. 2012). Although spatial and temporal variation in zooplankton biomass has been observed (e.g. Dalpadado et al. 2012, Johannesen et al. 2012), long-term data series to study the effect of climatic variability on copepod dynamics have been scarce (Tande et al. 2000, Eiane & Tande 2009), and several previous studies in the Barents Sea did not identify a clear association between temperature variation and the dynamics of *C. finmarchicus* (Tande et al. 2000, Stige et al. 2009, 2014, Dalpadado et al. 2012). Note, however, that the data analysed in these studies were limited to the upper water layer (0–50 m depth) (Tande et al. 2000, Stige et al. 2009), a few selected years (Tande et al. 2000) and/or aggregated biomass data (Stige et al. 2009, 2014, Dalpadado et al. 2012).

A notable exception, the Knipovich Polar Research Institute of Marine Fisheries and Oceanography (PINRO, Murmansk, Russia) collected zooplankton data during their ichthyoplankton surveys in the Norwegian and Barents Seas between 1959 and 1993. Some of these data have previously been analysed, with results available in Russian (Degtereva 1973, 1979, Antipova et al. 1974, Degtereva et al. 1990, Nesterova 1990, Drobysheva & Nesterova 2005; Tande et al. 2000 also analysed some of these data). Analyses of data from the Kola section (along 33.5°E) showed a positive association between temperature and zooplankton biomass in spring during the 1960s (Antipova et al. 1974), and earlier plankton development during warmer years when 8 yr of contrasting temperatures in the 1970s and 1980s were compared (Drobysheva & Nesterova 2005).

The Russian survey data on both ichthyoplankton and zooplankton have recently been digitised, and we here report on the first analyses of the complete dataset of *C. finmarchicus* stage-specific abundance. The data cover both shelf areas in the Norwegian and Barents Seas where variation in Atlantic water inflow is believed to be a main regulator of *C. finmarchicus* biomass (Helle & Pennington 1999, Dalpadado et al. 2003, Edvardsen et al. 2003a), and Norwegian Sea off-shelf areas considered as sources of *C. finmarchicus* to the shelves (Slagstad & Tande 1996, 2007, Halvorsen et al. 2003, Edvardsen et al. 2006). The long time span, high spatial resolution and coverage, region (subarctic) and separation into developmental stages make this dataset unique among climate effect studies on zooplankton (Richardson 2008, Mackas et al. 2012). Using spatiotemporal statistical analyses, we investigated associations between temperature and *C. finmarchicus* abundance, separating responses to temperature between different developmental stages, depths, seasons and geographical areas. This enabled us to shed light on whether temperature effects act primarily on abundances, vertical distribution or phenology.

MATERIALS AND METHODS

Zooplankton data

Zooplankton data were collected by PINRO during their ichthyoplankton surveys in spring (April–May) and summer (June–July) between 1959 and 1993. Sampling methods are described by Nesterova (1990). In brief, plankton samples were collected in the northeastern Norwegian Sea and southwestern

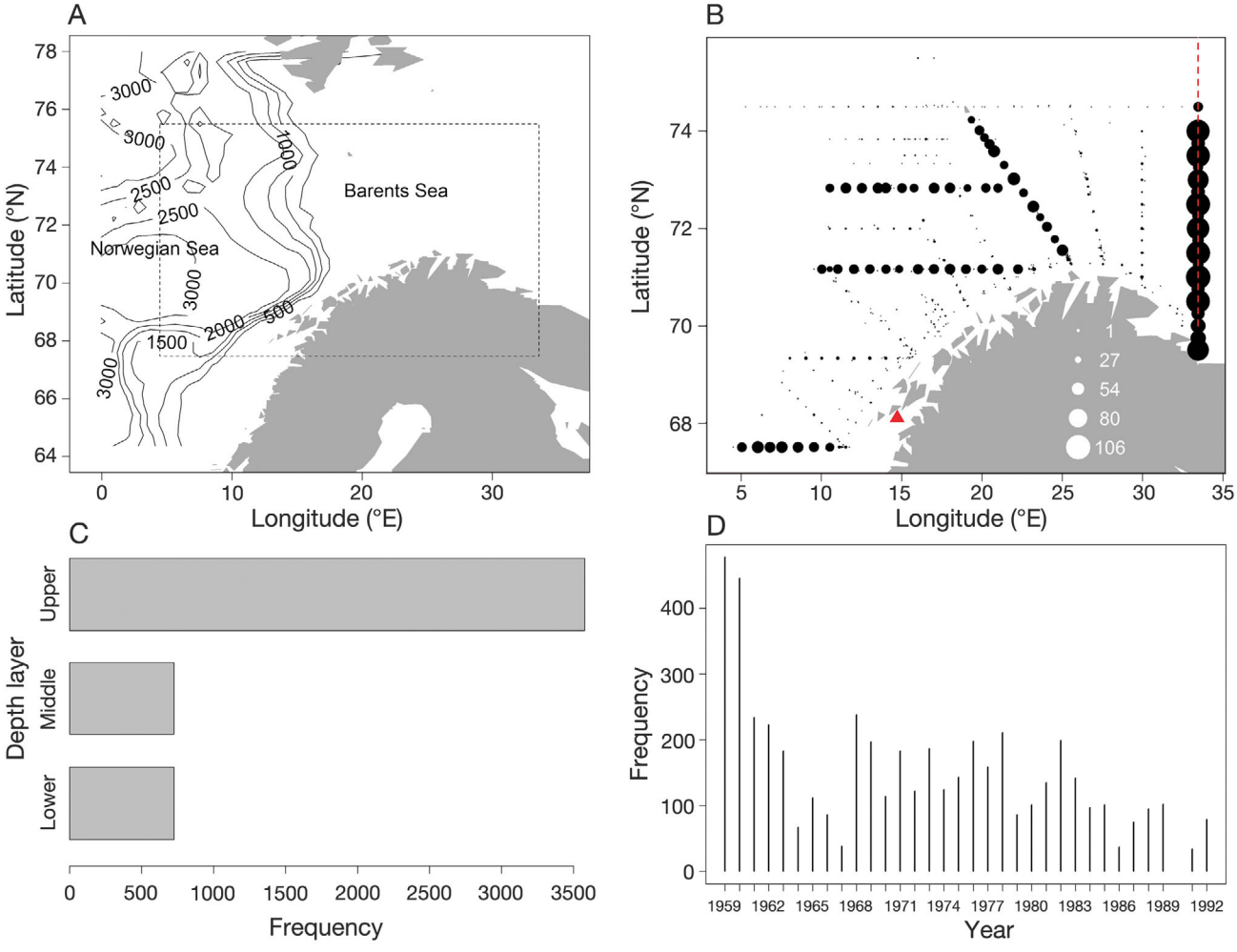

Fig. 1. (A) Study region (dashed area) with depth contours at every 500 m. (B–D) Distribution of sampling stations with stage-specific *Calanus finmarchicus* abundance data (n = 5026) by (B) geographical position, (C) depth layer (Upper: upper sampling depth ≤20 m and lower sampling depth ≤60 m, Middle: upper sampling depth 40–60 m and lower sampling depth ≤120 m, Lower: upper sampling depth >90 m) and (D) year. In (B), the size of the mapped circles reflects the number of times a station was sampled during the period 1959 to 1992. The positions of the Skrova station and the Kola section are marked with a red triangle and a red dashed line, respectively

Barents Sea along specific transects and depth layers (Fig. 1). The gear used was a Juday plankton net (37 cm diameter opening, 180 µm mesh size) with a closing mechanism, towed vertically from the lower depth to the upper depth of the sample. The main component of zooplankton biomass in the area and the dataset is *Calanus finmarchicus* (Nesterova 1990). For a total of around 5000 samples, specimens of this species were recorded as stage-specific abundance, expressed as ind. m^{-3}, accounting for the opening area of the net and the depth hauled. While nauplii are difficult to determine to species and were recorded as *Calanus* sp., *C. finmarchicus* copepodites (CI–CV) and adult males and females (CVI-M and CVI-F) were discriminated from other calanoid copepods.

There was some year-to-year variation in the stations sampled and depths hauled, particularly during the early years of the programme. In some years, sampling effort was reduced (specifically, no samples were collected in spring 1967, and no stage-specific counts were recorded in 1990 or 1993). All samples were in the dataset described by an 'upper sampling depth' (i.e. the shallowest depth of the vertical haul) and a 'lower depth' (i.e. the bottom of the haul). In most cases, the depths hauled fell within these 3 depth categories: 0–50 m, 50–100 m and 100 m–bottom. However, some samples deviated from this

scheme. In order to encompass as many samples as possible, we formulated the following new depth categories: Upper: upper sampling depth ≤20 m and lower sampling depth ≤60 m (n = 3578); Middle: upper sampling depth 40–60 m and lower sampling depth ≤120 m (n = 724); Lower: upper sampling depth >90 m (n = 724). Less than 5% of the samples were excluded when using these categories (n = 256). These were mainly samples covering a large depth interval (e.g. from the surface to several hundred meters), but also some samples falling between the set intervals (e.g. from 30 to 60 m) or with missing depth information.

Due to their small size, nauplii are under-sampled by the mesh size used (Hernroth 1987, Nichols & Thompson 1991). Considering this, in addition to the uncertainties in species determination of nauplii, we therefore present results for total nauplii abundances only (N total), which should be interpreted with caution. Abundances of adult males (CVI-M) were 0-inflated; 60% of the samples contained no males, compared to 25% for females (CVI-F) and 10–20% for nauplii and copepodite stages. *C. finmarchicus* males are known to appear earlier than females after overwintering, and die off sooner after fertilisation (Melle et al. 2004). As the data indicated that the spring survey was too late to sample males during their main appearance, the abundance data on adult males (CVI-M) were not included in the analyses of temperature associations described below.

Table 1. Model equations describing general patterns of *Calanus finmarchicus* abundance (Eqs. 1 & 2) and temperature associations in abundances (Eqs. 3–6). Z: stage-specific abundance, β: intercept, s(j): smooth function of day-of-year, s(d): smooth function of average sampling depth, te(x,y): 2-dimensional tensor product of longitude and latitude, l: indicator variable of season (spring or summer), s(Y): random effect of year, ε: random error, te(x,y,j): 2-dimensional tensor product of longitude and latitude (2-dimensional smooth) and day-of-year (1-dimensional smooth), s(T): smooth function of temperature anomaly, T: linear function of temperature anomaly. See Supplement 1 at www.int-res.com/articles/suppl/m517p085_supp.pdf for further details on model terms

Model	Equation	Eq. number
General		
Spatial, seasonal and vertical variation	$Z = \beta + s(j) + s(d) + te(x,y)l + s(Y) + \varepsilon$	1
Interaction between position and day of year	$Z = \beta + te(x,y,j) + \varepsilon$	2
Temperature effects		
Simple temperature effect	$Z = \beta + s(j) + s(d) + te(x,y)l + s(T) + \varepsilon$	3
Seasonally varying temperature effect	$Z = \beta + s(j) + s(d) + te(x,y)l + s(T)l + \varepsilon$	4
Spatially varying temperature effect	$Z = \beta + s(j) + te(x,y)l + te(x,y)lT + \varepsilon$	5
Spatially and temporally varying temperature effect	$Z = \beta + te(x,y,j) + te(x,y,j)T + \varepsilon$	6

Ocean temperatures

To assess associations between year-to-year variation in *C. finmarchicus* abundance and regional temperature, we used monthly mean sea temperature observations from the Kola section (along 33.5°E in the Barents Sea, 0–200 m depth) provided by PINRO (Tereshchenko 1996), and monthly temperature observations from the Skrova station in Vestfjorden, Lofoten Islands (68.1°N, 14.7°E, 0–200 m; Institute of Marine Research, Aure & Østensen 1993) (Fig. 1B). Vertically averaged (0–200 m) seasonal indices of these 2 temperature series were calculated by averaging observations from the months December (from the previous year) to February (Winter index), March to May (Spring index) and June to August (Summer index). To study associations between *C. finmarchicus* abundance and local temperature variation (spatially and seasonally), we used temperature estimates corresponding to the date (day, month, year) and position (latitude, longitude) of samples from a numerical ocean model hindcast archive (Lien et al. 2013). The model domain includes the Nordic Seas and the Barents Sea back to 1959 at 4 km resolution, and it realistically represents the variability in the Atlantic water masses in the zooplankton survey area (Lien et al. 2013). Three depth-integrated temperature indices were calculated per station by averaging local temperature estimates from 0, 10, 20 and 50 m (Upper), 50 and 100 m (Middle) and 100 and 250 m (Lower). Local temperature anomalies were calculated by extracting the residuals from a generalised additive model (GAM, Hastie & Tibshirani 1990, Wood 2006) where the local temperature index described above was modelled as a function of position, day-of-year and depth layer (see Eq. S1 in Supplement 1 at www.int-res.com/articles/suppl/m517p085_supp.pdf). These local temperature anomalies can be interpreted as deviances from the expected temperature at the position, day-of-year and depth of a zooplankton sample.

General patterns of *C. finmarchicus* abundance

Year-to-year variation in *C. finmarchicus* abundance was assessed by constructing year- and season-specific indices of stage-specific abundances. These seasonal abundance indices were constructed by extracting year-specific intercepts from a GAM formulated separately for spring and summer samples, where the natural logarithm of observed stage-specific abundances (with 1 added to avoid taking the logarithm of 0) was a function of day-of-year, sampling depth and location (Eq. S2 in Supplement 1). The indices can be interpreted as mean stage-specific abundances for a given season and year, taking into account year-to-year variability in sampling stations (both in time and space).

Spatial, seasonal and vertical variation in abundance was explored by fitting GAMs where observed stage-specific abundances ($\log_e[n+1]$) were a function of location, day-of-year and depth (Eq. 1 in Table 1). The effect of location could vary between spring and summer, defined as the transition between May and June (Day-of-year 150). An alternative version of Eq. (1) where the effect of depth on abundance could vary with season was formulated to investigate whether vertical distribution patterns differed between spring and summer (Eq. S3 in Supplement 1).

We hypothesised that seasonal variation in abundances might differ geographically (e.g. earlier appearance in the southern parts of the surveyed area; Manteufel 1941, Loeng & Drinkwater 2007). To visualise seasonal variation in abundances in different areas, we extracted model predictions from an alternative model (Eq. 2 in Table 1) where the effects of geographical position and day-of-year interact. Predicted abundances from late April (Day 115) to mid-July (Day 194) in the upper water layer (lower sampling depth ≤60 m) were computed for 3 locations: (1) off-shelf in the northeastern Norwegian Sea (69.7°N, 15.0°E), (2) in the Barents Sea entrance south of Bjørnøya (72.7°N, 19.5°E) and (3) in the Barents Sea proper (73.0°N, 30.5°E).

Associations with temperature

Associations between stage-specific abundances and regional temperature were quantified by calculating the Spearman rank correlation coefficient (r_S) between seasonal abundance indices and temperature indices from the Kola section and Skrova station. To account for autocorrelation in the time series, the effective number of degrees of freedom in the significance test for the correlation was adjusted according to the method described by Quenouille (1952) and modified by Pyper & Peterman (1998).

Associations between stage-specific *C. finmarchicus* abundances and local temperature anomalies were investigated with statistical analyses (GAMs) of spatially and temporally resolved observation data. Before the analyses, the observation data were assigned to 1 of the 3 depth categories decscribed in 'Zooplankton data' above: upper, middle or lower.

GAMs with various levels of complexity (Eqs. 3–6 in Table 1, Eq. S4 in Supplement 1) were investigated to address how associations between local temperature anomalies and stage-specific abundances of *C. finmarchicus* (1) differ between developmental stages, depths and seasons, (2) differ between different geographical areas and (3) shape variation in abundances throughout the spring and summer seasons.

(1) *Simple additive temperature effect*. In the simplest case, we assumed that temperature has a similar additive effect on abundances ($\log_e[n+1]$) across space and time (Eq. 3 in Table 1). The first part of the model formulation corresponds to the first part of Eq. (1) and constitutes the null-model to which a smooth function of local temperature anomaly was added (see Supplement 1 for further details). Further, to investigate whether the temperature effect differed seasonally and between depth layers, we added a factor variable of season (Eq. 4 in Table 1) and depth (Eq. S4 in Supplement 1) to the temperature term.

The following more complex models were only explored for samples from the surface layer, corresponding to the depth layer with the highest abundances during the growth season (Tande 1988b, Dale & Kaartvedt 2000, this study).

(2) *Spatially varying temperature effect*. To investigate whether the association between temperature and abundance differs between areas, we explored spatially varying coefficient models (Hastie & Tibshirani 1993), where the effect of temperature is assumed to be linear at any given location, but the slope of the temperature term can change smoothly and non-linearly in space and can differ between seasons (Eq. 5 in Table 1). Site-specific predictions of the temperature term were extracted, and significantly positive slope coefficients (for which the 2.5% percentile of the bootstrap distribution of the slope value was >0) or significantly negative slope coefficients (for which the 97.5% percentile of the bootstrap distribution was <0) were mapped. The bootstrap procedure is explained in the final paragraph below.

(3) *Spatially and temporally varying temperature effect*. To further investigate whether, and how, zooplankton phenology is influenced by temperature, and how this varies across areas, the temperature effect was modelled as a linear function varying smoothly with both geographical position and day-of-year (Eq. 6 in Table 1). Predicted daily abundances from late April (Day 115) to mid-July (Day 194) in the 3 locations previously described (see 'General patterns of *C. finmarchicus* abundance' above) were extracted for a colder-than-average scenario and a warmer-than-average scenario. For the colder scenario, temperatures were set to be 1°C below the expected temperature for a given time and position (i.e. temperature anomalies = −1), and for the warmer scenario, temperatures were set at 1°C above the expected (i.e. temperature anomalies = +1).

The different models (Eq. 1–6 in Table 1) were compared to null-models, only accounting for spatiotemporal variation in the data with genuine cross-validation (GCV), a measure of predictive power, and R^2, a measure of the proportion of data variation explained by the model. For the comparison, models were only fitted for data from the upper water layer, not including the effect of sampling depth. To account for within-year spatial autocorrelation which might lead to erroneous identification of significant effects (Zuur et al. 2007), 95% confidence intervals of the model effects were computed for all model formulations using nonparametric bootstrapping (1000 samples with replacement) with year as the sampling unit (Hastie et al. 2009). Further details on the calculation of GCV and model comparison are given in Supplement 2 at www.int-res.com/articles/suppl/m517p085_supp.pdf. All analyses were implemented in R (R Development Core Team 2014), using the mgcv library for GAMs (Wood 2013).

RESULTS

Temperature variation

Ocean temperature measurements from the Kola section and Skrova station fluctuated over the years of the study, with a cold period in the late 1970s, and generally increasing temperatures since the 1980s (Fig. 2) (as described by Johannesen et al. 2012). The local temperature estimates for the surveyed area generally increased from spring to summer, with highest temperatures occurring in the Norwegian Sea coastal areas compared to open Norwegian Sea and Barents Sea areas.

General dynamics in *C. finmarchicus* abundance

Temporal variation

Stage-specific abundances fluctuated throughout the years of the survey, without displaying any clear upward or downward trends (Fig. 3). The seasonal variation in abundances from spring to summer displayed a transition between increasingly older developmental stages throughout the spring and summer. On average, abundances of nauplii and stages CI–CII were higher in spring than summer, while the opposite was found for stages CIII–CV (Fig. 3). Abundances of CVI-F were generally higher in spring than summer, while CVI-M were only present in low abundance in both seasons. Predicted abundances from early spring to late summer in the upper water layer (Eq. 2 in Table 1) for a selected Norwegian Sea location (69.7°N, 15.0°E) indicated that abundances of nauplii and stages CI–CIII generally peaked during (or possibly before) the early parts of the spring survey, with indications of a second peak during late summer (Fig. 4, Location 1). Abundances of CIV, CV and CVI-F were relatively stable or increased throughout spring and summer. The seasonal dynamics were delayed in locations farther north and east in the surveyed area (Fig. 4, Locations 2 and 3), where abundances of nauplii remained higher during the surveyed period than in the southernmost location (but also decreased); CI–CIII seemed to peak around the transition between spring and summer (Day 150), and CIV and CV peaked later in summer, or possibly after the summer survey. In Locations 2 and 3, CVI-F were present in low abundance during the surveyed period. CVI-M were present in low abundance in Locations 1 and 2, and nearly absent in Location 3.

Spatial variation

The spatial variation of *C. finmarchicus* stage-specific abundances is illustrated in Fig. 5 as predicted abundances per position (Eq. 1 in Table 1) at median sampling depth (28 m) and median sampling day in spring (Day 129: 9 May) and in summer (Day 175: 4 July). In spring, the highest abundances of nauplii and stages CI–CIII were generally found off the Norwegian coast and in the southern Barents Sea, while in summer, the distribution centre was relocated farther north in the Norwegian and Barents Seas. Abundances of CIV were highest in the Norwegian Sea and the Barents Sea entrance in spring, with a shift to in-

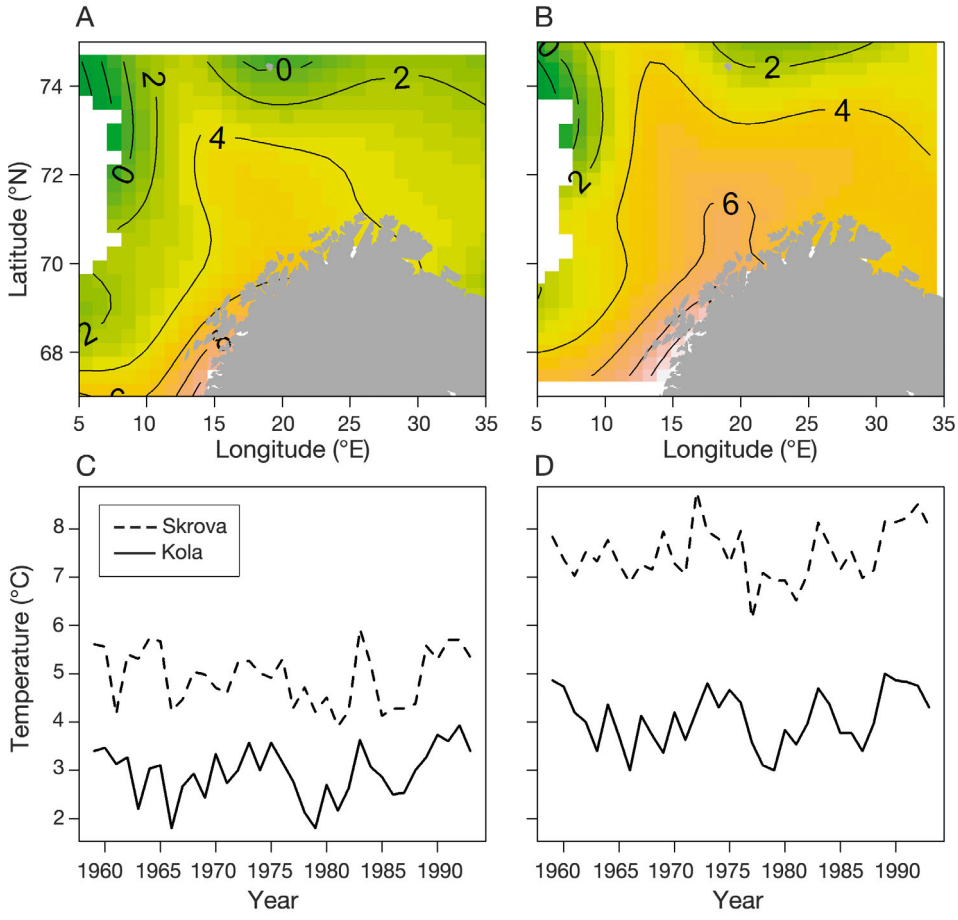

Fig. 2. Spatiotemporal variation in temperature during the course of the study. Local temperature estimates (°C) at the survey stations (see Fig. 1B), averaged over the years 1959 to 1992 and 0 to 250 m depth, in (A) spring and (B) summer. Year-to-year variation in temperature indices (°C) from the Kola section (solid line) and Skrova station (dashed line) in (C) spring and (D) summer. Local temperature estimates were interpolated in space using a generalised additive model with local temperature as a function of a tensor product smooth of longitude and latitude. See 'Materials and methods' for calculation of regional temperature indices

creased abundances in the Barents Sea in summer. There was less seasonal difference in the spatial distribution of stages CV and CVI-F, which were found in higher abundances in the Norwegian Sea than in the Barents Sea in both spring and summer. Stage CVI-M were found primarily in the Norwegian Sea area.

Vertical variation

Abundances of all stages were highest in the upper 50 m and decreased in deeper water (Fig. S1 in Supplement 3 at www.int-res.com/articles/suppl/m517p085_supp.pdf), although stages CIV, CV and CVI-F also showed a slight increase in abundances from around 100 to 200 m. An alternative model with a seasonally varying depth effect (Eq. S3 in Supplement 1) indicated that this second peak was more pronounced in summer than in spring (Fig. S2 in Supplement 3). The influence of position, day-of-year and sampling depth on stage-specific abundances is shown in Table S1 in Supplement 3.

Associations between temperature and *C. finmarchicus* abundance

Regional temperature

Correlations between seasonal abundance indices of nauplii and copepodite stages CI–CIV and Kola and Skrova temperatures were generally positive in spring and negative in summer (Table S2 in Supplement 3). Statistically significant correlations were identified for stages CII–CIV in spring and summer and for stage CI in summer. No significant correlations were observed between regional temperature indices and abundances of stages CV or CVI-F.

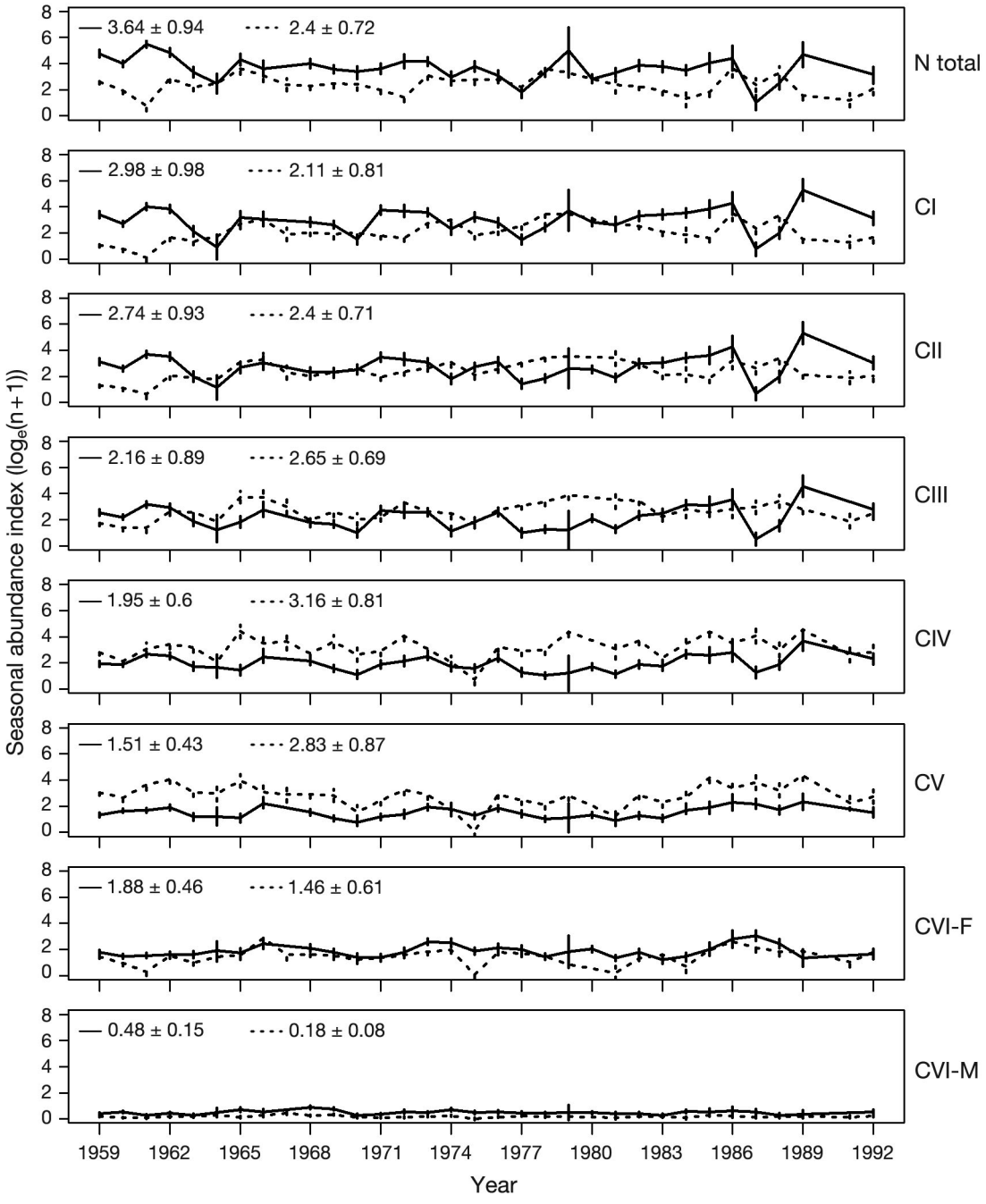

Fig. 3. Year-to-year variation in *Calanus finmarchicus* stage-specific seasonal abundance indices ($\log_e$[n+1]) in spring (solid lines) and summer (dashed lines). Abundance indices are year-specific intercepts from Eq. S2 in Supplement 1 at www.int-res.com/articles/suppl/m517p085_supp.pdf. The vertical lines mark the nominal 95% confidence interval (not accounting for spatial autocorrelation) of the abundance indices (solid lines for spring, dashed lines for summer). Also displayed are, per developmental stage, the overall mean and standard deviation of the spring and summer indices. N total: total nauplii abundance, CI–CVI: stage-specific copepodite abundances; M: male; F: female

Local temperature anomalies

(1) *Simple additive temperature effect.* In the simplest case (Eq. 3 in Table 1), we assumed that the effect of temperature variation on abundance does not change across space or in time but can differ between developmental stages. The results indicated a weakly positive but non-significant temperature effect on abundances of nauplii and stages CI–CIV, and a significant positive association for stages CV

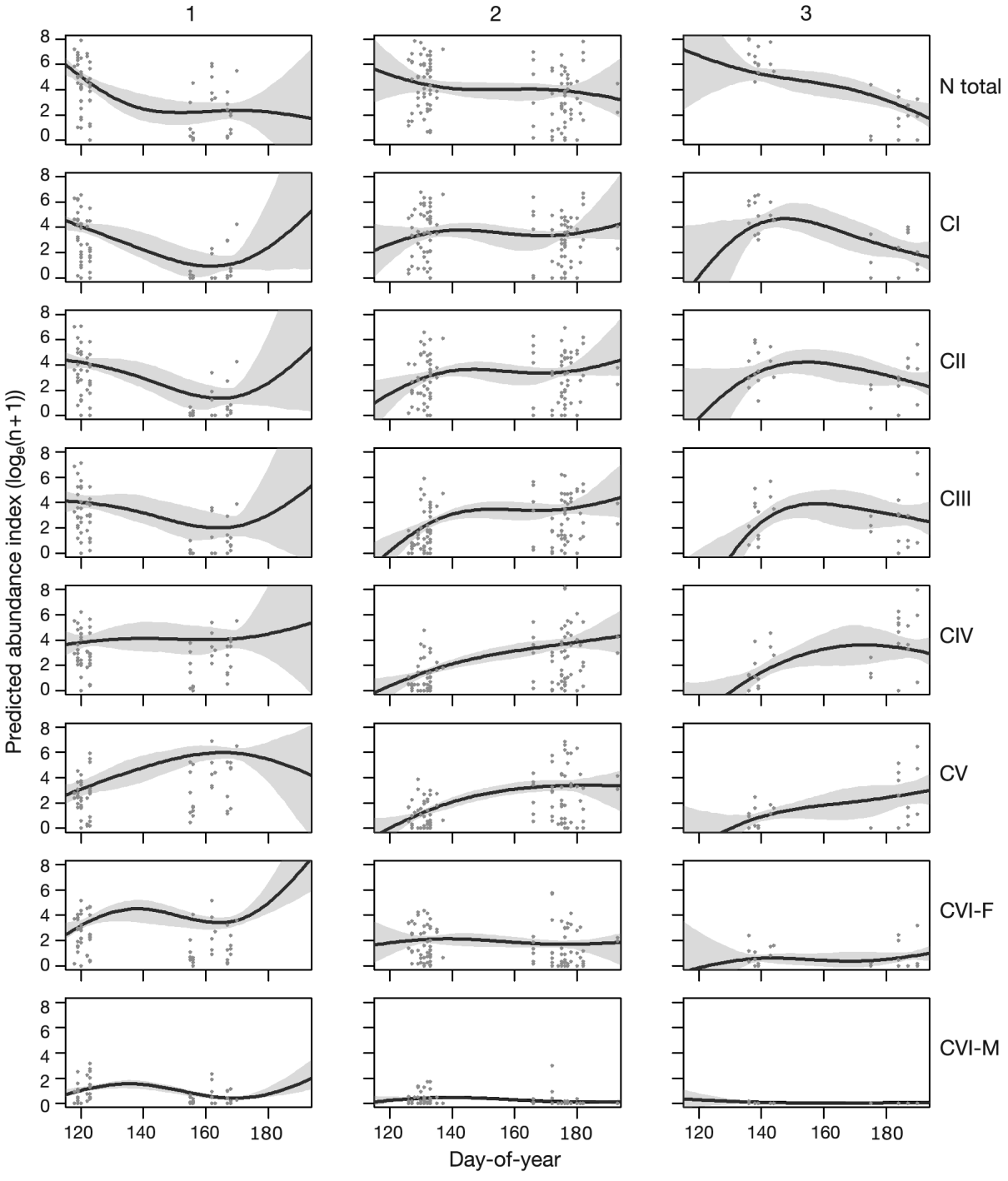

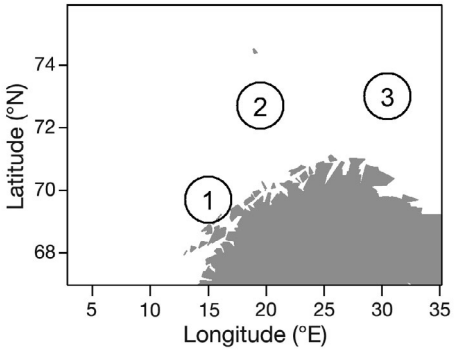

Fig. 4. Predicted abundances (plots) of *Calanus finmarchicus* developmental stages (log$_e$[n+1]) throughout the spring and summer seasons in 3 locations (map): 1 (left column), off-shelf in the north-eastern Norwegian Sea (69.7° N, 15.0° E); 2 (centre column), in the Barents Sea entrance south of Bjørnøya (72.7° N, 19.5° E); and 3 (right column), in the Barents Sea proper (73.0° N, 30.5° E). Predictions were extracted from Eq. 2 in Table 1, based on pooled data from the upper water layer for the period 1959 to 1992. Shaded area: 95% confidence interval from bootstrap procedure. Grey dots: sampled stage-specific abundances (log$_e$[n+1]) from stations within 50 km of each location. N total: total nauplii abundance, CI–CVI: stage-specific copepodite abundances; M: male; F: female

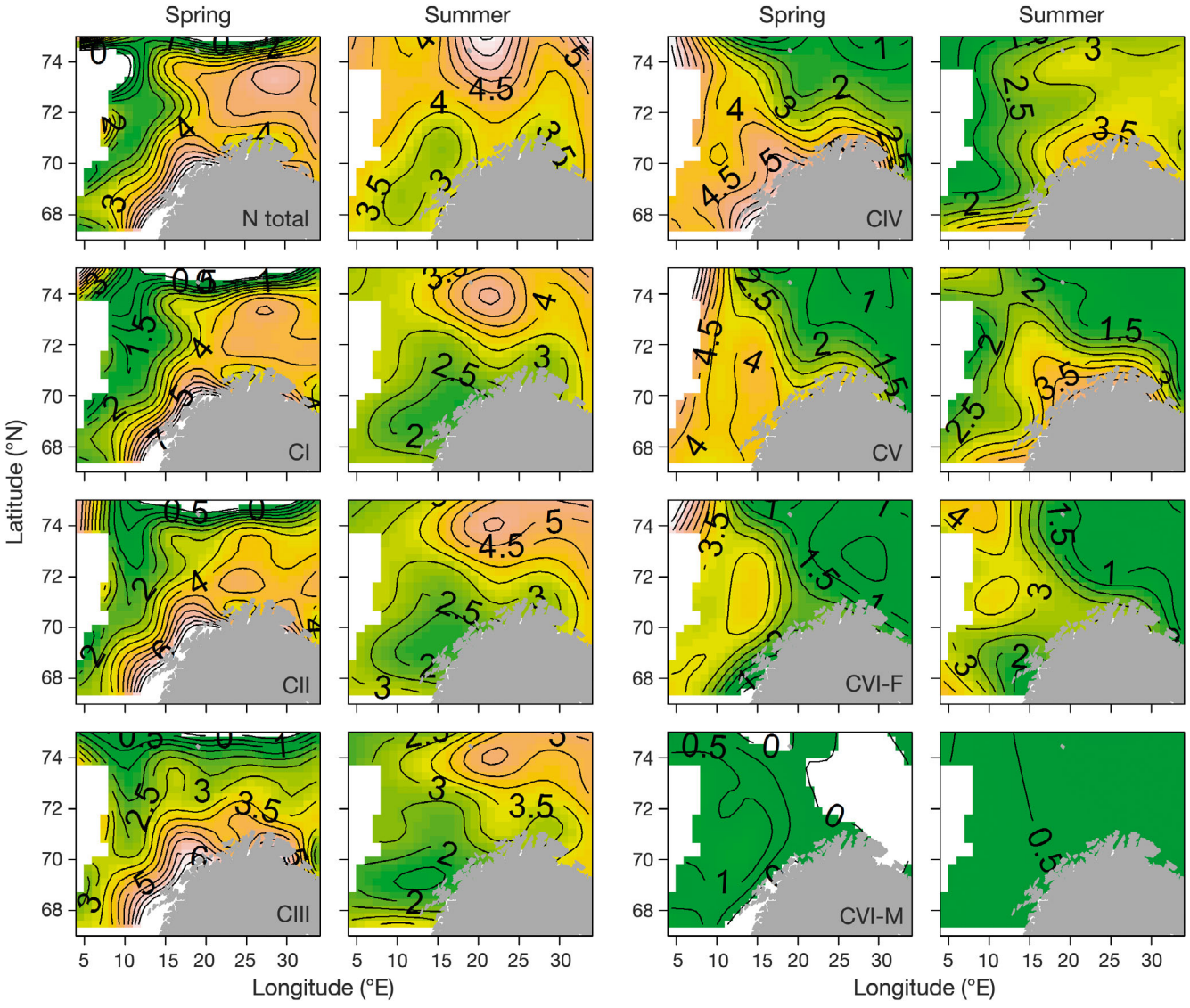

Fig. 5. Predicted stage-specific abundances ($\log_e[n+1]$, Eq. 1) of *Calanus finmarchicus* in the study area in spring and summer, at averaged values for sampling depth (28 m) and day-of-year (spring, Day 129: 9 May; summer, Day 175: 4 July), based on pooled data for the period 1959 to 1992. The numbered isolines mark the predicted stage-specific abundances, from green areas with the relatively lowest abundances, to orange/red areas with the relatively highest abundances. Note that model predictions are more uncertain for areas with low data coverage (see Fig. 1B). N total: total nauplii abundance, CI–CVI: stage-specific copepodite abundances; M: male; F: female

and CVI-F (Fig. 6, left). However, when we let the temperature effect differ between spring and summer (Eq. 4 in Table 1), a more detailed picture emerged. Positive temperature anomalies were associated (1) with above-average abundances of nauplii and CI–CIV in spring, (2) with below-average abundances of these stages in summer and (3) with above-average abundances of CV and CVI-F in both spring and summer (Fig. 6, middle and right). The associations for CIV–CV in summer did not significantly differ from 0 (the 95% confidence interval of the additive effect surrounded 0). We found few indications of a differing effect of temperature with depth (Fig. S3 in Supplement 3). The confidence intervals for the temperature effects in different depth layers were generally overlapping, with a possible exception of nauplii and CI–CIII in summer, for which the negative association with temperature was only observed in the upper water layers. Based on these findings, we proceeded with the more complex model investigations looking only at temperature effects on abundance in the upper water layer.

(2) *Spatially varying temperature effect.* Slope coefficient values from a spatially varying coefficient model (Eq. 5 in Table 1) mapped per sampling position (Fig. 7) reflected the seasonal patterns from the

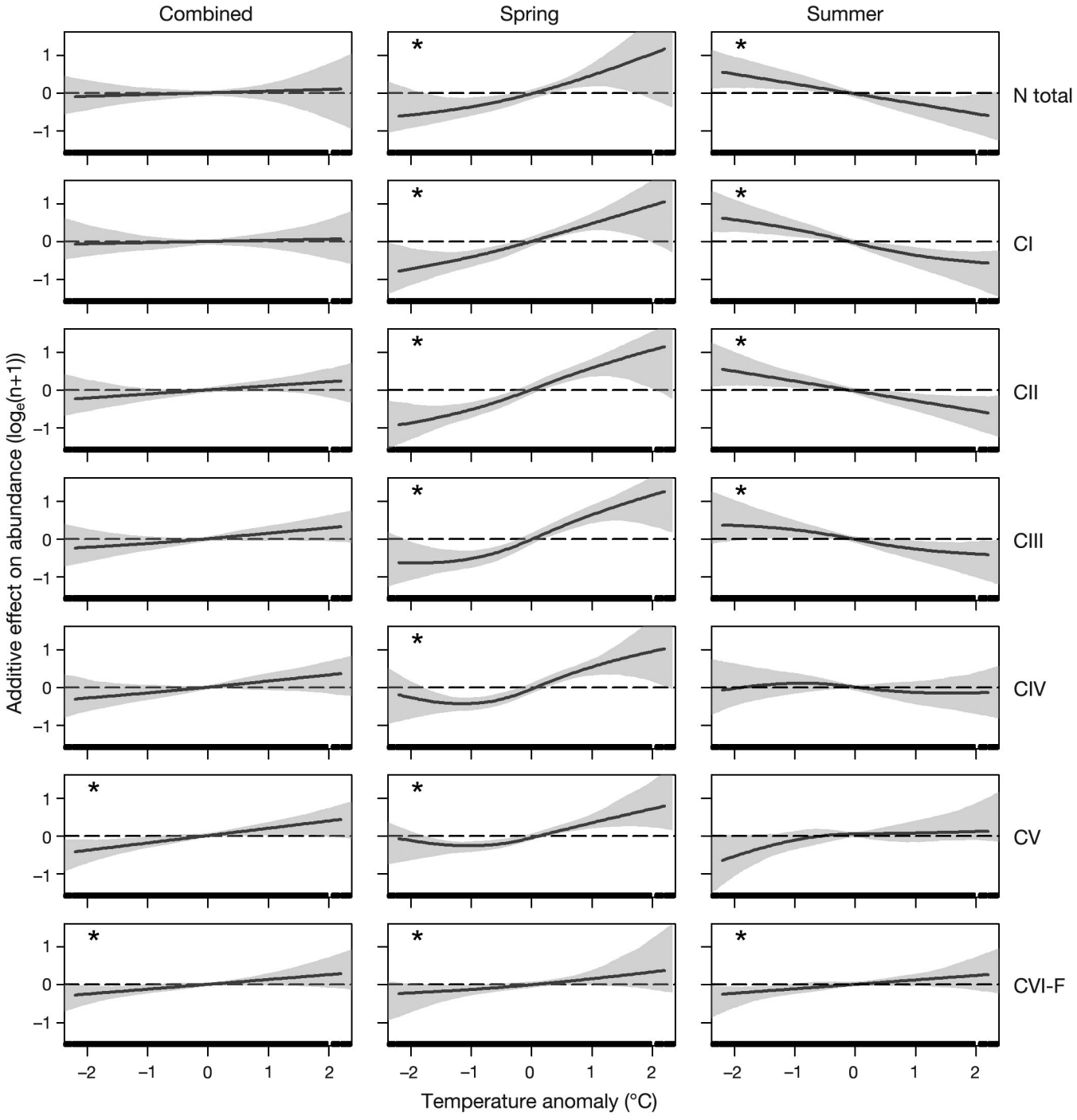

Fig. 6. Additive effect of local temperature anomalies on *Calanus finmarchicus* stage-specific abundances (log$_e$[n+1]). Left column: additive temperature effect estimated for spring and summer combined (Eq. 3 in Table 1). Centre and right columns: additive effect estimated for spring and summer separately (Eq. 4 in Table 1). Shaded area: 95% confidence interval from bootstrap procedure. Dashed line: 0 effect isoline. Stars indicate a significant association, i.e. that the effect differs from 0 in parts of the covariate's range. N total: total nauplii abundance, CI–CVI: stage-specific copepodite abundances; F: female

simple additive model (Fig. 6), but displayed some spatial variation in the strength of the temperature association. For nauplii, the positive association in spring was restricted to west of around 24°E, and the negative association in summer to the east of this border. The largest spatial extent of significant temperature associations was found for stages CI–CIII, with significant positive associations in spring in most of the survey area (except the northernmost transects for CI and CIII). Negative associa-

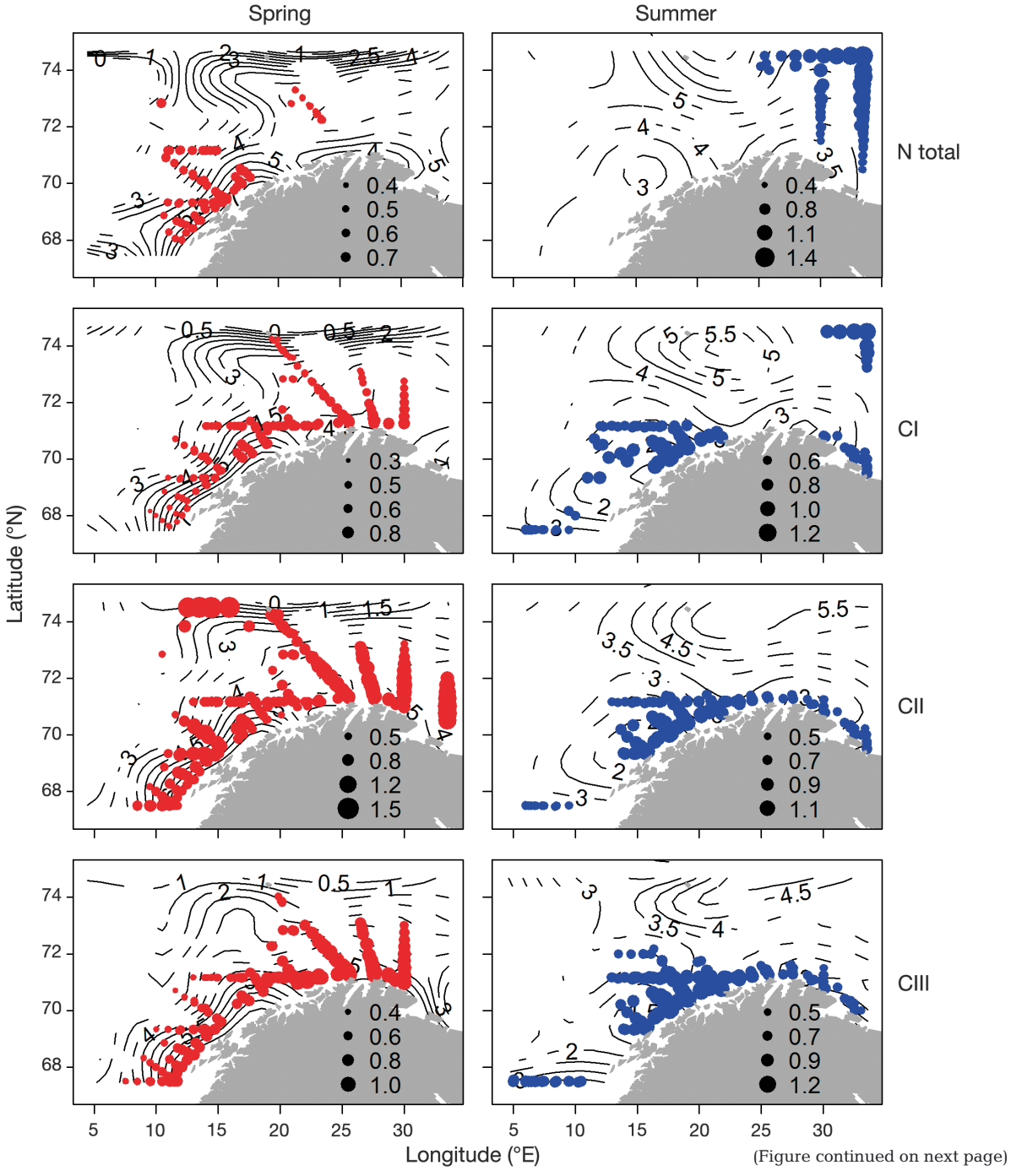

(Figure continued on next page)

Fig. 7. Significantly negative (blue) or positive (red) slope coefficients for a linear temperature effect on *Calanus finmarchicus* stage-specific abundances (Eq. 5 in Table 1) in spring and summer. The size of the circles reflects the magnitude of the slope coefficient. The numbered isolines show predicted abundances ($\log_e[n+1]$) when a temperature effect is excluded, corresponding to Fig. 5. N total: total nauplii abundance, CI–CVI: stage-specific copepodite abundances; F: female

tions in summer were mainly found along the Norwegian shelf edge and the southernmost Barents Sea. Abundances of CIV–CV were positively associated with temperature in spring, and higher slope values were predicted in areas with generally higher abundances in the Norwegian Sea and in the southern Barents Sea. In summer, negative (for CIV) or positive (for CIV and CV) associations were identified within smaller areas. Abundances of adult females (CVI-F) were positively associated with temperature only in restricted areas in both spring and summer.

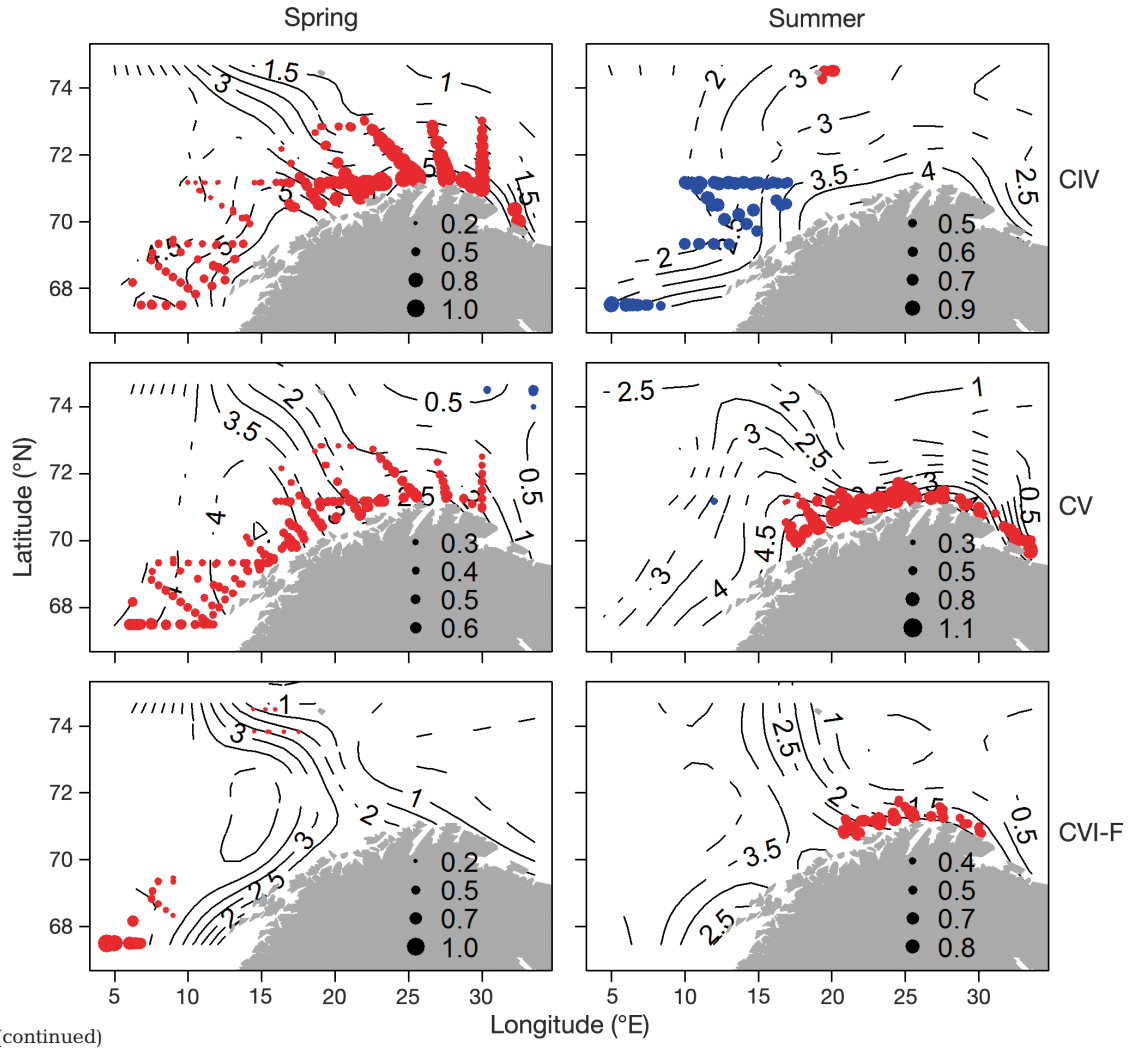

Fig. 7 (continued)

(3) *Spatially and temporally varying temperature effect.* The seasonal difference in the temperature association for younger copepodite stages indicated an effect on phenology rather than on total abundances only. To further explore this hypothesis, we formulated a model where the response to temperature could vary smoothly both with position and day-of-year (Eq. 6 in Table 1). Model predictions for a warmer-than-average and a colder-than-average scenario indicated earlier abundance peaks in the warmer-than-average scenario for nauplii and CI–CIII (Fig. 8), but not all combinations of stage and location showed significant differences between the 2 scenarios. For stages CIV and CV, temperature generally seemed to determine abundances rather than seasonal timing (except perhaps CIV in Location 1), but the differences were only significant for Location 2. Abundances of CVI-F did not differ significantly between the scenarios.

Model comparison

The different models (Eqs. 1–6 in Table 1) were compared by their GCV and R^2 values (Table 2, see Supplement 2 for details). In comparison to a null model without a temperature effect (Eq. 1), model predictive power improved for stage CV when adding a simple additive temperature term (Eq. 3), and for nauplii and copepodite stages CI–CIV when allowing for a differing temperature association in spring and summer (Eq. 4). A spatially varying coefficient model (Eq. 5) explained more of the data variation compared to the simpler models for all stages, and improved model predictive power for CII and CIII. For nauplii, CI, CIV–CV and CVI-F, the GCV values indicated that this model was over-parameterised. Allowing for a spatially and temporally varying temperature effect (Eq. 6) improved model predictive power for nauplii and stages CI–CIV when compared to a corresponding null model without temperature (Eq. 2).

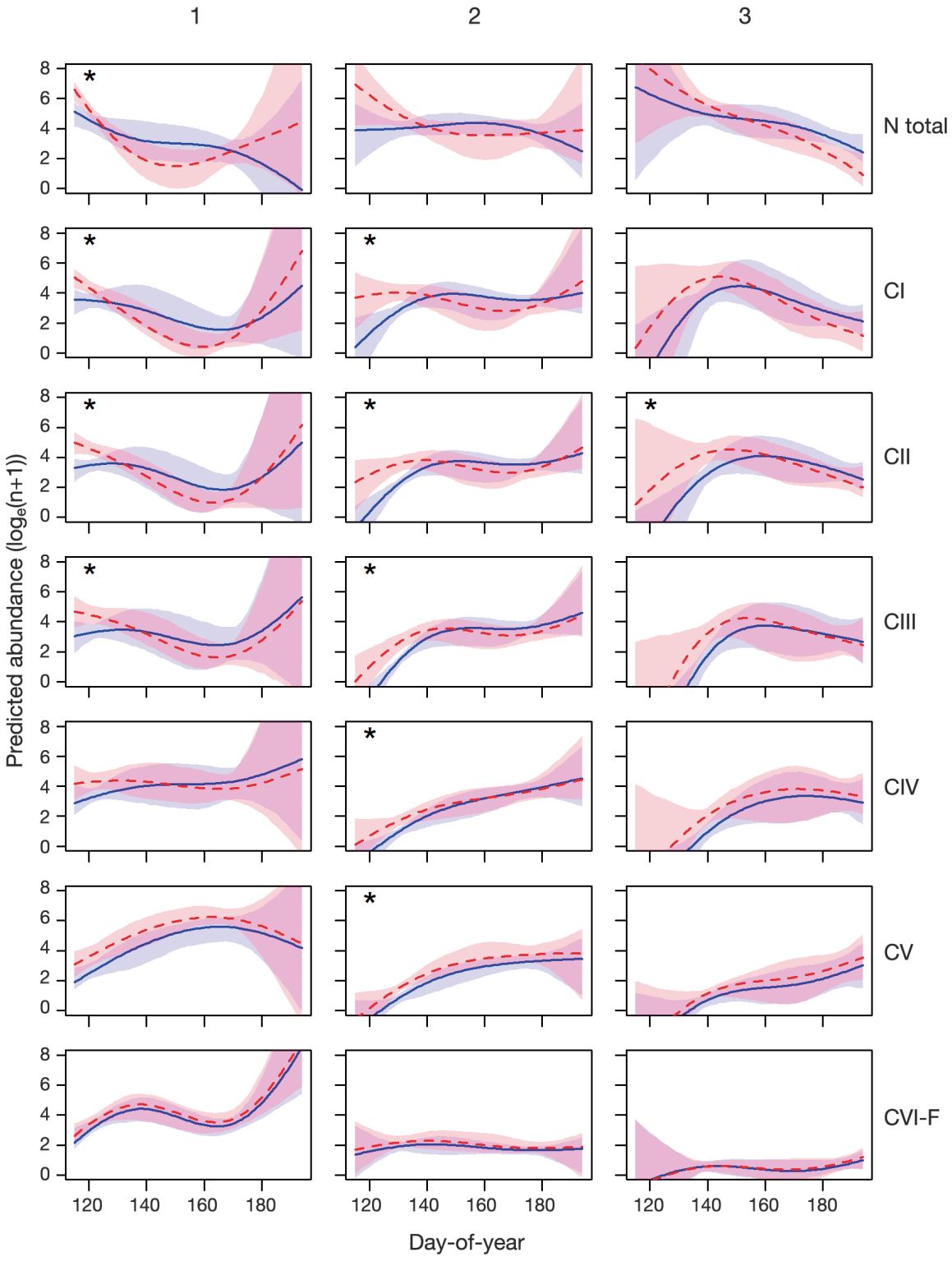

Fig. 8. Predicted abundances of *Calanus finmarchicus* developmental stages ($\log_e$[n+1]) under warm (red dashed line) and cold (blue solid line) temperature scenarios (Eq. 6 in Table 1) for 3 selected locations (see Fig. 4). Significant differences between the temperature scenarios (periods of non-overlapping confidence intervals) are marked with a star. Shaded areas: 95% confidence intervals from bootstrap procedure. N total: total nauplii abundance, CI–CVI: stage-specific copepodite abundances; F: female

Table 2. R^2 and genuine cross-validation (GCV) for different models of the temperature effect on *Calanus finmarchicus* stage-specific abundances, compared to null models without the temperature effect included. Two different null models were formulated, one without interactions (Eq. 1, left side of the table) and one with interaction between position and day (Eq. 2, right side of the table). For each of the 2 sets of models, the highest R^2 and lowest GCV scores are highlighted in **bold**. The numbers in the model name correspond to the equation number (see Table 1 and details in Supplement 1 at www.int-res.com/articles/suppl/m517p085_supp.pdf). Note that for the comparison, models were only fitted for data from the upper water layer, not including the effect of sampling depth. Add.: additive, N total: total nauplii abundance, CI–CVI: stage-specific copepodite abundances; F: female

Stage	Without interactions								Interaction between position and day			
	Null model (1)		Simple Add. (3)		Seasonal (4)		Spatial (5)		Null model (2)		Spatial by day (6)	
	R^2	GCV	R^2	GCV	R^2	GCV	R^2	GCV	R^2	GCV	R^2	GCV
N total	0.328	1.965	0.329	1.973	**0.349**	**1.947**	**0.349**	1.959	0.328	1.945	**0.354**	**1.941**
CI	0.357	1.785	0.357	1.795	0.384	**1.756**	**0.386**	1.764	0.352	1.789	**0.381**	**1.784**
CII	0.316	1.699	0.318	1.701	0.348	1.662	**0.353**	**1.660**	0.309	1.709	**0.342**	**1.700**
CIII	0.263	1.746	0.266	1.748	0.296	1.720	**0.302**	**1.715**	0.250	1.760	**0.282**	**1.748**
CIV	0.270	1.773	0.273	1.773	0.285	**1.765**	**0.290**	1.766	0.249	1.794	**0.267**	**1.793**
CV	0.439	1.629	0.447	**1.624**	0.449	1.629	**0.453**	1.648	0.413	**1.645**	**0.428**	**1.645**
CVI-F	0.537	**1.292**	**0.539**	1.294	**0.539**	1.297	**0.540**	1.304	0.517	**1.299**	**0.522**	1.303

DISCUSSION

We analysed data on *Calanus finmarchicus* abundances in the northeastern Norwegian Sea and southwestern Barents Sea from a recently digitised dataset. The long time-span, biannual sampling regime and high spatial resolution of the data enabled us to explore both temporal (year-to-year and seasonal) and spatial variation of stage-specific *C. finmarchicus* abundances. Furthermore, by extracting local temperature estimates from a numerical ocean model hindcast archive, we could analyse associations between local temperature anomalies and abundances. According to our results, abundances of copepodite stages CI–CIII in the northeastern Norwegian Sea and southwestern Barents Sea generally peaked, respectively, early in spring or around the transition between spring and summer (Fig. 4), and were positively correlated with increased temperatures in spring, with the opposite association in summer. Similar associations were identified when correlating abundances with regional temperature observations (Table S2 in Supplement 3) and local temperature anomalies (Fig. 6). Our results further indicated that abundances of stages CIV–CV peaked in summer or possibly after the summer survey (Fig. 4), and were positively associated with temperature in spring, with a weaker association in summer (negative for CIV, positive for CV). The temperature associations were present across a large area for young copepodite stages (Fig. 7), with positive associations in spring in areas with generally higher copepodite abundances off the Norwegian coast and in the southwestern Barents Sea (Fig. 5). In summer, negative associations were primarily confined to the southern parts of the surveyed area, and were less pronounced in Barents Sea areas with generally higher copepodite concentrations in summer.

We found few indications of differing temperature effects with depth (Fig. S3 in Supplement 3), which would be expected if temperature variation influenced vertical distribution rather than total abundances. On the other hand, the results indicated a temperature effect on phenology, particularly affecting the seasonal timing of young copepodite stages. The observed temperature associations can be related to (1) direct physiological effects of temperature or (2) indirect effects of temperature through other environmental factors. We will discuss these 2 alternatives in the following sections.

Direct effects of temperature

Carbon-specific growth rates are known to be higher and more temperature-sensitive for stages CI–CIV than CV (Eiane & Tande 2009), and laboratory experiments have shown that development time from eggs to CV decreases with increased temperatures (Tande 1988a, Pedersen & Tande 1992, Campbell et al. 2001). Faster development could explain the observed association between temperature and abundances of young stages (positive in spring and negative in summer), as a higher proportion of the population would have developed into older stages by the end of May during warm years. The spatial distribution of the temperature associations for

young stages (Fig. 7) could also reflect a temperature effect on growth rates, where increased temperatures speed up the regular northward shift in copepodite production from spring to summer, increasing copepodite abundances in the northeastern Norwegian Sea areas in spring, but reducing abundances in the same areas in summer. Furthermore, increased temperatures have been associated with earlier spawning (Ellertsen et al. 1987, Orlova et al. 2010) and increased egg production (Hirche et al. 1997), additional factors that could lead to both earlier appearance and increased abundances of young copepodite stages. In a previous investigation of the Russian survey data on total biomass of *C. finmarchicus*, Nesterova (1990) noted more year-to-year variation in spring than summer biomass, which was hypothesised to depend on the timing of *C. finmarchicus* spawning. During cold years, spawning occurs later (end of April) and biomass remains low for a long period, with the opposite situation for warmer years.

Temperature might also affect survival from one copepodite stage to the next. A laboratory study showed increased copepodite mortality at lower temperature (Tande 1988a), and the author suggested that in cold regions, a certain temperature increase during the growth season might be necessary for successful development from copepodite stage CI to stages CIV and CV (see also Pedersen & Tande 1992). Generally, a temperature increase reduces stage duration and thus the time to be preyed upon, so the chance of surviving to the next stage should increase, even if temperature does not affect mortality rates per se. However, contrasting results were found in a field study in the Northwest Atlantic (Plourde et al. 2009), where *C. finmarchicus* mortality was positively linked to temperature.

For older stages, a positive temperature association in spring would be expected if an earlier abundance peak of young stages with increased temperatures propagates into an earlier (spring) peak of older stages. Additionally, if egg production increases (Hirche et al. 1997), or a higher proportion of young copepodite stages survives (Tande 1988a, Pedersen & Tande 1992) with increased temperatures, we would expect higher abundances of older stages in both spring and summer. The results from a model with a spatiotemporally varying temperature effect (Eq. 6, Table 1) seemed to support this hypothesis, and indicated that abundances of young stages peak earlier during warmer years, while for older copepodite stages temperature apparently affects amplitude rather than timing (Fig. 8).

Indirect effects of temperature

Associations between temperature and *C. finmarchicus* abundance might result from direct physiological effects on spawning, growth and survival as discussed above. But other factors associated with temperature variation influence *C. finmarchicus* dynamics, such as food availability (primary productivity; e.g. Hirche et al. 1997, Melle & Skjoldal 1998, Head et al. 2000, Campbell et al. 2001) and inflow of Atlantic water masses bringing both zooplankton and warmer water from the Norwegian Sea to the Barents Sea (Helle & Pennington 1999, Dalpadado et al. 2003, Edvardsen et al. 2003b).

Models and ocean satellite data have suggested that during a warming period in the Barents Sea between 1998 and 2006, the spring bloom started progressively earlier (Johannesen et al. 2012, Harrison et al. 2013). While no routinely collected ocean colour data from the Barents Sea are available prior to 1998, it is likely that warmer periods were accompanied by earlier spring blooms also in the past. *In situ* studies on both sides of the North Atlantic have found positive associations between *C. finmarchicus* egg production and food availability (levels of chl *a*), but not with temperature, indicating that the main link between temperature and *C. finmarchicus* production is through the spring bloom (Gislason 2005, Runge et al. 2006, Head et al. 2013a,b). However, laboratory experiments have found that *C. finmarchicus* egg production increases with a combination of both temperature and food (Plourde & Runge 1993, Hirche et al. 1997, Campbell et al. 2001). Without available information on food availability, we cannot determine whether the associations between temperature and *C. finmarchicus* abundance detected in the present study are due to direct physiological effects, or to temperature effects on primary production. The same holds for other field studies relating increased temperatures to earlier spawning (Ellertsen et al. 1987, Nesterova 1990, Orlova et al. 2010) or increased egg production (Hirche et al. 1997) without considering the role of the spring bloom.

In advective systems such as the Norwegian and Barents Seas, water transport can also influence temperature associations in *C. finmarchicus* dynamics. Atlantic water inflow into the Barents Sea both brings zooplankton from the Norwegian Sea and warmer water potentially improving the growth conditions (Helle & Pennington 1999, Dalpadado et al. 2003). Therefore, the effects of temperature and advection on *C. finmarchicus* dynamics in the Bar-

ents Sea are profoundly linked. Specifically, increased advection of Atlantic water can (1) create more favourable temperature conditions in the Barents Sea, (2) increase the inflow of spawning females from the Norwegian Sea, potentially producing more eggs due to favourable temperature and food conditions in the past, and (3) trigger an earlier spring bloom by increasing Barents Sea temperatures. The positive associations observed between temperature and abundances of adult females in the present study might thus be explained by increased advection from upstream areas. Similarly, the observed temperature associations of both abundances and timing of nauplii and young copepodite stages could be due to (1) increased inflow of warmer water creating favourable growth conditions, (2) the effect of advection on abundances of spawning females and egg production and (3) the effect of advection on spring bloom dynamics potentially improving food availability.

However, while advection certainly is important in Barents Sea areas where Atlantic water inflow is believed to be an essential regulator of zooplankton biomass (Helle & Pennington 1999, Dalpadado et al. 2003, Edvardsen et al. 2003a), we also identified temperature associations in Norwegian Sea off-shelf areas considered as sources of *C. finmarchicus* to the Norwegian and Barents Sea shelves (Slagstad & Tande 1996, 2007, Halvorsen et al. 2003, Edvardsen et al. 2006). The presence of a seasonally differing temperature association (Fig. 7) and predicted earlier abundance peak with increased temperature (Fig. 8) in these areas supports the presence of a temperature effect on the phenology of young stages of *C. finmarchicus*.

In summary, it is difficult to disentangle the true mechanisms behind the temperature associations observed in this study, but it is likely that both advection and spring bloom dynamics are essential driving factors. Importantly, our results indicate the presence of temperature associations that differ between developmental stages, seasons and areas. Further studies should consider the importance of resolution when assessing the combined effects of temperature and other variables such as primary production and advection. Similar conclusions were drawn by Persson et al. (2012), who identified temperature associations in *C. glacialis* biomass in the White Sea only when data were finely resolved in time and developmental stages. Similarly to the present study, a positive correlation was found between spring temperatures and young stages (nauplii and CI–CIII), with an earlier peak of these stages during warmer years. A following decline of young stages later in summer was not observed, but older stages disappeared earlier in autumn during warm years, possibly due to a migration into 'cold-water refuges' in deeper water. No indications of a temperature effect on vertical distribution of *C. finmarchicus* were found in the present study, but the Arctic species *C. glacialis* in the White Sea is likely more sensitive to higher-than-average temperatures than the subarctic *C. finmarchicus*, which in the northern Norwegian Sea and Barents Sea is in the northern range of its distribution (Conover 1988, Hirche & Kosobokova 2007).

CONCLUSIONS

Temperature is considered one of the major factors shaping marine zooplankton dynamics (Edwards & Richardson 2004, Richardson 2008). While some studies have shown a positive association between year-to-year variation in zooplankton biomass and temperature along the Kola section (Antipova et al. 1974, Degtereva 1979), other studies have not identified a clear link between temperature and *C. finmarchicus* abundance or biomass in the Barents Sea (Tande et al. 2000, Stige et al. 2009, Dalpadado et al. 2012, Johannesen et al. 2012). The results from the present study indicate that this might be related to the coarse spatiotemporal resolution and/or use of aggregated biomass data in previous studies. Climate effects on phenology are known to vary across functional groups and trophic levels (Edwards & Richardson 2004). Our results indicate that variation also exists among developmental stages of the same species, emphasising the value of detailed data in ecological climate effect studies.

Studies of temperature effects on zooplankton phenology have typically shown a pattern of 'earlier when warmer' (McGinty et al. 2011, Mackas et al. 2012). Changes in seasonal timing can have cascading impacts on the ecosystem, as formalised in the match/mismatch hypothesis (Hjort 1914, Ellertsen et al. 1989, Cushing 1990, Beaugrand et al. 2003, Durant et al. 2007). A temperature increase due to climate change, which is predicted to be particularly pronounced in Arctic regions (Stocker et al. 2014), might, according to our results, trigger an earlier peak of *C. finmarchicus* copepodites. Based on these findings, it is potentially the predators on the youngest stages of *C. finmarchicus* that are most prone to experience a mismatch with their prey in a warmer climate.

Acknowledgements. This study is a deliverable of the Nordic Centre for Research on Marine Ecosystems and Resources under Climate Change (NorMER), which is funded by the Norden Top-level Research Initiative subprogramme 'Effect Studies and Adaptation to Climate Change'. P.D. and L.C.S were supported by the Research Council of Norway (RCN) through the SVIM project (project no. 196685). We are thankful to scientists and staff at Knipovich Polar Research Institute of Marine Fisheries and Oceanography (PINRO, Murmansk) who collected, sorted and digitised the zooplankton data, and for their collaboration with the use of these data. We thank Dr. Natalia Yaragina for her contribution during the data inspection, Dr. Lorenzo Ciannelli for useful input on GAMs, Dr. Andrey Dolgov and Dr. Øystein Langangen for valuable comments on the original version of the manuscript, and 4 anonymous reviewers for their comments, which significantly improved the paper.

LITERATURE CITED

Antipova TV, Degtereva AF, Timokhina AA (1974) Multiannual changes in biomass of plankton and benthos in the Barents Sea. Materialy Rybokhozyaistvennykh Issledovanii Severnogo Basseina (Materials of Fisheries Research in the Northern Basin) 21:80–87 (in Russian)

Aure J, Østensen Ø (1993) Hydrographic normals and long-term variations in Norwegian coastal waters. Fisken Havet 6:1–75

Beaugrand G, Brander KM, Lindley JA, Souissi S, Reid PC (2003) Plankton effect on cod recruitment in the North Sea. Nature 426:661–664

Campbell RG, Wagner MM, Teegarden GJ, Boudreau CA, Durbin EG (2001) Growth and development rates of the copepod *Calanus finmarchicus* reared in the laboratory. Mar Ecol Prog Ser 221:161–183

Conover RJ (1988) Comparative life histories in the genera *Calanus* and *Neocalanus* in high latitudes of the northern hemisphere. Hydrobiologia 167-168:127–142

Cushing DH (1990) Plankton production and year-class strength in fish populations: an update of the match/mismatch hypothesis. Adv Mar Biol 26:249–293

Dale T, Kaartvedt S (2000) Diel patterns in stage-specific vertical migration of *Calanus finmarchicus* in habitats with midnight sun. ICES J Mar Sci 57:1800–1818

Dalpadado P, Ingvaldsen R, Hassel A (2003) Zooplankton biomass variation in relation to climatic conditions in the Barents Sea. Polar Biol 26:233–241

Dalpadado P, Ingvaldsen RB, Stige LC, Bogstad B, Knutsen T, Ottersen G, Ellertsen B (2012) Climate effects on Barents Sea ecosystem dynamics. ICES J Mar Sci 69: 1303–1316

Degtereva A (1973) The relationship between abundance and biomass of plankton and the temperature in the south-western part of the Barents Sea. Trudy PINRO 33: 13–23 (in Russian)

Degtereva A (1979) Regularities in plankton quantitative development in the Barents Sea. Trudy PINRO 43:22–53 (in Russian)

Degtereva A, Nesterova L, Panasenko V (1990) Forming of feeding zooplankton in the feeding grounds of capelin in the Barents Sea. In: Rass T, Drobysheva S (eds) Food resources and trophic relations of fishes in North Atlantic. PINRO Press, Murmansk, p 24–33 (in Russian)

Drobysheva SS, Nesterova VN (2005) Long-term variations in zooplankton population parameters as shown by the data collected along the Kola section. In: Ozltigin VK (ed) 100 years of oceanographic observations along the Kola Section in the Barents Sea. Papers of the international symposium. PINRO Press, Murmansk, p 77–84

Durant JM, Hjermann DØ, Ottersen G, Stenseth NC (2007) Climate and the match or mismatch between predator requirements and resource availability. Clim Res 33: 271–283

Edvardsen A, Slagstad D, Tande KS, Jaccard P (2003a) Assessing zooplankton advection in the Barents Sea using underway measurements and modelling. Fish Oceanogr 12:61–74

Edvardsen A, Tande KS, Slagstad D (2003b) The importance of advection on production of *Calanus finmarchicus* in the Atlantic part of the Barents Sea. Sarsia 88:261–273

Edvardsen A, Pedersen JM, Slagstad D, Semenova T, Timonin A (2006) Distribution of overwintering *Calanus* in the North Norwegian Sea. Ocean Sci Discuss 3:25–53

Edwards M, Richardson AJ (2004) Impact of climate change on marine pelagic phenology and trophic mismatch. Nature 430:881–884

Eiane K, Tande KS (2009) Meso and macrozooplankton. In: Sakshaug E, Johnsen G, Kovacs K (eds) Ecosystem Barents Sea. Tapir Academic Press, Trondheim, p 209–234

Ellertsen B, Fossum P, Solemdal P, Sundby S, Tilseth S (1987) The effect of biological and physical factors on the survival of Arcto-Norwegian cod and the influence on recruitment variability. In: Loeng H (ed) The effect of oceanographic conditions on distribution and population dynamics of commercial fish in the Barents Sea. Proc Third Soviet-Norwegian Symposium, Murmansk, 26-28 May 1986. Institute of Marine Research, Bergen, p 101–126

Ellertsen B, Fossum P, Solemdal P, Sundby S (1989) Relation between temperature and survival of eggs and first-feeding larvae of northeast Arctic cod (*Gadus morhua* L.). Rapp P-V Reun Cons Int Explor Mer 191:209–219

Gislason A (2005) Seasonal and spatial variability in egg production and biomass of *Calanus finmarchicus* around Iceland. Mar Ecol Prog Ser 286:177–192

Halvorsen E, Tande KS, Edvardsen A, Slagstad D, Pedersen OP (2003) Habitat selection of overwintering *Calanus finmarchicus* in the NE Norwegian Sea and shelf waters off Northern Norway in 2000–02. Fish Oceanogr 12: 339–351

Harrison WG, Børsheim KY, Li WKW, Maillet GL and others (2013) Phytoplankton production and growth regulation in the Subarctic North Atlantic: a comparative study of the Labrador Sea-Labrador/Newfoundland shelves and Barents/Norwegian/Greenland seas and shelves. Prog Oceanogr 114:26–45

Hastie T, Tibshirani R (1990) Generalized additive models. Chapman & Hall, London

Hastie T, Tibshirani R (1993) Varying-coefficient models. J R Stat Soc 55:757–796

Hastie T, Tibshirani R, Friedman J (2009) The elements of statistical learning: data mining, inference, and prediction, 2nd edn. Springer, New York, NY

Head EJH, Harris LR, Campbell RW (2000) Investigations on the ecology of *Calanus* spp. in the Labrador Sea. I. Relationship between the phytoplankton bloom and reproduction and development of *Calanus finmarchicus* in spring. Mar Ecol Prog Ser 193:53–73

Head EJH, Harris LR, Ringuette M, Campbell RW (2013a) Characteristics of egg production of the planktonic copepod, *Calanus finmarchicus*, in the Labrador Sea: 1997–2010. J Plankton Res 35:281–298

Head EJH, Melle W, Pepin P, Bagøien E, Broms C (2013b) On the ecology of *Calanus finmarchicus* in the Subarctic North Atlantic: a comparison of population dynamics and environmental conditions in areas of the Labrador Sea-Labrador/Newfoundland Shelf and Norwegian Sea Atlantic and coastal waters. Prog Oceanogr 114:46–63

Helle K, Pennington M (1999) The relation of the spatial distribution of early juvenile cod (*Gadus morhua* L.) in the Barents Sea to zooplankton density and water flux during the period 1978 – 1984. ICES J Mar Sci 56:15–27

Hernroth L (1987) Sampling and filtration efficiency of two commonly used plankton nets: a comparative study of the Nansen net and the Unesco WP 2 net. J Plankton Res 9:719–728

Hirche HJ, Kosobokova K (2007) Distribution of *Calanus finmarchicus* in the northern North Atlantic and Arctic Ocean — expatriation and potential colonization. Deep-Sea Res II 54:2729–2747

Hirche HJ, Meyer U, Niehoff B (1997) Egg production of *Calanus finmarchicus*: effect of temperature, food and season. Mar Biol 127:609–620

Hjort J (1914) Fluctuations in the great fisheries of northern Europe viewed in the light of biological research. Rapp P-V Reun Cons Int Explor Mer 20:1–228

Hoegh-Guldberg O, Bruno JF (2010) The impact of climate change on the world's marine ecosystems. Science 328: 1523–1528

Johannesen E, Ingvaldsen RB, Bogstad B, Dalpadado P and others (2012) Changes in Barents Sea ecosystem state, 1970-2009: climate fluctuations, human impact, and trophic interactions. ICES J Mar Sci 69:880–889

Karamushko O, Karamushko L (1995) Feeding and bioenergetics of the main commercial fish of the Barents Sea on the different stages of ontogenesis. Russian Academy of Science, Kola Science Center, Apatity

Lien VS, Gusdal Y, Albretsen J, Melsom A, Vikebø F (2013) Evaluation of a Nordic Seas 4 km numerical ocean model hindcast archive (SVIM), 1960–2011. Fisken Havet 7: 1–80

Loeng H, Drinkwater K (2007) An overview of the ecosystems of the Barents and Norwegian Seas and their response to climate variability. Deep-Sea Res II 54: 2478–2500

Mackas DL, Greve W, Edwards M, Chiba S and others (2012) Changing zooplankton seasonality in a changing ocean: comparing time series of zooplankton phenology. Prog Oceanogr 97-100:31–62

Manteufel BP (1941) Plankton and herring in the Barents Sea. Trudy PINRO 7:125–218 (in Russian)

McGinty N, Power AM, Johnson MP (2011) Variation among northeast Atlantic regions in the responses of zooplankton to climate change: Not all areas follow the same path. J Exp Mar Biol Ecol 400:120–131

Melle W, Skjoldal HR (1998) Reproduction and development of *Calanus finmarchicus, C. glacialis* and *C. hyperboreus* in the Barents Sea. Mar Ecol Prog Ser 169:211–228

Melle W, Ellertsen B, Skjoldal HR (2004) Zooplankton: the link to higher trophic levels. In: Skjoldal HR (ed) The Norwegian Sea ecosystem. Tapir Academic Press, Trondheim, p 137–202

Nesterova VN (1990) Plankton biomass along the drift route of cod larvae (reference material). PINRO, Murmansk (in Russian)

Nichols JH, Thompson AB (1991) Mesh selection of copepodite and nauplius stages of four calanoid copepod species. J Plankton Res 13:661–671

Orlova EL, Boitsov VD, Nesterova VN (2010) The influence of hydrographic conditions on the structure and functioning of the trophic complex plankton–pelagic fishes–cod. Knipovich Polar Research Institute of Marine Fisheries and Oceanography (PINRO), Murmansk

Pedersen G, Tande KS (1992) Physiological plasticity to temperature in *Calanus finmarchicus*. Reality or artefact? J Exp Mar Biol Ecol 155:183–197

Persson J, Stige LC, Stenseth NC, Usov N, Martynova D (2012) Scale-dependent effects of climate on two copepod species, *Calanus glacialis* and *Pseudocalanus minutus*, in an Arctic-boreal sea. Mar Ecol Prog Ser 468:71–83

Plourde S, Runge JA (1993) Reproduction of the planktonic copepod *Calanus finmarchicus* in the Lower St. Lawrence Estuary: relation to the cycle of phytoplankton production and evidence for a *Calanus* pump. Mar Ecol Prog Ser 102:217–227

Plourde S, Pepin P, Head EJH (2009) Long-term seasonal and spatial patterns in mortality and survival of *Calanus finmarchicus* across the Atlantic Zone Monitoring Programme region, Northwest Atlantic. ICES J Mar Sci 66: 1942–1958

Pörtner HO, Karl D, Boyd PW, Cheung W and others (2014) Ocean systems. In: Field CB, Barros VR, Dokken DJ, Mach KJ and others (eds) Climate change 2014: impacts, adaptation, and vulnerability. Part A: global and sectoral aspects. Contribution of Working Group II to the Fifth Assessment Report of the Intergovernmental Panel on Climate Change. Cambridge University Press, Cambridge, p 411–484

Pyper BJ, Peterman RM (1998) Comparison of methods to account for autocorrelation in correlation analyses of fish data. Can J Fish Aquat Sci 55:2127–2140

Quenouille MH (1952) Associated measurements. Butterworth, London

R Development Core Team (2014) R: a language and environment for statistical computing. R Foundation for Statistical Computing, Vienna. Available at www.r-project.org/

Richardson AJ (2008) In hot water: zooplankton and climate change. ICES J Mar Sci 65:279–295

Runge JA, Plourde S, Joly P, Niehoff B, Durbin E (2006) Characteristics of egg production of the planktonic copepod, *Calanus finmarchicus*, on Georges Bank: 1994–1999. Deep-Sea Res II 53:2618–2631

Sakshaug E, Johnsen G, Kovacs K (eds) (2009) Ecosystem Barents Sea. Tapir Academic Press, Trondheim

Slagstad D, Tande KS (1996) The importance of seasonal vertical migration in across shelf transport of *Calanus finmarchicus.* Ophelia 44:189–205

Slagstad D, Tande KS (2007) Structure and resilience of overwintering habitats of *Calanus finmarchicus* in the Eastern Norwegian Sea. Deep-Sea Res II 54:2702–2715

Stige LC, Lajus DL, Chan KS, Dalpadado P, Basedow S, Berchenko I, Stenseth NC (2009) Climatic forcing of zooplankton dynamics is stronger during low densities of planktivorous fish. Limnol Oceanogr 54:1025–1036

Stige LC, Dalpadado P, Orlova E, Boulay AC, Durant JM, Ottersen G, Stenseth NC (2014) Spatiotemporal statistical analyses reveal predator-driven zooplankton fluctua-

tions in the Barents Sea. Prog Oceanogr 120:243–253
Stocker TF, Qin D, Plattner GK, Tignor M and others (eds) (2014) Climate change 2013: the physical science basis. Contribution of Working Group I to the Fifth Assessment Report of the Intergovernmental Panel on Climate Change. Cambridge University Press, Cambridge
Tande KS (1988a) Aspects of developmental and mortality rates in *Calanus finmarchicus* related to equiproportional development. Mar Ecol Prog Ser 44:51–58
Tande KS (1988b) An evaluation of factors affecting vertical distribution among recruits of *Calanus finmarchicus* in three adjacent high-latitude localities. Hydrobiologia 167-168:115–126
Tande K, Drobysheva S, Nesterova V, Nilssen EM, Edvardsen A, Tereschenko V (2000) Patterns in the variations of copepod spring and summer abundance in the north-eastern Norwegian Sea and the Barents Sea in cold and warm years during the 1980s and 1990s. ICES J Mar Sci 57:1581–1591
Tereshchenko VV (1996) Seasonal and year-to-year variations of temperature and salinity along the Kola meridian transect. ICES CM 1996/C:11. ICES, Copenhagen
Wood SN (2006) Generalized additive models: an introduction with R. Chapman & Hall/CRC, Boca Raton, FL
Wood SN (2013) mgcv: GAMs with GCV smoothness estimation and GAMMs by REML/ PQL. R package. Version 1.7–24. http://lojze.lugos.si/~darja/software/r/library/mgcv/html/mgcv-package.html
Zuur A, Ieno E, Smith G (2007) Analysing ecological data. Springer Press, New York, NY

Editorial responsibility: Alejandro Gallego, Aberdeen, UK

Submitted: April 11, 2014; Accepted: August 30, 2014
Proofs received from author(s): November 21, 2014

The following supplements accompany the article

Temperature effects on *Calanus finmarchicus* vary in space, time and between developmental stages

Kristina Øie Kvile[1,*], Padmini Dalpadado[2], Emma Orlova[3,†], Nils C. Stenseth[1], Leif C. Stige[1]

[1]**Centre for Ecological and Evolutionary Synthesis (CEES), Department of Biosciences, University of Oslo, PO Box 1066 Blindern, 0316 Oslo, Norway**

[2]**Institute of Marine Research, PO Box 1870 Nordnes, 5817 Bergen, Norway**

[3]**Knipovich Polar Research Institute of Marine Fisheries and Oceanography, Knipovich-St. 6, 183763 Murmansk, Russia**

*Corresponding author: k.o.kvile@ibv.uio.no

Marine Ecology Progress Series 517: 85–104 (2014)

Supplement 1. Supplementary modelling material

Further background on generalised additive models (GAMs) can be found in Hastie & Tibshirani (1990) and Wood (2006). Note that the smooth terms are constrained to have a mean of 0 in order for the model to be identifiable (Wood 2006). Random effects are treated as smooths by setting 'bs = re' when specifying the smooth in the mgcv library (Wood 2013). Smooth functions varying with a linear or factor variable are implemented using the 'by' operator within the smooth function in the mgcv library. We used a tensor product (setting 'te' instead of 's' when formulating the GAMs in the mgcv library) for the effect of geographical position because the isotropy in longitude and latitude measurements is reduced when we approach the poles.

Equations described in the main text (Eqs. 1-6 in Table 1)

Eq. (1): Spatial, seasonal and vertical variation

$$Z_{l,t,d} = \beta + s_1(j_t) + s_2(d_d) + te(x_l,y_l)l_f + s_3(Y) + \varepsilon_{l,t,d}$$

$Z_{l,t,d}$ is stage-specific abundance ($\log_e$ [n+1]) at location l, time t and depth d; β is the intercept; $s_1(j_t)$ and $s_2(d_d)$ are 1-dimensional smooth functions of, respectively, day-of-year and average sampling depth (cubic regression splines with maximally 3 degrees of freedom [df]); $te(x_l,y_l)$ is a 2-dimensional tensor product of longitude and latitude representing the effect of position (thin-plate regression splines with maximally 6 df each); l_f is an indicator variable of season (spring or summer) multiplied with the tensor product of longitude and latitude; $s_3(Y)$ is a random effect of year added to capture year-to-year variation not explained by seasonal or spatial variation; and $\varepsilon_{l,t,d}$ is a random error term.

Eq. (2): Interaction between position and day-of-year

$$Z_{l,t} = \beta + te(x_l,y_l,j_t) + \varepsilon_{l,t}$$

$Z_{l,t}$, β and $\varepsilon_{l,t}$ correspond to similar terms in Eq. (1), while $te(x_l,y_l,j_t)$ is an interaction term between position and day-of-year, formulated as a tensor product of a 2-dimensional smooth function of longitude and latitude (thin-plate regression spline with maximally 7 df) and a 1-dimensional smooth function of day-of-year (cubic regression spline with maximally 3 df). The position term (longitude and latitude) was formulated here as a 2-dimensional smooth (instead of 2 separate smooths) to avoid over-parameterisation of the model. We investigated the model for samples from the upper water layer only to facilitate comparison with the more complex temperature model (Eq. 6 in Table 1 of the main text), and to isolate seasonal variation in the upper waters from seasonal vertical migration.

Eq. (3): Temperature effect varying between stages

$$Z_{l,t,d} = \beta + s_1(j_t) + s_2(d_d) + te(x_l,y_l)l_f + s_3(T_{l,t,d}) + \varepsilon_{l,t,d}$$

$Z_{l,t,d}$, β, $s_1(j_t)$, $s_2(d_d)$, $te(x_l,y_l)l_f$ and $\varepsilon_{l,t,d}$ correspond to the first part of Eq. (1) and form the null-model core of the model formulation. $s_3(T_{l,t,d})$ is a 1-dimensional smooth function of local temperature anomaly (cubic regression spline with maximally 3 df).

Eq. (4): Seasonally varying temperature effect

$$Z_{l,t,d} = \beta + s_1(j_t) + s_2(d_d) + te(x_l,y_l)l_f + s_3(T_{l,t,d})l_f + \varepsilon_{l,t,d}$$

$Z_{l,t,d}$, β, $s_1(j_t)$, $s_2(d_d)$, $te(x_l,y_l)l_f$, $s_3(T_{l,t,d})$ and $\varepsilon_{l,t,d}$ correspond to similar terms in Eq. (3). l_f is an indicator variable of season (spring or summer) that is multiplied with the smooth function of local temperature anomaly ($s_3(T_{l,t,d})$).

Eq. (5) Spatially varying temperature effect

$$Z_{l,t} = \beta + s_1(j_t) + te_1(x_l,y_l)l_f + te_2(x_l,y_l)l_fT_{l,t} + \varepsilon_{l,t}$$

$Z_{l,t}$, β, $s_1(j_t)$, $te_1(x_l,y_l)l_f$ and $\varepsilon_{l,t}$ correspond to the first part of Eq. (1) and form the null-model core of the model formulation, but as the model is formulated for samples from the upper depth layer only, the smooth function of depth is removed. $te_2(x_l,y_l)l_fT_{l,t}$ is a 2-dimensional tensor product smooth of longitude and latitude (thin-plate regression splines with maximally 3 df each) that is multiplied with a factor variable of season (l_f) and with a linear temperature term ($T_{l,t}$).

Eq. (6): Spatially and temporally varying temperature effect

$$Z_{l,t} = \beta + te_1(x_l,y_l,j_t) + te_2(x_l,y_l,j_t)T_{l,t} + \varepsilon_{l,t}$$

$Z_{l,t}$, β, $te_1(x_l,y_l,j_t)l_f$ and $\varepsilon_{l,t}$ correspond to the first part of Eq. (2) and constitute the null-model core of the model formulation. $te_2(x_l,y_l,j_t)$ is a tensor product of a 2-dimensional smooth function of longitude and latitude (thin-plate spline with maximally 3 df) and a 1-dimensional smooth function of day-of-year (cubic regression spline with maximally 2 df). This second interaction term is multiplied by a linear term of temperature anomaly, $T_{l,t}$. The null-model base of the model formulation was changed compared to the previous model formulations (Eqs. 3–5) to assess whether adding a linear temperature term varying smoothly with position and day-of-year to a model already capturing the interaction between the variables would improve the model's predictive power. The degrees of freedom in the second interaction term had to be reduced to avoid over-parameterisation of the model.

Additional equations (Eqs. S1–S4)

Eq. (S1): Estimation of local temperature anomalies

$$T_{l,t,d} = \beta + te(x_l,y_l) + s(j_t)l_d + d_d + \varepsilon_{l,t,d}$$

$T_{l,t,d}$ is a local temperature estimate extracted from a numerical ocean model hindcast archive (Lien et al. 2013) at location l, time t and depth d (see main text for details); β is the intercept; $te(x_l,y_l)$ is a 2-dimensional tensor product of longitude and latitude (natural cubic regression splines with maximally 4 df each); $s(j_t)$ is a 1-dimensional smooth function of day of year (cubic regression spline with maximally 4 df), multiplied by l_d, a factor variable of depth layer (upper, middle or lower); d_d is a factor variable of depth layer (upper, middle or lower); and $\varepsilon_{l,t,d}$ is a random error term.

Eq. (S2): Indices of annual spring and summer stage-specific abundances

$$Z_{l,t,d} = f(Y) + s_1(j_t) + s_2(d_d) + te(x_l,y_l) + \varepsilon_{l,t,d}$$

Indices were constructed by extracting year-specific intercepts from the model, formulated separately for spring and summer samples. $Z_{l,t,d}$ is stage-specific abundance ($\log_e$ [n+1]) at location l, time t and depth d; $f(Y)$ is a year-specific intercept; $s_1(j_t)$ and $s_2(d_d)$ are 1-dimensional smooth functions of, respectively, day-of-year and average sampling depth (cubic regression splines with maximally 3 df); $te(x_l,y_l)$ is a 2-dimensional tensor product of longitude and latitude (thin-plate regression splines with maximally 6 df each); and $\varepsilon_{l,t,d}$ is a random error term.

Eq. (S3): Seasonally varying depth effect

$$Z_{l,t,d} = \beta + s_1(j_t) + s_2(d_d)l_f + te(x_l,y_l)l_f + s_3(Y) + \varepsilon_{l,t,d}$$

$Z_{l,t,d}$, β, $s_1(j_t)$, $s_2(d_d)$, $te(x_l,y_l)l_f$, $s_3(Y)$ and $\varepsilon_{l,t,d}$ correspond to similar terms in Eq. (1). l_f is an indicator variable of season (spring or summer) multiplied with the smooth function of depth.

Eq. (S4): Seasonally and vertically varying temperature effect

$$Z_{l,t,d} = \beta + s_1(j_t) + s_2(d_d) + te(x_l,y_l)l_f + s_3(T_{l,t,d})l_{f,d} + \varepsilon_{l,t,d}$$

$Z_{l,t,d}$, β, $s_1(j_t)$, $s_2(d_d)$, $te(x_l,y_l)l_f$, $s_3(T_{l,t,d})$ and $\varepsilon_{l,t,d}$ correspond to similar terms in Eq. (3). $l_{f,d}$ is an indicator variable of both season (spring or summer) and depth (upper, middle or lower) that is multiplied with the smooth function of local temperature anomaly ($s_3(T_{l,t,d})$). The temperature term is thus allowed to vary between all combinations of season and depth layer.

LITERATURE CITED

Hastie T, Tibshirani R (1990) Generalized additive models. Chapman & Hall, London

Lien VS, Gusdal Y, Albretsen J, Melsom A, Vikebø F (2013) Evaluation of a Nordic Seas 4 km numerical ocean model hindcast archive (SVIM), 1960-2011. Fisken Havet 7:1–80

Wood SN (2006) Generalized additive models: an introduction with R. Chapman & Hall/CRC, Boca Raton, FL

Wood SN (2013) mgcv: GAMs with GCV smoothness estimation and GAMMs by REML/ PQL. R package. Version 1.7–24. http://lojze.lugos.si/~darja/software/r/library/mgcv/html/mgcv-package.html

Supplement 2. Genuine cross-validation and model comparison

Models were compared with genuine cross-validation (GCV) by considering year as the sampling unit. This measure was chosen as data samples were not independent in space or time within years, possibly leading to positive auto-correlation in the model residuals. Using generalised CV or AIC in model selection would in this case likely favour over-parameterised models. GCV was calculated as the mean of the mean-squared predictive error from 1000 models formulated from datasets where data from 1 randomly chosen year were removed, and the observations from the removed year were predicted from a new model based on the reduced dataset. The GCV increases with high complexity and low predictive power, and models with lower GCV values are therefore better. Significance of model terms was assessed by comparing GCV and R^2 (the proportion of data variation explained by the model) with and without the model term in question, and by plotting the model term and assessing whether the 95% bootstrap intervals of the model effect differed from 0. The number of knots (i.e. the flexibility of the model terms / degrees of freedom) in model terms were also determined by minimising the GCV, and by generally keeping model complexity within ecologically reasonable limits.

Supplement 3. Additional figures and tables

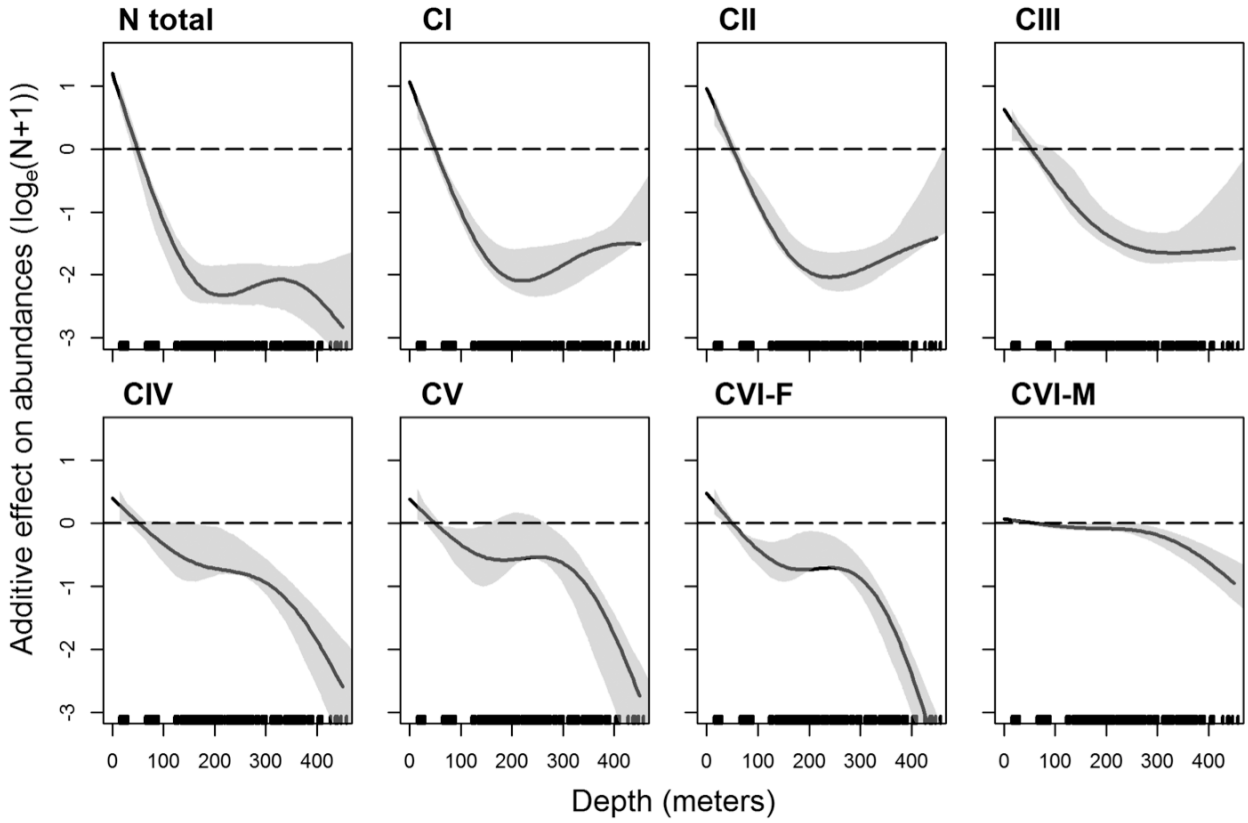

Fig. S1. Additive effect of depth on *Calanus finmarchicus* stage-specific abundances ($\log_e$[n+1]) (see Eq. 1 in Table 1 of the main text and Supplement 1). Shaded area: 95% confidence interval from bootstrap procedure. Dashed line: 0 effect isoline. N total: total nauplii abundance, CI–CVI: stage-specific copepodite abundances, F: female, M: male

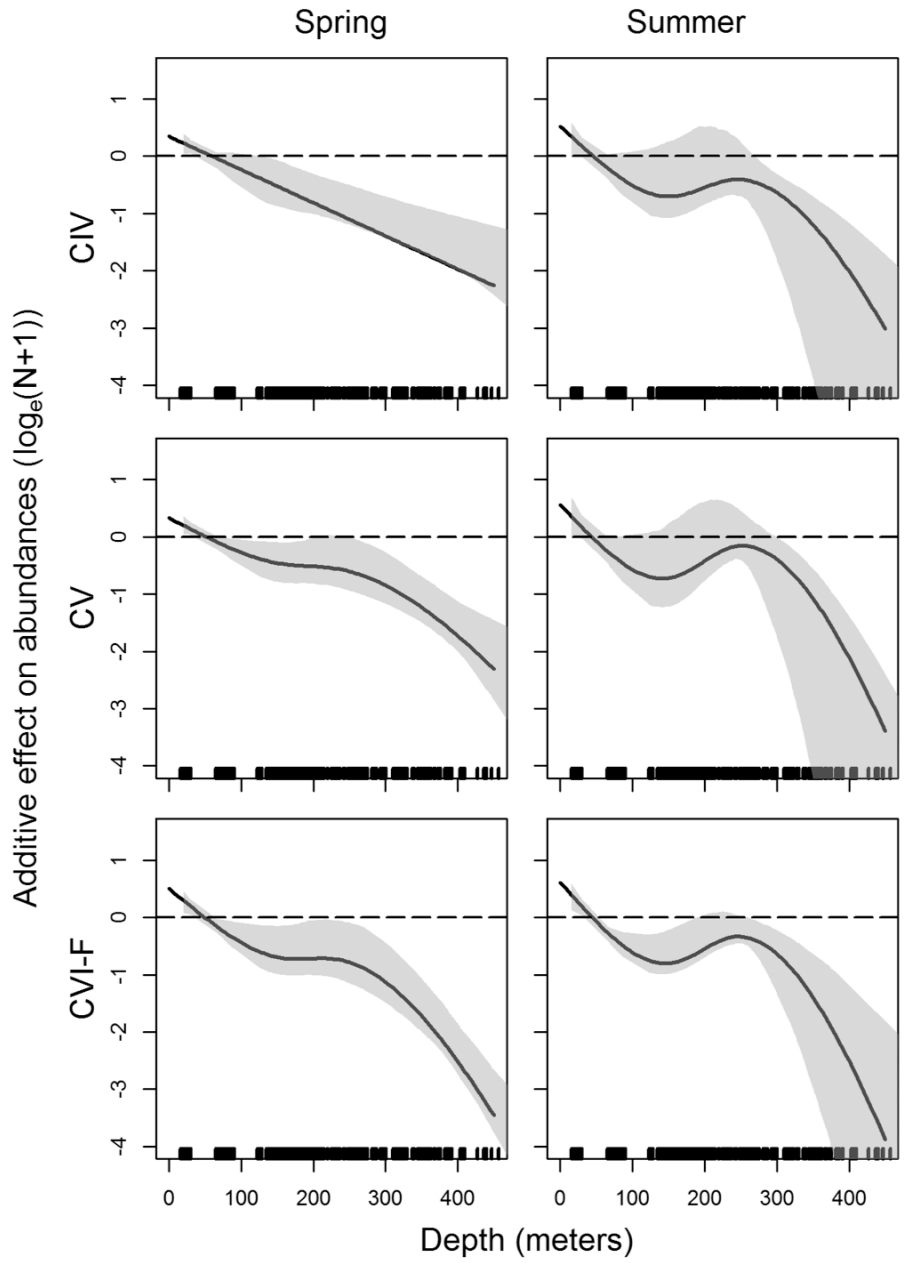

Fig. S2. Additive effect of depth on abundances ($\log_e$[n+1]) of *Calanus finmarchicus* copepodite stages CIV–CVI-F (female) in spring (left) and summer (right) (see Eq. S3 in Supplement 1). Shaded area: 95% confidence interval from bootstrap procedure. Dashed line: 0 effect isoline

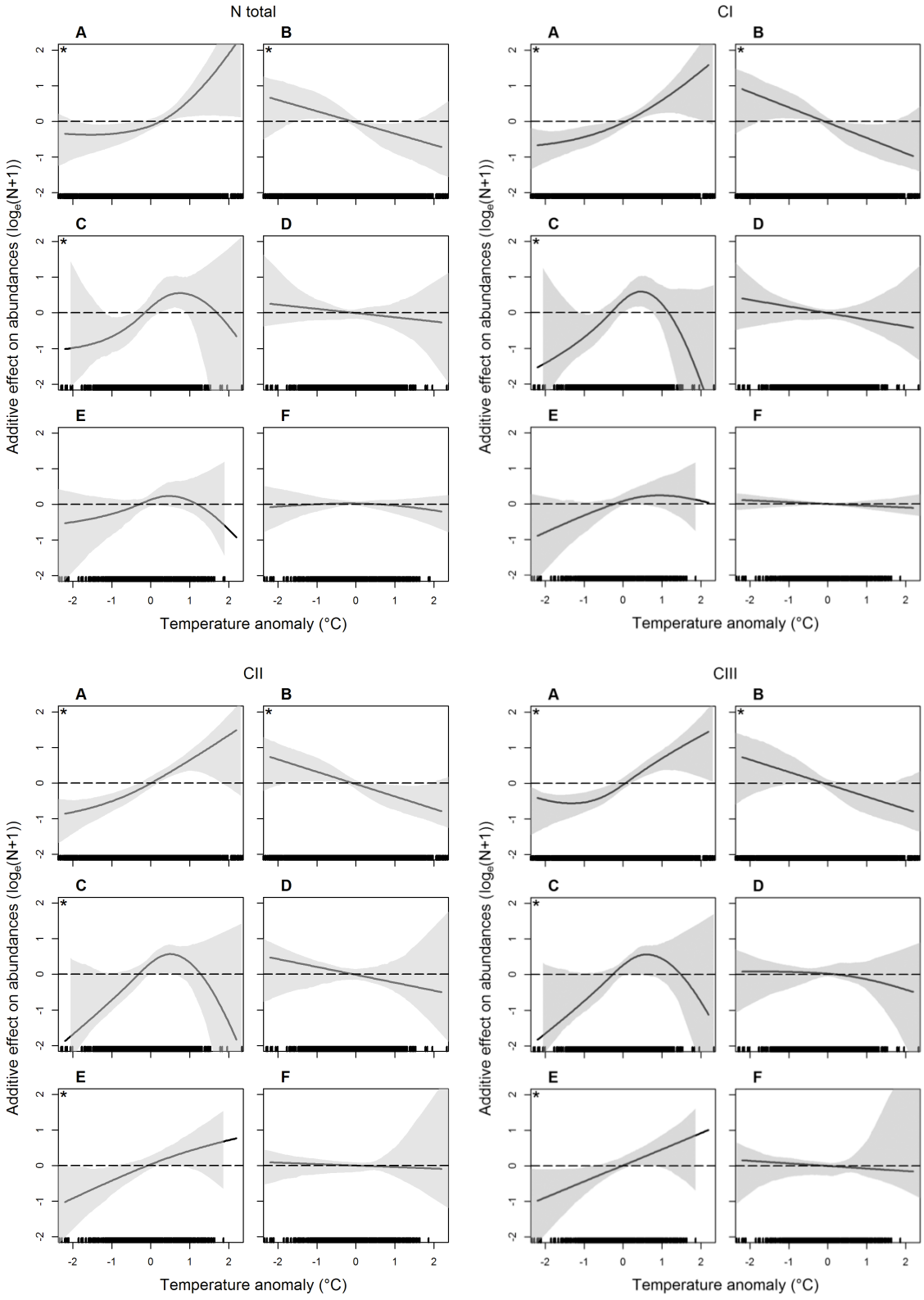
N total
CI
CII
CIII
A
B
C
D
E
F
*
Additive effect on abundances (log$_e$(N+1))
Temperature anomaly (°C)
-2
-1
0
1
2

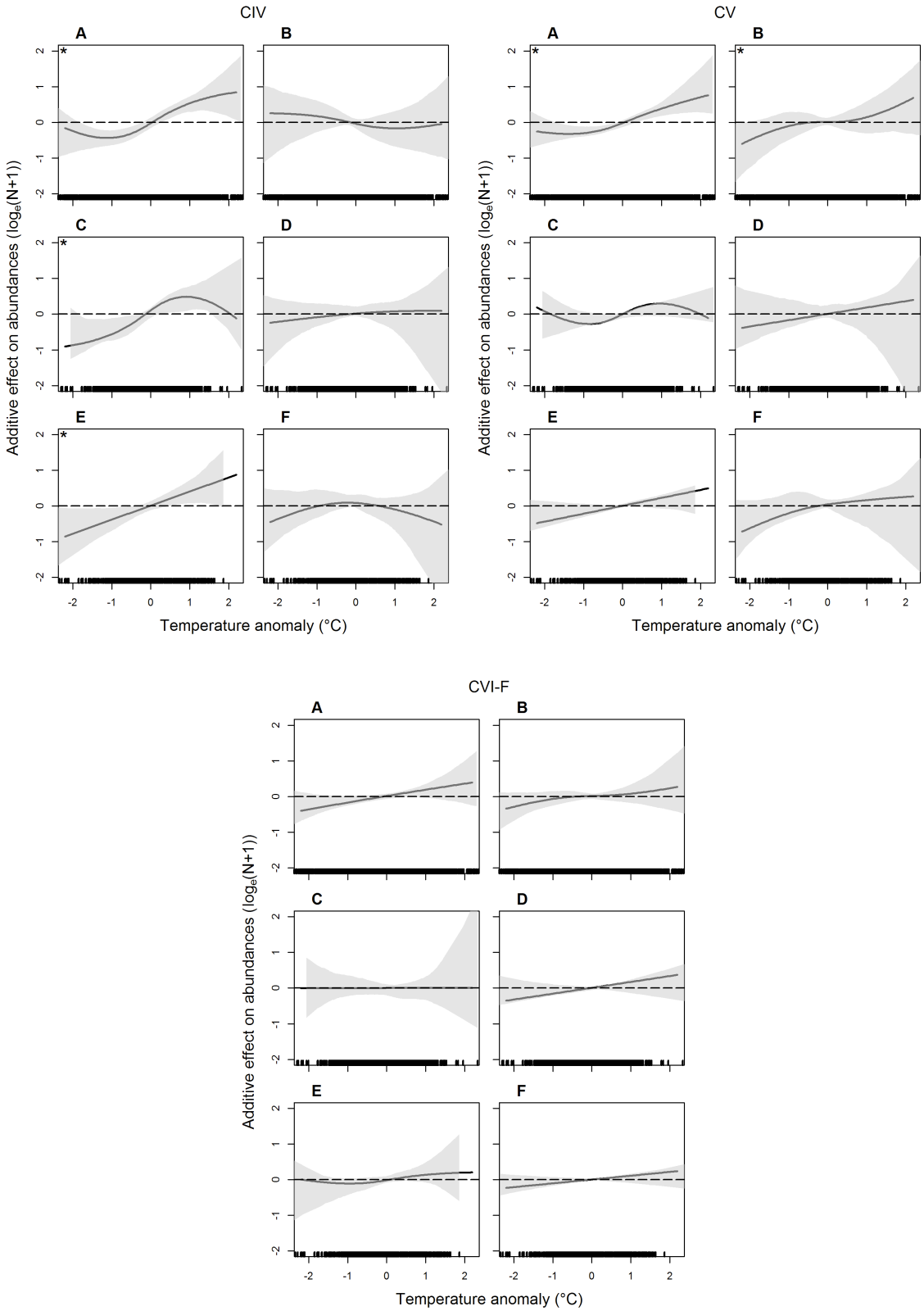

Fig. S3. Additive effect of local temperature anomalies on *Calanus finmarchicus* stage-specific abundances ($\log_e$[n+1]) compared across depth layers and seasons (Eq. S4 in Supplement 1). Six panels are displayed for each development stage: (A) upper water layer in spring; (B) upper water layer in summer; (C) middle water layer in spring; (D) middle water layer in summer; (E) lower water layer in spring; (F) lower water layer in summer. Shaded area: 95% confidence interval from bootstrap procedure. Dashed line: 0 effect isoline. Stars indicate a significant association, i.e. that the effect differs from 0 in parts of the covariates' range. N total: total nauplii abundance, CI–CVI: stage-specific copepodite abundance, F: female

Table S1. Importance of variables explaining general spatiotemporal variation in *Calanus finmarchicus* abundance: R^2 and genuine cross-validation (GCV) for models with all predictors (see Eq. 1 in Table 1 of the main text and Supplement 1, 'full model') and models with 1 term omitted. The difference in R^2 from the full model indicates the amount of data variation explained by the variable in question. The difference in GCV indicates the reduction in model predictive power when removing the variable. The most important variable(s) in terms of R^2 and GCV per developmental stage are shown in **bold**. N total: total nauplii abundance, CI–CVI: stage-specific copepodite abundance, F: female, M: male

	Full model		**– Position**		**– Day**		**– Depth**	
	R^2	**GCV**	**R^2**	**GCV**	**R^2**	**GCV**	**R^2**	**GCV**
N total	0.45	1.85	**0.28**	2.03	0.36	**3.88**	0.30	2.07
CI	0.45	1.67	**0.24**	1.92	0.39	**3.10**	0.31	1.89
CII	0.40	1.64	**0.18**	1.87	0.37	**2.10**	0.26	1.84
CIII	0.30	1.70	**0.10**	1.87	0.26	**1.88**	0.22	1.80
CIV	0.26	1.73	**0.14**	1.82	0.16	**3.81**	0.23	1.78
CV	0.37	1.62	**0.18**	1.79	0.22	**4.47**	0.34	1.67
CVI-F	0.50	1.27	**0.24**	**1.51**	0.49	1.27	0.43	1.38
CVI-M	0.42	0.48	**0.19**	0.55	0.39	**0.74**	0.40	0.49

Table S2. Spearman rank correlation coefficients (r_s) between *Calanus finmarchicus* stage-specific seasonal abundance indices (Eq. S2 in Supplement 1) and temperature indices from the Kola section and Skrova station. Significance level: *p < 0.05, **p < 0.01, ***p < 0.001. N total: total nauplii abundance, CI–CVI: stage-specific copepodite abundance, F: female

		Spring abundance						
	Temperature	N	CI	CII	CIII	CIV	CV	CVI–F
Kola	**Winter**	0.13	0.07	0.21	0.16	0.14	–0.03	–0.22
	Spring	0.2	0.2	0.34	0.29	0.32	0.15	–0.22
	Summer	0.18	0.26	0.39*	0.39*	0.45*	0.26	–0.16
Skrova	**Winter**	0.13	0.03	0.15	0.2	0.18	–0.04	–0.2
	Spring	0.04	–0.03	0.06	0.12	0.14	–0.07	–0.26
	Summer	0.18	0.23	0.35*	0.36*	0.41*	0.15	–0.1
		Summer abundance						
		N	CI	CII	CIII	CIV	CV	CVI–F
Kola	**Winter**	–0.21	–0.39*	–0.47*	–0.58**	–0.47*	–0.16	–0.12
	Spring	–0.29	–0.49*	–0.52**	–0.63**	–0.46*	–0.12	–0.08
	Summer	–0.35	–0.51*	–0.51*	–0.58**	–0.39*	–0.08	–0.04
Skrova	**Winter**	–0.01	–0.33	–0.39	–0.37	–0.28	0.04	0.01
	Spring	–0.13	–0.42*	–0.45*	–0.42*	–0.34	–0.02	–0.02
	Summer	–0.2	–0.39	–0.38	–0.39	–0.17	0.01	0.13

Disentangling the mechanisms behind climate effects on zooplankton

Kristina Øie Kvile[1,*], Øystein Langangen[1], Irina Prokopchuk[2], Nils Chr. Stenseth[1], Leif Chr. Stige[1]

[1]Centre for Ecological and Evolutionary Synthesis (CEES), Department of Biosciences, University of Oslo, PO Box 1066 Blindern, 0316 Oslo, Norway

[2]Knipovich Polar Research Institute of Marine Fisheries and Oceanography (PINRO), 6 Knipovich Street, 183763 Murmansk, Russia

Keywords: bottom-up control, *Calanus finmarchicus*, climate, ecosystem dynamics, spring bloom, zooplankton, trophic regulation, mechanisms

Abstract

In order to make realistic projections of population responses to climate change, there is a need for improved knowledge on the mechanisms by which climate affects ecosystems. Here, we quantify climate effects on *Calanus finmarchicus* in the north-eastern Norwegian Sea and south-western Barents Sea. By combining oceanographic drift models and statistical analyses of field data from 1959 to 1993 and investigating effects across several trophic levels, we are able to elucidate pathways by which climate influences zooplankton. The results show that spatially resolved *C. finmarchicus* biomass in summer is positively linked to temperature at back-calculated positions in spring. However, a warm spring does not lead to increased annual mean summer biomass. These apparently conflicting findings reflect that more *C. finmarchicus* originate from warmer than colder areas, but in warm springs, overall *C. finmarchicus* biomass is already high, and population growth from spring to summer is reduced. Furthermore, a combination of shallow mixed-layer-depth and increased wind in spring relates to both increased chlorophyll biomass in spring and *C. finmarchicus* biomass in summer, suggesting that *C. finmarchicus* biomass in summer is influenced by bottom-up effects of food-availability. Our study illustrates that improved understanding of climate effects can be obtained when different data sets and different methods are combined in a unified approach.

Introduction

Climate change has been correlated to various responses in zooplankton phenology, distribution, abundance and composition (Richardson, 2008; Beaugrand, 2014), but the controlling mechanisms behind the associations are often elusive. For example, a change in temperature might directly affect zooplankton physiology (Hirst & Bunker, 2003) or indirectly influence zooplankton through effects on their prey (Richardson & Schoeman, 2004) or ecosystem trophic structure (O'Connor *et al.*, 2009). In order to make realistic projections of climate effects on marine ecosystems, there is a need for improved understanding of the mechanisms by which climate affects the different trophic levels.

The Atlantic waters of the Norwegian Sea-Barents Sea ecosystem (NS-BS) support a highly productive ecosystem hosting several large fish stocks (Sakshaug *et al.*, 2009a). The area experienced increased water temperatures during the past decades (Johannesen *et al.*, 2012), and is like other high-latitude regions predicted to warm substantially throughout the 21st century (IPCC, 2014). Climate simulations further suggest globally increased ocean stratification, accompanied by decreased primary production in temperate regions, but increased primary production in the subarctic (including the Barents Sea) (Chust *et al.*, 2014).

Calanus finmarchicus dominates mesozooplankton biomass and is the main predator on phytoplankton throughout the North Atlantic (Nesterova, 1990; Melle *et al.*, 2014). In the NS-BS, young stages of *C. finmarchicus* are preyed upon by larvae of demersal fish, and older stages by various pelagic stocks (Melle *et al.*, 2004, 2014). Several studies have indicated that *C. finmarchicus* in the NS-BS is top-down controlled, particularly by Barents Sea capelin (Hassel *et al.*, 1991; Orlova *et al.*, 2002; Stige *et al.*, 2014a) and Norwegian spring-spawning herring (Dalpadado *et al.*, 2000; Prokopchuk & Sentyabov, 2006). Consistent effects of climate or food availability have on the other hand rarely been demonstrated *in situ* (Tande *et al.*, 2000; Dalpadado *et al.*, 2014; Kvile *et al.*, 2014).

Zooplankton's free-floating nature is an obstacle to field studies; for example, in the NS-BS the Norwegian Atlantic Current and the Norwegian Coastal Current (Fig. 1a) can transport a zooplankter several hundred km during its development time (Paper III, this dissertation). The use of individual based particle tracking models is considered a valuable approach to understand the effects of advection on zooplankton dynamics (Ji *et al.*, 2010). While the results of such models commonly are compared and calibrated with

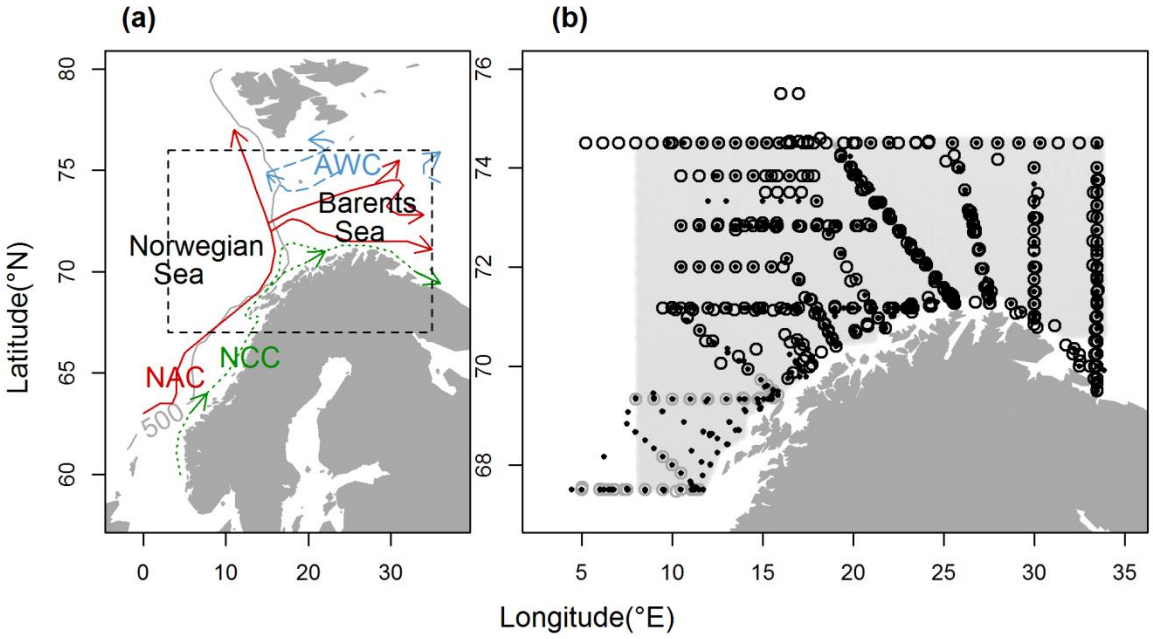

Fig. 1. (a) Map of the study area and the position of survey stations (dashed box). The main surface currents are: the Norwegian Atlantic Current (NAC, solid arrows), the Norwegian Coastal Current (NCC, dotted arrows) and Arctic Water Currents (AWC, dashed arrows). The 500 m depth contour (grey line) marks the approximate division between the Norwegian Sea and the Barents Sea/Norwegian continental shelf. (b) Survey stations, pooled for all years and separated in spring (bullets) and summer (open circles). Summer stations removed from the analyses are marked as grey. The initial particle release area is shaded grey.

observation data, they are rarely directly used in statistical analyses of observation data (but see Baumann *et al.*, 2006; Hidalgo *et al.*, 2012; Stige *et al.*, 2014b).

In this study, we use simulated zooplankton distributions from particle tracking and environmental conditions experienced during drift as input in a statistical model of *C. finmarchicus* field data from 1959 to 1993. Taking advection into account, we can quantify environmental effects integrated over the zooplankton's expected past habitat. Specifically, our aim is to understand how much of the variation in observed *C. finmarchicus* biomass in the NS-BS in summer is explained by (1) advection from observed distributions in spring to summer and variation in (2) temperature, (3) mixed-layer-depth and (4) wind (a proxy for mixing and turbulence). By assessing the relationships between the same physical variables and chlorophyll, a proxy for phytoplankton biomass, we are able to elucidate the pathways by which climate influences zooplankton in the NS-BS.

We show how combining state-of-the art drift modelling and spatiotemporal statistical analyses of long-term field data can improve our understanding of the mechanisms behind climate effects in marine systems. By investigating effects across

trophic levels, we highlight how changes in water column properties can influence food conditions for zooplankton, and in turn the zooplankton biomass available as prey for higher trophic levels.

Materials and methods

Zooplankton data

Zooplankton data were collected in spring (April-May) and summer (June-July) from 1959 to 1993 by PINRO (Nesterova, 1990). Samples were collected with a Juday net with closing mechanism (37 cm opening diameter, 180 µm mesh). Developmental stages of *C. finmarchicus* were recorded as ind./m^3, and total biomass (mg wet weight/m^3) was estimated from stage-specific individual weights (Kanaeva, 1962). The survey covered the north-eastern Norwegian Sea and south-western Barents Sea (Fig. 1) and depth layers approximately 0-50 m, 50-100 m, 100 m-bottom. There was some year-to-year variation in the stations sampled, and no records of *C. finmarchicus* were available from spring 1967, or summer 1980, 1990, 1991 and 1993.

Modelling drift from spring to summer

We modelled plankton drift routes from spring to summer each year with available *C. finmarchicus* data from both seasons. Particles representing a certain unity of biomass were tracked from spring to summer using a Lagrangian particle-tracking model (Ådlandsvik & Sundby, 1994), forced by a numerical ocean model hindcast archive (Lien *et al.*, 2013). The archive was constructed with the use of the Regional Ocean Modelling System (Shchepetkin & McWilliams, 2005), and provides hydrographic information for the NS-BS at daily intervals from 1959, with 4 by 4 km horizontal resolution and 32-layer terrain following vertical resolution.

We released particles within the survey area (Fig. 1b) with an initial distribution based on the spring observations of *C. finmarchicus*. Specifically, we extracted predictions from a generalised additive model (GAM) (Wood, 2006) describing spatiotemporal variation in *C. finmarchicus* biomass in spring. The model accounts for variation in space, time (day-of-year) and depth, and includes three random effects which capture overall year-to-year variation in biomass and yearly anomalies in the spatial patterns (Eq. A1, Appendix 1). We extracted year-specific predictions for all 25 831 grid cells in the release

area, at the median sampling day in spring (12th of May) and three depths: the median sampling depth (27.5 m), 10 m and 40 m. Each year, we released 100 000 particles. Thus, while the number of particles was not weighted by total biomass in spring, their spatial distribution was influenced by both general patterns and year-to-year variation in spring observations.

After release, particles drifted at their fixed depths until summer, when they were "sampled" at the day and positions of summer survey stations (within a 20 km radius). At each day of drift, we stored information about the particles' position, ambient sea temperature (at 27.5 m), mixed-layer-depth (MLD) and wind speed (at 10 m above the surface). MLD was defined as the depth where the difference in density (calculated from temperature and salinity profiles) from the surface layer was 0.125 kg/m^3 (Olsen *et al.*, 2003). For a fully mixed water column, MLD was set at 250 m, or at the local bottom depth if this was less than 250 m.

Statistical analyses

Spatial variation: We used the output from the particle tracking in a spatial statistical analysis of bottom-up effects in spring on summer biomass of *C. finmarchicus*. The response variable was spatiotemporal observation data on *C. finmarchicus* biomass in summer, and the explanatory variables included the number of particles "sampled" in a station and the average temperature, MLD and wind experienced by these particles during the first week of drift (12th-18th of May). We used a fixed week to ensure that the environmental variables represented equally long time periods for all samples (the sampling day differed between stations). We also tested to average the environmental conditions from the release date to the first day of the summer survey (1st of June, 18 days).

We first modelled spatial variation in summer biomass as a function of smooth additive effects of particle influx, and temperature, MLD and wind speed at back-calculated positions in spring (Eq. 1, Table 1). A random year effect was included to account for inter-annual variation in spring biomass and population growth from spring to summer. We also tested a number of alternative models with interactions, including varying coefficient models (Hastie & Tibshirani, 1993) where the effect of one covariate is assumed to be linear, but the slope of the effect varies smoothly with a second covariate. We tested twelve plausible interactions among effects of particle influx, temperature, MLD and wind, and proceeded with a varying coefficient model with a linear effect of wind (centred at zero) varying smoothly as a function of MLD (Eq. 2). None of the other

Table 1. Statistical models used in the (1-2) spatial and (3-4) time-series analyses of *C. finmarchicus* biomass in summer, and (5-6) the analysis of chlorophyll (Chl) biomass in spring. MLD: mixed-layer-depth, d.f.: degrees of freedom. *T*, *MLD*, *W* and *Chl* are average values between the 12th and 18th of May, *Z*, *P* and *MLD* and *Chl* are natural log-transformed, and *Z* and *P* added a constant of one.

	Eq. number	Model formulation	Symbols	
Spatial	**1.**	Additive	$Z_{l,t}$	Summer biomass in location *l*, time *t*
		$Z_{l,t} = \beta + s_1(P_{l,t}) + s_2(T_{l,t}) + s_3(MLD_{l,t}) + s_4(W_{l,t}) + b_t + \varepsilon_{l,t}$	β	Intercept
			s	1D smooth function, max. 3 d.f.
			P	Particle influx
	2.	Varying-coefficient	T	Temperature at back-calculated positions in spring
		$Z_{l,t} = \beta + s_1(P_{l,t}) + s_2(T_{l,t}) + s_3(MLD_{l,t}) + s_4(MLD_{l,t}) * W_{l,t} + b_t + \varepsilon_{l,t}$	MLD	MLD at back-calculated positions in spring
			W	Wind speed at back-calculated positions in spring
			b	Random effect of year
			ε	Error
Time-series	**3.**	Additive	$ZSum_y$	Mean summer biomass in year *y*
		$ZSum_y = \beta + s_1(ZSpr_y) + s_2(T_y) + s_3(MLD_y) + s_4(W_y) + \varepsilon_y$	β	Intercept
			s	1D smooth function, max. 2 d.f.
			$ZSpr_y$	Mean biomass in spring in year *y*
	4.	Varying-coefficient	T	Mean temperature in spring in year *y*
		$ZSum_y = \beta + s_1(ZSpr_y) + s_2(T_y) + s_3(MLD_y) + s_4(MLD_y) * W_y + \varepsilon_y$	MLD	Mean MLD in spring in year *y*
			W	Mean wind speed in spring in year *y*
			ε	Error
Chlorophyll	**5.**	Additive	$Chl_{l,y}$	Mean Chl in location *l*, year *y*
		$Chl_{l,y} = \beta + s_1(T_{l,y}) + s_2(MLD_{l,y}) + s_3(W_{l,y}) + b_t + \varepsilon_{l,y}$	β	Intercept
			s	1D smooth function, max. 3 d.f.
			T	Mean temperature in location *l*, year *y*
	6.	Varying-coefficient	MLD	Mean MLD in location *l*, year *y*
		$Chl_{l,y} = \beta + s_1(T_{l,y}) + s_2(MLD_{l,y}) + S_3(MLD_{l,y}) * W_{l,y} + b_t + \varepsilon_y$	W	Mean wind speed in location *l*, year *y*
			b	Random effect of year
			ε	Error

interactions were statistically significant or improved the model compared to a simple additive formulation.

Year-to-year variation: To assess if the relationships inferred from the spatial analysis reflected effects on year-to-year variation in overall *C. finmarchicus* biomass in summer, we conducted a time-series analysis testing the effects of annual mean temperature, MLD, wind and *C. finmarchicus* biomass in spring on annual mean summer biomass. As in the spatial analysis, we tested a purely additive model (Eq. 3) and a varying-coefficient model with an interaction between the effects of MLD and wind (Eq. 4). The calculation of indices of annual mean spring- and summer biomass, temperature, MLD and wind is described in Appendix 1. In all the statistical models of summer biomass (Eqs. 1-4), we only included samples from the upper water layer, corresponding to the drift depths of particles. All samples from depths < 60 m were included in this category. Furthermore, we excluded some observations in the area's southern boundary (south of 69.74°N, Fig. 1b), where, due to the northward currents, particle influx likely underestimated the potential drift into the station (see Appendix 1).

Food availability: Finally, to explore if the relationships inferred from the analyses above could reflect food availability, we analysed the effects of temperature, MLD and wind on chlorophyll (Chl) biomass. Remotely sensed Chl data from the NS-BS are not available at a regular scale prior to 1998, but with ocean model hindcast data until 2011, we could investigate relationships between the physical variables and spatiotemporally overlapping Chl. We downloaded Chl biomass data (mg/m^3) from 1998 to 2011 in the NS-BS from the GlobColour Project (http://www.globcolour.info), specifically, the global GSM-merged product for oceanic water (Maritorena *et al.*, 2010), at daily intervals and 25 by 25 km horizontal resolution. For each grid cell and year, we averaged Chl during the same week as in the zooplankton analyses (12th-18th of May, Appendix 2, Fig. A2), and aggregated temperature (at 27.5 m), wind speed (at 10 m above surface) and MLD from the ocean model on the same spatiotemporal resolution. We again tested a purely additive model (Eq. 5) and a varying coefficient model with an interaction between the effects of MLD and wind (Eq. 6).

Model validation: To account for within-year spatial autocorrelation, we computed 95 % confidence intervals of the spatial effects using nonparametric bootstrapping (1000 samples with replacement) with year as the sampling unit (Hastie *et al.*, 2009). Statistical significance was determined based on whether the confidence intervals differed from zero during the covariates' range. We used the adjusted R^2 and genuine cross-validation (GCV)

(for the spatial analyses) or AIC (for the time-series analyses) to compare models and the relative contributions of model terms (see Appendix 1). All models were formulated in the mgcv library in R (Wood, 2013; R Development Core Team, 2014), with the random-effect specification bs="re".

Results

Bottom-up effects on *C. finmarchicus*

The varying-coefficient models (Eqs. 2 and 4) were superior to the purely additive models (Eqs. 1 and 3) in terms of predictive power and variation explained in both the spatial and time-series analysis (Appendix 3, Table A1). Also, averaging the physical variables over the first week of drift instead of 18 days improved the models, and we proceed with the results using the first week (see Discussion for further details). The variables used are illustrated in Appendix 2, Fig. A3. In short, the spatial patterns in *C. finmarchicus* summer biomass, particle influx and temperature at back-calculated positions in spring were relatively predictable between years, with highest values in the south-western parts of the study area. The variation in MLD and wind was on the other hand better explained by year than space (Appendix 3, Table A2).

The results of the varying-coefficient models indicated that spatial variation in summer biomass was positively associated with particle influx and temperature experienced by the particles in spring (Fig. 2a, b). Year-to-year variation in summer biomass was positively related to spring biomass, but negatively related to high mean temperatures in spring (Fig. 2e, f). The interaction effect between MLD and wind at back-calculated positions in spring indicated a positive effect of wind on biomass in summer at shallow MLD; at deep MLD, wind had no effect (Fig. 2d). The lowest biomass was observed with the combination of shallow MLD and low wind (Appendix 2, Fig. A4). The combined effect of mean MLD and wind in spring on mean summer biomass had similar directions as in the spatial analysis, but were statistically non-significant ($p>0.05$). The spatial model explained around 30 % of the variation in summer biomass (Appendix 3, Table A1), with the random year-effect, particle influx and temperature terms each explaining around 12, 5 and 3 %, respectively. The interaction effect between MLD and wind only explained 1.6 %; nevertheless, the effect estimate was substantial. E.g., for a

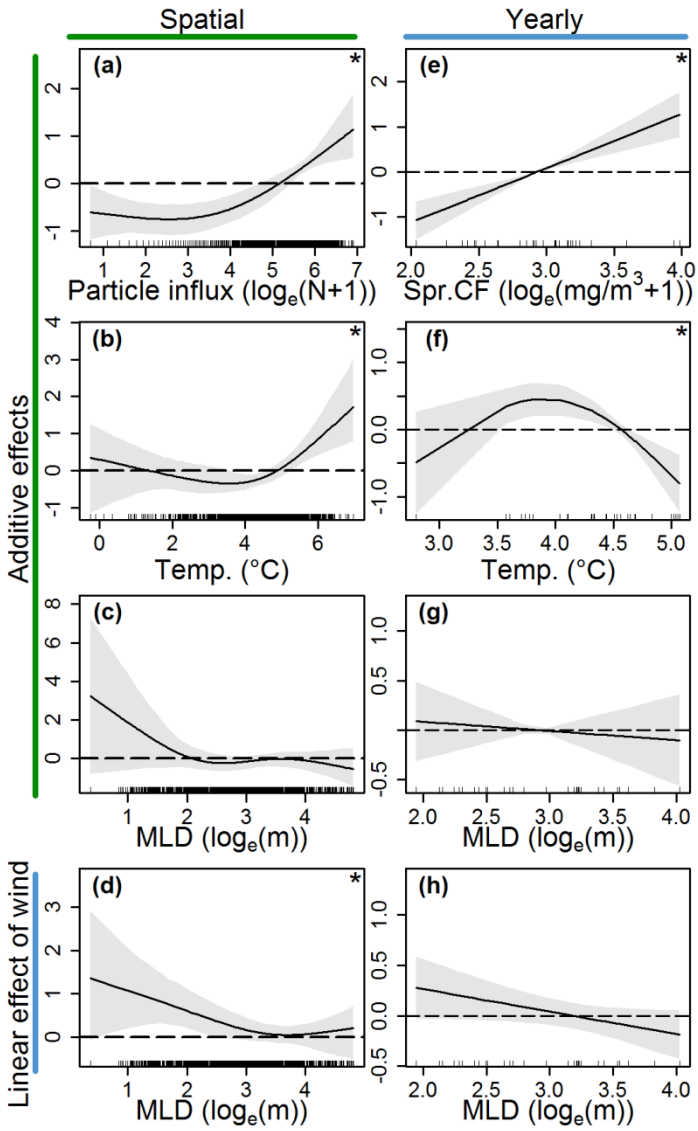

Fig. 2. Climate effects on zooplankton biomass. Lines and shaded areas show partial effects with 95 % confidence intervals from generalised additive models of (a-d) spatial (Eq. 2, Table 1) or (e-h) year-to-year variation (Eq. 4, Table 1) in *C. finmarchicus* biomass ($\log_e$(mg/m^3+1)) in summer. The rug along the x-axis indicates the location of observations. Significant associations ($p<0.05$) are marked with asterisks.

back-calculated MLD around 7 m, the regression coefficient of the wind effect was approx. 0.6, translating into an 82 % increase in summer biomass with an increase in wind of 1 m/s.

With a purely additive model, the effects of MLD and wind were non-significant ($p>0.05$), both in explaining spatial and year-to-year variation in summer biomass (Appendix 2, Figs. A5, A6). MLD and wind were positively correlated in both analyses (Appendix 3, Tables A3, A4); however, removing one of the two did not turn the remaining variable statistically significant.

The yearly indices of spring biomass and temperature were also positively correlated (Appendix 3, Table A4). If the spring biomass variable was removed from the time-series analysis, the temperature effect disappeared, indicating that summer biomass was not statistically different after warm or cold springs. An alternative model with the difference between the spring- and summer biomass indices as a function of spring

temperature also gave a negative association ($p<0.05$) with temperatures above approximately 4.5°C. Specifically, at higher spring temperatures, the overall increase in biomass from spring to summer approached zero.

Environmental effects on chlorophyll

The varying-coefficient model (Eq. 6) was also superior to the purely additive formulation (Eq. 5) in the analysis of environmental effects on spatial variation in Chl biomass (Appendix 3, Table A5). The results indicated that Chl biomass in spring was negatively associated with deep MLD, and the effect of increased wind was positive at shallow MLD, but negative at deep MLD (Figs. 3, A4). The effect of temperature was statistically non-significant ($p>0.05$). The model explained 17 % of the variation in the Chl data (Appendix 3, Table A5). The associations with MLD and wind using a purely additive model formulation indicated negative effects of deep MLD and low wind speed (Appendix 2, Fig. A7).

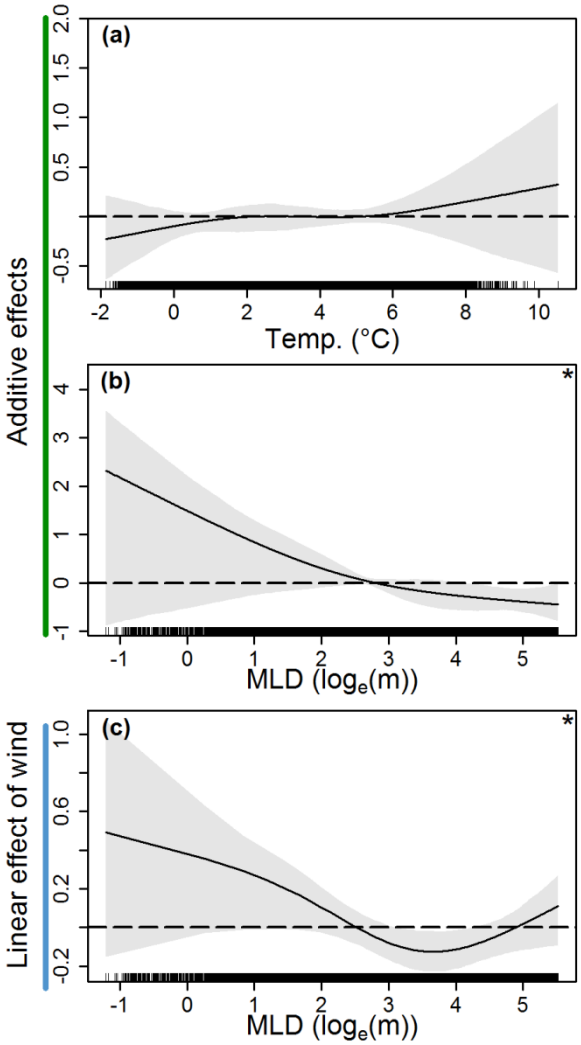

Fig. 3. Climate effects on chlorophyll biomass. Lines and shaded areas show partial effects with 95 % confidence intervals from the generalised additive model of spatial variation in chlorophyll (loge(mg/m3)) in spring (Eq. 6, Table 1). The rug along the x-axis indicates the location of observations. Significant associations ($p<0.05$) are marked with asterisks.

Discussion

We have analysed field data of *C. finmarchicus* biomass in the NS-BS using particle tracking to bridge observations from spring to summer. Accounting for drift, we found indications of bottom-up climate effects on *C. finmarchicus*. Wind and MLD likely influence *C. finmarchicus* through the lower trophic level, while temperature appears to have different effects on local and regional scales. We summarise the results and their implications below and in Fig. 4.

Temperature effects

Temperature had seemingly conflicting effects on local and regional scales. While spatially resolved biomass was positively linked to temperature at back-calculated positions in spring, year-to-year variation in summer biomass was negatively related to mean spring temperature, but only if mean spring biomass was accounted for. It appears that in warm springs, biomass levels tend to be relatively high, and the relative growth from spring to summer is reduced (Fig. 4b). Kvile *et al.* (2014) also showed that associations between ambient temperature and abundances of *C. finmarchicus* copepodites (CI-CIII) were positive in spring, but negative in summer, likely due to an earlier production peak. Further biomass growth after a warm spring might be limited by (1) competition for food; (2) predation by planktivorous fish or other predators removing "surplus production" (Stige *et al.*, 2009); and/or (3) earlier descent to overwintering. Manteifel (1941) reported reduced *C. finmarchicus* biomass in Barents Sea areas with mass development of ctenophores, which occurred earlier during warm years. Also, it was noted that *C. finmarchicus* descended earlier to overwintering after high temperatures in June. Kvile *et al*. (2014), however, did not find indications of temperature effects on the depth distribution of *C. finmarchicus* at the time of the summer survey.

The positive association between spatially resolved biomass in summer and back-calculated temperatures in spring likely reflects that more *C. finmarchicus* originate from warmer areas (Fig. 4a). This might be a result of the warmer, south-western areas being near the core areas for *C. finmarchicus* in the Norwegian Sea. Furthermore, temperature might directly (Hirche *et al.*, 1997; Campbell *et al.*, 2001) or through temperature effects on food availability (Feng *et al.*, 2014) influence growth rate and egg production. The observed relationship mostly reflect effects on stages CIV-CV, which dominate biomass in summer. Considering that it takes around 40 days from egg to CIV at typical ambient

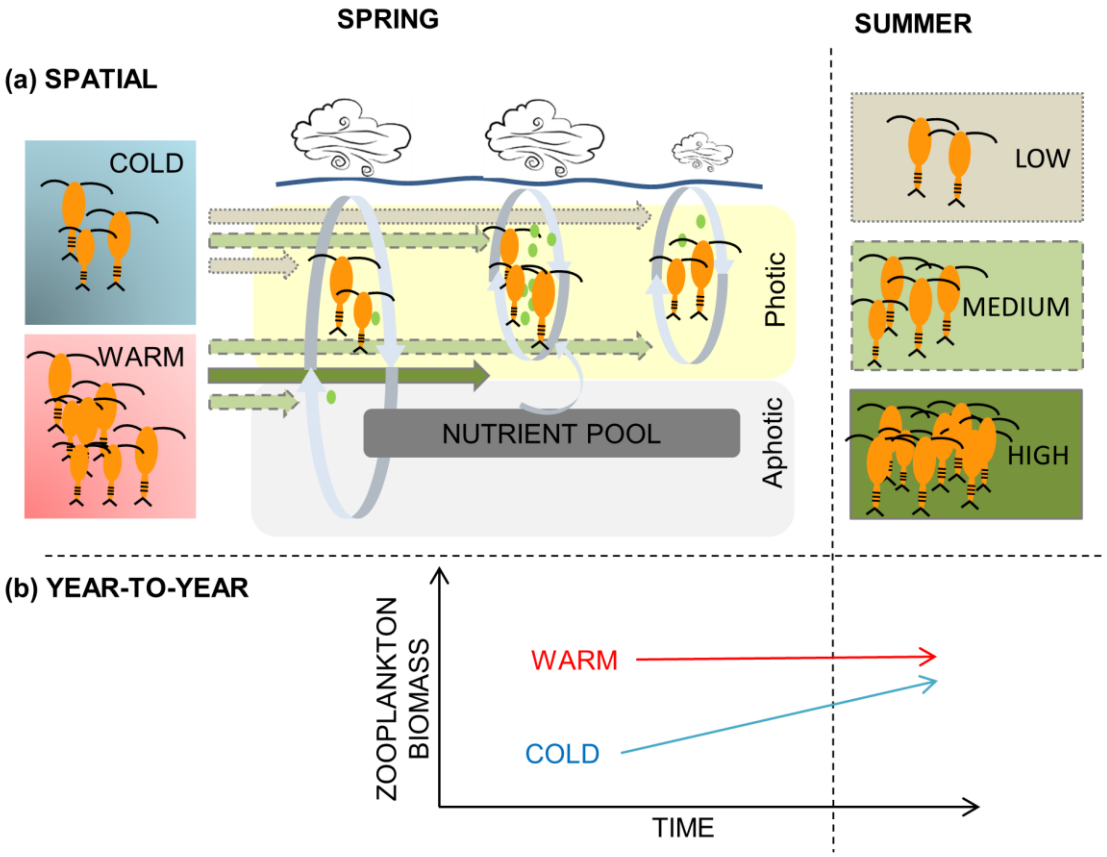

Fig. 4. Schematic presentation of results: More *C. finmarchicus* originate from warm than cold areas (a), but in a warm spring, mean biomass is high, and overall growth from spring to summer is lower than after a cold spring (b). The combination of shallow mixed-layer-depth (MLD) and strong winds favours phytoplankton production, which positively influences *C. finmarchicus* growth and/or egg production (a). In result, the combination of high temperature, shallow MLD and increased wind in spring leads to high summer biomass on a local scale (solid arrow), while alternative combinations with lower temperature, increased MLD and wind, or reduced MLD and wind, result in medium or low summer biomass (dashed or dotted arrows).

temperatures in the NS-BS (Campbell *et al.*, 2001), these stages are likely spawned in late April or May, depending on the sampling day in summer. The environmental variables are recorded during this period; thus, the observed associations might reflect effects on egg production by the parent generation, or on early growth conditions for copepodites sampled in summer.

Bottom-up effects of food

Most field studies to date have indicated that food availability is more important for *C. finmarchicus* egg production than direct effects of temperature (Runge *et al.*, 2006; Melle *et al.*, 2014). The phytoplankton spring bloom in the Atlantic waters of the NS-BS

primarily depends on a temperature-driven stabilisation of the water column (Rey, 2004; Sakshaug *et al.*, 2009b) (but see Behrenfeld & Boss, 2014), with commonly a single peak in spring. Large blooms typically take place when the MLD is shallower than 40-60 m (Sakshaug *et al.*, 2009b), thus, our spring data generally cover a period when the MLD is stabilised and nutrient availability might limit phytoplankton growth. During these periods, episodic wind-driven mixing can increase nutrient availability and prolong the spring bloom.

According to the trophodynamic phasing hypothesis (Parsons, 1988), a prolonged phytoplankton bloom can increase the temporal overlap between phytoplankton and zooplankton production. Brodeur & Ware (1992) found a positive relationship between winter winds and zooplankton biomass in summer, and hypothesised that a prolonged, less intense phytoplankton bloom allowed zooplankton to graze more efficiently than a short, intense bloom. We observed that a combination of shallow MLD and increased wind in spring was positively related to Chl biomass in spring and similarly to *C. finmarchicus* biomass in summer. Thus, there might be an optimal compromise between water column stability, keeping phytoplankton within the photic layer, and wind-induced mixing, renewing the nutrient supply for phytoplankton growth (Fig. 4a).

Wind-induced turbulence can also influence contact rates between zooplankton and its prey (Kiørboe & Saiz, 1995) and predators (MacKenzie *et al.*, 1994). However, the similar shapes of the MLD-wind interaction across trophic levels suggest bottom-up effects on productivity rather than predator-prey encounter rates. Nonetheless, it should be noted that while we found a significant effect of wind in the spatial analysis and not in the time-series analysis, the wind fields varied more between years than in space. The reduction in the number of data points in the time-series analysis likely increased the uncertainty of the effect estimates, but this might indicate that the wind-effect is spurious, or a proxy for something different acting at a local scale.

Including drift in statistical data analyses

Long-term data series of plankton are rare, and often restricted to single locations or seasons (Mackas & Beaugrand, 2010). Here, we analysed 30 years of data from two seasons, covering a large area in the NS-BS, and the particle tracking approach allowed us to investigate associations between the sampled zooplankton and the environment likely experienced in the past. Still, uncertainties in both the data and the model should be kept in mind when interpreting the results.

First, the zooplankton data are not evenly distributed in space and time. As the particle seeding model was based on the spring survey data, it is more uncertain in areas and years with reduced sampling effort, and fine spatial structures should be interpreted with caution. Transport to the edges of the study area in summer might be underestimated, although we reduced this bias by excluding the southernmost stations from the summer data. Also, the survey does not cover the Norwegian Sea proper, including *C. finmarchicus* core areas. Our results therefore apply to the highly advective shelf seas in the NS-BS rather than the core distribution areas.

Secondly, while the ocean model hindcast realistically represents both hydrography and the main transport patterns in the Atlantic waters in the NS-BS, both ocean current speed and temperature is slightly underestimated (Lien *et al.*, 2013). Also, random model noise will generate uncertainties in the analyses. We tested to average the environmental variables in the spatial analysis from the first day of drift until the first day of the summer survey (18 days), which, compared to using the first week of drift, resulted in weaker effects of MLD and wind. Possibly, the physical conditions early in the season, as represented by the first week, are particularly important for recruitment to the generation sampled later in summer, while conditions later in the season are less important. Alternatively, the difference in the results might be coincidental.

Finally, we restricted both particle drift and summer biomass data to the upper water layer. Since vertical positioning within the upper water can have large impacts on drift trajectories (Vikebø *et al.*, 2007), we released particles at three different depths. However, while *C. finmarchicus* is mainly confined to the upper 50 m in spring, older stages (CIV-CVI) might have a deeper distribution, in particular after June when descent to overwintering begins (Falkenhaug *et al.*, 1997; Dale & Kaartvedt, 2000). Focusing on the upper water layer might underestimate observed biomass in the statistical analysis, in particular towards the end of the summer survey.

Disentangling mechanisms behind climate effects

Lower trophic levels have typically been viewed as bottom-up controlled (Ware & Thomson, 2005; Greene, 2013), but several studies have demonstrated that top-down control might be important in cold, species-poor systems (Frank *et al.*, 2006; Petrie *et al.*, 2009). In order to project population responses to climate change, it is vital to understand the controlling mechanisms, but empirical evidence for either bottom-up or top-down control of zooplankton in the NS-BS has been elusive (Stige *et al.*, 2014a). Here, we show

that a combination of temperature, drift and water column properties can influence growth of *C. finmarchicus* biomass from spring to summer. While there is uncertainty associated with these results, the similar shapes of the MLD-wind interaction effect on both chlorophyll in spring and *C. finmarchicus* biomass in summer strongly suggest bottom-up effects of food availability. Understanding climate effects on water column stability and wind fields, in addition to temperature, will be important in order to foresee future conditions for animals dependent on zooplankton for dinner.

Acknowledgements

This study is a deliverable of the Nordic Centre for Research on Marine Ecosystems and Resources under Climate Change (NorMER), funded by the Norden Top-level Research Initiative sub- programme 'Effect Studies and Adaptation to Climate Change'. We are grateful to scientists and staff at PINRO who collected, sorted and digitised the zooplankton data, and to Padmini Dalpadado for comments on an earlier version of the manuscript.

References

Baumann H, Hinrichsen H-H, Möllmann C, Köster FW, Malzahn AM, Temming A (2006) Recruitment variability in Baltic Sea sprat (*Sprattus sprattus*) is tightly coupled to temperature and transport patterns affecting the larval and early juvenile stages. *Canadian Journal of Fisheries and Aquatic Sciences*, **63**, 2191–2201.

Beaugrand G (2014) Pelagic ecosystems and climate change. In: *Global Environmental Change*, Vol. 19 (ed Freedman B), pp. 141–150. Springer Netherlands, Dordrecht.

Behrenfeld MJ, Boss ES (2014) Resurrecting the ecological underpinnings of ocean plankton blooms. *Annual review of marine science*, **6**, 167–94.

Brodeur RD, Ware DM (1992) Long-term variability in zooplankton biomass in the subarctic Pacific Ocean. *Fisheries Oceanography*, **I**, 32–38.

Campbell RG, Wagner MM, Teegarden GJ, Boudreau CA, Durbin EG (2001) Growth and development rates of the copepod *Calanus finmarchics* reared in the laboratory. *Marine Ecology Progress Series*, **221**, 161–183.

Chust G, Allen JI, Bopp L et al. (2014) Biomass changes and trophic amplification of plankton in a warmer ocean. *Global Change Biology*, **20**, 2124–2139.

Dale T, Kaartvedt S (2000) Diel patterns in stage-specific vertical migration of *Calanus finmarchicus* in habitats with midnight sun. *ICES Journal of Marine Science*, **57**, 1800–1818.

Dalpadado P, Ellertsen B, Melle W, Dommasnes A (2000) Food and feeding conditions of Norwegian spring-spawning herring (*Clupea harengus*) through its feeding migrations. *ICES Journal of Marine Science*, **57**, 843–857.

Dalpadado P, Arrigo KR, Hjøllo SS et al. (2014) Productivity in the Barents Sea - response to recent climate variability. *PloS one*, **9**, e95273.

Falkenhaug T, Tande KS, Semenova T (1997) Diel , seasonal and ontogenetic variations in the vertical distributions of four marine copepods. *Marine Ecology Progress Series*, **149**, 105–119.

Feng J, Stige L, Durant J et al. (2014) Large-scale season-dependent effects of temperature and zooplankton on phytoplankton in the North Atlantic. *Marine Ecology Progress Series*, **502**, 25–37.

Frank KT, Petrie B, Shackell NL, Choi JS (2006) Reconciling differences in trophic control in mid-latitude marine ecosystems. *Ecology Letters*, **9**, 1096–1105.

Greene CH (2013) Towards a more balanced view of marine ecosystems. *Fisheries Oceanography*, **22**, 140–142.

Hassel A, Skjoldal HR, Gjøsæter H, Loeng H, Omli L (1991) Impact of grazing from capelin (*Mallotus villosus*) on zooplankton: a case study in the northern Barents Sea in August 1985. *Polar Research*, **10**, 371–388.

Hastie T, Tibshirani R (1993) Varying-coefficient models. *Journal of the Royal Statistical Society*, **55**, 757–796.

Hastie T, Tibshirani R, Friedman J (2009) *The Elements of Statistical Learning: Data Mining, Inference, and Prediction, 2nd ed.* Springer, New York, 745 pp.

Hidalgo M, Gusdal Y, Dingsor GE et al. (2012) A combination of hydrodynamical and statistical modelling reveals non-stationary climate effects on fish larvae distributions. *Proceedings of the Royal Society B: Biological Sciences*, **279**, 275–283.

Hirche H-J, Meyer U, Niehoff B (1997) Egg production of *Calanus finmarchicus*: effect of temperature, food and season. *Marine Biology*, **127**, 609–620.

Hirst AG, Bunker AJ (2003) Growth of marine planktonic copepods: global rates and patterns in relation to chlorophyll a, temperature, and body weight. *Limonology And Oceanography*, **48**, 1988–2010.

IPCC (2014) *Climate Change 2014: Synthesis Report. Contribution of Working Groups I, II and III to the Fifth Assessment Report of the Intergovernmental Panel on Climate Change* (eds Core Writing Team, Pachauri RK, Meyer LA). Geneva, 151 pp.

Ji R, Edwards M, Mackas DL, Runge JA, Thomas AC (2010) Marine plankton phenology and life history in a changing climate: current research and future directions. *Journal of Plankton Research*, **32**, 1355–1368.

Johannesen E, Ingvaldsen RB, Bogstad B et al. (2012) Changes in Barents Sea ecosystem state, 1970-2009: climate fluctuations, human impact, and trophic interactions. *ICES Journal of Marine Science*, **69**, 880–889.

Kanaeva IP (1962) Mean weight of copepods of Central and Northern Atlantic, the Norwegian and Greenland Seas. *M. Pishchepromizdat*, **46**, 253–266 (in Russian).

Kiørboe T, Saiz E (1995) Planktivorous feeding in calm and turbulent environments, with emphasis on copepods. *Marine Ecology Progress Series*, **122**, 135–146.

Kvile K, Dalpadado P, Orlova E, Stenseth N, Stige L (2014) Temperature effects on *Calanus finmarchicus* vary in space, time and between developmental stages. *Marine Ecology Progress Series*, **517**, 85–104.

Lien VS, Gusdal Y, Albretsen J, Melsom A, Vikebø F (2013) Evaluation of a Nordic Seas 4 km numerical ocean model hindcast archive (SVIM), 1960-2011. *Fisken og Havet*, **7**, 1–80.

Mackas DL, Beaugrand G (2010) Comparisons of zooplankton time series. *Journal of Marine Systems*, **79**, 286–304.

MacKenzie BR, Miller TJ, Cyr S, Leggett WC (1994) Evidence for a dome-shaped relationship between turbulence and larval fish ingestion rates. *Limnology and Oceanography*, **39**, 1790–1799.

Manteifel BP (1941) Plankton and herring in the Barents Sea. *Trudy PINRO. Transactions of the Knipovich Polar Scientific Institute of Sea-Fisheries and Oceanography Murmansk*, **7**, 125–218 (in Russian).

Maritorena S, D'Andon OHF, Mangin A, Siegel DA (2010) Merged satellite ocean color data products using a bio-optical model: Characteristics, benefits and issues. *Remote Sensing of Environment*, **114**, 1791–1804.

Melle W, Ellertsen B, Skjoldal HR (2004) Zooplankton: The link to higher trophic levels. In: *The Norwegian Sea Ecosystem* (ed Skjoldal HR), pp. 137–202. Tapir Academic Press, Trondheim.

Melle W, Runge J, Head E et al. (2014) The North Atlantic Ocean as habitat for *Calanus finmarchicus*: Environmental factors and life history traits. *Progress in Oceanography*, **129**, 244–284.

Nesterova VN (1990) *Plankton biomass along the drift route of cod larvae (reference material)*. PINRO, Murmansk (in Russian), 64 pp.

O'Connor MI, Piehler MF, Leech DM, Anton A, Bruno JF (2009) Warming and resource availability shift food web structure and metabolism. *PLoS Biology*, **7**, 3–8.

Olsen A, Johannessen T, Rey F (2003) On the nature of the factors that control spring bloom development at the entrance to the Barents Sea and their interannual variability. *Sarsia*, **88**, 379–393.

Orlova EL, Boitsov VD, Nesterova VN, Ushakov NG (2002) Composition and distribution of copepods, a major prey of capelin in the central Barents Sea, in moderate and warm years. *ICES Journal of Marine Science*, **59**, 1053–1061.

Parsons TR (1988) Trophodynamic phasing in theoretical, experimental aud natural pelagic ecosystems - Lecture by the member awarded the Oceanographical Society of Japan Prize for 1988. *Journal of the Oceanographical Society of Japan*, **44**, 94–101.

Petrie B, Frank KT, Shackell NL, Leggett WC (2009) Structure and stability in exploited marine fish communities: Quantifying critical transitions. *Fisheries Oceanography*, **18**, 83–101.

Prokopchuk I, Sentyabov E (2006) Diets of herring, mackerel, and blue whiting in the Norwegian Sea in relation to *Calanus finmarchicus* distribution and temperature conditions. *ICES Journal of Marine Science*, **63**, 117–127.

R Development Core Team (2014) R: A language and environment for statistical computing. *R Foundation for Statistical Computing, Vienna, Austria. URL http://www.R-project.org/*.

Rey F (2004) Phytoplankton: the grass of the sea. In: *The Norwegian Sea Ecosystem* (ed Skjoldal HR), pp. 97–136. Tapir Academic Press, Trondheim.

Richardson AJ (2008) In hot water: zooplankton and climate change. *ICES Journal of Marine Science*, **65**, 279–295.

Richardson AJ, Schoeman DS (2004) Climate impact on plankton ecosystems in the Northeast Atlantic. *Science (New York, N.Y.)*, **305**, 1609–12.

Runge JA, Plourde S, Joly P, Niehoff B, Durbin E (2006) Characteristics of egg production of the planktonic copepod, *Calanus finmarchicus*, on Georges Bank: 1994–1999. *Deep Sea Research Part II: Topical Studies in Oceanography*, **53**, 2618–2631.

Sakshaug E, Johnsen G, Kovacs K (eds.) (2009a) *Ecosystem Barents Sea*. Tapir Academic Press, Trondheim.

Sakshaug E, Johnsen G, Kristiansen S, Quillfeldt C von, Rey F, Slagstad D, Thingstad F (2009b) Phytoplankton and primary production. In: *Ecosystem Barents Sea* (eds Sakshaug E, Johnsen G, Kovacs K), pp. 167–207. Tapir Academic Press, Trondheim, Norway.

Shchepetkin AF, McWilliams JC (2005) The regional oceanic modeling system (ROMS): a split-explicit, free-surface, topography-following-coordinate oceanic model. *Ocean Modelling*, **9**, 347–404.

Stige LC, Lajus DL, Chan K-S, Dalpadado P, Basedow S, Berchenko I, Stenseth NC (2009) Climatic forcing of zooplankton dynamics is stronger during low densities of planktivorous fish. *Limnology and Oceanography*, **54**, 1025–1036.

Stige LC, Dalpadado P, Orlova E, Boulay A-C, Durant JM, Ottersen G, Stenseth NC (2014a) Spatiotemporal statistical analyses reveal predator-driven zooplankton fluctuations in the Barents Sea. *Progress in Oceanography*, **120**, 243–253.

Stige LC, Langangen Ø, Yaragina NA et al. (2014b) Combined statistical and mechanistic modelling suggests food and temperature effects on survival of early life stages of Northeast Arctic cod (*Gadus morhua*). *Progress in Oceanography*, **134**, 138–151.

Tande K, Drobysheva S, Nesterova V, Nilssen EM, Edvardsen A, Tereschenko V (2000) Patterns in the variations of copepod spring and summer abundance in the northeastern Norwegian Sea and the Barents Sea in cold and warm years during the 1980s and 1990s. *ICES Journal of Marine Science*, **57**, 1581–1591.

Vikebø F, Jørgensen C, Kristiansen T, Fiksen Ø (2007) Drift, growth, and survival of larval Northeast Arctic cod with simple rules of behaviour. *Marine Ecology Progress Series*, **347**, 207–219.

Ware DM, Thomson RE (2005) Bottom-up ecosystem trophic dynamics determine fish production in the Northeast Pacific. *Science (New York, N.Y.)*, **308**, 1280–1284.

Wood SN (2006) *Generalized additive models: an introduction with R*. Chapman and Hall/CRC, Boca Raton, Florida.

Wood SN (2013) mgcv: GAMs with GCV smoothness estimation and GAMMs by REML/ PQL. R package. Version 1.7–24.

Ådlandsvik B, Sundby S (1994) Modelling the transport of cod larvae from the Lofoten area. *ICES Mar Sci. Symp.*, **198**, 379–392.

Appendix 1. Supplementary methods

(a) Particle release model

100 000 particles were released within the survey area each spring based on predictions from the following generalized additive model (GAM) describing spatiotemporal variation of *C. finmarchicus* biomass in spring:

$$Z_{l,t,d} = \beta + s_1(j_t) + s_2(d_d) + te(x_l, y_l) + b_{0t} + b_{1t} * x_l + b_{2t} * y_l + \varepsilon_{l,t,d} \quad \textbf{Eq. A1}$$

$Z_{l,t,d}$ is the natural logarithm of *C. finmarchicus* biomass (added a constant of 1) in location *l*, time *t* and depth *d*; β is the intercept; $s_1(j_t)$ and $s_2(d_d)$ are 1D smooth functions of the day-of-year and average depth of the sample (with maximum 3 degrees of freedom (d.f.) each); $te(x_l, y_l)$ is a 2D tensor product smooth function of the position of the sample (with max. 5 d.f. for each basis function); and ε is a random error term. *x* and *y* represent distance (in km) south-west to north-east (approx. alongshore) and south-east to north-west (approx. onshore-offshore), respectively. To construct *x* and *y* we first transformed the geographical coordinates (longitude and latitude) to Azimuthal Equidistant projection centred at the median position of all samples (71.5°N, 20.25°E), and then added (to construct *x*) or subtracted (to construct *y*) the resulting distance in the longitudinal direction from the resulting distance in the latitudinal direction.

We included three random effects in the model: a random year-effect (b_{0t}) capturing year-to-year variation in biomass not explained by season or space; and two random year-effects (b_{1t}, b_{2t}) varying with linear terms of *x* and *y*, quantifying yearly anomalies in the spatial patterns. b_{0t} affects year-to-year variation in the intercept of model predictions, while $b_{1t*}x_l$ and $b_{2t*}y_l$ affect year-to-year variation in spatial distribution. The model explained 46 % of the variation in the data (adj. $R^2 = 0.459$).

(b) Calculation of yearly indices for the time-series analysis

Indices of spring- and summer biomass were constructed by extracting year-specific intercepts ($\beta+b_0$) from the particle release model (Eq. A1) formulated for spring- and summer samples separately. To avoid influences of survey design in the indices of year-to-year variation in environmental conditions, we extracted information for the same set of locations every year (Fig. A1, Appendix 2), spanning the whole area of possible particle origins. The selected locations are the centred (centre-of-gravity) release position of the particles sampled in each summer survey station, pooled for all years (in total 1325

locations). We averaged environmental information from the ocean model for these locations between the 12th and 18th of May to estimate yearly indices of temperature (°C at 27.5 m depth), MLD ($\log_e$(m)) and wind (m/s at 10 m above surface).

(c) Exclusion of observations in the area's boundary

In the statistical analyses of *C. finmarchicus* summer biomass (Eqs. 1-4, Table 1, main text), we excluded some observations in the area's boundaries where potential drift into the station likely was underestimated. Based on the general surface currents patterns in the NS-BS (Fig. 1a, main text), we expected this bias to be strongest along the southern, and potentially western, boundaries. Based on northward drift from the southern boundary (67.5-68°N), and eastward drift from the western boundary (8.5-9°E), from the release date (12th of May), to the median day of the summer survey (28th of June), we excluded stations south of the median final position of particles drifting from the south (69.74°N, Fig. 1b, main text). While the relatively strong northward drift indicated that a high proportion of *C. finmarchicus* south of this limit originate from areas to the south of the particle release area, there was no strong longitudinal trend in the drift pattern, and we did not exclude any station based on longitude.

(d) GCV for model validation

Genuine cross-validation (GCV) was calculated to compare the predictive power of spatial models. Since data samples were not independent in space or time within years, possibly leading to positive auto-correlation in the model residuals, using generalised CV or AIC would likely favour over-parameterised models. The GCV score is the mean of the mean square prediction error of 1000 models formulated for a dataset with one year randomly removed, predicting the data in the removed year. The GCV increases with high complexity and low predictive power. The random-effect of year could not be included when calculating GCV scores, and was for this purpose replaced by a smooth function of the annual mean spring biomass index (in Eqs. 1-2, Table 1, main text). For the Chl models (Eqs. 5-6), we replaced the random year effect with an index of year-to-year variation in the Chl data. This index was constructed by taking the year-specific intercept ($\beta+b_{0y}$) in the following GAM with Chl biomass as a function of a tensor product smooth function of longitude and latitude and a random effect of year:

$$Z_{l,y} = \beta + te(lon_l, lat_l) + b_{0y} + \varepsilon_{l,y} \qquad \textbf{Eq. A2}$$

Appendix 2. Supplementary figures

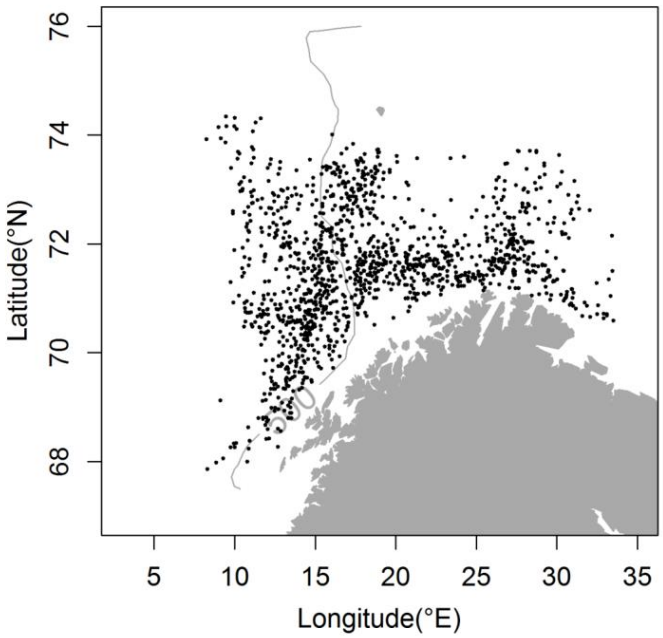

Fig. A1. Locations used to extract information to calculate yearly indices of annual mean temperature, MLD and wind. The locations are the centred (centre-of-gravity) release position of the particles sampled in each summer survey station, pooled for all years (in total 1325 locations).

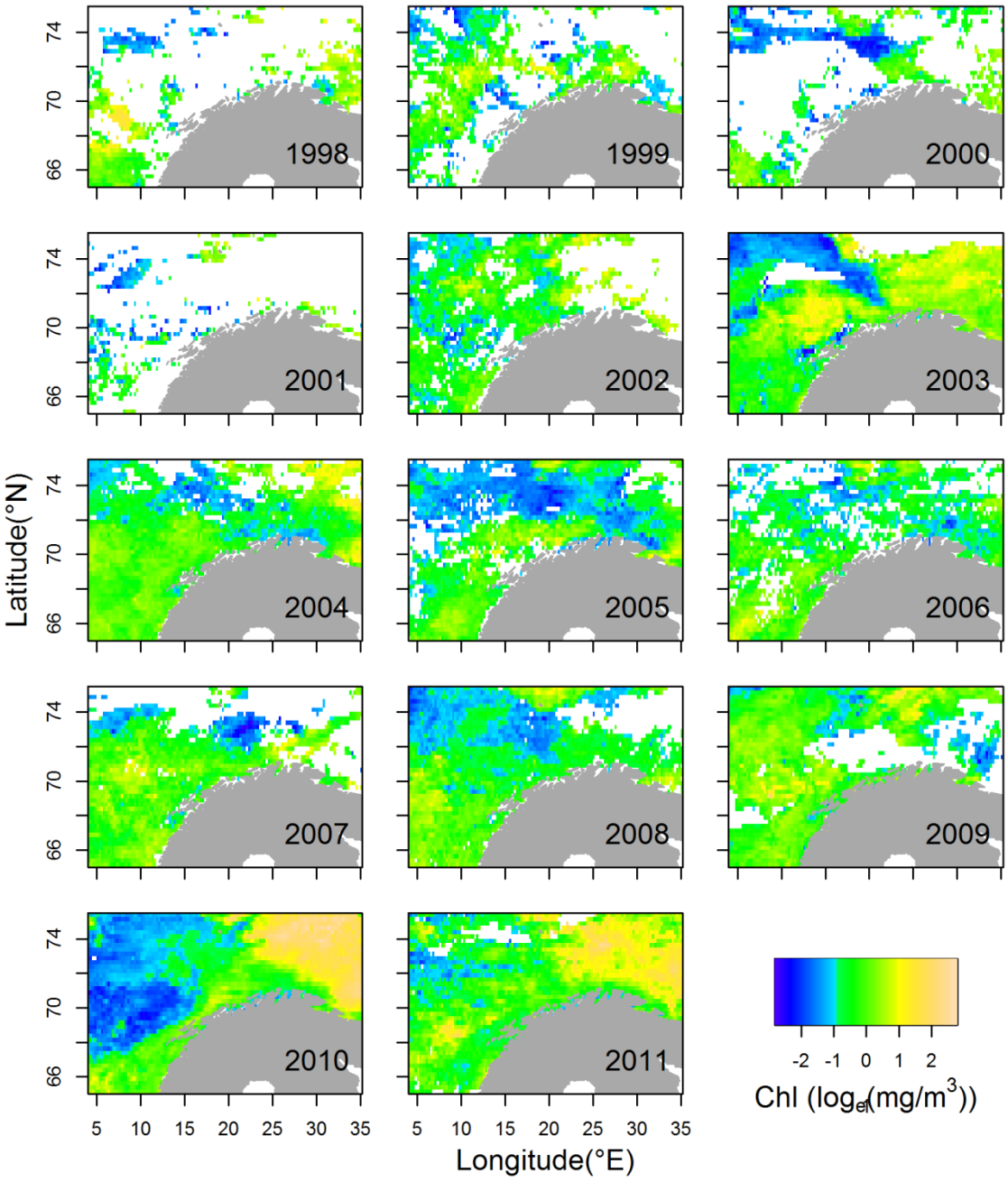

Fig. A2. The data used as response variable in the analyses of chlorophyll (Chl) biomass (Eqs. 5-6, Table 1, main text). The data are averages of daily Chl biomass ($\log_e(mg/m^3)$) between the 12th and 18th of May for each 25 by 25 km grid cell (in total 3600 cells) and year. Total data coverage was 65 %, white areas are missing values.

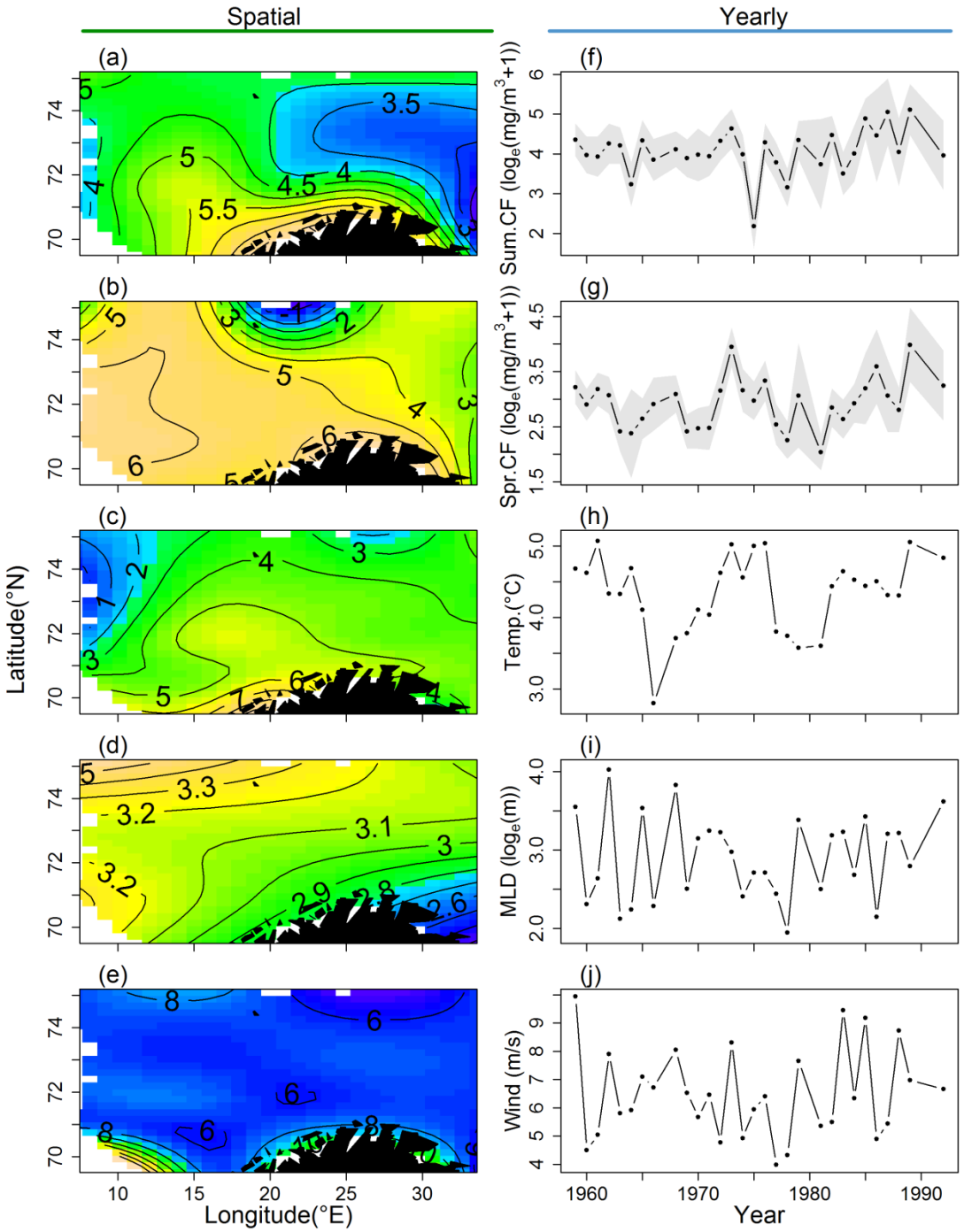

Fig. A3. The variables used in the spatial (a-e) and time-series (f-j) analyses of *C. finmarchicus* biomass. The spatial data are pooled for all years and interpolated using a tensor product smooth function of longitude and latitude, and include (a) *C. finmarchicus* summer biomass ($\log_e$ (mg/m^3+1)), (b) particle influx ($\log_e$(N+1)), (c) temperature (°C), (d) MLD ($\log_e$(m)) and (e) wind speed (m/s). Note that (c-e) are average conditions experienced by the particles prior to sampling in the locations indicated while (h-j) are average conditions across the area. Shaded area: 95 % confidence intervals of the biomass indices.

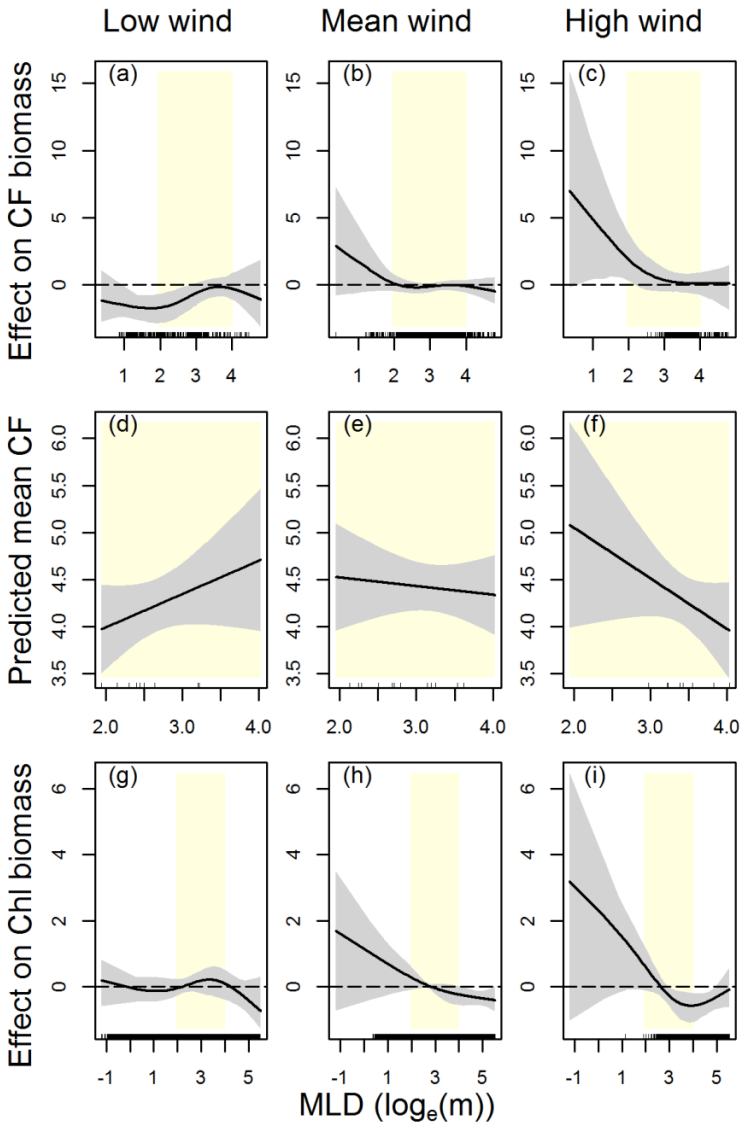

Fig. A4. Combined effects of MLD and wind on (a-c) spatially resolved *C. finmarchicus* biomass, (d-f) annual mean *C. finmarchicus* biomass or (g-i) spatially resolved chlorophyll (Chl) biomass. Predicted effects on spatially resolved *C. finmarchicus* biomass ($\log_e(mg/m^3+1)$) in summer (Eq. 2, Table 1, main text) are shown for wind speed fixed at (b) the mean value (6.5 m/s) or 3 m/s (a) below or (c) above the mean. Predicted annual mean *C. finmarchicus* biomass ($\log_e(mg/m^3+1)$) in summer (Eq. 4, Table 1, main text) is shown for annual mean wind speed fixed at (e) the mean value (6.4 m/s) or 2 m/s (d) below or (f) above the mean. Predicted effects on spatially resolved Chl biomass ($\log_e(mg/m^3)$) in spring (Eq. 6, Table 1, main text) are shown for wind speed fixed at (h) the mean value (6.4 m/s) or 3 m/s (g) below or (i) above the mean. The yellow areas indicate overlapping MLD values in the three analyses, and the grey areas 95 % confidence intervals. The rug on the x-axis indicates the locations of MLD data for the wind speed interval represented by the given panel.

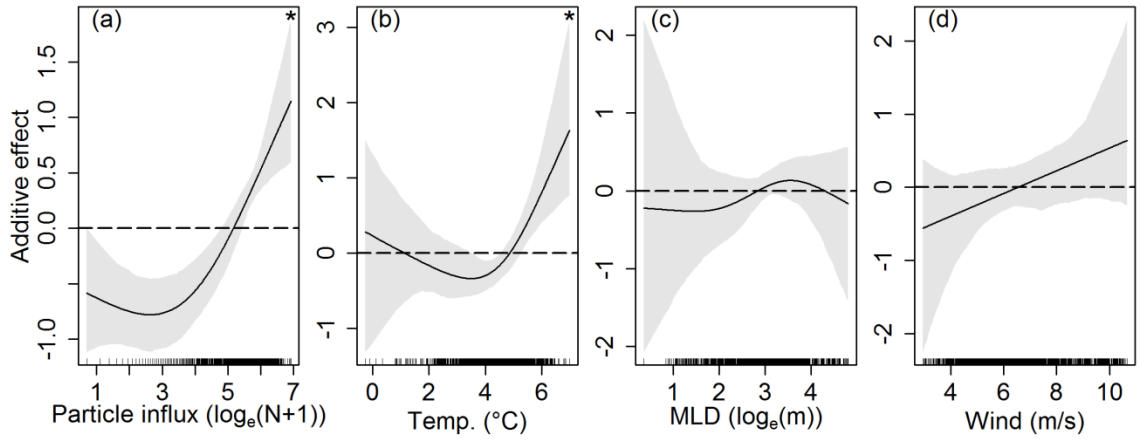

Fig. A5. Results from the spatial analysis (Eq. 1, Table 1, main text), showing the purely additive effects of (a) particle influx, (b) temperature, (c) MLD and (d) wind at back-calculated positions in spring on *C. finmarchicus* biomass ($\log_e(mg/m^3+1)$) in summer. The shaded area indicates the 95 % confidence interval, and the rug along the x-axis the location of observations. Significant associations ($p<0.05$) are marked with asterisks.

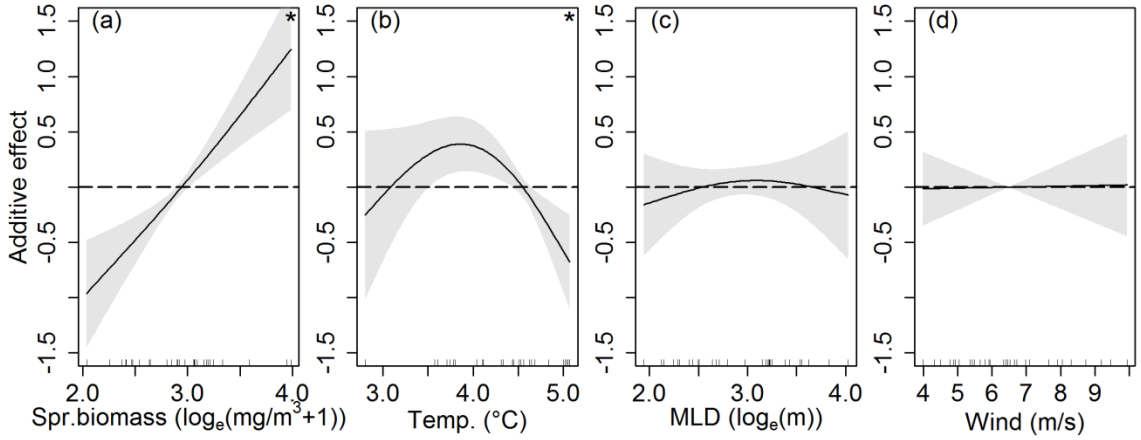

Fig. A6. Results of the time series analyses (Eq. 3, Table 1, main text), showing the purely additive effects of annual mean (a) *C. finmarchicus* biomass, (b) temperature, (c) MLD and (d) wind in spring on annual mean *C. finmarchicus* biomass ($\log_e(mg/m^3+1)$) in summer. The shaded area indicates the 95 % confidence interval, and the rug along the x-axis the location of observations. Significant associations ($p<0.05$) are marked with asterisks.

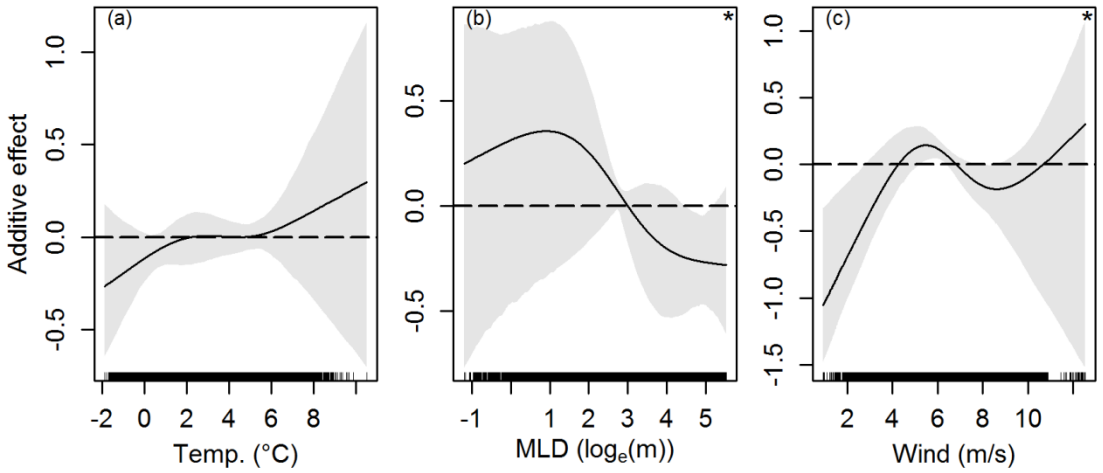

Fig. A7. Results from the analysis of chlorophyll biomass ($\log_e$(mg/m^3)) (Eq. 5, Table 1, main text), showing the purely additive effects of (a) temperature, (b) MLD and (c) wind. All variables are mean values between the 12th and 18th of May per 25 km grid cell and year (1998-2011). The shaded area indicates the 95 % confidence interval, and the rug along the x-axis the location of observations. Significant associations ($p<0.05$) are marked with asterisks.

Appendix 3. Supplementary tables

Table A1. Comparison of the predictive power (GCV/AIC) and variation explained (adjusted R^2) for the purely additive formulation (upper) and the varying-coefficient formulation (lower) in the spatial (left) and time-series (right) analyses of *C. finmarchicus* summer biomass, and partial R^2 for the different model terms, calculated by removing one covariate at a time while keeping all other variables in the model.

	Spatial		Time-series	
Additive	GCV	1.873	AIC	43.924
	R^2	0.295	R^2	0.459
	Model term	Partial R^2	Model term	Partial R^2
	Particle influx	0.058	Spring biomass	0.433
	Temperature	0.026	Temperature	0.182
	MLD	0.002	MLD	0.000
	Wind	0.003	Wind	-0.023
	Year	0.126		
Variable-coefficient	GCV	1.830	AIC	41.316
	R^2	0.308	R^2	0.495
	Model term	Partial R^2	Model term	Partial R^2
	Particle influx	0.054	Spring biomass	0.489
	Temperature	0.028	Temperature	0.245
	MLD	0.006	MLD	-0.016
	MLD*Wind	0.016	MLD*Wind	0.013
	Year	0.119		

Table A2. The proportion of the variation in the data used in (a) the spatial analysis explained by space and (b) the time-series analysis explained by year. All values are adjusted R^2, of a model where (a) the data used the spatial analysis (Eqs. 1-2, Table 1, main text) are explained by a tensor-product smooth spline of longitude and latitude, or (b) the data used to construct variables for the time-series analysis (Eqs. 3-4, Table 1, main text) are explained by a factor-variable of year. MLD, particle influx and spring- and summer biomass were natural log-transformed to reduce the influence of outliers, and biomass and particle influx were added a constant of one to avoid taking the logarithm of zero.

Variable	a. Space	b. Year
Temperature	0.55	0.25
MLD	0.08	0.43
Wind	0.03	0.74
Particle influx	0.69	
Spring biomass		0.10
Summer biomass	0.24	0.16

Table A3. Kendall tau rank correlation coefficient (R_k) and statistical significance (p-values) of the correlation between the covariates in the spatial analyses (Eqs. 1-2, Table 1, main text).

	R_k	p
Particles–Temperature	0.08	<0.05
Particles–MLD	0.06	<0.05
Particles–Wind	0.04	<0.05
Temperature–MLD	-0.13	<0.05
Temperature–Wind	-0.05	<0.05
MLD–Wind	0.40	<0.05

Table A4. Kendall tau rank correlation coefficient (R_k) and statistical significance (p-values) of the correlation between the indices used as covariates in the time series analyses (Eqs. 3-4, Table 1, main text).

	R_k	p
Spring biomass–Temperature	0.44	<0.05
Spring biomass–MLD	0.25	0.058
Spring biomass–Wind	0.19	0.145
Temperature–MLD	0.01	0.972
Temperature–Wind	0.03	0.804
MLD–Wind	0.48	<0.05

Table A5. Comparison of the predictive power (GCV) and variation explained (adjusted R^2) for the purely additive formulation (upper) and the varying-coefficient formulation (lower) in the analysis of chlorophyll biomass (Eqs. 5-6, Table 1, main text), and partial R^2 for the different model terms.

Additive	GCV	0.788
	R^2	0.156
	Model term	Partial R^2
	Temperature	0.003
	MLD	0.027
	Wind	0.018
	Year	0.052
Variable-coefficient	R^2	0.171
	GCV	0.787
	Model term	Partial R^2
	Temperature	0.003
	MLD	0.023
	MLD*Wind	0.032
	Year	0.053

Coupling a hydrodynamic model with biological survey data gives new insight into long-term variation in *Calanus finmarchicus* spawning areas

Kristina Øie Kvile[1,*], Øyvind Fiksen[2,3], Irina Prokopchuk[4], Anders Frugård Opdal[2,3]

[1]Centre for Ecological and Evolutionary Synthesis (CEES), Department of Biosciences, University of Oslo, PO Box 1066 Blindern, 0316 Oslo, Norway

[2]Uni Research and Hjort Centre for Marine Ecosystem Dynamics, PO Box 7810, 5020 Bergen, Norway

[3]Department of Biology and Hjort Centre for Marine Ecosystem Dynamics, University of Bergen, PO Box 7803, 5020 Bergen, Norway

[4] Knipovich Polar Research Institute of Marine Fisheries and Oceanography (PINRO), 6 Knipovich Street, 183763 Murmansk, Russia

Keywords: advection, copepod, ocean currents; spawning, zooplankton, climate, Norwegian Sea, Barents Sea

Abstract

Calanus finmarchicus is the dominant mesozooplankton species in the Atlantic waters of the Norwegian Sea and Barents Sea. Knowledge of the spatial distribution and timing of *C. finmarchicus* recruitment is important to understand the dynamics of both foraging migrations of pelagic fish and recruitment success of demersal and pelagic fish stocks. In this study, we use large-scale spatiotemporal survey data (33 years in both Norwegian Sea and Barents Sea areas) coupled with drift trajectories from a hydrodynamic model to back-calculate and map the spatiotemporal distribution of *C. finmarchicus* from copepod to egg, and thus potential adult spawning areas.

Assuming overwintering in the Norwegian Sea, our results suggest that copepodites observed along three Norwegian Sea survey transects originate from relatively limited areas in the transects' surroundings off the shelf-edge. In some years, however, strong ocean currents, possibly linked to climatological events, apparently transport eggs and copepodites long distances northward along the shelf edge. Copepodites sampled in the Barents Sea entrance are a mix of locally spawned individuals and long-distance-travellers from a narrow band along the shelf edge, while copepodites found farther east in the Barents Sea are most likely exclusively spawned on the Barents Sea shelf. A low number of drift-trajectories from overwintering areas in the Norwegian Sea reached the easternmost Barents Sea transect (33.5°E). This could indicate that copepodites observed here partly descend from individuals from other overwintering areas, such as Norwegian fjords or the Barents Sea shelf.

Introduction

Several large fish stocks feed within the Atlantic waters of the Norwegian Sea and Barents Sea (NS-BS), and copepods constitute an important part of their diet. *Calanus finmarchicus* is the dominant copepod species in the NS-BS, and plays a key role as phytoplankton grazer during the spring bloom (Rey, 2004). Nauplii and younger copepodite stages are in turn an important food source for various larval and juvenile fish (e.g. cod, haddock, herring) while older copepodite stages and adults are preyed upon by pelagic fish (e.g. herring, capelin and mackerel) (Melle *et al.*, 2004; Loeng & Drinkwater, 2007; Eiane & Tande, 2009). Knowledge of the spatiotemporal distribution of *C. finmarchicus* recruitment is therefore important to understand both large-scale foraging migrations and the recruitment success of demersal fish stocks. Specifically, it has been hypothesised that the abundance and timing of *C. finmarchicus* nauplii and copepodites is an important driver for recruitment success of Atlantic cod larvae (Hjort, 1914; Ellertsen *et al.*, 1989; Cushing, 1990; Sundby, 2000; Kristiansen *et al.*, 2011) and that herring migrations in the Norwegian Sea are timed after the seasonal cycle of *C. finmarchicus* (Gislason & Astthorsson, 2002; Broms *et al.*, 2012).

In late winter, adult *C. finmarchicus* ascend from overwintering in the deep waters of the Norwegian Sea (Halvorsen *et al.*, 2003; Slagstad & Tande, 2007; Melle *et al.*, 2014) or fjord basins (Hirche, 1983; Kaartvedt, 1996). The new generation is spawned in the upper waters in early spring. The intensity of spawning increases with food availability and is highest during the spring bloom (April-May) (Diel & Tande, 1992; Niehoff *et al.*, 1999; Melle *et al.*, 2014), but a significant proportion of the total egg production occurs during the pre-bloom period (Niehoff *et al.*, 1999; Stenevik *et al.*, 2007).

The NS-BS is governed by the Norwegian Atlantic Current, which brings relatively warm and saline Atlantic water northward in the Norwegian Sea and into the Barents Sea (Fig. 1) (Loeng 1991, Blindheim 2004). Closer to the Norwegian coast, the upper water masses are dominated by the northbound cooler and fresher Norwegian Coastal Current, which follows the coastline into the Barents Sea. Both adults and the new generation of *C. finmarchicus* might be transported within and out of the Norwegian Sea depending on ambient ocean current dynamics (Edvardsen *et al.*, 2003a; Torgersen & Huse, 2005; Samuelsen *et al.*, 2009).

Since the distribution of zooplankton species such as *C. finmarchicus* depends not only on recruitment and mortality, but largely on advection, it is difficult to understand the

spatial distribution and timing of recruitment based on field data alone (Pedersen *et al.*, 2001; Speirs *et al.*, 2004). This would require near complete sampling coverage in space and time, which is obviously difficult in the open ocean. Available data typically provide a snapshot of the abundance and structure of zooplankton in the area and time of sampling, and additionally, the earliest life stages of *C. finmarchicus* (eggs and nauplii) are too small to be well represented by the sampling gear commonly used (Hernroth, 1987; Nichols & Thompson, 1991).

The combination of hydrodynamic models and individual-based models/particle tracking, often termed coupled physical-biological models, provides a tool to study the spatial dynamics of planktonic organisms. For the NS-BS, this modelling approach has gained considerable attention during the past decades, and it has been applied in numerous studies, both for early life stages of fish (e.g. Ådlandsvik & Sundby, 1994; Vikebø *et al.*, 2007; Opdal *et al.*, 2011), and *C. finmarchicus* (e.g. Bryant *et al.*, 1998; Torgersen & Huse, 2005; Samuelsen *et al.*, 2009).

Some of these studies investigated the degree of retention of *C. finmarchicus* in the Nordic Seas and advection onto the Norwegian continental shelf or into the Barents Sea. Bryant *et al.* (1998) found that *C. finmarchicus* populations could be retained for several years within the Norwegian Sea gyres in the Norwegian and Lofoten basins. However, individuals present farther north were rapidly flushed out of the model domain, for example into the Barents Sea. Torgersen & Huse (2005) found on the other hand that on-shelf transport from the Norwegian Sea was lower than expected, and that zooplankton advection into the Barents Sea was almost exclusively from the Norwegian continental shelf. They hypothesised that the coarse resolution of the oceanographic model (20˟20 km) caused an underestimation of the cross-shelf transport. This hypothesis was somewhat confirmed by Samuelsen *et al.* (2009), who observed an overall increase in cross-shelf transport when applying an embedded model with finer grid resolution (4.5˟4.5 km).

In most cases, coupled physical-biological models are formulated based on assumptions derived from field or experimental studies, and the results are compared to available field data. However, in recent years several studies on fish larval dynamics have explicitly coupled the output from particle tracking models with field data (Hidalgo *et al.*, 2012; Hufnagl *et al.*, 2014; Langangen *et al.*, 2014; Stige *et al.*, 2014). Here we apply a similar approach using information from large-scale biological field data of *C. finmarchicus* copepodites (33 years in both Norwegian Sea and Barents Sea areas) to represent endpoints of modelled drift trajectories, enabling us to estimate the yearly

spatiotemporal distribution of eggs, and thus potential adult spawning locations. With this approach, we ask the following questions:

- Where and when could the eggs giving rise to the observed copepodites in the NS-BS have been spawned?
- Is there variation in the predicted spawning locations between years?
- How important are climatic drivers for the dynamics of the back-calculated spawning locations?

Materials and methods

Survey data

The Knipovich Polar Research Institute of Marine Fisheries and Oceanography (PINRO, Murmansk, Russia) collected zooplankton data during bi-annual surveys between 1959 and 1992. These data have recently been digitised and are described in Nesterova (1990) and Kvile *et al.* (2014). Samples were collected with a Juday plankton net (37 cm diameter opening, 180 µm mesh size) with a closing mechanism, and specimens of *C. finmarchicus* were recorded as stage-specific abundances (ind. m^{-3}). In the present study we were interested in the variation in abundances of the new generation (G1), and therefore focused on abundance data of copepodite stages CI-CIV collected in spring (mid-April to late May). This period covers the mid- to late peak period of stages CI-CIII and early accumulation of stage CIV for south-western parts of the study area, and the early peak period of these stages for north-eastern parts of the study area (Kvile *et al.*, 2014). We did not include information on the stages CV-CVI, since they likely belong to the overwintered generation (G0), or on nauplii, which due to their small size are under-sampled by the mesh size used (Hernroth, 1987; Nichols & Thompson, 1991).

Further, we only used data collected in the upper water (0-60 m depth), corresponding to the depth layer with highest abundances of young copepodites during the growth season (Tande, 1988; Unstad & Tande, 1991; Dale & Kaartvedt, 2000; Kvile *et al.*, 2014). Finally, to avoid bias due to inter-annual variation in survey coverage, we only included data from repeatedly sampled transects, and within these transects, we only included survey stations sampled the same number of times or more as the average for that transect (i.e., if the stations in transect x had on average been sampled 5 times each, we excluded stations sampled four times or less). This resulted in three off-shelf transects and

five on-shelf transects (Fig. 1), with a minimum number of stations sampled per year ranging from 4 (NS.Open3) to 14 (Kola). Since the number of stations sampled varied between years, and the minimum of stations required excluded some transects for some of the years, the total number of stations per year ranged from a minimum of 6 (1959, only one transect included) to 66 (1975, all transects included).

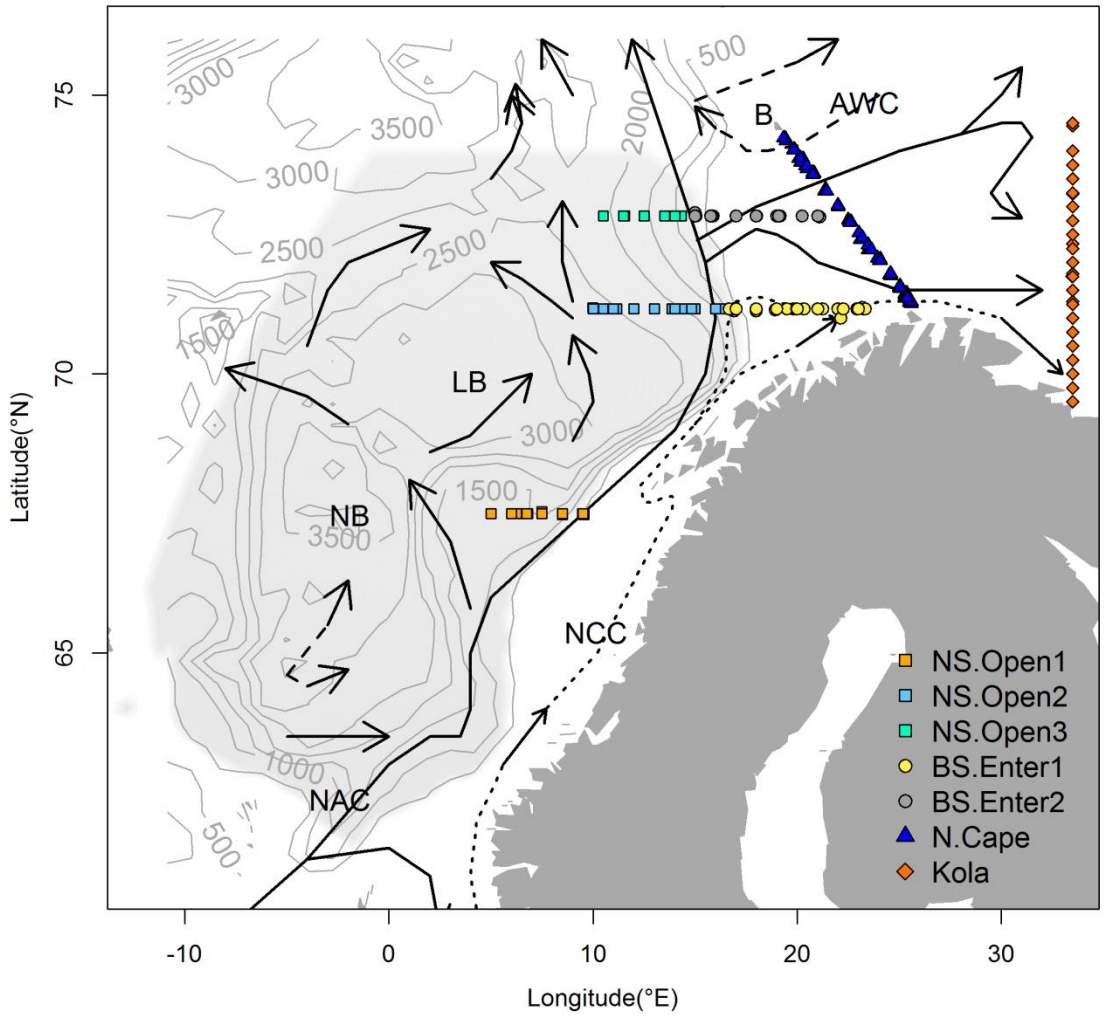

Fig. 1. The Norwegian and Barents Seas with depth contours at every 500 meters and the main surface currents indicated. Sampling transects are marked with different colours and symbols. Solid arrows: North Atlantic Current (NAC); dotted arrows: Norwegian Coastal Current (NCC); dashed arrows: Arctic water currents (AWC); NB: Norwegian Basin; LB: Lofoten Basin; B: Bjørnøya; grey shaded area: initial particle seeding area. The NAC branch which follows the 500 m depth contour northward and branches into the Barents Sea is the Norwegian Atlantic Current.

Particle-tracking

To simulate past ocean transport in the NS-BS, we extracted results from a numerical ocean model hindcast archive (Lien *et al.*, 2013, 2014), coupled to a regional ocean model system (ROMS, Haidvogel *et al.* (2008)). This archive provides hydrographic information for the NS-BS at daily intervals from 1959, with 4×4 km horizontal resolution and 32-layer terrain following vertical resolution, and has been shown to realistically reproduce observed hydrographic conditions and circulation features in these areas (Lien *et al.*, 2013). Particles representing possible origins of the new generation of *C. finmarchicus* (G1) spawned by individuals recently ascended from overwintering (G0) were seeded with an idealised homogenised Norwegian Sea-distribution. The distribution was constrained to avoid geographical bias regarding the origin of parents, assuming that shelf areas are too shallow to provide important overwintering sites (i.e. similarly as Samuelsen *et al.* (2009) and Hjøllo *et al.* (2012)). The seeding area was defined as every grid cell in the Norwegian Sea with bottom depth > 500 m, to the north of Shetland and the Faroese Islands, to the east of Iceland and Jan Mayen, and to the south of 74°N (Fig. 1). Each particle was seeded in the centre of a grid cell and fixed at 20 m depth, resulting in a total of 57 869 particles.

Particles were released 1st of March every year between 1959 and 1992. This coincides approximately with the start of the phytoplankton spring bloom (pre-bloom) in the Norwegian Sea (Rey, 2004). According to observations in the Norwegian Sea, *C. finmarchicus* egg production is usually initiated during the pre-bloom phase (March-April), and peaks during the main bloom period (May) (Niehoff *et al.*, 1999; Melle *et al.*, 2004, 2014; Stenevik *et al.*, 2007). To test for sensitivity to different features of the particle-tracking model, we ran the model simulation with deeper and shallower particle depths (20m ± 10m) and earlier and later release dates (1st of March ± 15 days).

Back-calculation of spawning location and time

To record particle drift trajectories and ambient temperature exposure, we applied a Lagrangian particle-tracking model (Ådlandsvik & Sundby, 1994). The particles were advected horizontally according to ambient velocities, using a Runge Kutta 4th order scheme with no diffusion. After drifting for up to three months, particles were "sampled" at the time and position of survey stations, within a three-day interval and 20 km radius (we also tested 20±5 km radius). Thus, for each survey station, in addition to the data on

observed copepodites, we obtained information on the number of simulated particles present at the time of the survey and their past trajectories.

We back-calculated the approximate age (in days) of observed copepodite stages CI-CIV in each station using the Belehrádek temperature function $D = a(T - \alpha)^b$, where D is development time (days), T is temperature (°C), α and b are constants, and a is a stage-specific parameter (from Campbell *et al.* (2001), Table A1, Appendix 2). The function gives the time between the median day of the egg period and the point when 50 % of the copepods have reached a specific stage (about 45 days from egg to CIV at 4°C). For a given station, the temperature experienced by an observed copepodite prior to sampling was assumed to equal the average temperature experienced by the particles "sampled" in the station, throughout their drift trajectories from the release date (1st of March) to the survey date. We first estimated particle-specific development times using the average temperature experienced by the particle in question, and then averaged these particle-specific estimates to get station-specific estimates (one value per development stage present). From the estimated development times, we could derive particle and station (averaged) specific spawning days, i.e. the sampling day minus the estimated development times for the four copepodite stages.

We identified potential spawning locations, i.e. locations where the observed copepodite stages could have been present as eggs, by back-calculating the particles "sampled" at a station to their position at the estimated (particle-specific) spawning dates. Since up to four stages (CI-CIV) with increasing ages could be present in a station, up to four different spawning locations could be estimated from each particle trajectory. If no particles were "sampled" in a station at the time of the survey, no back-calculated egg locations could be calculated. In addition to keeping track of all potential back-calculated spawning locations (up to four per particle sampled in a station), we also averaged these as the centre of gravity (CoG) spawning locations (one for each copepodite stage present in a station), giving all particles equal weight.

We predicted egg abundances at the time of spawning using a reversed exponential decay formula, $Ne_i = \frac{Nc_i}{e^{-\sum_1^i M_i D_i}}$, where the number of eggs (Ne_i) needed to yield the observed abundance of stage i copepodites (Nc_i) in a specific station depend on the cumulative mortality experienced up to that stage given (1) stage-specific instantaneous

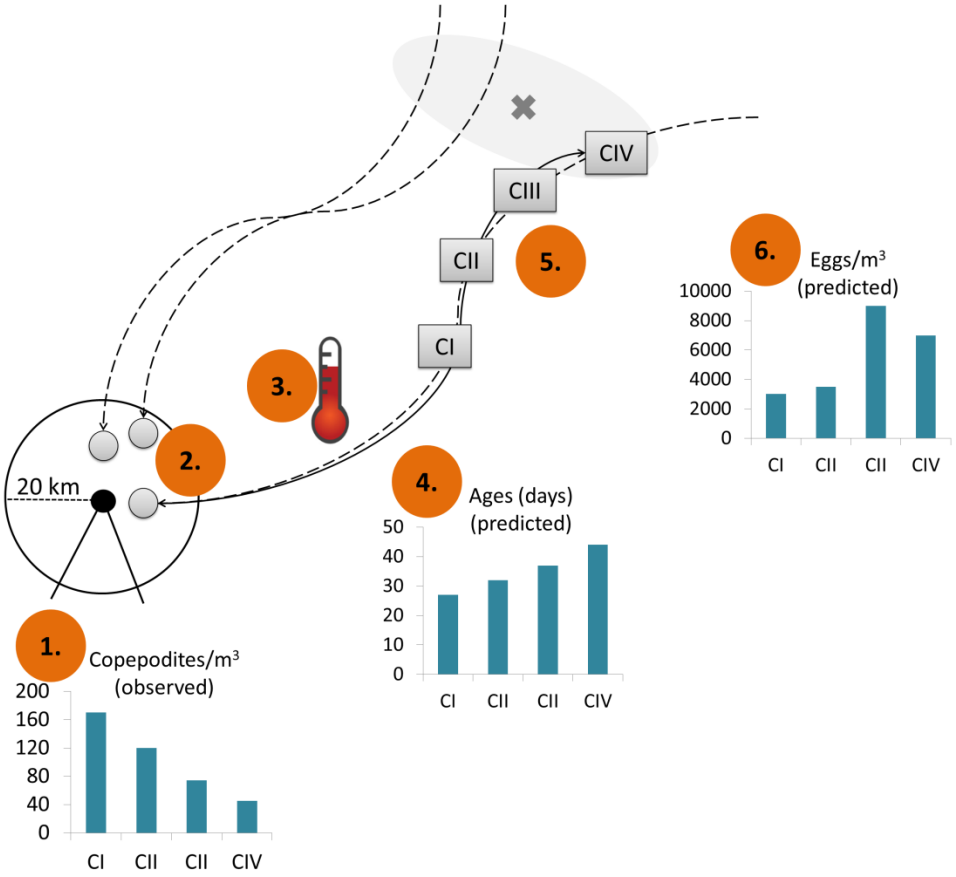

Fig. 2. The back-calculation approach step-by-step

1: At every survey station (black dot), we know the observed abundances of *C. finmarchicus* copepodite stages CI-CIV.

2: Within a three-day interval around the true sampling date, and a 20 km radius around the true sampling position, we "sample" modelled particles representing generation G1 copepodites (grey circles).

3: We estimate the average temperature experienced by the sampled particles during their drift trajectories from the release date to the sampling day (dashed arrows) using the ocean model output.

4: Using temperature-dependent development functions, we calculate the ages of the observed copepodite stages.

5: We find potential spawning locations by back-calculating the sampled particles through their past drift trajectories (solid arrows) until the estimated stage-specific egg spawning days (shown for the lower particle as grey squares). We also calculate CoGs spawning locations for each stage present as an average of all the particles sampled (shown as a grey cross for CIV).

6: Based on the observed copepodite abundances (Step 1), their estimated ages (Step 4) and stage-specific mortality estimates from the literature, we calculate the egg abundances needed to give rise to the observed copepodite abundances.

mortality rates suggested for the Nordic Seas by Aksnes & Blindheim (1996) (Table A2, Appendix 2), which were available for all relevant stages (eggs, NI-NVI, CI-CIV). Similarly as above, we first estimated particle-specific egg abundances using particle-specific development times, and then averaged these values to get mean estimates per station. See Fig. 2 for an overview of the back-calculation approach.

Analyses

Variation in spawning locations and time

Based on the back-calculation approach described above, we derived the following properties per transect:

1. CoG spawning locations. The sum of all CoG back-calculated spawning locations estimated for the stations in one transect.
2. Total potential spawning locations. The sum of all back-calculated spawning locations estimated from all particles sampled in the stations in one transect.
3. Drift distance (km) from egg to copepodite (CI-CIV). The distance between a survey station and its back-calculated stage-specific CoG spawning locations, summarised within each transect.
4. Development time (days) from egg to copepodite (CI-CIV), summarised within each transect.
5. Spawning period. The sum of all spawning days estimated for the stations in one transect.

Environmental effects on inter-annual variation in spawning time and locations

To understand the forcing behind the observed patterns in spawning locations and timing we related year-to-year variation in the features listed above with environmental variation using correlation analyses (Spearman rank correlation). In the significance test for the correlation, the effective number of degrees of freedom was adjusted to account for autocorrelation in the time-series following the method described by Quenouille (1952), modified by Pyper & Peterman (1998).

Single values per transect and year were obtained by calculating the CoG of the CoG spawning locations, the standard deviations of the longitudes and latitudes of the total potential spawning locations (a measure of the extent of the area), and the average drift distance and development time. To avoid confounding the variation in the variables with the developmental state of the sampled population, we only used the values for copepodite

stage CIV for the correlation analyses. With the exception of the total potential spawning locations, all features were weighted by the natural logarithm of the egg abundances back-calculated from the observed abundances of stage CIV.

As climate indices we used the winter (December-March) North Atlantic Oscillation (NAO) index (Hurrell & National Center for Atmospheric Research Staff, 2013) and sea temperature measurements from the Kola transect in the Barents Sea (70.5-72.5°N, 33.5°E) (Tereschenko 1996, provided by PINRO) (Appendix 1, Fig. A1). Both time-series are known to reflect the variation in the Atlantic waters of the NS-BS (Ottersen & Stenseth, 2001; Ingvaldsen & Loeng, 2009). A vertically averaged (0-200 m) Kola winter index was calculated from monthly values in January-April (i.e., similar approach as Ottersen & Stenseth 2001).

Results

Overview of the survey data

The sampling survey generally covered the seven transects in a southwest-northeast direction, starting in the southernmost Norwegian Sea transect (NS.Open1) in mid-late April, moving northwards to the transects at 71.17°N (NS.Open2 and BS.Enter1) and at 72.83°N (NS.Open3 and BS.Enter2) in early-mid May, and then eastward to the N.Cape- and Kola transects (Fig. 3). On average, both the total observed copepodite abundance (CI-CIV) and the contribution of the youngest copepodites (CI-CII) to the total abundance was higher for the on-shelf than the off-shelf transects.

Spawning locations and egg to copepodite transport

For a general overview of the potential spawning locations for *C. finmarchicus* copepodites sampled in the different transects, we pooled the back-calculated station-specific CoG spawning locations for all years and copepodite stages CI-CIV (Fig. 4). For the three off-shelf transects (NS.Open1-3), most back-calculated CoG spawning locations are found in a relatively limited area south of the transects. A few spawning locations are also estimated to the north, or in a larger distance south of the transects. The CoG spawning locations estimated for the two transects in the Barents Sea entrance (BS.Enter1-2) form a narrow band along the shelf edge south of the transects. In addition, there is an aggregation of

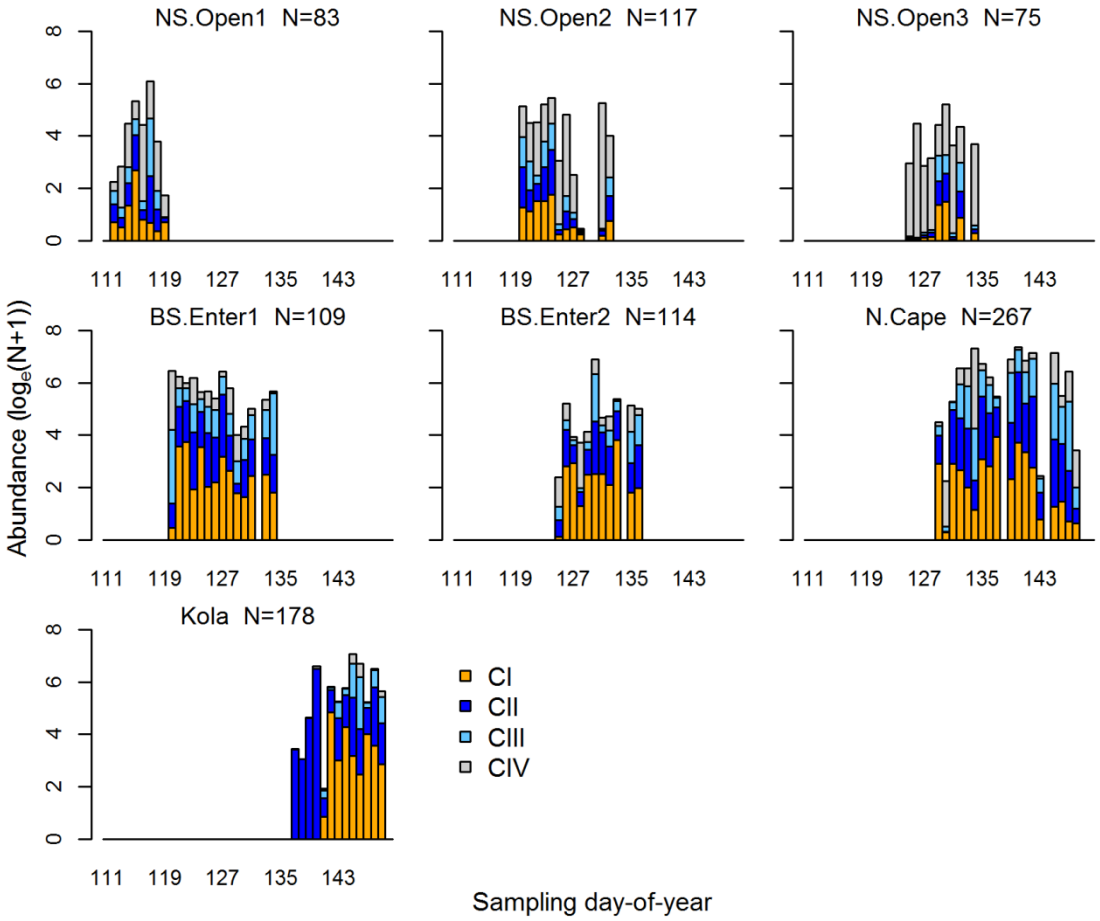

Fig. 3. Transect-specific abundances of copepodites per sampling day-of-year, averaged over all sampled years. The proportion of different stages is marked with different colours. X-axis: Day counting from the 1st of January. Y-axis: Average abundance of pooled stages CI-CIV (natural logarithm scale, added one to avoid negative values). N: total number of samples. Note that the exponential of the proportional (stage-specific) logarithmic values does not give the correct stage-specific abundances if more than one stage is present.

spawning locations on the shelf around, and north of, the transects, which is larger for BS.Enter1 than BS.Enter2. For the more eastern N.Cape transect, almost all back-calculated CoG spawning locations are found west of the transect on the Barents Sea shelf. Similarly, all CoG spawning locations for copepodites sampled on the Kola transect are found on the Barents Sea shelf. However, this estimate is based on only 22 particles sampled in 18 different stations in 1973 and 1975. For the other eight years investigated no particles were sampled at the Kola transect. The year-to-year variation in CoG spawning locations is shown in Figs. A2 and A3 (Appendix 1). Note that since we could only back-

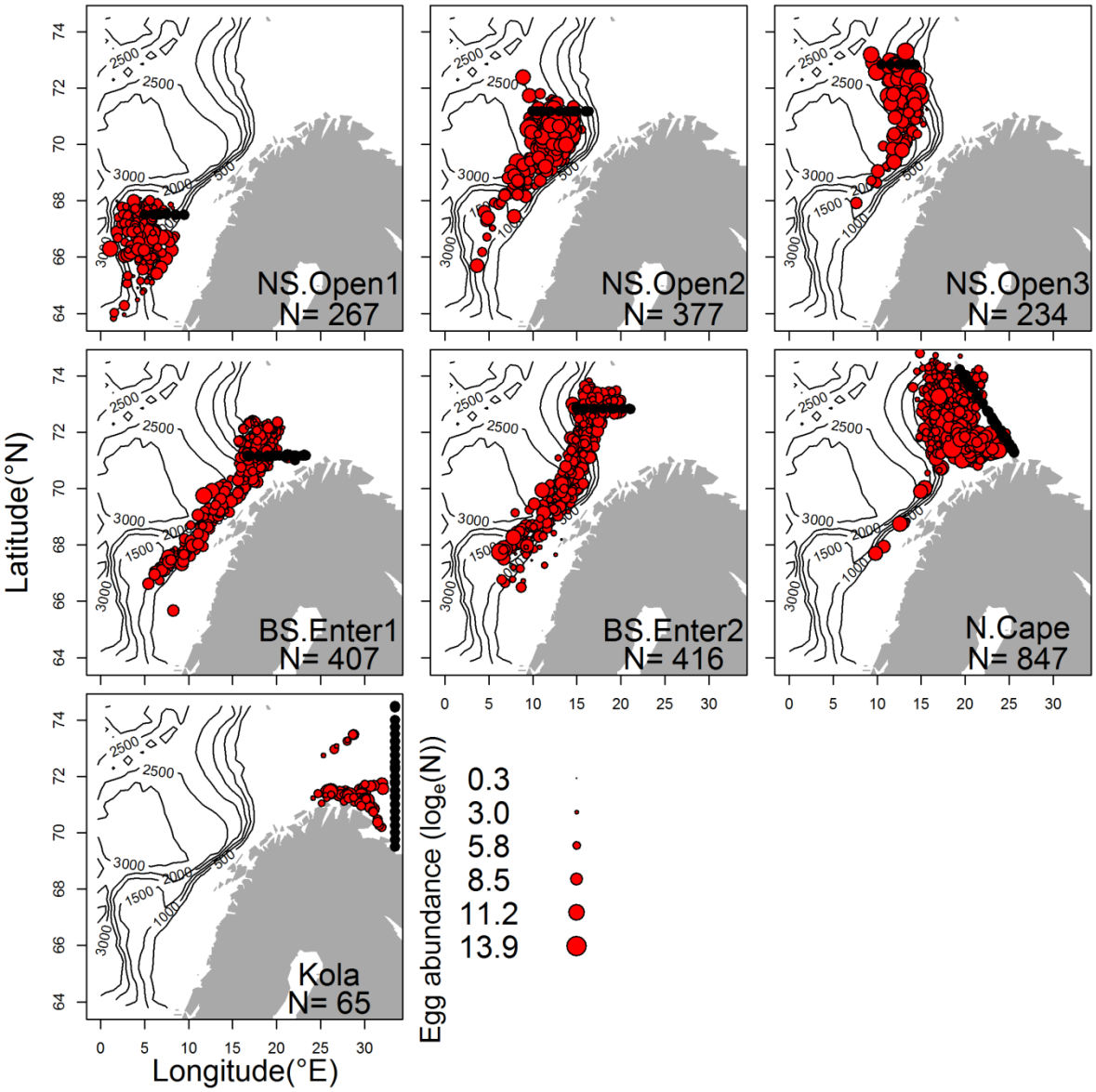

Fig. 4. Back-calculated CoG spawning locations (red dots) for different transects (black dots), pooled for all years and copepodite stages (CI-CIV). The size of dot is proportional to the egg abundance (natural logarithm) back-calculated to that location. N: Total number of back-calculated CoG spawning locations for each transect (number of stations sampled which received at least one particle * number of stages present in each of these stations).

calculate spawning locations and timing for the Kola transect for two years, it is excluded from the estimates of year-to-year variation.

Fig. 5 shows the variation in drift distance, development time and drift speed between the back-calculated CoG spawning locations and the survey stations. We use the period from egg to copepodite stage CIV as an example, but since development times of all stages present in a specific station were calculated using the same temperature history, drift

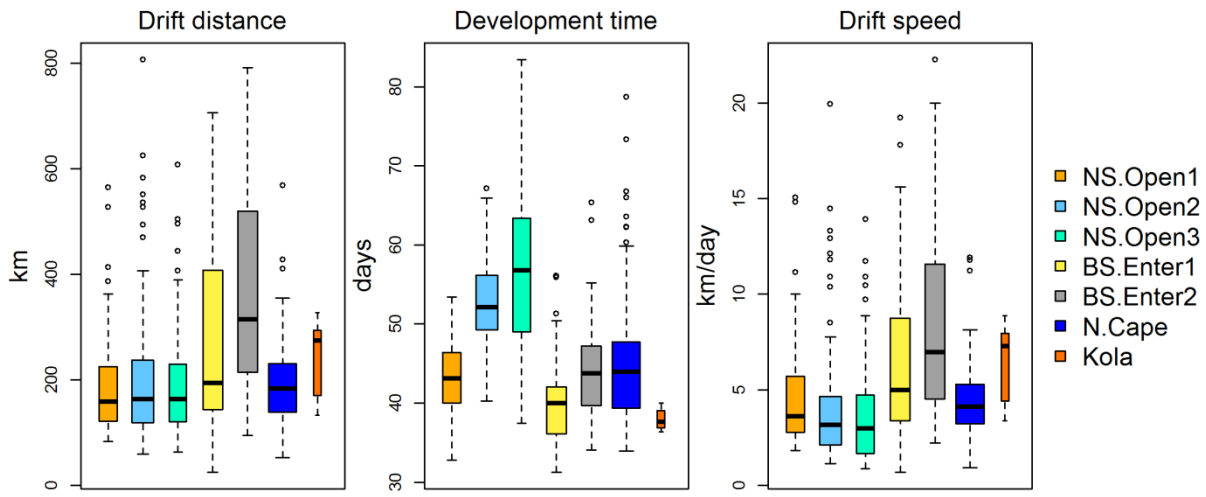

Fig. 5. Variation in drift distances (left), development time (middle) and drift speed (right) from egg to copepodite stage CIV for the different transects, pooled for all years. The box plots show the following properties: the median (black horizontal line), the interquartile range (coloured box), the adjacent values (dashed whiskers) and outliers (open dots). The width of the boxes is proportional to the transect sample size.

distances and development times are approximately proportional, but shorter and less variable, for the younger stages. The distance between survey stations and the back-calculated CoG spawning location varied more within than between transects (Fig. 5, left). For the three Norwegian Sea transects, the interquartile range of the drift distance from egg to CIV copepodites was approximately 120 to 240 km. Both the median and the variation in drift distances are higher for the two Barents Sea entrance transects, in particular for BS.Enter2, where egg-CIV drift distances are estimated to exceed 215 km for 75 % of the sampled stations. For the N. Cape and Kola transects, egg-CIV drift distances are on average around 180 and 275 km, respectively.

The estimated egg-CIV development times and drift speeds (drift distance/ development time) show that the larger variation in drift distance for the two Barents Sea entrance transects is driven by a higher and more variable drift speed, and not development time (Fig. 5, middle and right). Egg-CIV development time is estimated to be around 40 days for all transects except NS.Open2 and NS.Open3, where the median is 52 and 57 days, respectively. Year-to-year variation in egg-CIV drift distance and development time is shown in Fig. A4.

The total potential back-calculated spawning locations per transect and year is shown in Fig. A5 and yearly estimates of the variation in the total potential spawning locations for stage CIV (longitude and latitude standard deviations) in Fig. A6 (Appendix 1). In the off-shelf Norwegian Sea, the total potential back-calculated spawning locations form in some years a relatively circular feature around the transects, and in other years extend in a long belt along the shelf edge south of the transects and/or south of the Lofoten Basin. For the two transects in the Barents Sea entrance, the spawning locations often stretch far south along the shelf edge, and a varying number of locations are situated on the shelf between years. Eggs later transported as copepodites to the N.Cape transect are, for most years investigated, predominantly spawned on the Barents Sea shelf. Similarly, for the Kola transect, all potential spawning locations estimated for the two years with available information were restricted to the Barents Sea shelf.

Timing of spawning

The back-calculated spawning period is estimated to start earlier, and peak earlier, for the Norwegian Sea transects compared to the Barents Sea transects (Fig. 6 and Table A3, Appendix 2). The spawning period is estimated to fall between early March and early April for copepodites sampled in the Norwegian Sea, mid-March to mid-April for the Barents Sea entrance, and in mid-March to early May or mid-April to early May for the N.Cape and Kola transects, respectively.

It is important to keep in mind that these estimates are based on observations of the proportion of offspring surviving and recruiting into copepodite stages CI-CIV. Individuals not surviving past the earlier stages, or who were at the egg or naupliar or past the CIV stage at the time of sampling, are not included. The figures are therefore a truncated image of the true spawning period (see Discussion). Furthermore, the survey covered the different transects differently in time. For instance, the NS.Open1 transect was always sampled early, and the Kola transect late in the survey (Fig. 3).

Environmental effects on year-to-year variation in spawning dynamics

Overall there appears to be few consistent links between climate indices (NAO winter index and Kola winter temperature) and quantifiable features of spawning locations (Table 1). Both the climate indices are negatively correlated with mean development time, but for the other features, significant correlations only occur for 1 or 2 transects. The few

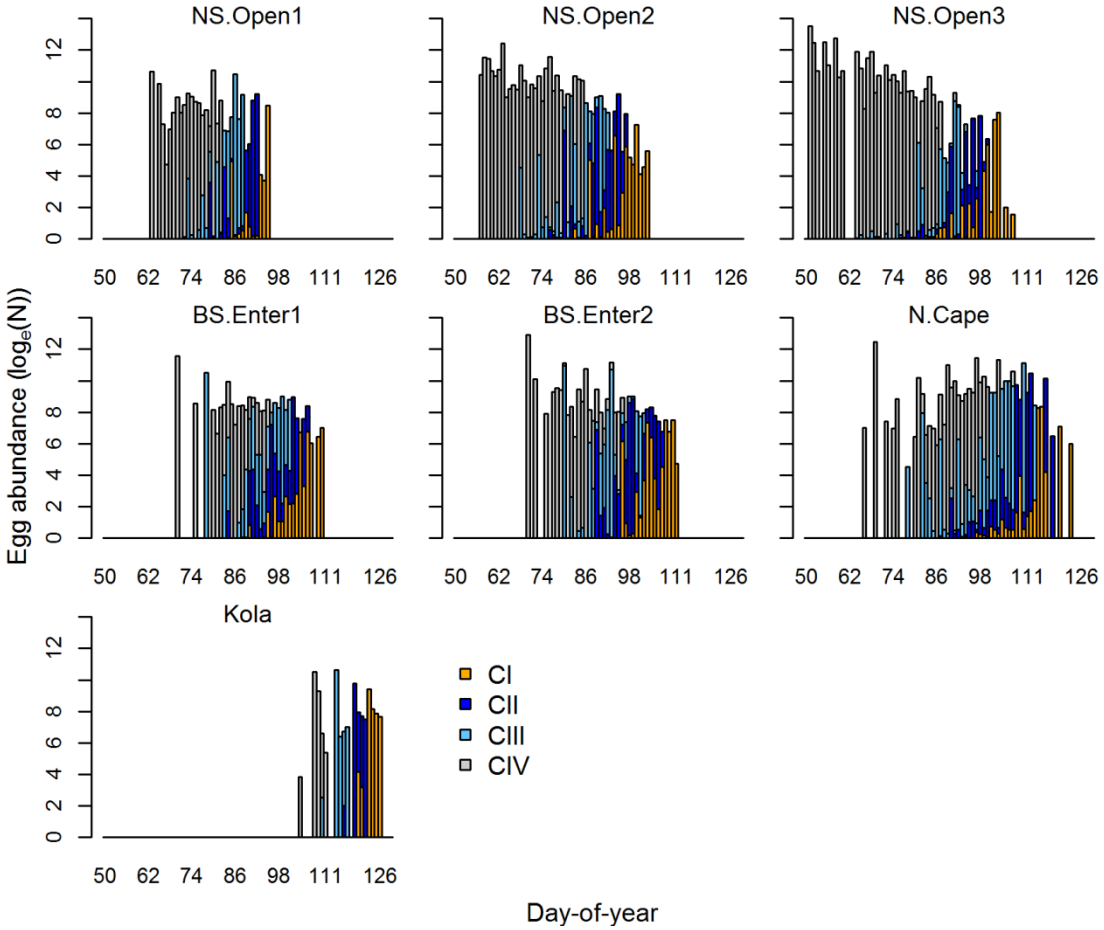

Fig. 6. Back-calculated spawning days and egg abundances per transects averaged for all years. X-axis: Back-calculated day-of-year, counting from the 1st of January. Y-axis: Back-calculated egg abundance summed for all stages (natural logarithm). The proportion of different eggs back-calculated from different stages is marked with different colours. Note that the exponential of the proportional (stage-specific) logarithmic values does not give the correct stage-specific egg abundance values if more than one stage is present.

correlations that occur might be random, or point to a tendency that the back-calculated spawning locations for the Norwegian Sea transects are located further south and west (i.e. farther away from the transects) in years with a positive NAO phase, and/or higher temperatures. This is indicated by some negative correlations between CoG latitude/longitude and NAO/temperature, and some positive correlations between mean drift distance/standard deviations of total spawning locations and NAO/temperature.

To illustrate the differences in the spatial dynamics of *C. finmarchicus* recruitment during a year with a negative (1969) versus a positive (1976) NAO phase, we plotted for these two years the total potential spawning locations (based on back-calculated spawning locations from all particles) for three of the transects (Fig. 7). In 1969, a year with a

negative NAO phase, the total potential spawning locations for the NS.Open2 transect are within a relatively limited area to the south of the transect, and their latitudinal standard deviation is below the overall mean (Fig. A6, Appendix 1). In 1976, a year with a positive NAO phase, the estimated spawning locations extend farther south along the shelf edge and to the south of the Lofoten Basin, which is reflected in higher-than-average longitudinal and latitudinal standard deviations (Fig. A6, Appendix 1), positive anomaly of egg-CIV drift distance (Fig. A4, Appendix 1) and negative anomalies of CoG longitude and latitude (Fig. A3, Appendix 1). For the BS.Enter1 and N.Cape transects the difference between the two years is not as striking, and 1976 is not characterised by more long-distance travellers than usual (Fig. A4, Appendix 1).

Sensitivity analyses

We tested the sensitivity of the back-calculating approach to (1) depth of the particles (2) particle release day and (3) sampling radius (Table A4, Appendix 2). There are differences in the number of particles sampled with different model setups. Specifically, for the on-shelf transects, earlier or later start date systematically increases (+11 to 533 %) or reduces (-8 to 90 %) the number of particles, respectively. For all transects, increasing or decreasing the sampling radius increases (+43 to 80 %) or reduces (-36 to 53 %) the number of particles, respectively. However, these differences do in most cases not seem to affect the results of the different analyses. The exception is the Kola transect, where the number of particles sampled in the "standard run" was very small (30), and changes in the pool of particles sampled have larger effects. Here, an increased number of particles sampled generally increases the number of spawning locations estimated in the vicinity of the transect (mean drift distance is reduced by 21 % in the "early" run) and influences the overall variation in spawning locations (the standard deviation of total spawning locations longitude and latitude differs from -100 to +149 % from the standard run depending on the model setup). The same tendency is found for the N.Cape transect. Changing the drift depth of the particles did not influence the results in any systematic manner.

Table 1. Spearman rank correlation coefficients (R_s) and statistical significance of the correlation (p) between climate indices (NAO winter index and Kola winter temperature) and yearly anomalies of (1-2) CoG spawning location longitude and latitude, (3) mean drift distance from egg to CIV, (4) mean development time from egg to CIV, and (5-6) variation in total spawning locations (longitude and latitude standard deviations). Significant correlations ($p \leq 0.05$) are shaded in grey. The Kola transect was not included since yearly values were only available for two years.

		1.CoG Lon		2.CoG Lat		3.Drift dist.		4.Dev.time		5.SD Lon		6.SD Lat	
	Transect	R_s	p	R_s	p	R_s	p	R_s	p	R_s	p	R_s	p
NAO	NS.Open1	-0.37	0.29	-0.32	0.29	0.22	0.26	-0.16	0.58	0.28	0.38	0.21	0.27
	NS.Open2	-0.16	0.51	-0.02	0.90	0.01	0.62	-0.03	0.71	0.27	0.46	0.34	0.30
	NS.Open3	-0.26	0.19	-0.53	0.01	0.58	0.01	-0.68	0.02	0.74	0.01	0.51	0.01
	BS.Enter1	0.11	0.87	0.03	0.91	-0.04	0.96	-0.64	0.05	0.31	0.18	0.37	0.23
	BS.Enter2	-0.13	0.52	0.08	0.97	0.09	0.68	-0.47	0.05	0.11	0.54	-0.10	0.95
	N.Cape	0.17	0.22	0.27	0.43	-0.31	0.29	-0.67	0.01	0.33	0.11	0.32	0.24
Kola temp.	NS.Open1	-0.06	0.95	-0.41	0.37	0.15	0.59	-0.69	0.04	-0.27	0.57	0.28	0.45
	NS.Open2	-0.54	0.10	-0.43	0.14	0.52	0.14	-0.32	0.11	0.41	0.25	0.57	0.18
	NS.Open3	-0.59	0.02	-0.46	0.35	0.48	0.26	-0.45	0.02	0.48	0.07	0.39	0.17
	BS.Enter1	0.39	0.17	0.33	0.20	-0.28	0.19	-0.80	0.00	0.02	0.97	0.16	0.74
	BS.Enter2	0.36	0.19	0.56	0.04	-0.52	0.08	-0.34	0.04	0.02	0.63	0.23	0.18
	N.Cape	0.17	0.59	0.44	0.07	-0.29	0.26	-0.58	0.01	0.34	0.40	-0.04	0.94

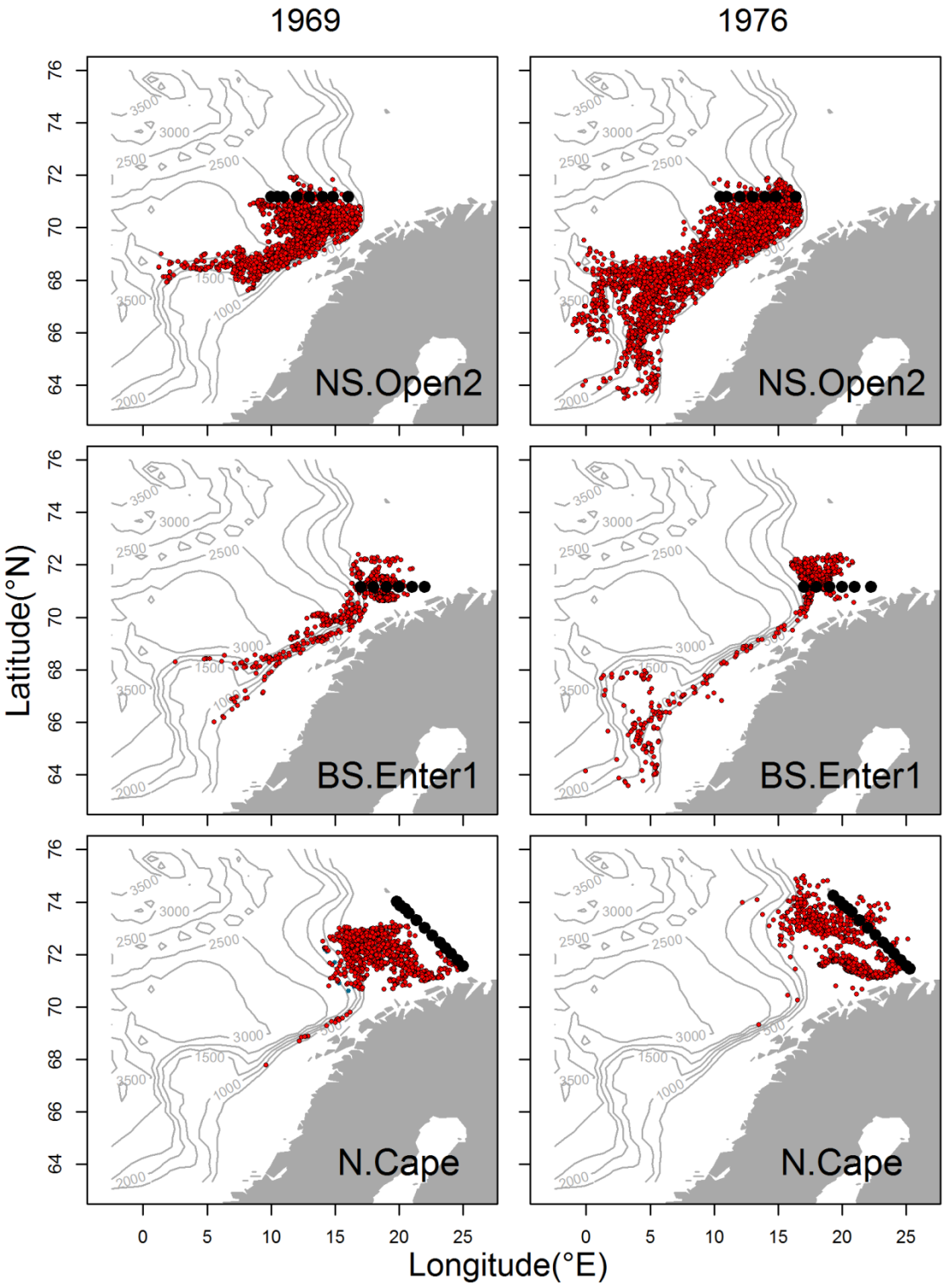

Fig. 7. Total potential spawning locations (red dots) for three transects (NS.Open2, BS.Enter1 and N.Cape, black dots) in 1969 (NAO-negative year, left) and 1976 (NAO-positive year, right). Spawning locations are back-calculated for all copepodite stages present in a station, based on all particles sampled in that station, and summed for all stations in the transect.

Discussion

Back-calculated spawning locations

The results showed that copepodites sampled in different transects, but also within the same transect, could have been subject to disparate current and temperature regimes and thus transport histories. Copepodites sampled in the Norwegian Sea were chiefly spawned less than 240 km upstream from the transects, while copepodites sampled in the Barents Sea entrance had in general a more mixed origin, from nearby shelf areas to several hundred kilometres south along the shelf edge (Figs. 4 and 5). Most copepodites sampled along the N.Cape transect farther east in the Barents Sea were likely spawned on the Barents Sea shelf. Similarly, from the few particles that reached the Kola transect, we could infer that copepodites sampled here likely originated from eggs spawned within the Barents Sea. The variation in drift distance was rather driven by drift speed than development time (Fig. 5), which in turn was driven by variation in ocean current speed or ambient temperature, respectively. Considering that the simulated particles did not possess any inherent behaviour, but were solely advected by ocean current hind casts, it is not surprising that the estimated spawning locations reflect the hydrodynamics in the NS-BS.

The dominant surface currents in the Norwegian Sea enter from the North Atlantic Ocean through two main channels, the Faroe-Shetland Channel (the Norwegian Atlantic Current) and the Iceland-Faroe ridge (the Faroe Current) (Blindheim, 2004). The Norwegian Atlantic Current has its main flow close to the Norwegian continental shelf (Fig. 1), and flows northward with a higher mean speed than the Faroe Current farther off-shelf. Along the path northward some water branches off westward and might enter the cyclonic gyres in the Norwegian and Lofoten Basins. The three Norwegian Sea transects are situated relatively close to the shelf edge where plankton transport likely is dominated by the Norwegian Atlantic Current, reflected in the positioning of most back-calculated spawning locations to the south along the shelf edge (Fig. 4).

Bryant *et al.* (1998) showed that *C. finmarchicus* is to a larger degree retained in the western and central Norwegian Sea, where the influence of gyres is strong, than in the eastern Norwegian Sea, where northward advection dominates. Speirs *et al.* (2004) also estimated that copepodites sampled within the Norwegian Sea gyre (at 66°N, 2°E), were primarily spawned within 50 km of the station. The fate of a zooplankton spawned in the central Norwegian Sea might thus largely differ from one spawned farther east. Retention

within gyres might explain the observed low influx from areas to the west of the Norwegian Sea transects.

Continuing north, one branch of the Norwegian Atlantic Current enters the Barents Sea. The main entrance is through Bjørnøyrenna, a trench about halfway between the Norwegian coast and Bjørnøya (Ingvaldsen & Loeng, 2009). The BS.Enter2 transect is situated in the Bjørnøyrenna area, and received the highest number of particles among the on-shelf transects (Table A4, Appendix 2). The more southern BS.Enter1 transect also received particles through Bjørnøyrenna, indicated by spawning locations estimated to the north of the transect (Figs. 4, A2, A5). Particles must also have crossed the shelf farther south, considering that for some years, potential spawning locations for the Barents Sea entrance transects were estimated on the Norwegian continental shelf. In fact, we observed the same for the Norwegian Sea transects, which implies that some particles were transported onto the Norwegian continental shelf, and then off again in direction of the Norwegian Sea transects.

In a recent study, Opdal & Vikebø (2015) identified two topographical features that appear to funnel much of the *C. finmarchicus* transport from the Norwegian Sea to the Norwegian shelf, namely the Træna trough in the Lofoten-Vesterålen area (67-70°N) and the Norwegian trench in the Møre area (62-64°N). Inspecting the total particle distribution for some years, we found that in addition to Bjørnøyrenna, cross-shelf transport happened in several areas along the Norwegian continental shelf (results not shown). However, the reoccurring presence of back-calculated on-shelf spawning locations at around 67^{o}N (Fig. A5) supports that the Træna trough is an important cross-shelf route for *C. finmarchicus* eggs and copepodites.

Transport of *C. finmarchicus* to the Barents Sea

Entering the Barents Sea, the Norwegian Atlantic Current slows down (Ingvaldsen & Loeng, 2009), and few particles reached the Kola transect within the time of the survey. Nevertheless, *C. finmarchicus* copepodites were present in the samples (Fig. 3). Several mechanisms might explain these findings: (1) presence of overwintering *C. finmarchicus* in the Barents Sea repopulating the area in spring, (2) advection of adult specimens from overwintering sites in fjords along the Norwegian coast or (3) model underestimation of transport into the Barents Sea.

It is generally debated to which extent the shallow Barents Sea is used for overwintering by *C. finmarchicus* (Tande, 1991; Aksnes & Blindheim, 1996; Arashkevich

et al., 2002), or if the new generation appearing in spring and summer are primarily advected from the Norwegian Sea (Skjoldal & Rey, 1989; Helle & Pennington, 1999; Edvardsen *et al.*, 2003b; Loeng & Drinkwater, 2007; Slagstad & Tande, 2007). It has been argued that due to the risk of the next generation being transported north outside favourable environmental conditions (Aksnes & Blindheim, 1996), and possibly fish predation in shallow shelf areas during winter (Bagøien *et al.*, 2001), *C. finmarchicus* is an expatriate in the Barents Sea. Also, the variability in zooplankton biomass in the Barents Sea has been shown to correlate with the strength of Atlantic water inflow (Helle & Pennington, 1999), and advected zooplankton biomass from the Norwegian Sea has been estimated to outnumber local production four times (Edvardsen *et al.*, 2003b).

However, other studies have demonstrated that changes in zooplankton biomass in the Norwegian Sea does not seem to affect the quantities in the Barents Sea entrance, and have estimated that local production is the most important contributor to *C. finmarchicus* biomass in the Barents Sea (Dalpadado *et al.*, 2012; Skaret *et al.*, 2014). Both field observations of overwintering *C. finmarchicus* in the Barents Sea (Manteifel, 1941; Pedersen, 1995) and a positive correlation between the inflow of Atlantic water one year and *C. finmarchicus* biomass in the Barents Sea the following year (Dvoretsky & Dvoretsky, 2014) support that *C. finmarchicus* might overwinter in the Barents Sea. The species also displays a broad range of overwintering depths in the Northwest Atlantic (Head & Pepin, 2007), including shallow shelf areas, and is known to overwinter in shallow waters in the Greenland Sea where cold Arctic Intermediate Water reaches the surface (Dale *et al.*, 1999),

Since the significance of overwintering in the Barents Sea is debated, we constrained the initial seeding distribution to Norwegian Sea areas with bottom depths below 500 m, which are known to be important overwintering areas (Melle *et al.*, 2004, 2014). If we had released particles within the Barents Sea, these would most likely have contributed significantly to the on-shelf transects. Note however, that due to the transport dynamics in the Barents Sea, *C. finmarchicus* would probably go extinct here after a few years if advection from the Norwegian Sea completely stopped (Skaret *et al.*, 2014).

Further, it is known that *C. finmarchicus* might overwinter in fjords along the Norwegian coast (Hirche, 1983; Kaartvedt, 1996). Eggs spawned by individuals ascending from fjords could potentially be transported with the Norwegian Coastal Current into the southern Barents Sea. Results from previous modelling studies have shown that both *C. finmarchicus* from the Norwegian continental shelf (Torgersen & Huse, 2005) and cod

eggs and larvae from coastal spawning grounds as far south as 58°N (Opdal *et al.*, 2011), end up in the Barents Sea due to the Norwegian Coastal Current. As inshore and fjord areas are not well resolved in the hydrodynamic model used in this study, it is to date not feasible to include fjords in the initial seeding distribution, but it should be considered in future work.

While the Norwegian Sea might not be the only source for *C. finmarchicus* copepodites observed in the Barents Sea in spring, the ocean model and/or the particle tracking procedure might also underestimate the transport of particles from the Norwegian Sea to the Barents Sea. First, we know that advancing the grid resolution from 20 km to 4.5 km increased cross-shelf transport (Torgersen & Huse, 2005; Samuelsen *et al.*, 2009), but we do not know whether the current resolution is sufficient for realistically recreating cross-shelf transport. According to Lien *et al.* (2013) the ocean model tends to underestimate current strength, and be more strongly controlled by topography than is realistic, which in turn would affect the model's ability to move particles across topographical structures such as the Norwegian continental shelf.

Secondly, earlier release day increased the number of particles advected into the Barents Sea (Table. A4, Appendix 2). Torgersen & Huse (2005) and Samuelsen *et al.* (2009) similarly found that earlier emergence from overwintering increased on-shelf transport, as westerly winds tend to be strongest in late winter/early spring. Earlier release date also generally increases the time available to reach the Barents Sea transects. But while the influx of particles increased with earlier release date, spawning was still estimated to take place primarily on the shelf (results not shown). One option is then that adults appearing in the surface in mid-February are advected in the upper water, and spawn after having drifted for some time. For the Kola transect, the number of particles sampled in the "early run" increased from a total of 30 to 190. Early appearance of females which are transported onto the shelf could thus be a source of *C. finmarchicus* to this area. On the other hand, in 77 % of the Kola stations (across all years) no particles were sampled even in the "early run".

Back-calculated spawning period

We found that the back-calculated spawning period from observed copepodite stages fell within a period from early March to early May, and started progressively later when we moved from the Norwegian Sea transects and eastward into the Barents Sea (Fig. 6, Table A3, Appendix 2). These general patterns reflect findings from field studies in the

Norwegian Sea showing that *C. finmarchicus* females produce eggs both during the phytoplankton pre-bloom (March-April) and the main bloom (May) (Niehoff *et al.*, 1999; Niehoff & Hirche, 2000; Stenevik *et al.*, 2007). For the Barents Sea, field studies suggest that egg production starts in mid-March with a peak in May (Diel & Tande, 1992; Melle & Skjoldal, 1998). However, variation in timing of the phytoplankton bloom between years (due to climatic variation) and in space (e.g. earlier bloom near the coast) make generalisations on the scale of the NS-BS difficult (Melle *et al.*, 2004, 2014; Bagøien *et al.*, 2012; Head *et al.*, 2013).

Speirs *et al.* (2004) back-calculated the main spawning period for copepodites sampled in the Norwegian Sea to be between the 10th of April and 10th of May, around a month later than our estimates for the Norwegian Sea. In general, our estimates fell within the early range of previous studies. The back-calculated spawning period was based on observations from a limited survey period, only including individuals who survived to the copepodite stages CI-CIV (temporal variation in mortality could influence the estimates), excluding eggs and naupliar stages. The results therefore clearly give a truncated picture of the actual spawning period in the NS-BS. Some egg production continues during the post-bloom period both in the Norwegian Sea and in the Barents Sea (Melle & Skjoldal, 1998; Stenevik *et al.*, 2007), and might even, at least in the south-western parts of the area, continue later in summer as G1 mature and spawn (Tande, 1991). Due to the timing of the survey, any spawning later than May is not included in the present study.

Environmental effects on back-calculated spawning locations and timing

To understand the forcing behind the observed year-to-year variation in estimated recruitment dynamics we correlated quantifiable features with commonly used climate indices. It is important to keep in mind that the ocean model is driven by climatic variation, in addition to topography, and that the results of the back-calculations are driven by the model, in addition to the observed data. We therefore expected that the results would reflect climatic variation. Considering this, it is perhaps surprising that the relations were relatively weak and inconsistent. This might be due to an underestimation in the ocean model of the effect of hydrographic variation compared to topography (Lien *et al.*, 2013). Alternatively, the climate indices used might not reflect smaller – or much larger – scale hydrographic variation which affects the observed patterns.

The most consistent correlations with regional climate indices were found for mean development time. These correlations are likely driven by the back-calculation approach

itself. Development time is calculated from the ambient temperature experienced by the simulated particles, and the Kola winter index likely reflects some of the temperature variation both in the Norwegian- and Barents Sea. A positive NAO phase is known to increase regional temperature in the NS-BS (Stenseth *et al.*, 2002), and can therefore influence development time through the same mechanism.

There was further a tendency that the back-calculated spawning locations for the Norwegian Sea transects were located farther upstream in years with a positive NAO phase, and/or higher temperatures. Atlantic water movement in the Norwegian Sea is influenced by the NAO. The Norwegian Atlantic Current tends to be stronger and closer to the coast during a positive NAO phase, and weaker and farther offshore during a negative phase (Blindheim, 2004; Sandø *et al.*, 2010). Considering that the Norwegian Sea transects were within the pathway of the Norwegian Atlantic Current, we expected that year-to-year variation in the current strength would be reflected in the estimated spawning locations. Specifically, in NAO-positive years eggs from potentially more distant spawning locations were transported into the survey transects (Fig. 7). This relationship did not emerge for the on-shelf transects. While a positive NAO index is associated with higher influx of Atlantic water and increased temperatures in the Barents Sea, the inflow is ultimately largely determined by local wind fields between Norway and Bjørnøya, and the effect of local atmospheric conditions can in periods reduce the link between the NAO index and Barents Sea climate (Ingvaldsen & Loeng, 2009). Potential relationships between the estimated spawning areas and time-series of local wind fields should be investigated in the future.

Future considerations

Two aspects of the present study should be given more attention in future investigations, namely the vertical distribution of particles, and the use of forward versus backward particle tracking. We will briefly discuss these issues below.

First, running the model with different drift depths (20m ± 10m) had little effect on back-calculated spawning areas and timing, and it thus seems that a 20 m drift depth covers the transport patterns within the upper water layer reasonably well. The earliest copepodite stages (CI-CIII) are primarily confined to the upper water layer (down to around 60 m) (Tande, 1988; Unstad & Tande, 1991; Dale & Kaartvedt, 2000), which was also found for the survey data (Kvile *et al.*, 2014). However, small differences in depth (10-30 m) could potentially have large impacts on drift trajectories in the NS-BS (Vikebø *et al.*, 2005, 2007; Fiksen *et al.*, 2007). Vikebø *et al.* (2005, 2007) found that fish larvae closer to the surface

(<20m) primarily drifted northwards and into the central Barents Sea with Atlantic currents through Bjørnøyrenna, while larvae in deeper waters (>40 m) tended to drift with the coastal current into the southern Barents Sea. In contrast to the present study, however, larvae were seeded on the Norwegian shelf, where the Norwegian coastal current plays a larger role.

While the youngest stages are confined to the upper waters, stage CIV can venture deeper (some CIV can enter overwintering, (Melle *et al.*, 2004)), which likely would influence drift trajectories in the present study. A more detailed examination of the effect of drift depth, potentially including dynamic, stage-specific vertical migrations, should be considered in future studies.

Secondly, we did a forward-in-time trajectory simulation (FITT), seeding a large and uniformly distributed number of particles in the Norwegian Sea, which is assumed to be the core distribution area of *C. finmarchicus*. Alternatively, seeding particles at the stations and running the simulation backwards in time (BITT) would require fewer particles and be more computationally efficient (most of the particles seeded with FITT end up outside the sampling stations). BITT would also circumvent some of the uncertainties in the present study, such as the date of release and the low number of particles that reached the Kola transect. If diffusion is not included and development is reversible (as in our simulations), a single particle BITT should equal that of a FITT (Batchelder, 2006).

However, in order to get a measure of variation in potential origins, diffusion cannot be ignored in BITT (Batchelder, 2006; Christensen *et al.*, 2007). Including diffusion leads to increased uncertainty as time progresses backward, and since dispersion does not operate identically forwards and backwards (Thygesen, 2011; Pepin *et al.*, 2013), BITT results should be interpreted as spatial probability fields of particle origins, likely being less conservative than FITT results. In addition, even using BITT, a number of initial considerations have to be made (e.g. the number and distribution of initial particles within the survey station). Nevertheless, testing both FITT and BITT (including diffusion) would likely expand our knowledge of potential spawning areas for *C. finmarchicus* in the NS-BS.

Summary

The use of coupled physical-biological models to study the dynamics of zoo- and ichthyoplankton has gained much popularity during the past decades (Miller, 2007), but to explicitly couple the models to observed biological data is a relatively novel approach. Here, we linked survey data of *C. finmarchicus* to the output of a hydrodynamic model to understand the spatiotemporal dynamics of *C. finmarchicus* spawning in the NS-BS. Due to the long time span and large spatial extent of the data, we could compare the results both across areas (off-shelf and on-shelf) and through time (1959 to 1992).

We identified three regions where, due to the hydrodynamics in the NS-BS, *C. finmarchicus* eggs and copepodites likely experience differing transport histories. (1) Off-shelf Norwegian Sea areas, where most copepodites likely were spawned in upstream areas < 240 km away; (2) The Barents Sea entrance, where copepodites could originate both from nearby shelf areas and several hundred kilometres south off-shelf; (3) Barents Sea, where most copepodites likely were spawned on the Barents Sea shelf. Few particles from the Norwegian Sea reached the Kola transect (33.5°E), which could indicate that the observed copepodites originate from additional sources. One interpretation is that *C. finmarchicus* dynamics in the Barents Sea is not, at least in the short-term, solely driven by advection from the Norwegian Sea, but also by local spawners (Dalpadado *et al.*, 2012; Skaret *et al.*, 2014). Further, this suggests that within the same season, predators on *C. finmarchicus* might encounter different food supplies in the Barents Sea compared to the Norwegian Sea.

From year to year, the back-calculated spawning areas for the Norwegian Sea and Barents Sea entrance transects varied between being mainly concentrated around the transects and stretching far south along the shelf edge, but any associations with climate variation were relatively weak and inconsistent. The effect of a positive NAO on the Norwegian Atlantic Current strength was somewhat visible in increased drift distances from egg to copepodite, and thus larger potential spawning areas within the eastern Norwegian Sea. This was not reflected in the Barents Sea, again pointing to the difficulties in predicting *C. finmarchicus* dynamics here based on patterns in the Norwegian Sea. For predators on *C. finmarchicus* early life stages, the location of the food source might thus be less stable, and potentially more dispersed, in the Norwegian Sea compared to south-western Barents Sea areas.

While this study has shed light on some aspects of *C. finmarchicus* recruitment dynamics, many issues remain unresolved. Specifically, we believe that the inclusion of fjords and inshore areas, and assessment of the relative contributions of spawners from these areas to the *C. finmarchicus* population in the Barents Sea should be investigated in future studies.

Aknowledgements

This study is a deliverable of the Nordic Centre for Research on Marine Ecosystems and Resources under Climate Change (NorMER), which is funded by the Norden Top-level Research Initiative sub-programme "Effect Studies and Adaptation to Climate Change". Hydrodynamic model results were made available by the Norwegian Meteorological Institute and the Institute of Marine Research, Norway, through the NRC funded SVIM-project. We are thankful to scientists and staff at Knipovich Polar Research Institute of Marine Fisheries and Oceanography, Murmansk, for providing the zooplankton data, and to L.C. Stige and Ø. Langangen for constructive comments on the manuscripts.

References

Aksnes DL, Blindheim J (1996) Circulation patterns in the North Atlantic and possible impact on population dynamics of *Calanus finmarchicus*. *Ophelia*, **44**, 7–28.

Arashkevich E, Wassmann P, Pasternak A, Wexels Riser C (2002) Seasonal and spatial changes in biomass, structure, and development progress of the zooplankton community in the Barents Sea. *Journal of Marine Systems*, **38**, 125–145.

Bagøien E, Kaartvedt S, Aksnes DL, Eiane K (2001) Vertical distribution and mortality of overwintering *Calanus*. *Limnology and Oceanography*, **46**, 1494–1510.

Bagøien E, Melle W, Kaartvedt S (2012) Seasonal development of mixed layer depths, nutrients, chlorophyll and *Calanus finmarchicus* in the Norwegian Sea – A basin-scale habitat comparison. *Progress in Oceanography*, **103**, 58–79.

Batchelder HP (2006) Forward-in-Time-/Backward-in-Time-Trajectory (FITT/BITT) Modeling of Particles and Organisms in the Coastal Ocean*. *Journal of Atmospheric and Oceanic Technology*, **23**, 727–741.

Blindheim J (2004) Oceanography and climate. In: *The Norwegian Sea Ecosystem* (ed Skjoldal HR), pp. 65–96. Tapir Academic Press, Trondheim.

Broms C, Melle W, Horne JK (2012) Navigation mechanisms of herring during feeding migration: the role of ecological gradients on an oceanic scale. *Marine Biology Research*, **8**, 461–474.

Bryant AD, Hainbucher D, Heath M (1998) Basin-scale advection and population persistence of *Calanus finmarchicus*. *Fisheries Oceanography*, **7**, 235–244.

Campbell RG, Wagner MM, Teegarden GJ, Boudreau CA, Durbin EG (2001) Growth and development rates of the copepod *Calanus finmarchics* reared in the laboratory. *Marine Ecology Progress Series*, **221**, 161–183.

Christensen A, Daewel U, Jensen H, Mosegaard H, St John M, Schrum C (2007) Hydrodynamic backtracking of fish larvae by individual-based modelling. *Marine Ecology Progress Series*, **347**, 221–232.

Cushing DH (1990) Plankton production and year-class strength in fish populations: an update of the match/mismatch hypothesis. *Advances in Marine Biology*, **26**, 249–293.

Dale T, Kaartvedt S (2000) Diel patterns in stage-specific vertical migration of *Calanus finmarchicus* in habitats with midnight sun. *ICES Journal of Marine Science*, **57**, 1800–1818.

Dale T, Bagøien E, Melle W, Kaartvedt S (1999) Can predator avoidance explain varying overwintering depth of *Calanus* in different oceanic water masses? *Marine Ecology Progress Series*, **179**, 113–121.

Dalpadado P, Ingvaldsen RB, Stige LC, Bogstad B, Knutsen T, Ottersen G, Ellertsen B (2012) Climate effects on Barents Sea ecosystem dynamics. *ICES Journal of Marine Science*, **69**, 1303–1316.

Diel S, Tande K (1992) Does the spawning of *Calanus finmarchicus* in high latitudes follow a reproducible pattern? *Marine Biology*, **113**, 21–31.

Dvoretsky VG, Dvoretsky AG (2014) Interannual fluctuations of zooplankton in the Kola Section (Barents Sea) in relation to environmental factors. *Biology Bulletin*, **41**, 378–386.

Edvardsen A, Slagstad D, Tande KS, Jaccard P (2003a) Assessing zooplankton advection in the Barents Sea using underway measurements and modelling. *Fisheries Oceanography*, **12**, 61–74.

Edvardsen A, Tande KS, Slagstad D (2003b) The importance of advection on production of *Calanus finmarchicus* in the Atlantic part of the Barents Sea. *Sarsia*, **88**, 261–273.

Eiane K, Tande KS (2009) Meso and macrozooplankton. In: *Ecosystem Barents Sea* (eds Sakshaug E, Johnsen G, Kovacs K), pp. 209–234. Tapir Academic Press, Trondheim.

Ellertsen B, Fossum P, Solemdal P, Sundby S (1989) Relation between temperature and survival of eggs and first-feeding larvae of northeast Arctic cod (*Gadus morhua* L.). *Rapports et Proces-Verbaux des Reunions du Conseil Inter- national pour l'Exploration de la Mer*, **191**, 209–219.

Fiksen Ø, Jørgensen C, Kristiansen T, Vikebø F, Huse G (2007) Linking behavioural ecology and oceanography: larval behaviour determines growth, mortality and dispersal. *Marine Ecology Progress Series*, **347**, 195–205.

Gislason A, Astthorsson OS (2002) The food of Norwegian spring-spawning herring in the western Norwegian Sea in relation to the annual cycle of zooplankton. *Sarsia*, **87**, 236–247.

Haidvogel DB, Arango H, Budgell WP et al. (2008) Ocean forecasting in terrain-following coordinates: Formulation and skill assessment of the Regional Ocean Modeling System. *Journal of Computational Physics*, **227**, 3595–3624.

Halvorsen E, Tande KS, Edvardsen A, Slagstad D, Pedersen OP (2003) Habitat selection of overwintering *Calanus finmarchicus* in the NE Norwegian Sea and shelf waters off Northern Norway in 2000-02. *Fisheries Oceanography*, **12**, 339–351.

Head E, Pepin P (2007) Variations in overwintering depth distributions of *Calanus finmarchicus* in the slope waters of the NW Atlantic continental shelf and the Labrador Sea. *Journal of Northwest Atlantic Fishery Science*, **39**, 49–69.

Head EJH, Melle W, Pepin P, Bagøien E, Broms C (2013) On the ecology of *Calanus finmarchicus* in the Subarctic North Atlantic: A comparison of population dynamics and environmental conditions in areas of the Labrador Sea-Labrador/Newfoundland Shelf and Norwegian Sea Atlantic and Coastal Waters. *Progress in Oceanography*, **114**, 46–63.

Helle K, Pennington M (1999) The relation of the spatial distribution of early juvenile cod (*Gadus morhua* L.) in the Barents Sea to zooplankton density and water flux during the period 1978-1984. *ICES Journal of Marine Science*, **56**, 15–27.

Hernroth L (1987) Sampling and filtration efficiency of two commonly used plankton nets. A comparative study of the Nansen net and the Unesco WP 2 net. *Journal of Plankton Research*, **9**, 719–728.

Hidalgo M, Gusdal Y, Dingsor GE et al. (2012) A combination of hydrodynamical and statistical modelling reveals non-stationary climate effects on fish larvae distributions. *Proceedings of the Royal Society B: Biological Sciences*, **279**, 275–283.

Hirche H-J (1983) Overwintering of *Calanus finmarchicus* and *Calanus helgolandicus*. *Marine Ecology Progress Series*, **11**, 281–290.

Hjort J (1914) Fluctuations in the great fisheries of northern Europe viewed in the light of biological research. *Rapports et Proces-Verbaux des Reunions du Conseil International pour l'Exploration de la Mer*, **20**, 1–228.

Hjøllo SS, Huse G, Skogen MD, Melle W (2012) Modelling secondary production in the Norwegian Sea with a fully coupled physical/primary production/individual-based *Calanus finmarchicus* model system. *Marine Biology Research*, **8**, 508–526.

Hufnagl M, Peck MA, Nash RDM, Dickey-Collas M (2014) Unravelling the Gordian knot! Key processes impacting overwintering larval survival and growth: A North Sea herring case study. *Progress in Oceanography*.

Hurrell J, National Center for Atmospheric Research Staff (2013) "The Climate Data Guide: Hurrell North Atlantic Oscillation (NAO) Index (PC-based)." Retrived from https://climatedataguide.ucar.edu/climate-data/hurrell-north-atlantic-oscillation-nao-index-pc-based.

Ingvaldsen RB, Loeng H (2009) Physical oceanography. In: *Ecosystem Barents Sea* (eds Sakshaug E, Johnsen G, Kovacs K), pp. 33–64. Tapir Academic Press, Trondheim.

Kaartvedt S (1996) Habitat preference during overwintering and timing of seasonal vertical migration of *Calanus finmarchicus*. *Ophelia*, **44**, 145–156.

Kristiansen T, Drinkwater KF, Lough RG, Sundby S (2011) Recruitment variability in North Atlantic cod and match-mismatch dynamics. *PloS one*, **6**, e17456.

Kvile K, Dalpadado P, Orlova E, Stenseth N, Stige L (2014) Temperature effects on *Calanus finmarchicus* vary in space, time and between developmental stages. *Marine Ecology Progress Series*, **517**, 85–104.

Langangen Ø, Stige LC, Yaragina NA, Ottersen G, Vikebø FB, Stenseth NC (2014) Spatial variations in mortality in pelagic early life stages of a marine fish (*Gadus morhua*). *Progress in Oceanography*, **127**, 96–107.

Lien VS, Gusdal Y, Albretsen J, Melsom A, Vikebø F (2013) Evaluation of a Nordic Seas 4 km numerical ocean model hindcast archive (SVIM), 1960-2011. *Fisken og Havet*, **7**, 1–80.

Lien VS, Gusdal Y, Vikebø FB (2014) Along-shelf hydrographic anomalies in the Nordic Seas (1960–2011): locally generated or advective signals? *Ocean Dynamics*, **64**, 1047–1059.

Loeng H (1991) Features of the physical oceanographic conditions of the Barents Sea. *Polar Research*, **10**, 5–18.

Loeng H, Drinkwater K (2007) An overview of the ecosystems of the Barents and Norwegian Seas and their response to climate variability. *Deep Sea Research Part II: Topical Studies in Oceanography*, **54**, 2478–2500.

Manteifel BP (1941) Plankton and herring in the Barents Sea. *Trudy PINRO. Transactions of the Knipovich Polar Scientific Institute of Sea-Fisheries and Oceanography Murmansk*, **7**, 125–218 (in Russian).

Melle W, Skjoldal H (1998) Reproduction and development of *Calanus finmarchicus, C. glacialis* and *C. hyperboreus* in the Barents Sea. *Marine Ecology Progress Series*, **169**, 211–228.

Melle W, Ellertsen B, Skjoldal HR (2004) Zooplankton: The link to higher trophic levels. In: *The Norwegian Sea Ecosystem* (ed Skjoldal HR), pp. 137–202. Tapir Academic Press, Trondheim.

Melle W, Runge J, Head E et al. (2014) The North Atlantic Ocean as habitat for *Calanus finmarchicus*: Environmental factors and life history traits. *Progress in Oceanography*, **129**, 244–284.

Miller T (2007) Contribution of individual-based coupled physical-– biological models to understanding recruitment in marine fish populations. *Marine Ecology Progress Series*, **347**, 127–138.

Nesterova VN (1990) *Plankton biomass along the drift route of cod larvae (reference material)*. PINRO, Murmansk (in Russian), 64 pp.

Nichols JH, Thompson AB (1991) Mesh selection of copepodite and nauplius stages of four calanoid copepod species. *Journal of Plankton Research*, **13**, 661–671.

Niehoff B, Hirche H (2000) The reproduction of *Calanus finmarchicus* in the Norwegian Sea in spring. *Sarsia*, **85**, 15–22.

Niehoff B, Klenke U, Hirche H, Irigoien X, Head R, Harris R (1999) A high frequency time series at Weathership M, Norwegian Sea, during the 1997 spring bloom:the reproductive biology of *Calanus finmarchicus*. *Marine Ecology Progress Series*, **176**, 81–92.

Opdal AF, Vikebø FB (2015) Long-term stability in modelled zooplankton influx could uphold major fish spawning grounds on the Norwegian continental shelf. *Canadian Journal of Fisheries and Aquatic Sciences*.

Opdal AF, Vikebø F, Fiksen Ø (2011) Parental migration, climate and thermal exposure of larvae: spawning in southern regions gives Northeast Arctic cod a warm start. *Marine Ecology Progress Series*, **439**, 255–262.

Ottersen G, Stenseth NC (2001) Atlantic climate governs oceanographic and ecological variability in the Barents Sea. *Limnology and Oceanography*, **46**, 1774–1780.

Pedersen G (1995) Why does a component of *Calanus finmarchicus* stay in the surface waters during the overwintering period in high latitudes? *ICES Journal of Marine Science*, **52**, 523–531.

Pedersen OP, Tande KS, Slagstad D (2001) A model study of demography and spatial distribution of *Calanus finmarchicus* at the Norwegian coast. *Deep Sea Research Part II: Topical Studies in Oceanography*, **48**, 567–587.

Pepin P, Han G, Head EJ (2013) Modelling the dispersal of *Calanus finmarchicus* on the Newfoundland Shelf: implications for the analysis of population dynamics from a high frequency monitoring site. *Fisheries Oceanography*, **22**, 371–387.

Pyper BJ, Peterman RM (1998) Comparison of methods to account for autocorrelation in correlation analyses of fish data. *Canadian Journal of Fisheries and Aquatic Sciences*, **55**, 2127–2140.

Quenouille MH (1952) *Associated Measurements*. Butterworth, London, 241 pp.

Rey F (2004) Phytoplankton: the grass of the sea. In: *The Norwegian Sea Ecosystem* (ed Skjoldal HR), pp. 97–136. Tapir Academic Press, Trondheim.

Samuelsen A, Huse G, Hansen C (2009) Shelf recruitment of *Calanus finmarchicus* off the west coast of Norway: role of physical processes and timing of diapause termination. *Marine Ecology Progress Series*, **386**, 163–180.

Sandø AB, Nilsen JEØ, Gao Y, Lohmann K (2010) Importance of heat transport and local air-sea heat fluxes for Barents Sea climate variability. *Journal of Geophysical Research*, **115**, C07013.

Skaret G, Dalpadado P, Hjøllo SS, Skogen MD, Strand E (2014) *Calanus finmarchicus* abundance, production and population dynamics in the Barents Sea in a future climate. *Progress in Oceanography*, **125**, 26–39.

Skjoldal HR, Rey F (1989) Pelagic production and variability of the Barents Sea ecosystem. In: *Biomass Yields and Geography of Large Marine Ecosystems* (eds Sherman K, Alexander LM), pp. 241–286. American Association for the Advancement of Science. Selected Symposia.

Slagstad D, Tande KS (2007) Structure and resilience of overwintering habitats of *Calanus finmarchicus* in the Eastern Norwegian Sea. *Deep Sea Research Part II: Topical Studies in Oceanography*, **54**, 2702–2715.

Speirs DC, Gurney WSC, Holmes SJ et al. (2004) Understanding demography in an advective environment: modelling *Calanus finmarchicus* in the Norwegian Sea. *Journal of Animal Ecology*, **73**, 897–910.

Stenevik EK, Melle W, Gaard E, Gislason A, Broms CTÅ, Prokopchuk I, Ellertsen B (2007) Egg production of *Calanus finmarchicus* — A basin-scale study. *Deep Sea Research Part II: Topical Studies in Oceanography*, **54**, 2672–2685.

Stenseth NC, Mysterud A, Ottersen G, Hurrell JW, Chan K-S, Lima M (2002) Ecological effects of climate fluctuations. *Science (New York, N.Y.)*, **297**, 1292–6.

Stige LC, Langangen Ø, Yaragina NA et al. (2014) Combined statistical and mechanistic modelling suggests food and temperature effects on survival of early life stages of Northeast Arctic cod (*Gadus morhua*). *Progress in Oceanography*, **134**, 138–151.

Sundby S (2000) Recruitment of Atlantic cod stocks in relation to temperature and advection of copepod populations. *Sarsia*, **85**, 277–298.

Tande KS (1988) An evaluation of factors affecting vertical distribution among recruits of *Calanus finmarchicus* in three adjacent high-latitude localities. *Hydrobiologia*, **167-168**, 115–126.

Tande KS (1991) *Calanus* in North Norwegian fjords and in the Barents Sea. *Polar Research*, **10**, 389–408.

Tereshchenko VV (1996) Seasonal and year-to-year variations of temperature and salinity along the Kola meridian transect. *ICES CM 1996/C: 11*.

Thygesen UH (2011) How to reverse time in stochastic particle tracking models. *Journal of Marine Systems*, **88**, 159–168.

Torgersen T, Huse G (2005) Variability in retention of *Calanus finmarchicus* in the Nordic Seas. *ICES Journal of Marine Science*, **62**, 1301–1309.

Unstad KH, Tande KS (1991) Depth distribution of *Calanus finmarchicus* and *C. glacialis* in relation to environmental conditions in the Barents Sea (eds Sakshaug E, Hopkins CCE, 0ritsland NA). *Polar Research*, **10**, 409–420.

Vikebø F, Sundby S, Adlandsvik B, Fiksen O (2005) The combined effect of transport and temperature on distribution and growth of larvae and pelagic juveniles of Arcto-Norwegian cod. *ICES Journal of Marine Science*, **62**, 1375–1386.

Vikebø F, Jørgensen C, Kristiansen T, Fiksen Ø (2007) Drift, growth, and survival of larval Northeast Arctic cod with simple rules of behaviour. *Marine Ecology Progress Series*, **347**, 207–219.

Ådlandsvik B, Sundby S (1994) Modelling the transport of cod larvae from the Lofoten area. *ICES Mar Sci. Symp.*, **198**, 379–392.

Appendix 1. Supplementary figures

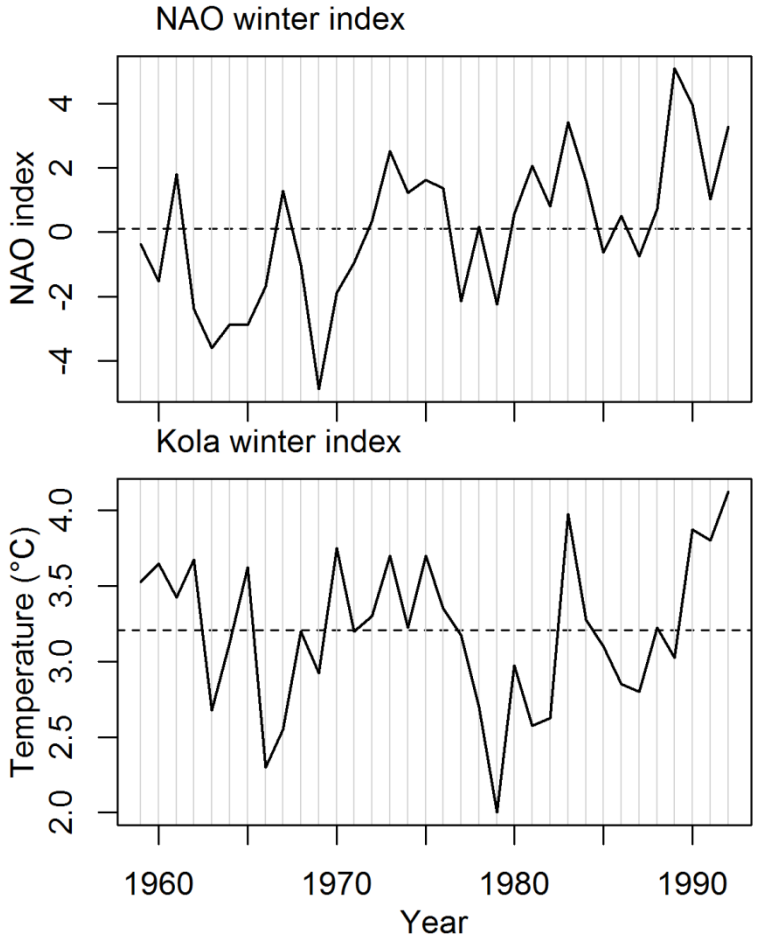

Fig. A1. Time series of the NAO winter index (upper) and the Kola winter index (lower). Dashed horizontal line: overall mean of the index for the years in question (1959-1992). The Kola winter index is the mean of the monthly mean values 0-200 m in January-April.

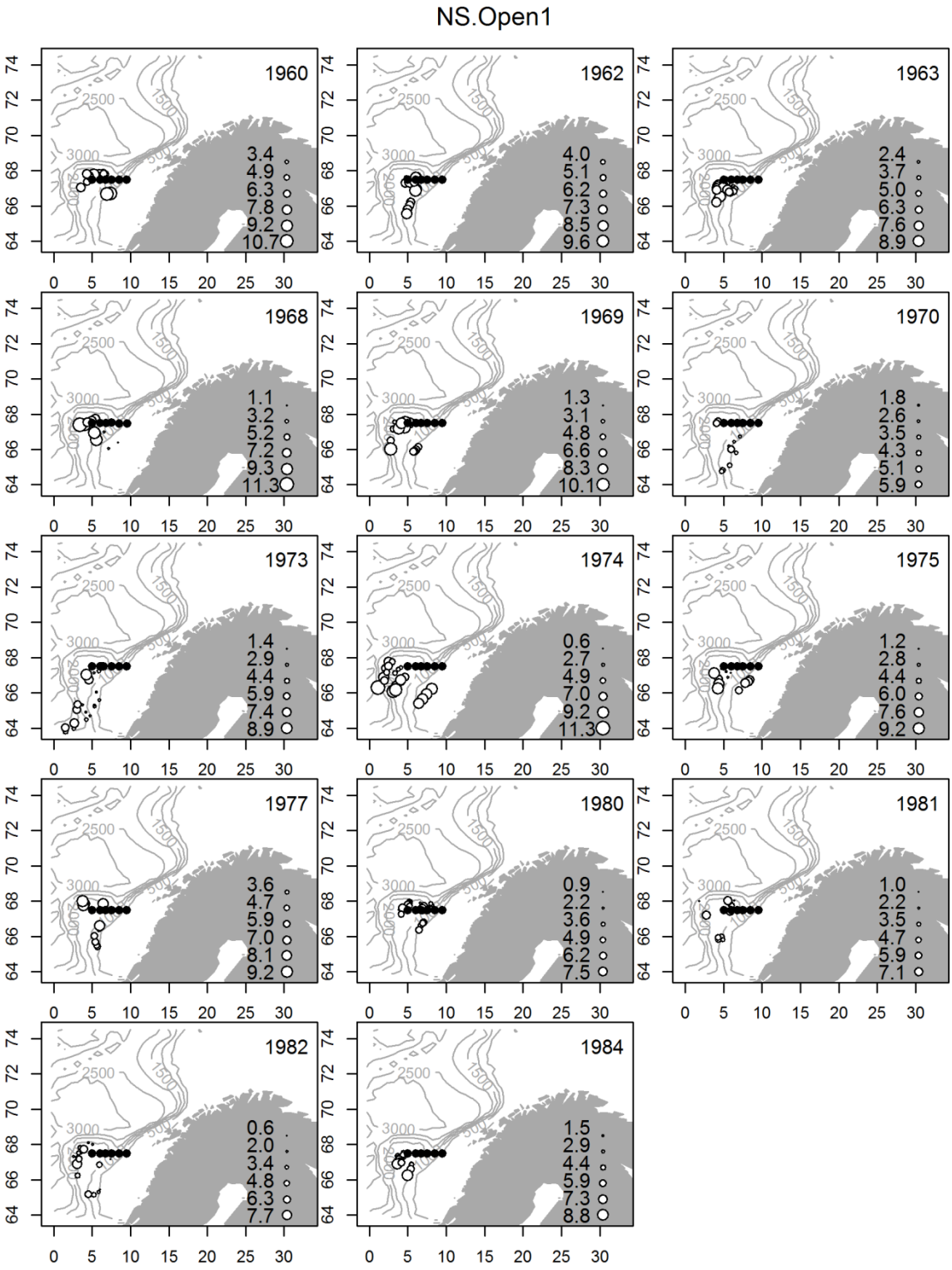

Fig. A2. Year-to-year variation in back-calculated CoG spawning locations (white dots) for different transects (black dots), pooled for all copepodite stages (CI-CIV). The size of dot is proportional to the egg abundance (natural logarithm) back-calculated to that location. The Kola transect is not displayed since estimates from only two years were available. X-axis: longitude, y-axis: latitude.

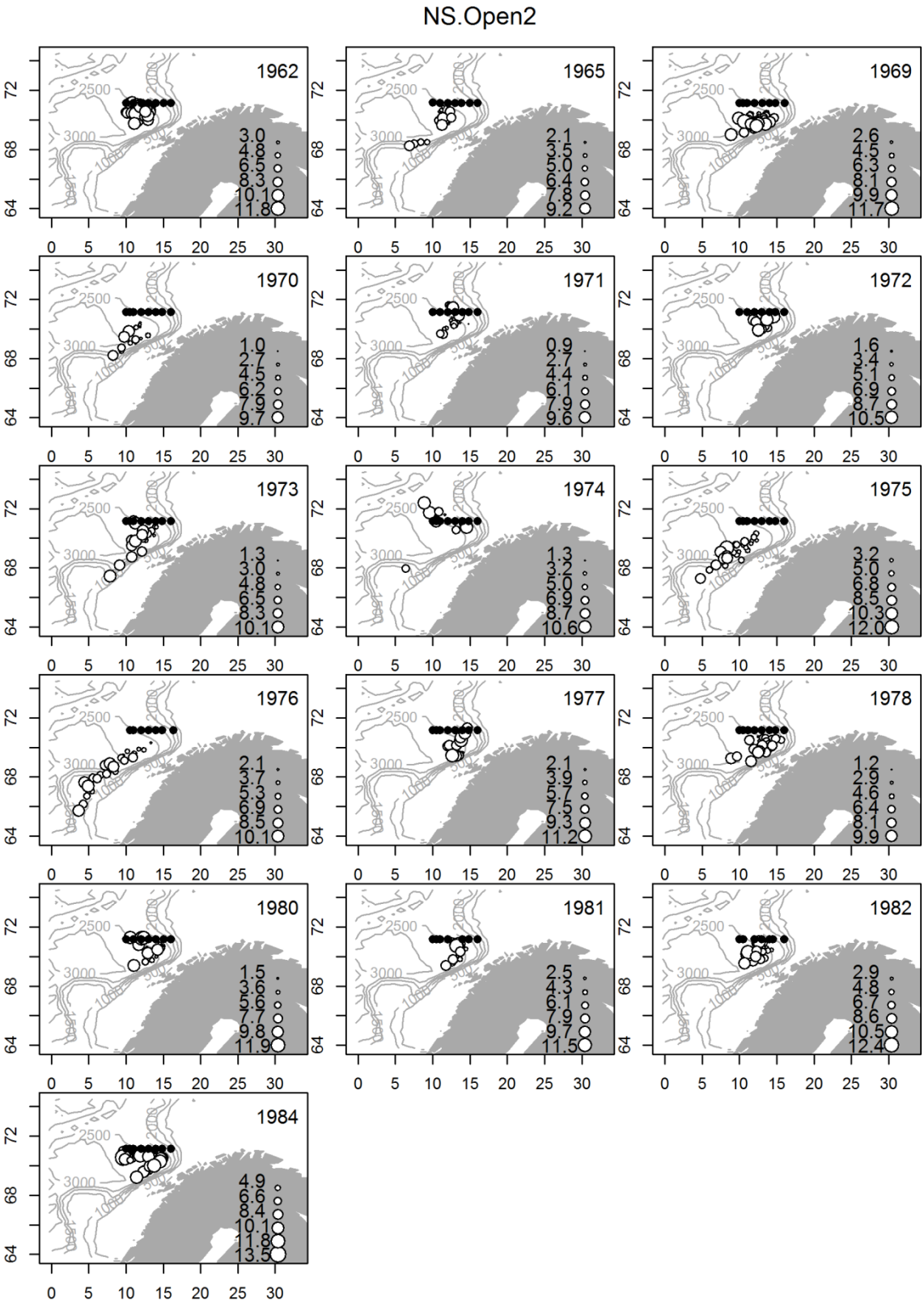

Fig. A2. (continued)

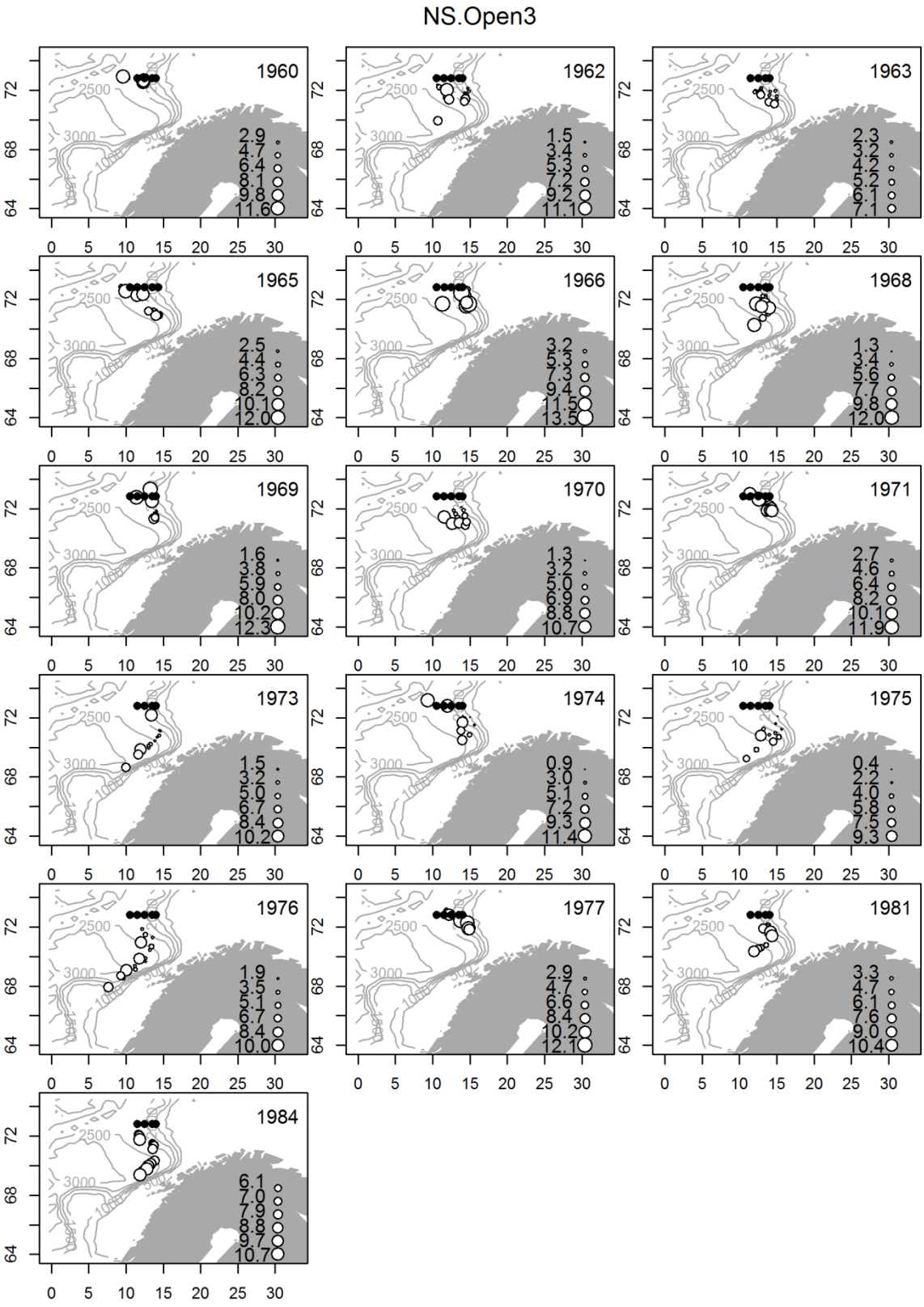

Fig. A2. (continued)

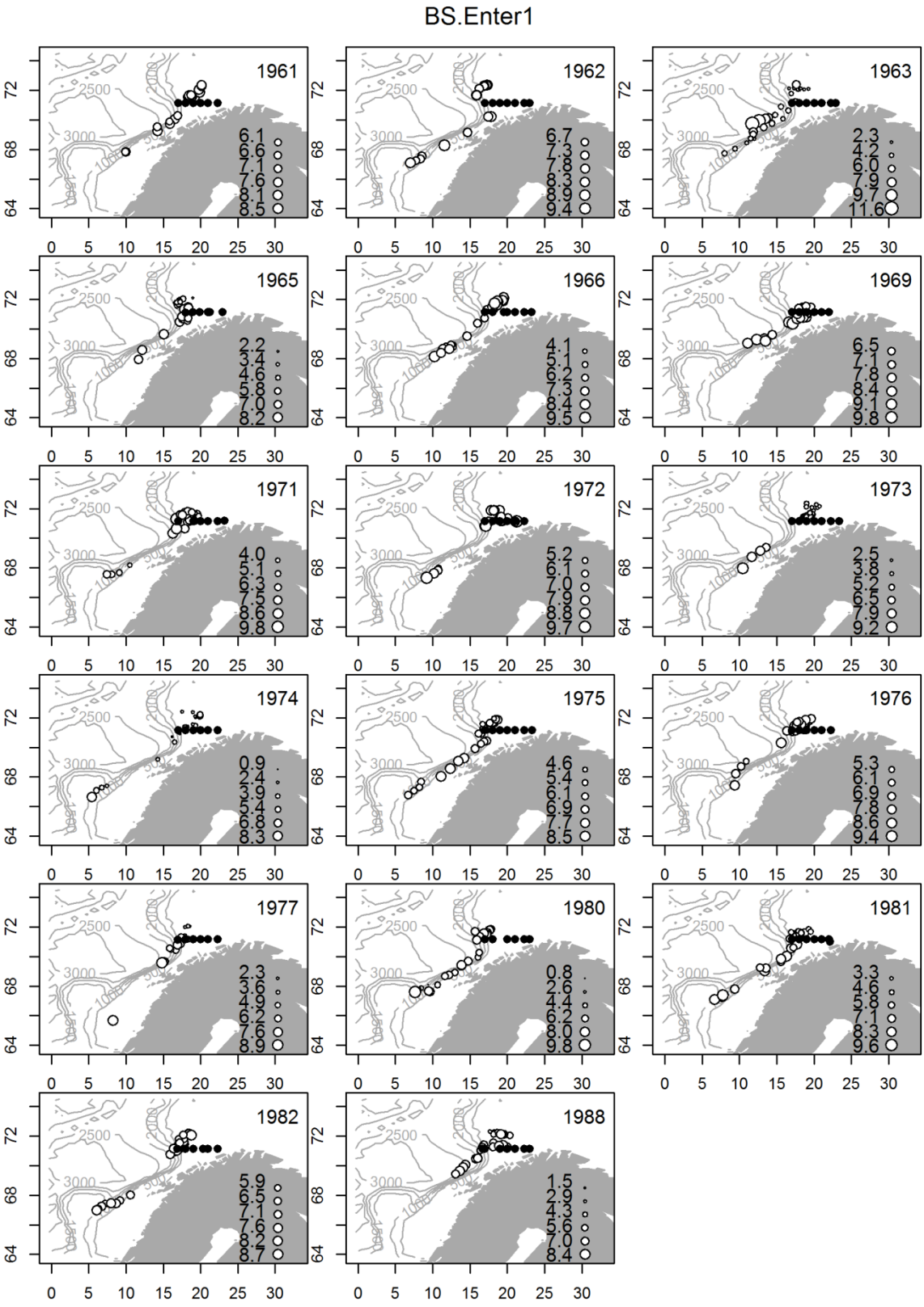

Fig. A2. (continued)

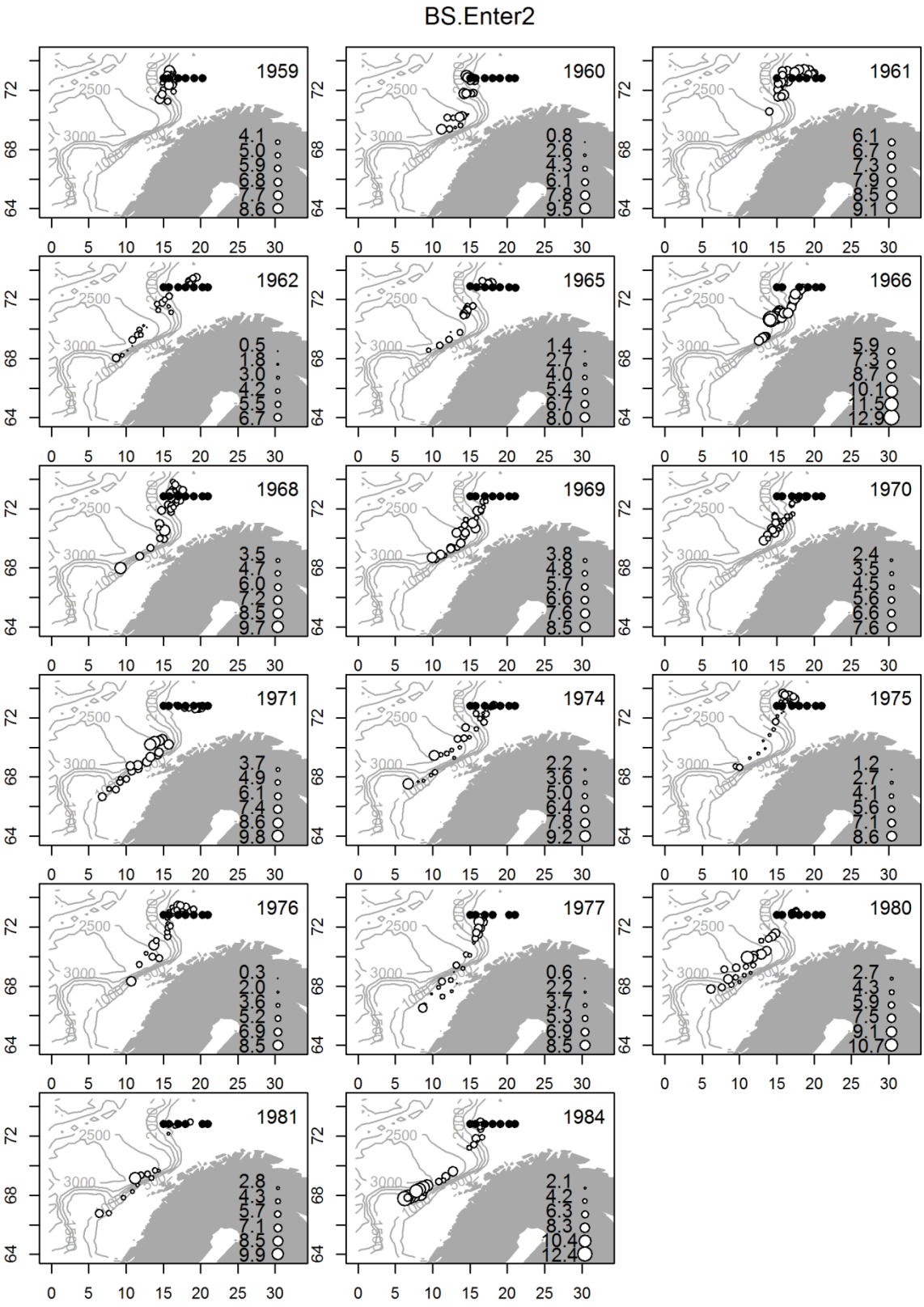

Fig. A2. (continued)

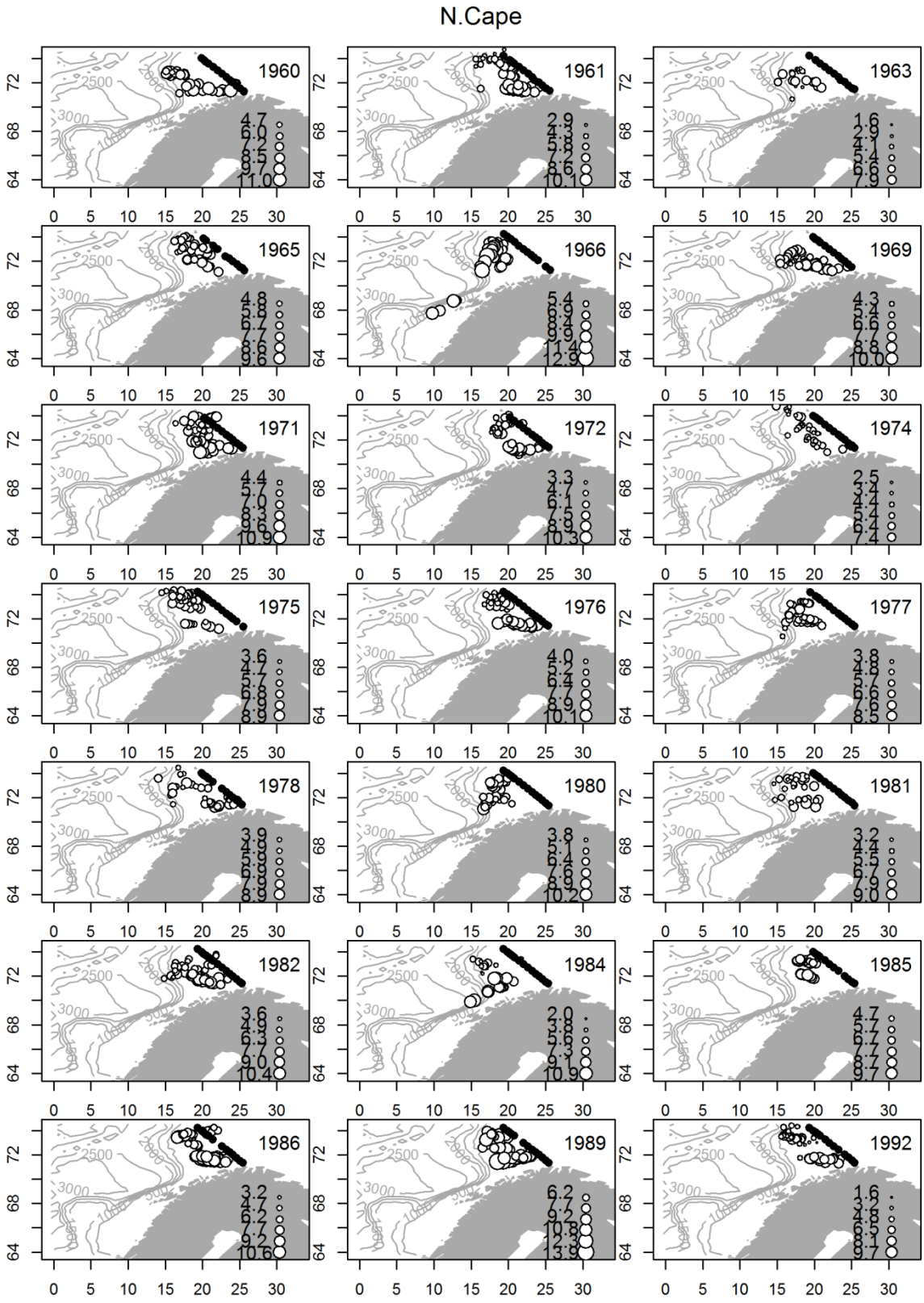

Fig. A2. (continued)

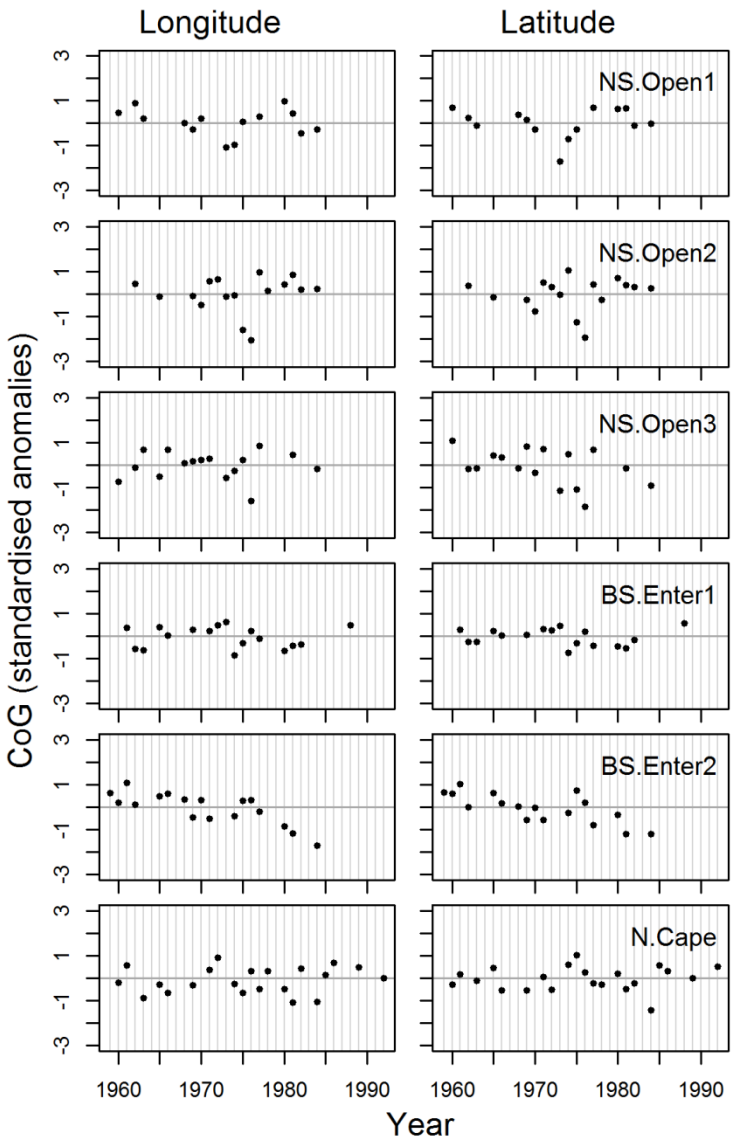

Fig. A3. Year-to-year variation in transect-specific longitude (left) and latitude (right) of the CoG spawning locations for stage CIV, displayed as standardised anomalies (yearly value-mean value for all years/standard deviation for all years). Grey horizontal line: zero isoline. The Kola transect is not displayed as we could only estimate the values for two years.

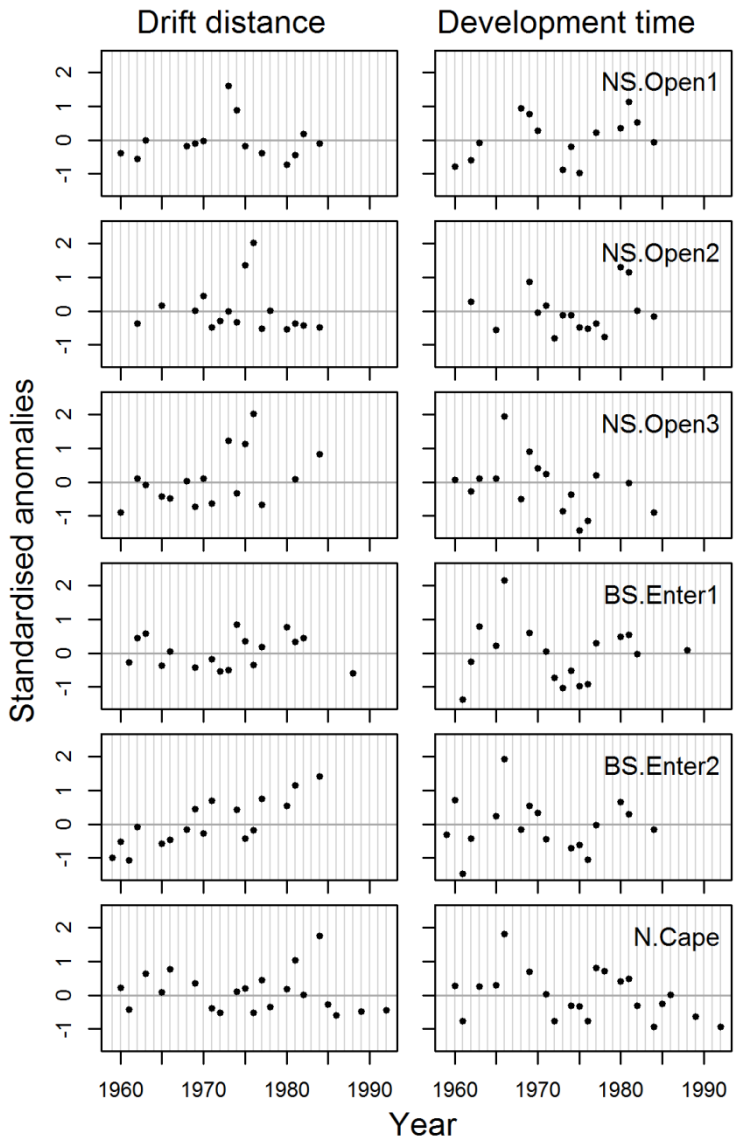

Fig. A4. Year-to-year variation in transect-specific mean drift distance (left) and development time (right) from egg to CIV, displayed as standardised anomalies (yearly mean value-mean value for all years/standard deviation for all years). Grey horizontal line: zero isoline. The Kola transect is not displayed as we could only estimate the values for two years.

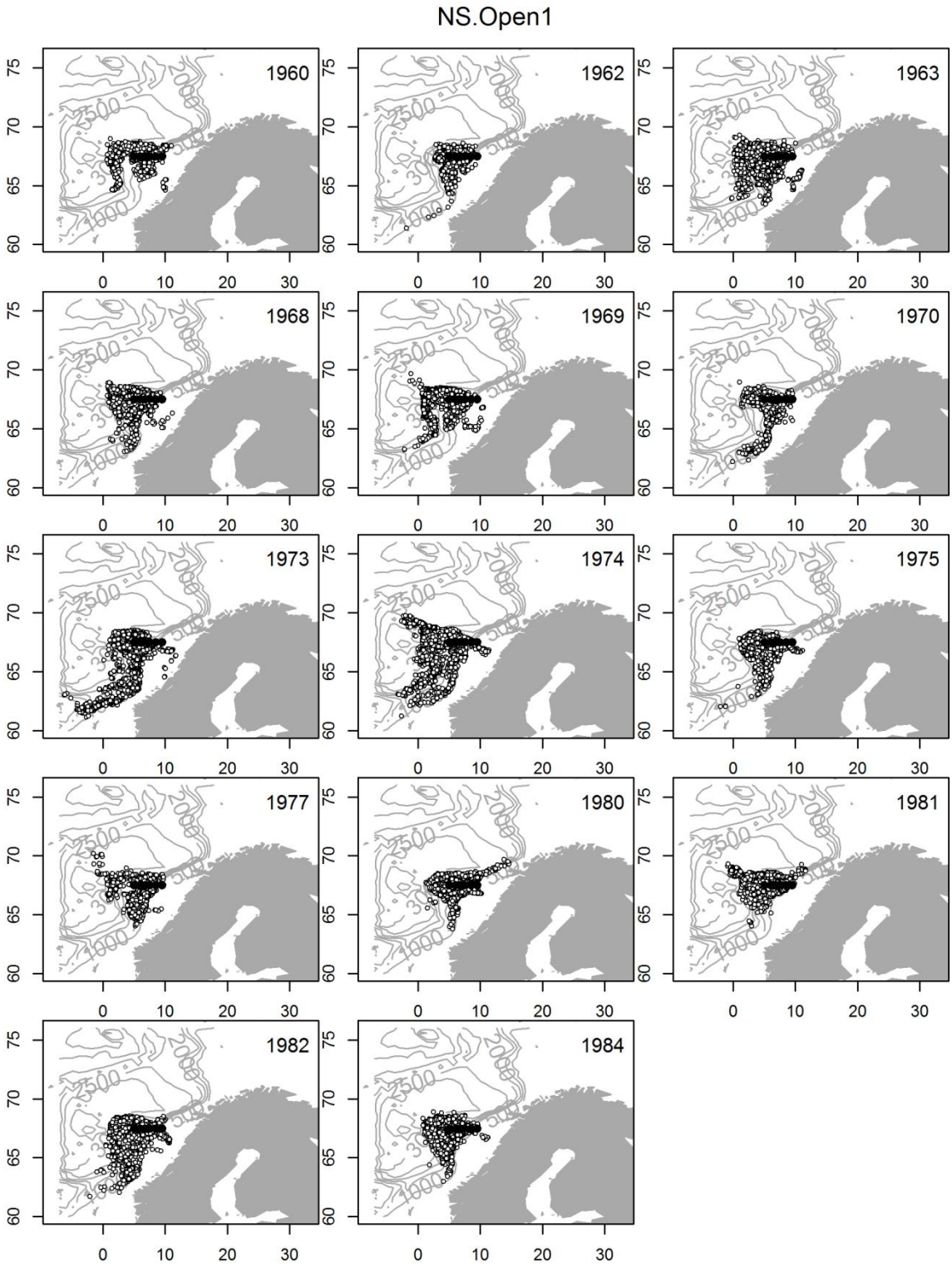

Fig. A5. Year-to-year variation in total potential spawning locations (white dots) for different transects (black dots). Each white dot represents one particle sampled and one copepodite stage present in the same station. The Kola transect is not displayed since estimates from only two years were available. X-axis: longitude, y-axis: latitude.

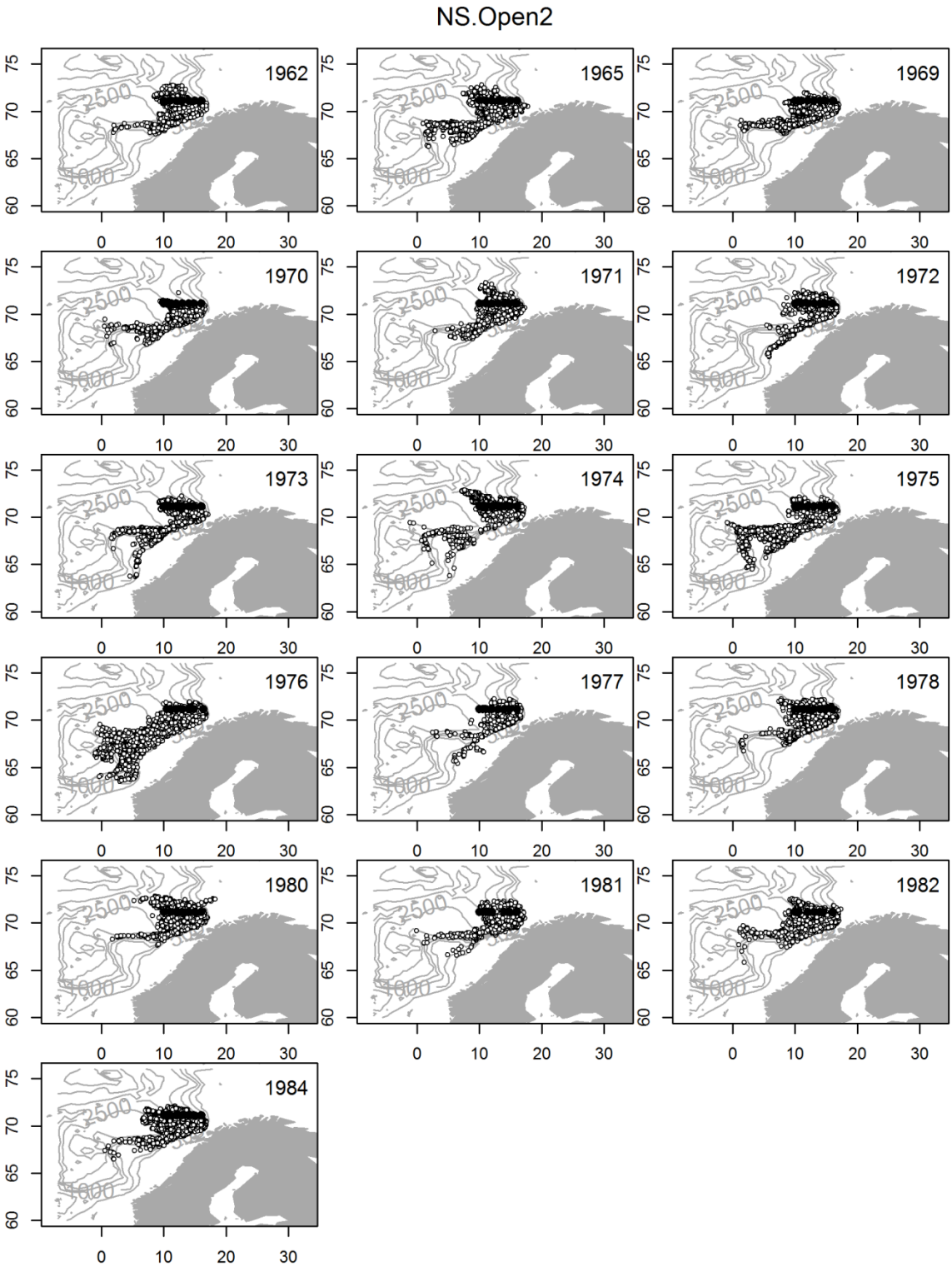

Fig. A5. (continued)

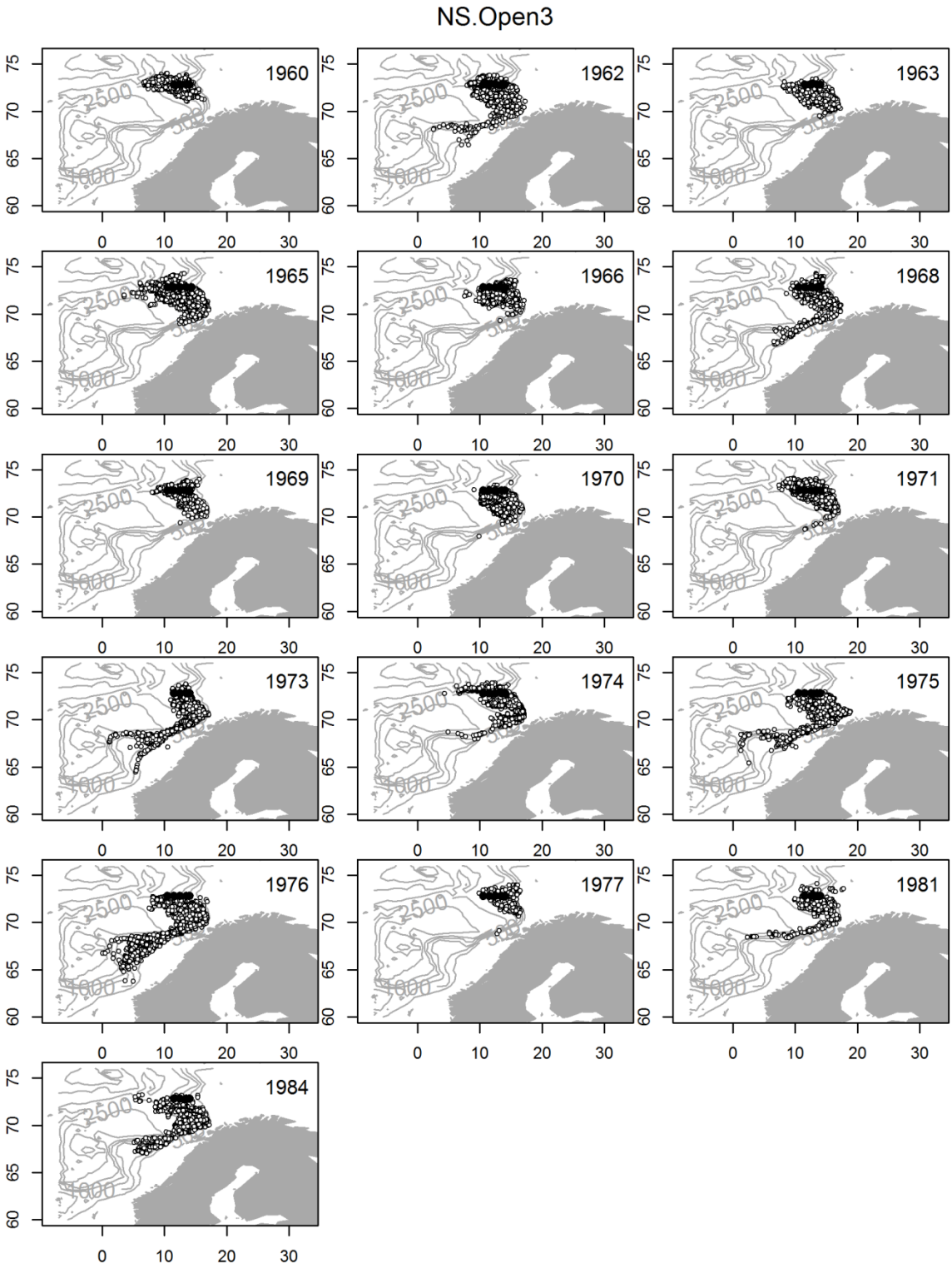

Fig. A5. (continued)

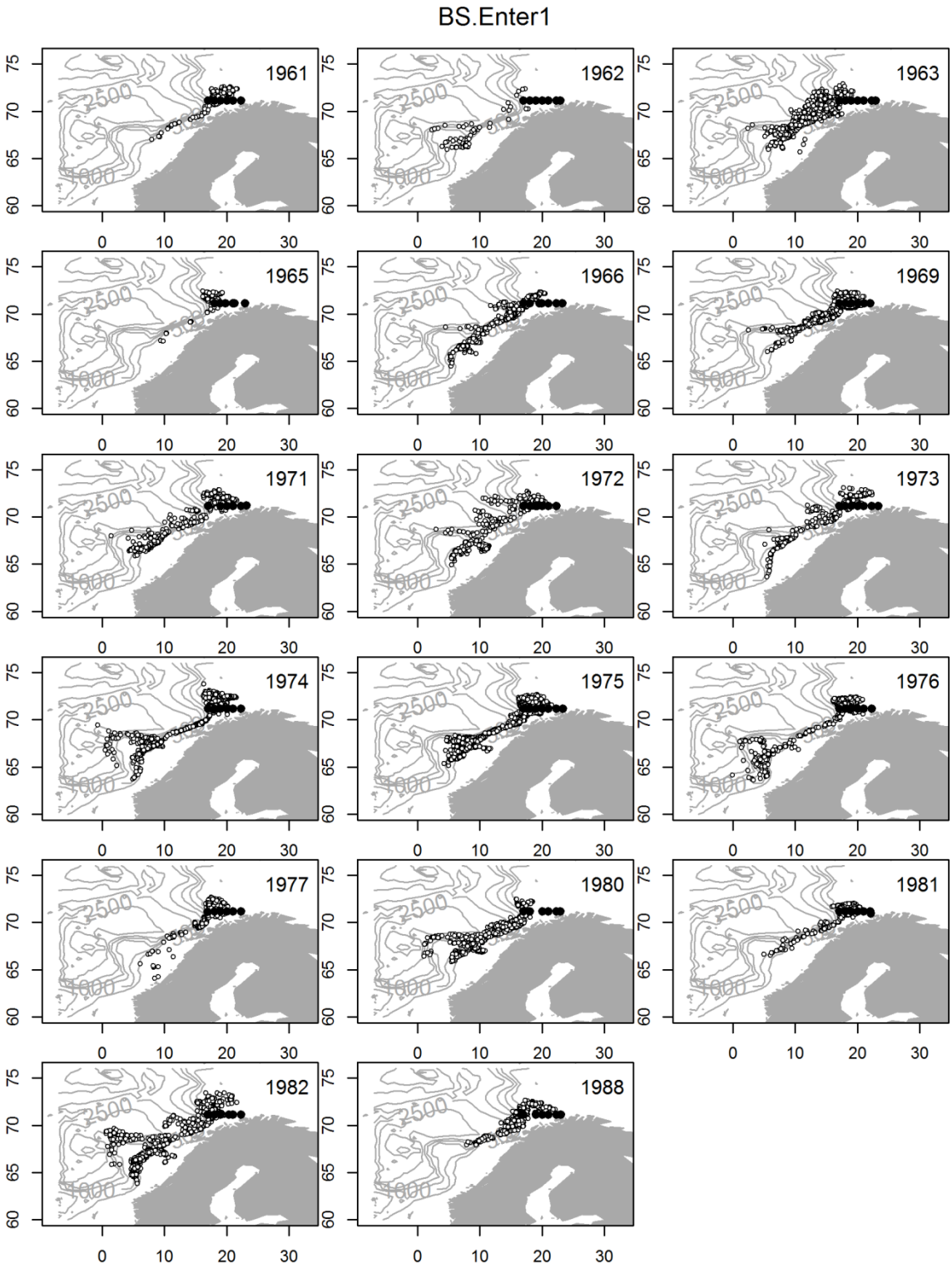

Fig. A5. (continued)

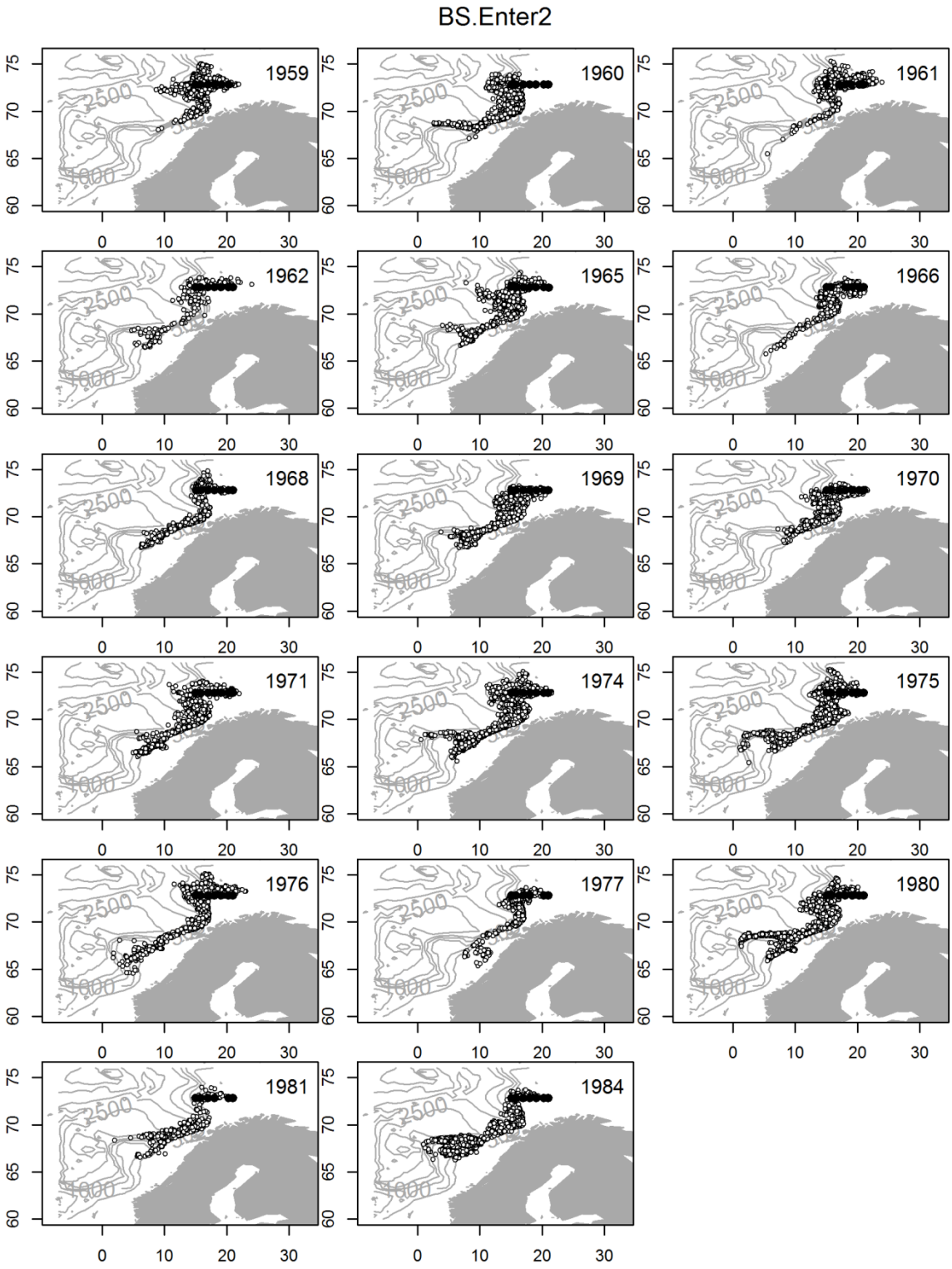

Fig. A5. (continued)

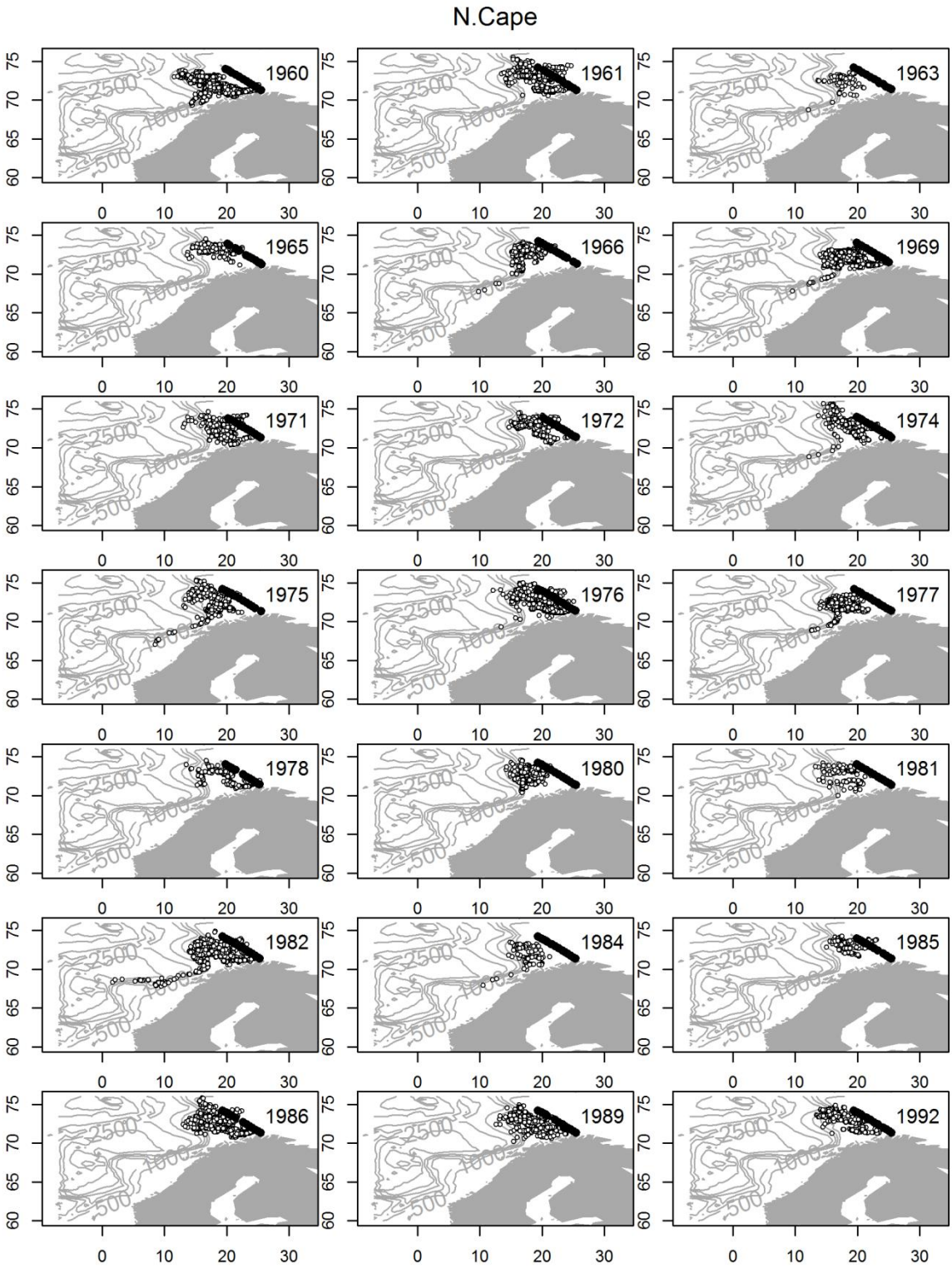

Fig. A5. (continued)

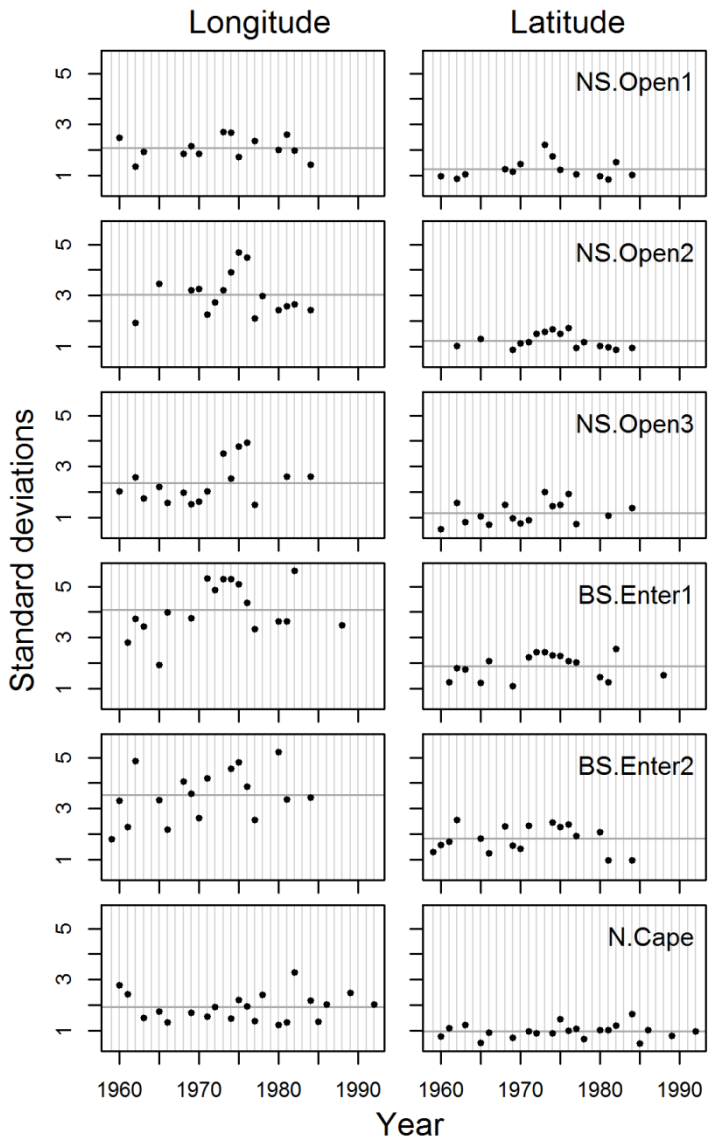

Fig. A6. Year-to-year variation in transect-specific standard deviations of total spawning area longitude (left) and latitude (right). Grey horizontal line: mean of the year and transect specific values. The Kola transect is not displayed as we could only estimate the values for two years.

Appendix 2. Supplementary tables

Table A1. Parameter values used to estimate development time using the Belehrádek temperature function $D = a(T - \alpha)^b$. D: days between the median day of the egg period and the time when 50 % of the copepods have reached a specific stage, T: temperature in °C, α: 9.11 and b: -2.05. Source: Campbell *et al.* (2001).

Stage	a
NI	595
NVI	4426
CI	5267
CII	6233
CIII	7370
CIV	8798

Table A2. Instantaneous mortality estimates (d^{-1}) used in the exponential decay formula to back-calculate egg abundances. Source: Aksnes & Blindheim (1996).

Stage	M
Egg	0.16
N	0.08
CI	0.16
CII	0.18
CIII	0.15
CIV	0.04

Table A3. Summary statistics of back-calculated spawning period per transect, pooled for all years and copepodite stages CI-CIV. Mean: weighted mean, using the back-calculated egg abundances as weights, min. and max.: minimum and maximum values

	Estimated spawning period		
Transect	**Mean**	**Min.**	**Max**
NS.Open1	79	63	95
NS.Open2	79	57	103
NS.Open3	78	51	107
BS.Enter1	94	70	110
BS.Enter2	95	70	111
N.Cape	101	66	123
Kola	118	104	126

Table A4. Percentage difference (±) between the original results with the model setup (1) release date 1st of March, drift depth 20 m, sampling radius 20 km ("standard"), and the following alternatives: (2) release date 1st of March, drift depth 10 m, sampling radius 20 km ("shallow"); (3) release date 1st of March, drift depth 30 m, sampling radius 20 km ("deep"); (4) release date 15th of February, drift depth 20 m, sampling radius 20 km ("early"); (5) release date 15th of March, drift depth 20 m, sampling radius 20 km ("late"); (6) release date 1st of March, drift depth 20 m, sampling radius 25 km ("large"); and (7) release date 1st of March, drift depth 20 m, sampling radius 15 km ("small"). The results listed are calculated using data for all years available, and include: (1) Total number of particles sampled per transect; (2-3) CoG spawning locations longitude and latitude; (4) mean drift distance from egg to CIV; (5) mean development time from egg to CIV; (6-7) standard deviations of total spawning area longitude and latitude for copepodites later sampled as CIV; and (8) mean spawning day of CIV. Differences above 10 % are shaded in grey.

		Values	**Percentage difference (±)**					
		1.Standard	**2.Shallow**	**3.Deep**	**4.Early**	**5.Late**	**6.Large**	**7.Small**
1.Number of particles	NS.Open1	8324	1.4	1.5	0.9	2.9	42.5	-38.0
	NS.Open2	11174	-3.5	-3.9	0.2	-0.8	45.5	-38.7
	NS.Open3	6683	13.3	-7.1	1.3	-2.8	49.2	-39.2
	BS.Enter1	3032	29.6	-14.0	35.0	-28.7	45.9	-40.5
	BS.Enter2	6007	-2.8	3.8	10.7	-8.0	44.3	-36.1
	N.Cape	3565	6.2	-1.5	63.8	-43.8	48.6	-39.5
	Kola	30	-33.3	-20.0	533.3	-90.0	80.0	-53.3
		1.Standard	**2.Shallow**	**3.Deep**	**4.Early**	**5.Late**	**6.Large**	**7.Small**
2.CoG longitude	NS.Open1	4.51	-3.6	5.7	-0.8	4.8	-1.1	0.7
	NS.Open2	11.17	-1.1	2.0	-0.6	2.5	-0.1	0.6
	NS.Open3	12.75	0.7	-1.0	-0.1	-0.1	-0.4	0.3
	BS.Enter1	14.71	-1.5	-1.9	1.8	-5.4	-0.9	-0.4
	BS.Enter2	12.90	-0.7	0.5	-0.1	-2.1	0.2	-0.2
	N.Cape	18.20	0.3	-0.6	3.7	-4.1	-0.7	0.0
	Kola	26.87	2.2	-2.6	6.5	-9.8	0.2	-0.4
3.CoG latitude	NS.Open1	66.83	0.0	0.0	-0.1	0.2	0.0	0.0
	NS.Open2	69.96	0.0	0.0	0.0	0.1	0.0	0.0
	NS.Open3	71.48	-0.4	0.2	0.0	0.0	0.0	0.0
	BS.Enter1	70.05	-0.1	-0.1	0.0	-0.4	-0.1	-0.1
	BS.Enter2	70.30	0.1	0.0	0.1	-0.2	0.0	0.0
	N.Cape	72.26	0.1	0.1	0.1	0.0	0.0	0.0
	Kola	71.37	0.2	0.7	0.4	0.0	0.1	-0.1
4.Drift distance	NS.Open1	191	0.6	-3.5	3.2	-5.1	1.0	-0.6
	NS.Open2	204	2.9	-4.0	0.3	-6.0	0.3	-1.3
	NS.Open3	200	13.3	-7.9	-0.4	-1.5	-0.1	-0.5
	BS.Enter1	258	4.2	4.6	-2.6	11.0	1.1	3.0
	BS.Enter2	361	-2.9	-0.6	-1.5	3.5	-2.0	1.8
	N.Cape	190	-4.7	1.4	-13.7	11.6	1.2	1.1
	Kola	249	2.1	7.0	-21.1	36.6	2.9	0.1

5.Development time	NS.Open1	43	1.7	-1.4	0.8	-1.8	0.3	-0.3
	NS.Open2	53	0.2	-0.8	0.7	0.0	0.2	-0.2
	NS.Open3	57	-2.0	0.6	-0.5	-0.5	0.3	-0.2
	BS.Enter1	40	-0.2	-0.4	0.6	-2.2	0.2	-0.4
	BS.Enter2	44	-0.1	-0.5	0.9	-0.7	0.5	-0.3
	N.Cape	45	0.6	-0.9	1.1	-2.0	0.3	-1.2
	Kola	38	4.0	8.6	11.9	3.0	1.4	-0.8
6.Longitude SD	NS.Open1	2.33	-1.6	-4.1	7.2	-6.5	1.6	-1.0
	NS.Open2	3.72	1.0	-6.1	2.6	-8.2	-0.1	0.2
	NS.Open3	2.88	0.3	-7.8	2.8	-2.1	-1.8	0.2
	BS.Enter1	4.99	5.5	1.1	-1.2	-3.9	-0.3	-1.1
	BS.Enter2	4.33	2.5	-5.2	3.6	-4.1	-0.8	0.0
	N.Cape	2.29	12.4	4.4	8.3	-12.3	5.0	-0.2
	Kola	2.58	44.6	-7.8	17.8	-100.0	11.2	7.4
7.Latitude SD	NS.Open1	1.49	-6.6	1.0	3.0	-3.1	0.6	0.4
	NS.Open2	1.48	4.2	-1.4	1.8	-3.4	-0.1	0.5
	NS.Open3	1.68	-2.9	-4.2	1.0	-0.7	-1.7	-1.2
	BS.Enter1	2.17	-6.7	0.4	-1.2	-4.7	-1.2	0.3
	BS.Enter2	2.11	1.8	1.9	5.8	-5.4	1.0	-0.2
	N.Cape	1.07	-0.3	9.8	-7.2	7.4	3.2	0.3
	Kola	0.38	149.9	99.9	96.7	-100.0	18.0	-20.3
8.Spawning day	NS.Open1	72	-1.0	0.8	-0.5	0.5	-0.2	0.1
	NS.Open2	71	-0.2	0.6	-0.4	0.6	-0.1	0.1
	NS.Open3	70	1.8	-0.6	0.5	0.0	-0.1	0.2
	BS.Enter1	85	0.1	0.0	-0.3	0.4	-0.2	0.3
	BS.Enter2	85	0.3	0.2	-0.6	0.5	-0.2	0.1
	N.Cape	91	-0.3	0.5	-0.7	0.9	-0.2	0.6
	Kola	109	-0.2	-3.4	-4.0	0.3	-0.2	-0.1

References Appendix 2

Aksnes DL, Blindheim J (1996) Circulation patterns in the North Atlantic and possible impact on population dynamics of *Calanus finmarchicus*. *Ophelia*, **44**, 7–28.

Campbell R, Wagner M, Teegarden GJ, Boudreau CA, Durbin EG (2001) Growth and development rates of the copepod *Calanus finmarchics* reared in the laboratory. *Marine Ecology Progress Series* **221**,161–183.

Corkett CJ, McLaren IA, Sevigny J-M (1986) The rearing of the marine calanoid copepods *Calanus finmarchicus* (Gunnerus), *C. glacialis* (Jaschnov) and *C. hyperboreus* (Kroyer) with comment on the equiproportional rule. *Syllogeus*, **58**, 539–546.

A statistical regression approach to estimate copepod mortality from spatiotemporal survey data

Kristina Øie Kvile[1]*, Leif Chr. Stige[1], Irina Prokopchuk[2], Øystein Langangen[1]

[1]Centre for Ecological and Evolutionary Synthesis (CEES), Department of Biosciences, University of Oslo, PO Box 1066 Blindern, 0316 Oslo, Norway

[2]Knipovich Polar Research Institute of Marine Fisheries and Oceanography (PINRO), 6 Knipovich Street, 183763 Murmansk, Russia

Keywords: Advection, mortality, statistical regression approach, vertical life table, zooplankton

Abstract

Mortality is notoriously difficult to estimate for zooplankton populations in the open ocean due to the confounding effect of advection. The vertical life table (VLT) approach is commonly used, but has been shown to be sensitive to both spatial and temporal trends in recruitment. Here, we estimate mortality rates of *Calanus finmarchicus* copepodites from spatiotemporally resolved data from the highly advective Norwegian Sea-Barents Sea ecosystem in spring and summer. We apply both the VLT and a statistical regression approach (SRA), specifically taking into account the effects of advection and varying recruitment. Testing the two methods on a simulated dataset shows that the SRA performs better than the VLT when trends in recruitment are present. Overall, the SRA appears to be a robust method for non-uniform, spatiotemporally resolved survey data influenced by advection. The estimated mortality rates are relatively low (0.03-0.07 d^{-1}) and indicate increased mortality for the oldest copepodite stage pair (CIV-CV) compared to the early copepodite stages. However, the differences are not statistically significant at the 5 % level, and comparing stage-specific mortality estimates from previous studies does not reveal any clear trends.

Introduction

The limited knowledge of mortality rates has been described as one of the main challenges in the modelling of marine population dynamics (Runge *et al.*, 2004). In contrast to attributes such as egg production and growth, which can be estimated by incubating specimens in the lab, mortality is a property of populations and must be determined in the field (Hirst & Kiørboe, 2002). But to estimate mortality rates for zooplankton populations in the open ocean is challenging due to the influence of advection (Aksnes & Ohman, 1996). Catching a different number of individuals one day compared to the next can reflect recruitment and mortality, but also transport in or out of the area. Following a zooplankton population in time to estimate mortality (horizontal methods) requires observations from a large enough area to minimise the effect of advection, which is rarely attainable in the open ocean. In addition, the estimation of mortality rates is hindered by spatiotemporal patchiness or bias in observation data, and uncertainty in parameters needed for the estimation (e.g. stage duration) (Ohman, 2012). Due to the limited knowledge of mortality rates, they are often assumed constant in zooplankton population models (Ohman *et al.*, 2004).

As a solution to the confounding effect of advection, Aksnes & Ohman (1996) proposed the vertical life table (VLT) approach. They argued that even in the presence of advection, the composition of zooplankton developmental stages may contain information about mortality and recruitment, assuming that different stages are equally influenced by advection and there is no strong cohort structure over time. The VLT has been applied in numerous studies (e.g. Möllmann, 2002; Plourde *et al.*, 2009; Melle *et al.*, 2014) and is typically advocated as a robust method in advective systems.

Recently however, the VLT was criticised for its sensitivity to advection, specifically, to spatial gradients in abundance (Gentleman *et al.*, 2012). Also, the method is known to be susceptible to temporal trends in recruitment (Aksnes & Ohman, 1996). Here, we apply a statistical regression approach (SRA) (Langangen *et al.*, 2014), an extension of the VLT which specifically incorporates the role of advection by modelling the effect of space, and accounts for trends in recruitment by inclusion of a seasonal term. It has previously been applied to estimate mortality of fish eggs (Langangen *et al.*, 2014), and is here adapted for the estimation of zooplankton mortality rates. We apply both the VLT and the SRA to estimate mortality rates of *Calanus finmarchicus* copepodites from long-term, spatiotemporally resolved observation data from the Norwegian Sea-Barents Sea

ecosystem (NS-BS). In addition, we compare the performance of the two methods on a simulated dataset mimicking the observation data with known mortality rates.

Materials and methods

The study system

The survey area covers the north-eastern Norwegian Sea and Norwegian continental shelf and south-western Barents Sea (Fig. 1). Mesozooplankton biomass in the area is dominated by *C. finmarchicus*, which typically has an annual life cycle at these latitudes (Eiane & Tande, 2009). Individuals of the adult stage (CVI) emerge in early spring from overwintering in the deep waters of the Norwegian Sea or fjords (Hirche, 1983; Kaartvedt, 1996; Melle *et al.*, 2004), and spawn in in the upper waters. The peak of the spawning period is typically in April-May in the Norwegian Sea (Melle *et al.*, 2004; Broms & Melle, 2007), and occurs progressively later from south-west to north-east into the Barents Sea. The new generation develops from eggs through six naupliar stages (NI-NVI) and five copepodite stages (CI-CV), and in summer (from around mid-June in the Norwegian Sea (Østvedt, 1955)), the older copepodite stages (mainly CV) start to descend for overwintering. The distribution of *C. finmarchicus* in the NS-BS is highly influenced by advection (Edvardsen *et al.*, 2003; Samuelsen *et al.*, 2009), in particular the northbound Norwegian Atlantic Current and Norwegian Coastal Current (Blindheim, 2004) (Fig. 1).

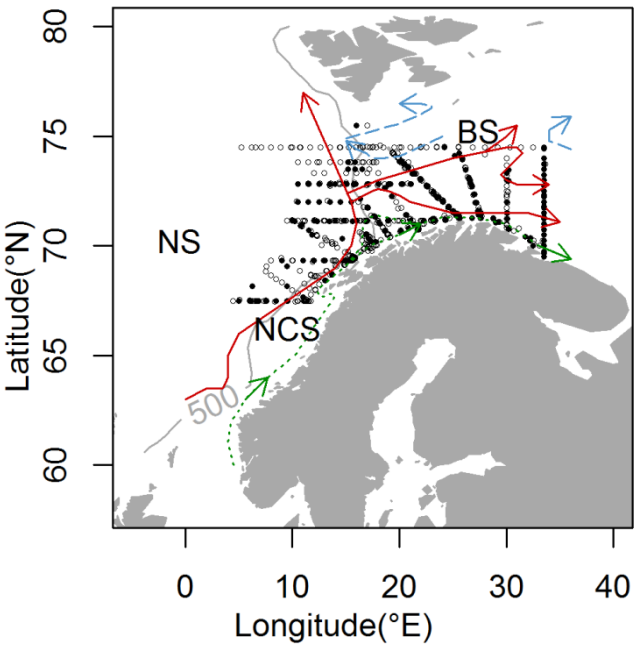

Fig. 1. Study area with survey stations pooled for all years (circles). Filled circles indicate stations with depth-integrated data. The 500 m depth contour (grey line) marks the approximate division between the Norwegian Sea (NS) and the Barents Sea (BS) and Norwegian continental shelf (NCS). The main surface currents in the area are the Norwegian Atlantic Current (red solid arrows), the Norwegian Coastal Current (green dotted arrows) and Arctic Water currents (blue dashed arrows).

Mortality estimation

To estimate instantaneous mortality (day^{-1}) of *C. finmarchicus* copepodite stages, we applied the vertical life table (VLT) approach (Aksnes & Ohman, 1996) and a statistical regression approach (SRA) (Langangen *et al.*, 2014). Both methods use information about the relative abundance of consecutive developmental stages, and do not require knowledge about absolute abundances. With the VLT, the instantaneous daily mortality rate (m) for the stage pair i and $i+1$ is the solution to the following equation, where v_i is the abundance of stage i and α_i is the duration of stage i:

$$\frac{v_i}{v_{i+1}} = \frac{e^{(m\alpha_i)}-1}{1-e^{(-m\alpha_{i+1})}} \qquad \textbf{(1)}$$

It is assumed that the mortality of stage i and i+1 is equal during a period corresponding to the combined duration of the two stages ($\alpha_i + \alpha_{i+1}$). To estimate the mortality rate for adults (q) and the preceding copepodite stage, the corresponding equation is:

$$\frac{v_{q-1}}{v_q} = e^{(m\alpha_{q-1})} - 1 \quad \textbf{(2)}$$

Mortality rates are estimated for all data samples separately, and average rates with uncertainty estimates can be calculated given a sufficient number of samples.

The SRA is an extension of the VLT which specifically incorporates the effect of advection and varying production. The mortality rate for two consecutive stages is found by estimating the effect of age (in days) on stage-specific abundance using the following generalized additive mixed model (GAMM):

$$ln(Z)_{l,t} = \beta_0 + s(spd_l) + te(lon_l, lat_l) + b_{0t} + (\beta_1 + b_{1t})A_l + \varepsilon_{l,t} \qquad \textbf{(3)}$$

The response variable is the natural log-transformed stage-specific abundance of individuals belonging to stage i or i+1 in station l and year t (zeros excluded). To account for variable duration of the stages i and i+1, abundance is divided by the estimated stage duration. The scaled abundance can be interpreted as the number of individuals of age A (days). The age of individuals in stage i is defined as the median day between the day of entry into stage i and into stage i+1 (see 'Estimation of development time'). The covariates include (1) spawning day (*spd*, i.e. the sampling day minus the estimated age) – accounting for seasonal variation in abundance; (2) sampling position (*lon*, longitude, *lat*, latitude) – accounting for horizontal advection from spawning; and (3) age (A) – accounting for

mortality (estimates -*m*). The model includes two random effects: (4) a random year effect (b_{0t}) accounting for year-to-year variation in total abundance and (5) a random year by age effect (b_{1t}) accounting for year-to-year variation in mortality. β_0 and β_1 are the fixed effects, *s* is a 1D smoothing spline, *te* a 2D tensor product smooth, and ε a normally distributed error term. In order to estimate confidence intervals of the mortality estimates (the age effect) we used a nonparametric bootstrap procedure (1000 samples with replacement), with year as the sampling unit (Hastie *et al.*, 2009).

The model was formulated using the gam function in the mgcv library in R, treating the random effects as smooths (setting the flag bs = "re") (Wood, 2013; R Development Core Team, 2014). The model code is given in Appendix 3, and can be downloaded using the following link: https://github.com/kristokv/SRA.

Field data

Stage-specific abundance data of *C. finmarchicus* (ind. m^{-3}) were collected by PINRO (Murmansk, Russia) from 1959 to 1993 in the north-eastern Norwegian Sea and south-western Barents Sea (Fig. 1). Two surveys were conducted per year, in spring (April-May) and summer (June-July). Samples were collected with a Juday plankton net with closing mechanism (37 cm diameter opening, 180 µm mesh size), towed vertically from the lower depth to the upper depth of the sample (Nesterova, 1990). The number of survey stations varied between years, and stage-specific data from both seasons were available from 30 years in total. We did not estimate mortality rates for eggs or naupliar stages, since these due to their small size likely are under-sampled by the mesh size used (Hernroth, 1987; Nichols & Thompson, 1991).

Most samples were taken from one of the following depth categories: Upper: upper sampling depth <=20 m and lower sampling depth <=60 m (n: 3359); Middle: upper sampling depth 40-60 m and lower sampling depth <= 120 m (n: 719); Lower: upper sampling depth > 90 m (n: 721). To avoid bias due to stage-specific vertical distribution patterns, depth-integrated data are typically used for mortality estimation. To ensure a good coverage of the water column, we summed abundances from different depth layers (multiplied by the number of meters hauled per layer) for all stations with samples from all three layers (Upper, Middle, Lower). This resulted in a total of 504 data points. We also applied the SRA on the full dataset (n: 4799). Since around 70 % of the samples were from the Upper layer, we weighted the data to reduce potential bias in the mortality estimates. Depth-specific weights were calculated as 1 divided by the fraction of samples from the

respective depth layer (Upper: 0.70, Middle: 0. 15, Lower: 0.15), and implemented using the "weights" argument when formulating the GAM.

Simulated data

To test the ability of the two methods to estimate mortality from the type of survey data available, we simulated a *C. finmarchicus* population with known mortality rates, and "sampled" this population to resemble the actual observations. For all years with available survey data, we simulated a population developing from egg-producing females (CVI) in spring to a mix of different developmental stages later in spring and summer. We used an individual-based model with a super-individual (SI) approach (Scheffer *et al.*, 1995), where each SI represents a set of individuals with similar drift history. Each SI initially represents a group of females producing eggs, which in turn develop into copepodites (the egg and naupliar stages are combined) and ultimately new adult females.

The initial distribution of SIs was based on modelled evolved overwintering fields in the Norwegian Sea (Hjøllo *et al.*, 2012), focusing on north-eastern areas overlapping with the survey area and adjacent areas from where copepods might drift into the survey area (65-72°N, 0-15°E, total number of 4 by 4 km grid cells: 15346) (Fig. 2). The initial number of adult females in each SI was similarly based on modelled evolved overwintering abundances (Hjøllo *et al.*, 2012), scaled to numbers between 100 and 3300. From this total distribution, we released 3000 randomly selected SIs daily between the 1st and 31st of March each year (in total 93 000 SIs per year).

After release, the SIs are transported passively at 25 m depth using an offline Lagrangian particle-tracking model (Ådlandsvik & Sundby, 1994), with hydrographic forcing from a numerical ocean model hindcast archive (Lien *et al.*, 2013, 2014). The archive was constructed with the use of the regional ocean modelling system (ROMS) (Shchepetkin & McWilliams, 2005; Haidvogel *et al.*, 2008). The hydrographic information is available for the NS-BS at daily intervals from 1959, with 4 by 4 km horizontal resolution and 32-layer terrain following vertical resolution. The diffusion coefficient was set at 100 m/s^2.

All adult females in a SI produce eggs at a constant, season-dependent rate. We used observed rates for the Norwegian Sea (Stenevik *et al.*, 2007) for pre-bloom (10 eggs female^{-1} d^{-1}), bloom (22 eggs female^{-1} d^{-1}) and post-bloom (18 eggs female^{-1} d^{-1}) conditions, defining pre-bloom as March-April, bloom as May and post-bloom as June-July. At each time step (day), the stage duration for all stages present in a SI, and the fraction of the total

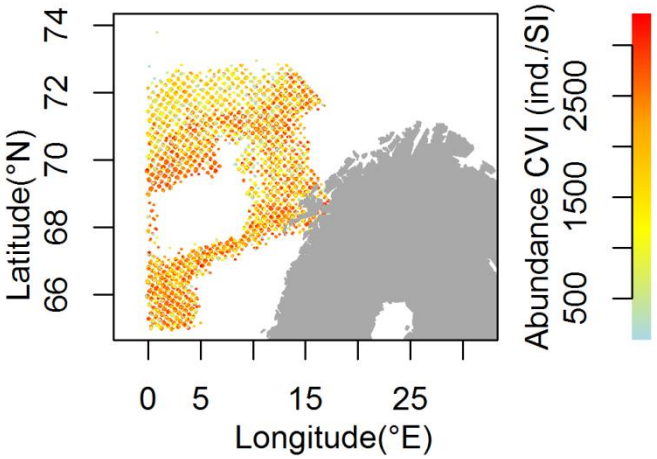

Fig. 2. Initial distribution of simulated super-individuals (SIs) and number of adult females (CVI) in each SI, based on evolved overwintering abundances (Hjøllo *et al.*, 2012). From this total distribution, we released 3000 randomly selected SIs daily between the 1st and 31st of March each year.

stage duration obtained by that day, are estimated using the ambient temperature at the current position (see 'Estimation of development time'). When individuals complete the duration of a stage, they move to the next. The individuals do not develop beyond the adult stage, thus, a female continues to produce eggs until she dies. At each time step, individuals are removed from the SI according to stage-specific instantaneous mortality rates. We ran the simulation three times with different mortality rates: (1) stage-specific mortality rates based on previous estimates for *C. finmarchicus* in the Northeast Atlantic (Melle *et al.*, 2014), (2) a high mortality scenario and (3) a low mortality scenario (Table 1).

After drifting for up to 150 days, the SIs were "sampled" at the day and position of actual spring and summer survey stations in the same year (within a 20 km radius). The stage-specific abundances summed from all SIs sampled in the survey stations were used as simulated data for the mortality estimation.

Table 1. Instantaneous mortality rates (d^{-1}) used in the simulations. The Base scenario is based on estimates for *C. finmarchicus* in the Northeast Atlantic (Melle *et al.*, 2014).

	Stage						
Scenario	Egg	CI	CII	CIII	CIV	CV	CVI
Base	0.230	0.090	0.105	0.075	0.030	0.025	0.020
High	0.200	0.200	0.200	0.200	0.200	0.200	0.200
Low	0.010	0.010	0.010	0.010	0.010	0.010	0.010

Estimation of development time

We estimated development time (*D*, in days) from egg to copepodite stage CI, and further for each developmental stage using the Bêlehrádek temperature function fitted for *C. finmarchicus*

$$D = a(T + 10.6)^{-2.05} \quad \textbf{(4)}$$

where *T* is temperature (°C) and *a* is a stage-specific constant. Since the ambient temperature estimates for a large fraction of the survey stations (~40%) were below 4°C, we used the coefficients given in Corkett *et al.* (1986) (see Discussion). The function gives the number of days from spawning until a given stage is reached. Stage duration of stage *i* was calculated as the difference between *D* for stage *i* and stage *i*+1, and the age of stage *i* as the midpoint between *D* for stage *i* and stage *i*+1. To estimate *D* during the simulation, we used the ambient temperature estimate from the position of the SI (at 25 m depth), according to the ocean model.

For the observation data, the past temperature experienced by the sampled copepodites is unknown. We therefore assumed *D* to be a function of temperature at the time and position of the survey station, specifically, the average of the ambient temperature estimates from 10, 50 and 100 m according to the ocean model hindcast archive (Lien *et al.*, 2013). To estimate *D* for the simulated dataset (after sampling of the SIs), we used the ambient temperature estimates at the time and position of survey stations and the drift depth of the SIs.

Additional analyses

To test the sensitivity of the VLT and the SRA to advection, varying egg production and varying (and unknown) temperature, we constructed three simplified simulated datasets. The simplest (Sim. 1) was a closed population (excluding drift), developing at fixed temperature (5°C) and reproducing at a constant rate (100 eggs per day, independent of the number of females present). This population was sampled at regular intervals after all stages reached stable abundances. The two other datasets were identical to the full simulation (including drift and only sampling SIs present at actual survey stations), but (Sim. 2) setting temperature and egg production fixed or (Sim. 3) setting only temperature fixed. Note that with fixed and known temperature, stage durations and ages of the "sampled" copepodites can be accurately estimated. See Table 2 for an overview of the different simulations.

To calculate realistic confidence intervals of the mortality estimates from the full simulation (Sim. 4), we added random noise with normal distribution and mean zero to the simulated data. The standard deviation of the noise term was calculated as the square root of the difference between the variance from the SRA model (Eq. 3) formulated for the actual observation data and the simulated data. We added this noise to the response variable in the SRA model for the simulated data (on the logarithmic scale), and retransformed to raw data values for the VLT.

Table 2. Overview of the different simulation runs used to construct simulated datasets. Var. prod.: varying egg production, var. temp.: varying temperature.

Sim. no.	Drift	Var. prod.	Var. temp.	Comments
Sim. 1	No	No	No	Closed population developing at 5°C, producing 100 eggs per day
Sim. 2	Yes	No	No	SIs drift according to ocean current hindcasts from the ocean model
Sim. 3	Yes	Yes	No	Egg production depends on month and number of females present in the SIs
Sim. 4	Yes	Yes	Yes	Development depends on ambient temperature hindcasts from the ocean model

Results

Simulated data

Using data from the simplest simulation (Sim. 1), both the VLT and the SRA accurately estimate mortality, with only minor deviations (Table 3). When mortality varies between the stages (Base) the estimates for CI-CII are closest to the average value for the two stages, for CII-CIII and CIII-CIV to the true value for the earlier stage, and for CIV-CV to the later stage. As the SRA requires estimates of age and stage duration of both stages in the stage pair, it cannot be used to estimate mortality for CV-CVI (adults). The estimates from the VLT are also less accurate for CV-CVI than the other stage pairs, and we continue focusing on the results for the copepodite stage pairs only.

Including drift and sampling at survey stations, but with fixed temperature and egg production (Sim. 2), the VLT tends to overestimate mortality in our dataset, especially for the older stage pairs (CIII-CIV and CIV-CV) (Table 3). This is because the stage distributions have not become stable at the time of the earliest samples in spring; abundances of older stages are still increasing while abundances of younger stages are

stable (Appendix 1, Fig. A1). If only mortality estimates from summer are included in the average, the bias is reduced (Appendix 2, Table A1). Including drift barely influences the SRA estimates compared to the estimates from the simpler simulation (Sim. 1). However, the SRA tends to underestimate mortality for CIV-CV, especially at the High mortality (0.2). At such high mortality rates, the true age of most sampled copepodites are likely earlier than the midpoint between the two stages. Re-estimating the ages by weighing the days between the two stages by the estimated mortality (e^{-m}) reduces this bias (Appendix 2, Table A1). For the other stages or mortality rates, the difference between the weighted and non-weighted ages is so small that the mortality estimates are barely affected.

When egg production depends on the number of females present in the SIs (Sim. 3), the VLT estimates are more biased, in particular for the High (0.2) or Low (0.01) mortality rates (Table 3). At these mortalities, there is a clear decrease (for 0.2) or increase (for 0.01) in abundances with time (Appendix 1, Fig. A2). As copepodites belonging to the younger of the two stages in the stage pair generally develop slightly before the older (the abundance of the younger stage increase, or decrease, slightly before the older stage), this leads to underestimation (for 0.2) or overestimation (for 0.01) of mortality. Season-specific estimates are more accurate when the rate of change in abundance is smaller (e.g. for the younger stage pairs in spring at Low mortality) (Appendix 2, Table A1). However, the season-specific VLT estimates are still generally more biased than the SRA estimates. The SRA performs better when data from both seasons are included (Appendix 2, Table A1). As for Sim. 2, the High (0.2) mortality rate for CIV-CV is underestimated, but improved by weighing the ages by the estimated mortality.

Including varying and unknown temperature (Sim. 4) increases most of the mortality estimates (Table 3). In spring and summer, temperatures at the sampling stations are generally higher than the ambient temperatures experienced by the SIs prior to sampling, leading to underestimation of stage duration and overestimation of mortality. A linear regression of temperature by day gave a slope of 0.05°C d^{-1}, which for the earliest stage pair (CI-CII) translates into an increase in 0.7°C from start to end of the duration of the stages combined (on average 14 days), or 1.5°C from spawning to sampling (on average 30 days). Decreasing the temperature estimates at the stations with 0.7°C for the

Table 3. Instantaneous mortality rates (d^{-1}) estimated from the simulated data using the VLT and the SRA, compared to the true values (shaded). Var. prod.: varying egg production, var. temp.: varying temperature.

					Simulation							
		True mortality			1. Simple		2. Drift		3. Var. prod.		4. Var. temp.	
		Per stage	Mean		VLT	SRA	VLT	SRA	VLT	SRA	VLT	SRA
Base	CI	0.090	CI-CII	0.098	0.097	0.097	0.100	0.094	0.080	0.090	0.100	0.117
	CII	0.105	CII-CIII	0.090	0.101	0.101	0.110	0.098	0.100	0.090	0.110	0.105
	CIII	0.075	CIII-CIV	0.053	0.072	0.071	0.090	0.069	0.080	0.070	0.090	0.081
	CIV	0.030	CIV-CV	0.028	0.024	0.024	0.070	0.015	0.070	0.010	0.090	0.041
	CV	0.025	CV-CVI	0.023	0.015		0.000		0.010		0.020	
	CVI	0.020										
High	CI	0.200	CI-CII	0.200	0.208	0.205	0.210	0.203	0.090	0.190	0.100	0.230
	CII	0.200	CII-CIII	0.200	0.216	0.216	0.230	0.214	0.110	0.180	0.120	0.206
	CIII	0.200	CIII-CIV	0.200	0.224	0.222	0.240	0.219	0.130	0.190	0.140	0.193
	CIV	0.200	CIV-CV	0.200	0.202	0.179	0.240	0.167	0.130	0.150	0.150	0.172
	CV	0.200	CV-CVI	0.200	0.212		0.120		0.080		0.100	
	CVI	0.200										
Low	CI	0.010	CI-CII	0.010	0.005	0.005	0.010	0.003	0.060	0.010	0.070	0.041
	CII	0.010	CII-CIII	0.010	0.009	0.009	0.020	0.007	0.080	0.010	0.080	0.027
	CIII	0.010	CIII-CIV	0.010	0.022	0.022	0.040	0.019	0.120	0.020	0.100	0.020
	CIV	0.010	CIV-CV	0.010	0.006	0.006	0.050	-0.002	0.120	-0.010	0.130	0.004
	CV	0.010	CV-CVI	0.010	0.029		0.020		0.110		0.140	
	CVI	0.010										

stage duration estimation (a conservative measure for the older stage pairs) reduces the overestimation of mortality rates (Appendix 2, Table A1).

Fig. 3 shows the mortality estimates from Sim. 4, with random noise added to the data and the temperature estimates at the stations decreased by 0.7°C. The confidence intervals for the VLT estimates are calculated from standard deviations of the mean, while for the SRA we applied a bootstrap procedure accounting for spatial autocorrelation. This gives more conservative (and broader) confidence intervals with the SRA than the VLT.

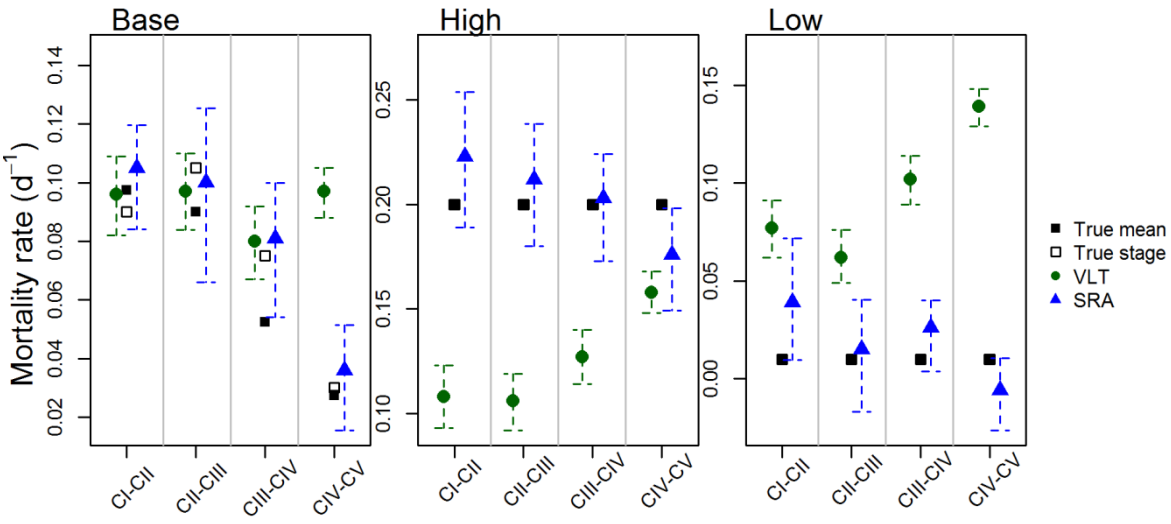

Fig. 3. Estimated mortality rates (d^{-1}) from the VLT (green dots) and the SRA (blue triangles) for data from the full simulation (Sim. 4) with (a) Base, (b) High, or (c) Low mortality rates (Table 1). The dashed arrows indicate 95 % confidence intervals of the estimates. Random noise was added to the simulated data, and the temperature estimates at the sampling stations (used to estimate stage duration after sampling) decreased with 0.7 °C. For the Base mortality (a), the true stage-specific mortality rate is plotted for the first of the two stages in the stage pair (white squares).

Observation data

For the depth-integrated observation data, the mortality estimates for CI-CII, CII-CIII and CIII-CIV are negative with the VLT and positive with the SRA (Fig. 4). For CIV-CV, the VLT estimates higher mortality than the SRA. Re-calculating the ages in the SRA model by weighing according to the estimated mortality rates increases the estimate for CIV-CV with 0.01. We also applied the SRA on the full dataset, weighing the observations to reduce the bias in number of samples per depth layer. The estimates from the complete

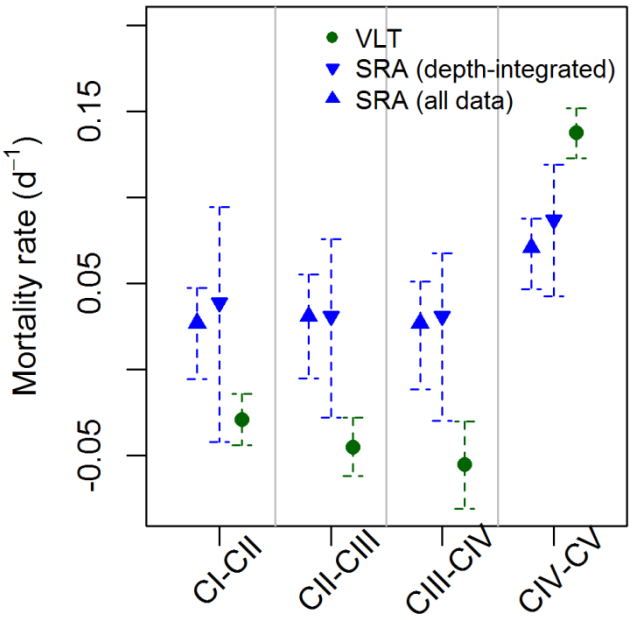

Fig. 4. Estimated mortality rates (d^{-1}) from the VLT (green dots) and the SRA (blue triangles) for the observation data, with 95 % confidence intervals of the estimates (dashed arrows). The SRA estimates are based on depth-integrated data (point-down triangles, n: 504), or all data weighted by depth layer (point-up triangles, n: 4799).

dataset are within the confidence intervals of the depth-integrated data (mean values: CI-CII: 0.03, CII-CIII: 0.03, CIII-CIV: 0.03, CIV-CV: 0.07), but the strong increase in the number of samples (from 504 to 4799) improves the confidence in the estimates (Fig. 4).

For the VLT, approximately 50 % of the station-specific mortality estimates for the three first stage pairs are negative, resulting in overall negative mortality rates. The negative estimates are primarily from summer; if the data are split into season, the estimates from spring are positive (mean values: CI-CII: 0.05, CII-CIII: 0.07, CIII-CIV: 0.11, CIV-CV: 0.16) and from summer negative for the first four stage pairs (mean values: CI-CII: -0.09, CII-CIII: -0.12, CIII-CIV: -0.17, CIV-CV: 0.12). Plotting the observed stage-specific abundances by day of year shows that CI-CIII generally decrease in summer, CV increases in spring, and CIV-CV both increase in summer (Fig. 5).

Discussion

Performance of the two methods

The mortality estimation for the simulated data showed that for a closed population with stable stage distribution, the VLT and the SRA were essentially identical, and both methods were able to capture the true mortality rates. Adding drift did not influence the mortality estimates as long as there were no strong trends in recruitment. If trends in recruitment were present, the SRA performed better than the VLT. An important

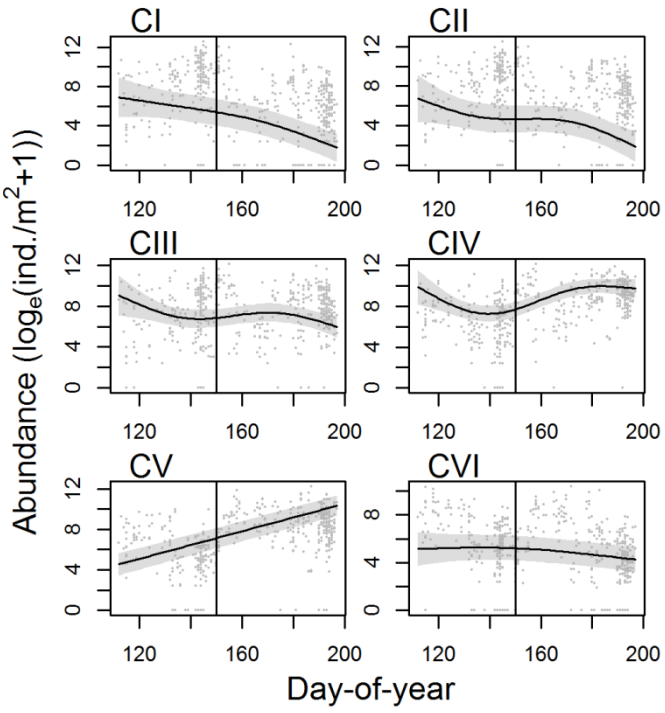

Fig. 5. Stage-specific abundance per day-of year. The smooth line is the predicted abundance from a GAM of the observation data (natural logarithm of depth-integrated abundance) as a function of sampling position (a 2D tensor product of longitude and latitude) and day (a 1D smooth function of day-of-year). The shaded area is the 95 % confidence interval of the predictions, grey dots are actual observations, and the vertical line marks the division between the spring and summer survey.

assumption of the VLT is that there are no strong trends in recruitment into a particular stage (Aksnes & Ohman, 1996). The method is relatively robust to random fluctuations in recruitment, but upward or downward trends lead to overestimation or underestimation of mortality, respectively (Aksnes & Ohman, 1996). When egg production depended on the number of females present (Sim. 3 and 4), there were strong downward trends in recruitment at High mortality, and upward trends at Low mortality. As expected, the VLT overestimated the Low mortality rate and underestimated the High mortality rate. The SRA specifically incorporates temporal variation in abundance through the effect of spawning day, and is therefore more appropriate for data with potential trends in recruitment.

In the actual survey data, abundances of younger stages (CI-CIII) tended to decrease in summer (indicating a downward trend in recruitment of these stages) while abundances of older stages (CIV-CV) tended to increase (indicating an upward trend in recruitment of these stages). The VLT should thus underestimate mortality for the younger stages, and overestimate mortality for the older stages. Comparing the results from the two methods seems to confirm this; the estimated mortality rates were lower (and negative) for the younger stages and higher for the older stage pair (CIV-CV) with the VLT than the SRA.

The simulations further showed that when trends in recruitment were present, the VLT performed better with season-specific data. This confirms that the method is more

appropriate for multiple samples obtained at the same time, reducing additional variability likely present in time series data (Aksnes & Ohman, 1996). The SRA performed better when the model was fitted to data from both seasons, benefitting from data covering more of the production curve of the stages in question. Still, season-specific estimates were generally better with the SRA than the VLT.

Horizontal methods, like the population surface method (Wood, 1994), follow the progression of a population through successive time points, but demand both frequent sampling in time (capturing the full abundance curve) and that the population sampled is closed, with minimal influence of advection (Aksnes *et al.*, 1997). In our dataset, the same station was generally visited only once or twice per year, and the number of stations sampled varied between years. Still, the SRA performed well in our most complex simulation, including drift and non-uniform distribution of egg-producing females. The method therefore seems to be a good alternative for non-uniform and "gappy" spatiotemporal data. It should be noted, however, that the method is more appropriate when data from several years are available (ideally more than two, see Appendix 1, Fig. A3). Including data from multiple years allows the model to separate trends in mortality from seasonal and spatial trends in abundances.

Estimated mortality rates

The simulations indicated that for observations resembling the actual survey data, the SRA performs better than the VLT. For the survey data, we obtained negative mortality estimates with the VLT for the three first stage pairs, indicating violations of the method's assumptions. Some authors exclude negative estimates when calculating average mortality rates (e.g. Pepin, 2013). However, according to Aksnes & Ohman (1996), all mortality estimates, also negative, should be included to obtain unbiased mean mortality rates when a sufficient number of samples are available.

The SRA estimates are in the lower end of previous mortality estimates for *C. finmarchicus*, in particular for the three youngest stage pairs (Fig. 6), but comparable to other estimates from the NS-BS region (see Table A2, Appendix 2, for a detailed overview of the previous studies). The differences between stage pairs in our study are not significant at the 5 % level, but indicate higher mortality for CIV-CV. It has been hypothesised that older (and larger) copepodites are subject to higher predation by visual predators (Eiane *et al.*, 2002). Also, stage CV might be more susceptible to food limitation since gonad maturation begins at this stage (Irigoien *et al.*, 2000). Trends in mortality with

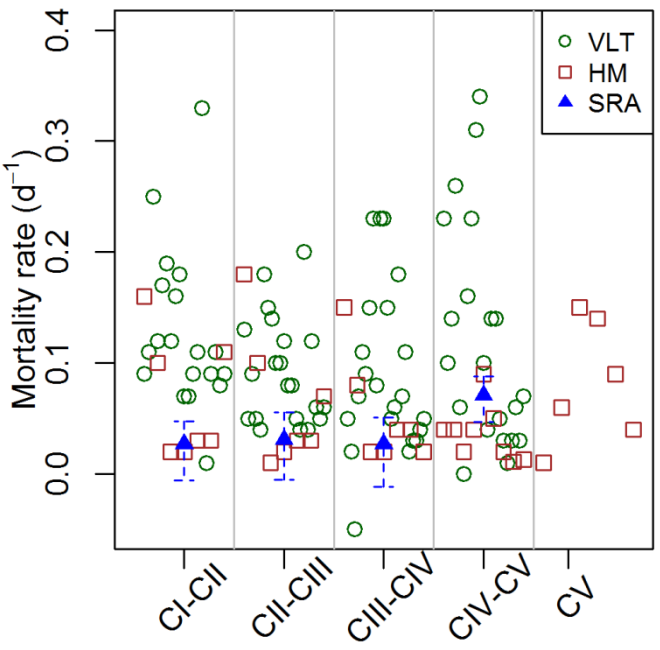

Fig. 6. Estimated instantaneous mortality rates (d^{-1}) from previous studies using the VLT (green dots) or horizontal methods (HM, brown squares) compared to results from this study (blue triangles). HM estimates are stage-specific, plotted for the first stage of the stage pair indicated. Mortality rates from this study are estimated with the SRA on the full dataset (weighted by depth), plotted with 95 % confidence intervals (dashed arrows). See Table A2 (Appendix 2) for information about the previous studies.

development stage are likely to vary between systems (Eiane *et al.*, 2002), and comparing estimates from previous studies does not reveal any clear trends (Fig. 6).

Stage duration estimates

A limitation to both the VLT and the SRA is the uncertainty in the estimated stage durations. First, it is assumed that stage durations are equal for all individuals in a sample (individuals of the same stage have exactly the same age), while they in reality might have experienced differing environments prior to sampling. Secondly, the past environment of the sampled individuals is unknown, and assumed equal to the sampling station. Introducing variable and unknown temperature (Sim. 4) introduced a bias with both methods. However, the effect was much smaller than introducing varying production (Sim. 3) on the VLT estimates, and taking into consideration the temperature increase with time reduced the bias with both methods. For the observation data, we used temperature estimates for the survey stations from the ocean model hindcast, not actual observations. This introduces an additional source of uncertainty. While the Atlantic water masses in the NS-BS are realistically represented by the model (Lien *et al.*, 2013), small scale variability is less accurately depicted than large scale patterns. Also, temperature tends to be underestimated (~0.5°C). We did therefore not decrease the temperature estimates further for the stage duration estimations in the observation data.

Thirdly, we followed the practice of Plourde *et al.* (2009) and used coefficients for stage duration estimation from Corkett *et al.* (1986), as these cover temperatures below the limits in the study by Campbell *et al.* (2001). However, most studies, also for high-latitude areas, apply the coefficients from the latter study (e.g. Thor *et al.*, 2008; Skardhamar *et al.*, 2011; Dvoretsky & Dvoretsky, 2013). These give shorter stage duration for stages CI-CIII and longer stage duration for CIV-CV relative to the coefficients provided by Corkett *et al*., resulting in higher mortality rates for the younger stages, and lower for the older stages (Plourde *et al.*, 2009). For our data, applying the coefficients from Campbell *et al*. would reduce the (non-significant) difference in mortality from the younger stage pairs to CIV-CV with the SRA, giving estimates between 0.04 and 0.06 d^{-1}.

Finally, we have considered development to be a function of temperature only, assuming excess food supply. We lack information on food availability overlapping with the survey data, but instances of food limitation would result in the stage durations being underestimated, and thereby the mortality rates overestimated. Previous studies have however found that doubling the stage durations, a realistic result of food limitation (Campbell *et al.*, 2001), does not influence the estimated mortality rates beyond the range of the confidence intervals presented here (approximately ±0.03) (Ohman *et al.*, 2002; Eiane & Ohman, 2004).

Concluding remarks

Zooplankton mortality rates are not constant in time and space, and can be linked to variation in food availability and temperature (Plourde *et al.*, 2009; Neuheimer *et al.*, 2010), predation pressure (Eiane *et al.*, 2002; Ohman *et al.*, 2008) or infectious agents (Kimmerer & McKinnon, 1990; Dunlap *et al.*, 2013). Several studies have indicated that zooplankton in the Barents Sea is top-down controlled by capelin, in particular in autumn and in areas to the north and east of our survey area (Hassel *et al.*, 1991; Dalpadado *et al.*, 2012; Stige *et al.*, 2014). In the presence of top-down control, we would excpect mortality to be positively correlated to predator abundance. The SRA provides annual estimates of mortality, but the uncertainties in these estimates are likely large, as shown for synthetic data in Langangen *et al.* (2014). Differing mortality rates in space or time can have large impacts on abundances (Appendix 1, Fig. A2), which should be considered when modelling zooplankton populations.

We have demonstrated that the SRA is more appropriate than the VLT when there are trends in recruitment, and that the method is well suited for data influenced by

advection. Statistical methods such as the SRA therefore seem like a promising tool to acquire knowledge of key population processes such as mortality from non-uniform, spatiotemporal survey data.

Acknowledgements

This work is a deliverable of the Norden Top-level Research Initiative sub-programme 'Effect Studies and Adaptation to Climate Change', and is a deliverable of the Nordic Centre for Research on Marine Ecosystems and Resources under Climate Change (NorMER). We are grateful to scientists and staff at PINRO who collected, sorted and digitised the zooplankton data. We also thank the authors who kindly provided or confirmed mortality estimates from previous studies.

References

Aksnes DL, Magnesen T (1983) Distribution, development, and production of *Calanus finmarchicus* in Lindåspollene, western Norway, 1979. *Sarsia*, **68**, 195–208.

Aksnes DL, Ohman MD (1996) A vertical life table approach to zooplankton mortality estimation. *Limnology and oceanography*, **41**, 1461–1469.

Aksnes D, Miller C, Ohman M, Wood S (1997) Estimation techniques used in studies of copepod population dynamics—a review of underlying assumptions. *Sarsia*, **82**, 279–296.

Arnkværn G, Daase M, Eiane K (2005) Dynamics of coexisting *Calanus finmarchicus*, *Calanus glacialis* and *Calanus hyperboreus* populations in a high-Arctic fjord. *Polar Biology*, **28**, 528–538.

Bagøien E, Kaartvedt S, Aksnes DL, Eiane K (2001) Vertical distribution and mortality of overwintering *Calanus*. *Limnology and Oceanography*, **46**, 1494–1510.

Blindheim J (2004) Oceanography and climate. In: *The Norwegian Sea Ecosystem* (ed Skjoldal HR), pp. 65–96. Tapir Academic Press, Trondheim.

Broms C, Melle W (2007) Seasonal development of *Calanus finmarchicus* in relation to phytoplankton bloom dynamics in the Norwegian Sea. *Deep Sea Research Part II: Topical Studies in Oceanography*, **54**, 2760–2775.

Campbell RG, Wagner MM, Teegarden GJ, Boudreau CA, Durbin EG (2001) Growth and development rates of the copepod *Calanus finmarchics* reared in the laboratory. *Marine Ecology Progress Series*, **221**, 161–183.

Corkett CJ, McLaren IA, Sevigny J-M (1986) The rearing of the marine calanoid copepods *Calanus finmarchicus* (Gunnerus), *C. glacialis* (Jaschnov) and *C. hyperboreus* (Kroyer) with comment on the equiproportional rule. *Syllogeus*, **58**, 539–546.

Dalpadado P, Ingvaldsen RB, Stige LC, Bogstad B, Knutsen T, Ottersen G, Ellertsen B (2012) Climate effects on Barents Sea ecosystem dynamics. *ICES Journal of Marine Science*, **69**, 1303–1316.

Dunlap DS, Ng TFF, Rosario K, Barbosa JG, Greco AM, Breitbart M, Hewson I (2013) Molecular and microscopic evidence of viruses in marine copepods. *Proceedings of the National Academy of Sciences of the United States of America*, **110**, 1375–80.

Dvoretsky VG, Dvoretsky AG (2013) The mortality levels of two common copepods in the Barents Sea. *Vestnik MGTU*, **16**, 460–465 (in Russian).

Edvardsen A, Tande KS, Slagstad D (2003) The importance of advection on production of *Calanus finmarchicus* in the Atlantic part of the Barents Sea. *Sarsia*, **88**, 261–273.

Eiane K, Ohman MD (2004) Stage-specific mortality of *Calanus finmarchicus*, *Pseudocalanus elongatus* and *Oithona similis* on Fladen Ground, North Sea, during a spring bloom. *Marine Ecology Progress Series*, **268**, 183–193.

Eiane K, Tande KS (2009) Meso and macrozooplankton. In: *Ecosystem Barents Sea* (eds Sakshaug E, Johnsen G, Kovacs K), pp. 209–234. Tapir Academic Press, Trondheim.

Eiane K, Aksnes DL, Ohman MD, Wood S, Martinussen MB (2002) Stage-specific mortality of *Calanus* spp. under different predation regimes. *Limnology and Oceanography*, **47**, 636–645.

Gentleman WC, Pepin P, Doucette S (2012) Estimating mortality: Clarifying assumptions and sources of uncertainty in vertical methods. *Journal of Marine Systems*, **105-108**, 1–19.

Gislason A, Eiane K, Reynisson P (2007) Vertical distribution and mortality of *Calanus finmarchicus* during overwintering in oceanic waters southwest of Iceland. *Marine Biology*, **150**, 1253–1263.

Haidvogel DB, Arango H, Budgell WP et al. (2008) Ocean forecasting in terrain-following coordinates: Formulation and skill assessment of the Regional Ocean Modeling System. *Journal of Computational Physics*, **227**, 3595–3624.

Hassel A, Skjoldal HR, Gjøsæter H, Loeng H, Omli L (1991) Impact of grazing from capelin (*Mallotus villosus*) on zooplankton: a case study in the northern Barents Sea in August 1985. *Polar Research*, **10**, 371–388.

Hastie T, Tibshirani R, Friedman J (2009) *The Elements of Statistical Learning: Data Mining, Inference, and Prediction, 2nd ed.* Springer, New York, 745 pp.

Heath MR, Rasmussen J, Ahmed Y et al. (2008) Spatial demography of *Calanus finmarchicus* in the Irminger Sea. *Progress in Oceanography*, **76**, 39–88.

Hernroth L (1987) Sampling and filtration efficiency of two commonly used plankton nets. A comparative study of the Nansen net and the Unesco WP 2 net. *Journal of Plankton Research*, **9**, 719–728.

Hirche H-J (1983) Overwintering of *Calanus finmarchicus* and *Calanus helgolandicus*. *Marine Ecology Progress Series*, **11**, 281–290.

Hirst A, Kiørboe T (2002) Mortality of marine planktonic copepods: global rates and patterns. *Marine Ecology Progress Series*, **230**, 195–209.

Hjøllo SS, Huse G, Skogen MD, Melle W (2012) Modelling secondary production in the Norwegian Sea with a fully coupled physical/primary production/individual-based *Calanus finmarchicus* model system. *Marine Biology Research*, **8**, 508–526.

Irigoien X, Harris RP, Head RN, Lindley JA, Harbour D (2000) Physiology and population structure of *Calanus finmarchicus* (Copepoda: Calanoida) during a Lagrangian tracer release experiment in the North Atlantic. *Journal of Plankton Research*, **22**, 205–221.

Kaartvedt S (1996) Habitat preference during overwintering and timing of seasonal vertical migration of *Calanus finmarchicus*. *Ophelia*, **44**, 145–156.

Kimmerer WJ, McKinnon a. D (1990) High mortality in a copepod population caused by a parasitic dinoflagellate. *Marine Biology*, **107**, 449–452.

Langangen Ø, Stige LC, Yaragina NA, Vikebø FB, Bogstad B, Gusdal Y (2014) Egg mortality of northeast Arctic cod (*Gadus morhua*) and haddock (*Melanogrammus aeglefinus*). *ICES Journal of Marine Science*, **71**, 1129–1136.

Li X, McGillicuddy DJ, Durbin EG, Wiebe PH (2006) Biological control of the vernal population increase of *Calanus finmarchicus* on Georges Bank. *Deep-Sea Research Part II: Topical Studies in Oceanography*, **53**, 2632–2655.

Lien VS, Gusdal Y, Albretsen J, Melsom A, Vikebø F (2013) Evaluation of a Nordic Seas 4 km numerical ocean model hindcast archive (SVIM), 1960-2011. *Fisken og Havet*, **7**, 1–80.

Lien VS, Gusdal Y, Vikebø FB (2014) Along-shelf hydrographic anomalies in the Nordic Seas (1960–2011): locally generated or advective signals? *Ocean Dynamics*, **64**, 1047–1059.

Matthews J, Hestad L, Bakke J (1978) Ecological studies in Korsfjorden, Western Norway. The generations and stocks of *Calanus hyperboreus* and *C. finmarchicus* in 1971-1974. *Oceanologica Acta*, **1**, 277–284.

Melle W, Ellertsen B, Skjoldal HR (2004) Zooplankton: The link to higher trophic levels. In: *The Norwegian Sea Ecosystem* (ed Skjoldal HR), pp. 137–202. Tapir Academic Press, Trondheim.

Melle W, Runge J, Head E et al. (2014) The North Atlantic Ocean as habitat for *Calanus finmarchicus*: Environmental factors and life history traits. *Progress in Oceanography*, **129**, 244–284.

Möllmann C (2002) Population dynamics of calanoid copepods and the implications of their predation by clupeid fish in the Central Baltic Sea. *Journal of Plankton Research*, **24**, 959–978.

Nesterova VN (1990) *Plankton biomass along the drift route of cod larvae (reference material)*. PINRO, Murmansk (in Russian), 64 pp.

Neuheimer AB, Gentleman WC, Pepin P, Head EJH (2010) Explaining regional variability in copepod recruitment: Implications for a changing climate. *Progress in Oceanography*, **87**, 94–105.

Nichols JH, Thompson AB (1991) Mesh selection of copepodite and nauplius stages of four calanoid copepod species. *Journal of Plankton Research*, **13**, 661–671.

Ohman MD (2012) Estimation of mortality for stage-structured zooplankton populations: What is to be done? *Journal of Marine Systems*, **93**, 4–10.

Ohman MD, Runge JA, Durbin EG, Field DB, Niehoff B (2002) On birth and death in the sea. *Hydrobiologia*, **480**, 55–68.

Ohman M, Eiane K, Durbin E, Runge J, Hirche H (2004) A comparative study of *Calanus finmarchicus* mortality patterns at five localities in the North Atlantic. *ICES Journal of Marine Science*, **61**, 687–697.

Ohman MD, Durbin EG, Runge J a., Sullivan BK, Field DB (2008) Relationship of predation potential to mortality of *Calanus finmarchicus* on Georges Bank, northwest Atlantic. *Limnology and Oceanography*, **53**, 1643–1655.

Pepin P (2013) Distribution and feeding of *Benthosema glaciale* in the western Labrador Sea: Fish-zooplankton interaction and the consequence to calanoid copepod

populations. *Deep-Sea Research Part I: Oceanographic Research Papers*, **75**, 119–134.

Plourde S, Pepin P, Head EJH (2009) Long-term seasonal and spatial patterns in mortality and survival of *Calanus finmarchicus* across the Atlantic Zone Monitoring Programme region, Northwest Atlantic. *ICES Journal of Marine Science*, **66**, 1942–1958.

R Development Core Team (2014) R: A language and environment for statistical computing. *R Foundation for Statistical Computing, Vienna, Austria. URL http://www.R-project.org/*.

Runge JA, Franks PS, Gentleman WC, Megrey BA, Rose KA, Werner FE, Zakardijan B (2004) Diagnosis and prediction of variability in secondary production and fish recruitment processes: developments in physical-biological modeling. *The Sea: The Global Coastal Ocean: Multiscale Interdisciplinary Processes*, **13**, 413–473.

Samuelsen A, Huse G, Hansen C (2009) Shelf recruitment of *Calanus finmarchicus* off the west coast of Norway: role of physical processes and timing of diapause termination. *Marine Ecology Progress Series*, **386**, 163–180.

Scheffer M, Baveco JM, Deangelis DL, Rose KA, Vannes EH (1995) Super-individuals a simple solution for modeling large populations on an individual basis. *Ecological Modelling*, **80**, 161–170.

Shchepetkin AF, McWilliams JC (2005) The regional oceanic modeling system (ROMS): a split-explicit, free-surface, topography-following-coordinate oceanic model. *Ocean Modelling*, **9**, 347–404.

Skardhamar J, Reigstad M, Carroll J, Eiane K, Wexels Riser C, Slagstad D (2011) Effects of mortality changes on biomass and production in *Calanus* spp. populations. *Aquatic Biology*, **12**, 129–145.

Stenevik EK, Melle W, Gaard E, Gislason A, Broms CTÅ, Prokopchuk I, Ellertsen B (2007) Egg production of *Calanus finmarchicus* — A basin-scale study. *Deep Sea Research Part II: Topical Studies in Oceanography*, **54**, 2672–2685.

Stige LC, Dalpadado P, Orlova E, Boulay A-C, Durant JM, Ottersen G, Stenseth NC (2014) Spatiotemporal statistical analyses reveal predator-driven zooplankton fluctuations in the Barents Sea. *Progress in Oceanography*, **120**, 243–253.

Thor P, Nielsen TG, Tiselius P (2008) Mortality rates of epipelagic copepods in the post-spring bloom period in Disko Bay, western Greenland. *Marine Ecology Progress Series*, **359**, 151–160.

Wood SNN (1994) Obtaining bith and mortality patterns from structured population trajectories. *Ecological Monographs*, **64**, 23–44.

Wood SN (2013) mgcv: GAMs with GCV smoothness estimation and GAMMs by REML/ PQL. R package. Version 1.7–24.

Østvedt OJ (1955) Zooplankton investigations from weather ship M in the Norwegian Sea. 1948-49. *Hvalrådets skrifter*, **40**, 1–93.

Ådlandsvik B, Sundby S (1994) Modelling the transport of cod larvae from the Lofoten area. *ICES Mar Sci. Symp.*, **198**, 379–392.

Appendix 1. Supplementary figures

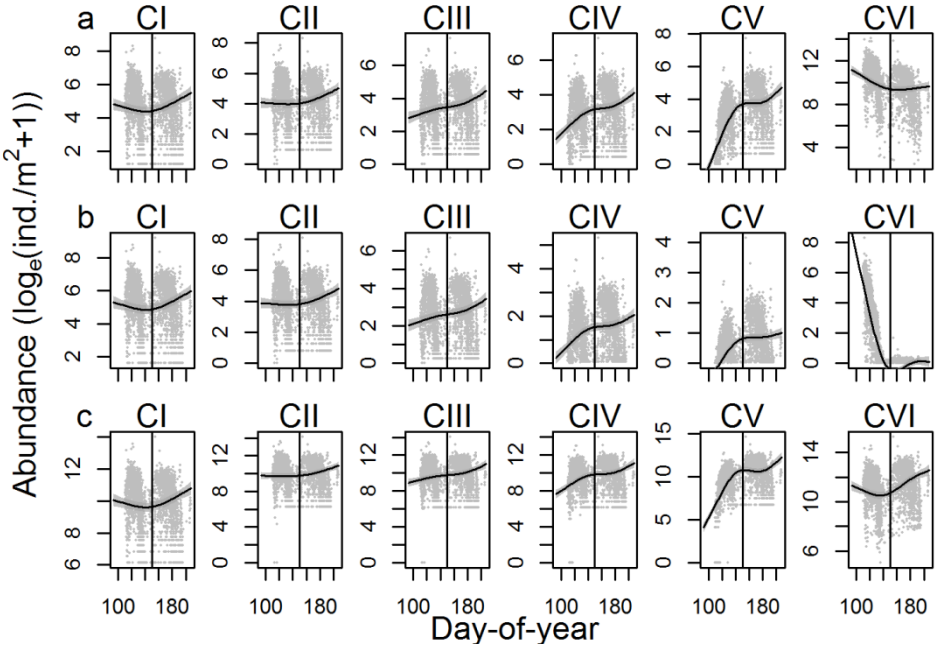

Fig. A1. Stage-specific abundances per day-of year from a simulation including drift, but with fixed temperature and egg production (Sim. 2). a: Base mortality, b: High mortality, c: Low mortality (Table I, main text). The smooth line is predicted abundance (natural logarithmic scale) from a GAM of the simulated data as a function sampling position (a two-dimensional tensor product of longitude and latitude) and day (a one-dimensional smooth function of day-of-year). Grey dots indicate the data points, the shaded area 95 % confidence interval of the predictions, and the vertical line the division between the spring and summer survey.

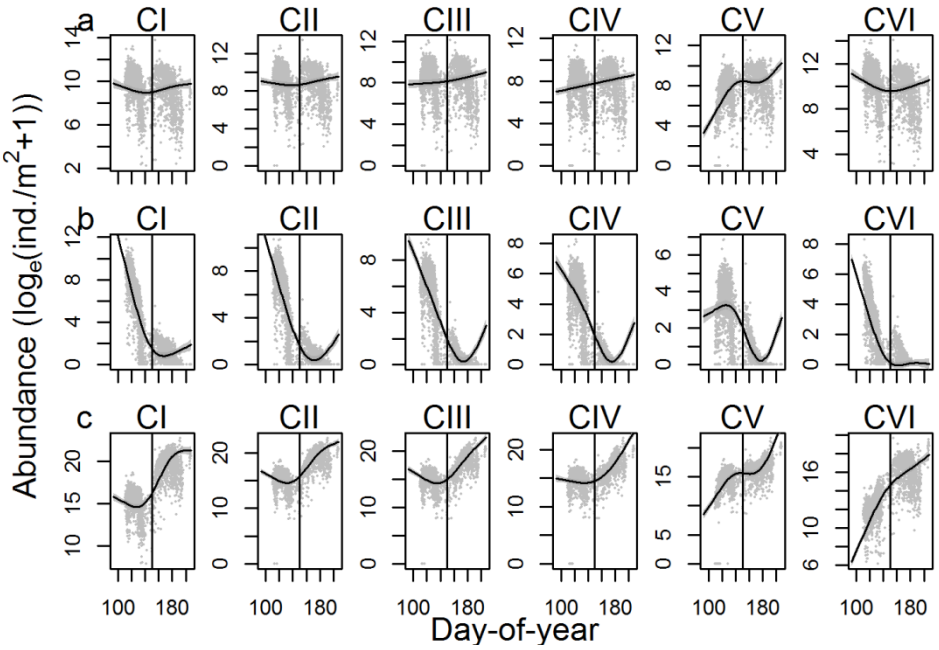

Fig. A2. Stage-specific abundances per day-of year from a simulation including drift and varying egg production, but with fixed temperature (Sim. 3). a: Base mortality, b: High mortality, c: Low mortality (Table 1, main text). The smooth line is predicted abundance (natural logarithmic scale) from a GAM of the simulated data as a function sampling position (a two-dimensional tensor product of longitude and latitude) and day (a one-dimensional smooth function of day-of-year). Grey dots indicate the data points, the shaded area 95 % confidence interval of the predictions, and the vertical line the division between the spring and summer survey.

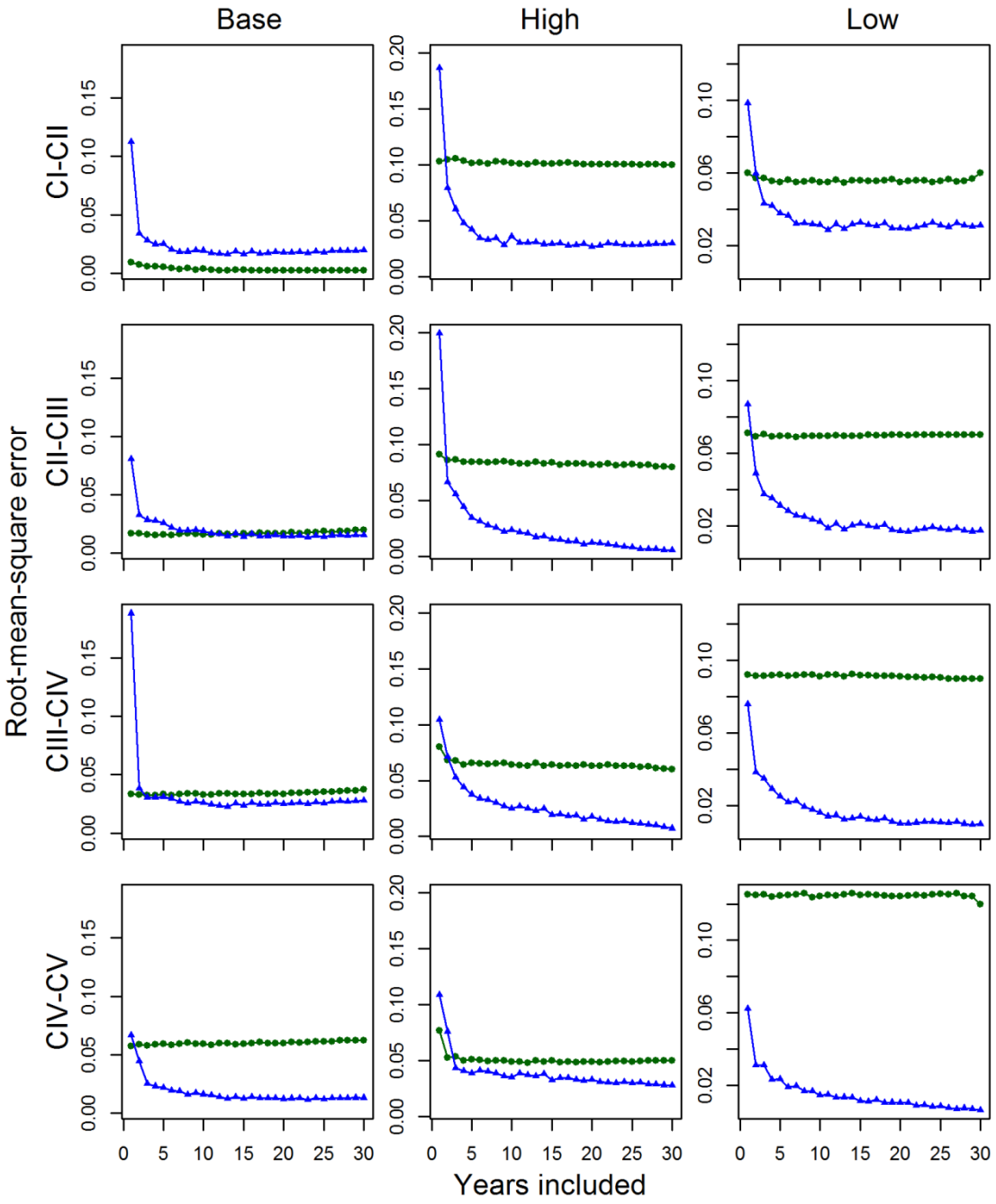

Fig. A3. Difference between estimated and true mortality rates for the full simulation (Sim. 4) depending on the number of years with data included. The panels show, per stage-pair and mortality rate, the root-mean-square error for 100 resamples of 1-30 randomly selected years included in the estimation with the VLT (green dots) and the SRA (blue triangles). For the Base scenario, the true mortality rates were considered as the arithmetic mean mortality for the two relevant stages (see Table I, main text). Note that 30 years of data equals the full dataset used in the analyses (Fig. 3, main text). The random effects were excluded from the SRA model when data from only one year was included.

Appendix 2. Supplementary tables

Table A1. Mortality estimates (d^{-1}) from the simulated data using the VLT and the SRA, compared to the true values (shaded). Orig.: original estimates, using the full datasets (equivalent to estimates given in Table III, main text); Spr.: Estimates based on spring samples only (April-May); Sum.: Estimates based on summer samples only (June-July); W.: Stage-specific ages re-estimated, weighted by the original mortality estimates; -0.70: Ambient temperature estimates used to calculate stage duration reduced by -0.70°C.

	True mortality				2. Drift					3. Varying egg production							4. Varying temperature			
					VLT			SRA		VLT			SRA				VLT		SRA	
	Per stage		Mean		Orig.	Spr.	Sum.	Orig.	W.	Orig.	Spr.	Sum.	Orig.	Spr.	Sum.	W.	Orig.	-0.70	Orig.	-0.70
Base	CI	0.090	CI-CII	0.098	0.100	0.110	0.100	0.094	0.094	0.080	0.090	0.080	0.090	0.071	0.073	0.090	0.100	0.090	0.117	0.104
	CII	0.105	CII-CIII	0.090	0.110	0.120	0.100	0.098	0.096	0.100	0.100	0.090	0.090	0.074	0.079	0.092	0.110	0.100	0.105	0.095
	CIII	0.075	CIII-CIV	0.053	0.090	0.110	0.070	0.069	0.069	0.080	0.100	0.070	0.070	0.049	0.050	0.067	0.090	0.080	0.081	0.074
	CIV	0.030	CIV-CV	0.028	0.070	0.110	0.020	0.015	0.014	0.070	0.100	0.030	0.010	-0.006	0.004	0.011	0.090	0.080	0.041	0.040
	CV	0.025	CV-CVI	0.023	0.000	0.000	0.000			0.010	0.010	0.020					0.020	0.010		
	CVI	0.020																		
High	CI	0.200	CI-CII	0.200	0.210	0.220	0.210	0.203	0.207	0.090	0.040	0.140	0.190	0.165	0.161	0.192	0.100	0.090	0.230	0.220
	CII	0.200	CII-CIII	0.200	0.230	0.240	0.220	0.214	0.214	0.110	0.090	0.120	0.180	0.175	0.138	0.184	0.120	0.110	0.206	0.199
	CIII	0.200	CIII-CIV	0.200	0.240	0.260	0.220	0.219	0.221	0.130	0.160	0.110	0.190	0.194	0.144	0.192	0.140	0.120	0.193	0.190
	CIV	0.200	CIV-CV	0.200	0.240	0.280	0.200	0.167	0.209	0.130	0.200	0.070	0.150	0.146	0.128	0.173	0.150	0.140	0.172	0.171
	CV	0.200	CV-CVI	0.200	0.120	0.030	0.210			0.080	0.100	0.060					0.100	0.090		
	CVI	0.200																		
Low	CI	0.010	CI-CII	0.010	0.010	0.010	0.010	0.003	0.003	0.060	0.010	0.100	0.010	-0.017	0.001	0.011	0.070	0.060	0.041	0.032
	CII	0.010	CII-CIII	0.010	0.020	0.030	0.010	0.007	0.007	0.080	0.020	0.140	0.010	-0.017	-0.001	0.013	0.080	0.070	0.027	0.020
	CIII	0.010	CIII-CIV	0.010	0.040	0.060	0.020	0.019	0.020	0.120	0.060	0.180	0.020	-0.001	0.007	0.023	0.100	0.090	0.020	0.015
	CIV	0.010	CIV-CV	0.010	0.050	0.100	0.010	-0.002	-0.003	0.120	0.090	0.140	-0.010	-0.022	-0.028	-0.018	0.130	0.120	0.004	0.001
	CV	0.010	CV-CVI	0.010	0.020	0.020	0.020			0.110	0.160	0.070					0.140	0.130		
	CVI	0.010																		

Table A2. Overview of previous studies providing *C. finmarchicus* instantaneous mortality rates (day^{-1}) included in Fig. 6 (main text). Eggs and naupliar stages are not included. 95%: 95% confidence interval; CPBM: coupled physical-biological model; DDE: Delay differential equation; F: Females; G1: 1st Generation: G2: 2nd generation; LR: Linear regression; LSE: Least square estimates; M: Males; NE: Northeast; NW: Northwest; PSM: Population surface method; SD: Standard deviation; SdE: Standard error; SW: Southwest; VLT: Vertical life table.

VERTICAL METHODS						**Stage**					**Ref.**
Area	**Year**	**Month**	**Sampling gear (mesh size)**	**Method**	**Statistic**	**CI-CII**	**CII-CIII**	**CIII-CIV**	**CIV-CV**	**CV-CVI**	
NE Atlantic (59°N, 20°W)	1996	Jun.	WP2 (200 µm)	VLT	Mean ± SdE		0.13±0.02	-0.09±0.02	0.23±0.02		[1][1]
							0.09±0.02	0.02±0.01	0.14±0.01		
							0.05±0.02	-0.05±0.03	0.26±0.02		
							0.05±0.02	0.05±0.01	0.10±0.01		
Georges Bank	1995-1999	Jan.-Jun.	Pump/Mocness (153 µm)	VLT	Median ± 95%	0.09±0.04	0.04±0.03	0.07±0.02	0.06±0.01	0.09±0.01 (M) 0.05±0.01 (F)	[2]
SW of Iceland	1997	Apr./Jun.	Multi Plankton Sampler (200 µm)	VLT	Mean ± 95%				0.00±0.035	0.19±0.05 (M) 0.13±0.04 (F)	[3]
Irminger Sea	2002	Apr./May (a) Jul./Aug. (b)	ARIES (200 µm)/ OCEAN (95 µm)	Mod. VLT	Mean ± SD	0.11±0.18 (a) 0.25±0.18 (b)		0.11 (a) 0.09 (b)			[4]
W Greenland	2001	Jun.	Pump (50 µm)	VLT	Mean ± SD	0.12±0.03	0.18±0.02	0.15±0.06			[5]
Labrador Sea	2006	Jun. (a) Aug.-Sep. (b)	Ring net (202 µm)/ Multinet (202 µm)	VLT	Mean ± 95%	0.17±0.07 (a) 0.19±0.11 (b)	0.15±0.06 (a) 0.14±0.09 (b)	0.23±0.14 (a) 0.08±0.05 (b)	0.16±0.08 (a) 0.23±0.14 (b)	0.09±0.03 (a) 0.39±0.06 (b)	[6]
Newfoundland Shelf	2006	Jun. (a) Aug.-Sep. (b)	Ring net (202 µm)/ Multinet (202 µm)	VLT	Mean ± 95%	0.12±0.04 (a) 0.16±0.08 (b)	0.10±0.03 (a) 0.10±0.09 (b)	0.23±0.06 (a) 0.23±0.09 (b)	0.31±0.04 (a) 0.34±0.12 (b)	0.03±0.01 (a) 0.22±0.06 (b)	
Newfoundland-Labrador	1999-2006	Jul. (a) Nov.-Dec. (b)	Ring net (202 µm)	VLT	Mean ± SdE	0.18±0.02 (a) 0.07±0.01 (b)	0.12±0.02 (a) 0.08±0.02 (b)	0.15±0.02 (a) 0.05±0.01 (b)	0.10±0.01 (a) 0.04±0.02 (b)	0.09±0.01 (a) 0.17±0.01 (b)	[7]
Gulf of St. Lawrence	1999-2006	Jun. (a) Nov. (b)				0.07±0.01 (a) 0.09±0.01 (b)	0.08±0.02 (a) 0.05±0.01 (b)	0.06±0.01 (a) 0.18±0.01 (b)	0.14±0.01 (a) 0.14±0.01 (b)	0.12±0.01 (a) 0.13±0.01 (b)	

Scotian Shelf	1999-2006	Apr.-May (a) Oct. (b)				0.11±0.01 (a) 0.33±0.05 (b)	0.04±0.01 (a) 0.20±0.06 (b)	0.07±0.01 (a) 0.11±0.02 (b)	0.05±0.01 (a) 0.03±0.00 (b)	0.04±0.01 (a) 0.44±0.02 (b)	
Barents Sea	2006	Aug.	Juday (168 µm)	VLT	Mean ± 95%	0.01	0.04±0.04	0.02±0.02	0.01	0.14±0.05 (F) 0.13±0.06 (M)	[8] [2]
NE Atlantic, Offhself	1971-2009	Not specified	WP2/Bongo/Multinet/LHPR(180-270	VLT	Mean ± SdE	0.09±0.01	0.12±0.01	0.03±0.01	0.03±0.01	0.02±0.02	[9] [2]
NE Atlantic, Shelf	1990-2010		WP2/Bongo (180-335 µm)			0.11±0.02	0.06±0.01	0.03±0.01	0.06±0.01	0.02±0.02	
NW Atlantic, Offshelf	1995-2006		Ring net (200 µm)			0.08±0.02	0.05±0.01	0.04±0.02	0.03±0.01	-0.04±0.03	
NW Atlantic, Shelf	1994-2009		Ring net (200 µm)			0.09±0.01	0.06±0.01	0.05±0.01	0.07±0.01	0.15±0.005	
HORISONTAL METHODS						**Stage**					
Area	**Year**	**Month**	**Sampling gear (mesh size)**	**Method**	**Statistic**	**CI**	**CII**	**CIII**	**CIV**	**CV**	**CVI**	
Korsfjorden (W Norway)	1971 (G1)	All year	Longhurst frame net	DDE	LSE			0.12	0.14	0.12	0.09	[10]
	1971 (G2)							0.10	0.16	0.16	0.03	
	1972 (G1)							0.04	0.07	0.46	0.49	
	1972 (G2)							0.02	0.02	0.02	0.15	
	1973 (G1)							0.14	0.23	0.43	0.11	
	1973 (G2)							0.04	0.06	0.04	0.06	
Lindåspollene (W Norway)	1979-1980	All year	Juday net (180 µm)	DDE	LSE	0.16	0.18	0.15	0.04	<0.01		[11]
Sørfjorden (W Norway)	1996	Feb.-Jun.	Multinet (180 µm)	PSM	Mean ± 95%	0.10±0.15	0.10±0.13	0.08±0.17	0.04±0.21	0.06±0.3		[12] [2]
Lurefjorden (W Norway)						0.02±0.19	0.01±0.09	0.02±0.11	0.02±0.05	0.15±0.08		
North Sea	1976	Mar.- Jun.	Niskin water bottles	PSM	Mean ± 95%	0.02	0.02	0.02	0.04±0.03	0.14±0.15	0.03±0.04 (F)	[13] [2]
Norwegian Sea	1997	Mar.-Jun.	WP2 (53 µm)	PSM	Mean ± 95%	0.03	0.03	0.04	0.09±0.09			[14]
Svalbard fjord (Arctic)	2001-2002	All year	WP2 (180 µm)	PSM	Mean ± 95%	0.03±0.03	0.03±0.05	0.04±0.06	0.05±0.06	0.09±0.14	0±0.07 (F)	[15] [2]
Georges Bank	1995-1999	Jan.-Jun.	Pump/Mocness (153 µm)	Inverse CPBM	Mean	0.11	0.07	0.02	0.02	0.04	0.09	[16] [3]

Sognefjorden (W Norway)	1995-1996	Oct.-Feb.	Kiel Multinet (180 µm)	LR	Mean ± 95%				0.01±0.01	[17][4]
Masfjorden (W Norway)									0.03±0.01	
Sørfjorden (W Norway)									0.01±0.01	
Lurefjorden (W Norway)									0.01±0.01	

[1]Different estimates are based on development times from different authors.
[2]Extracted from article figure (other estimates are confirmed by the authors).
[3]Not distinguished between species, but *C. finmarchicus* stage CIV dominated the sample
[3]Same data as ref. 2
[4]Not distinguished between *Calanus* species. Stage CV dominated the samples, but CIV and CVI were also present

References

1. Irigoien, X, Harris, RP, Head, RN, Lindley, JA & Harbour, D (2000) Physiology and population structure of *Calanus finmarchicus* (Copepoda: Calanoida) during a Lagrangian tracer release experiment in the North Atlantic. *J. Plankton Res.*, **22**, 205–221.
2. Ohman, MD, Runge, JA, Durbin, EG, Field, DB & Niehoff, B (2002) On birth and death in the sea. *Hydrobiologia*, **480**, 55–68.
3. Gislason, A, Eiane, K & Reynisson, P (2007) Vertical distribution and mortality of *Calanus finmarchicus* during overwintering in oceanic waters southwest of Iceland. *Mar. Biol.*, **150**, 1253–1263.
4. Heath, MR et al. 2008 Spatial demography of *Calanus finmarchicus* in the Irminger Sea. *Prog. Oceanogr.* **76**, 39–88.
5. Thor, P, Nielsen, TG & Tiselius, P (2008) Mortality rates of epipelagic copepods in the post-spring bloom period in Disko Bay, western Greenland. *Mar. Ecol. Prog. Ser.*, **359**, 151–160.
6. Pepin, P (2013) Distribution and feeding of *Benthosema glaciale* in the western Labrador Sea: Fish-zooplankton interaction and the consequence to calanoid copepod populations. *Deep. Res. Part I Oceanogr. Res. Pap.*, **75**, 119–134.
7. Plourde, S, Pepin, P & Head, EJH (2009) Long-term seasonal and spatial patterns in mortality and survival of *Calanus finmarchicus* across the Atlantic Zone Monitoring Programme region, Northwest Atlantic. *ICES J. Mar. Sci.*, **66**, 1942–1958.

8. Dvoretsky, VG & Dvoretsky, AG (2013) The mortality levels of two common copepods in the Barents Sea. *Vestn. MGTU*, **16**, 460–465 (in Russian).
9. Melle, W et al. (2014) The North Atlantic Ocean as habitat for *Calanus finmarchicus*: Environmental factors and life history traits. *Prog. Oceanogr.*, **129**, 244–284.
10. Matthews, J, Hestad, L & Bakke, J (1978) Ecological studies in Korsfjorden, Western Norway. The generations and stocks of *Calanus hyperboreus* and *C. finmarchicus* in 1971-1974. *Oceanol. Acta*, **1**, 277–284.
11. Aksnes, DL & Magnesen, T (1983) Distribution, development, and production of *Calanus finmarchicus* in Lindåspollene, western Norway, 1979. *Sarsia*, **68**, 195–208.
12. Eiane, K, Aksnes, DL, Ohman, MD, Wood, S & Martinussen, MB (2002) Stage-specific mortality of *Calanus* spp. under different predation regimes. *Limnol. Oceanogr.*, **47**, 636–645.
13. Eiane, K & Ohman, MD (2004) Stage-specific mortality of *Calanus finmarchicus, Pseudocalanus elongatus* and *Oithona similis* on Fladen Ground, North Sea, during a spring bloom. *Mar. Ecol. Prog. Ser.*, **268**, 183–193.
14. Ohman, M, Eiane, K, Durbin, E, Runge, J & Hirche, H (2004) A comparative study of *Calanus finmarchicus* mortality patterns at five localities in the North Atlantic. *ICES J. Mar. Sci.*, **61**, 687–697.
15. Arnkværn, G, Daase, M & Eiane, K (2005) Dynamics of coexisting *Calanus finmarchicus, Calanus glacialis* and *Calanus hyperboreus* populations in a high-Arctic fjord. *Polar Biol.*, **28**, 528–538.
16. Li, X, McGillicuddy, DJ, Durbin, EG & Wiebe, PH (2006) Biological control of the vernal population increase of *Calanus finmarchicus* on Georges Bank. *Deep. Res. Part II Top. Stud. Oceanogr.*, **53**, 2632–2655.
17. Bagøien, E, Kaartvedt, S, Aksnes, DL & Eiane, K (2001) Vertical distribution and mortality of overwintering *Calanus*. *Limnol. Oceanogr.*, **46**, 1494–1510.

Appendix 3. Model code

```
#Script to estimate mortality for copepodite stage-pairs using a
#statistical regression approach
#Created by Kristina Kvile, August 2015
#Written for R (https://www.r-project.org/)
#Requires the library mgcv (Mixed GAM Computation Vehicle with
GCV/AIC/REML Smoothness Estimatio,n, S.Wood)
#https://cran.r-project.org/web/packages/mgcv/index.html

library(mgcv) #Load library
load("dat.rda") #Load data frame

#dat.rda contains the following variables (columns):
#Sampling time and position:
# 1.Month, 2.Year 3.Lat (Latitude, decimal degree),4.Lon (Longitude,
#decimal degree)
# 5.Day (Julian day of sampling), 6.Season (Spring or summer), 7.Temp
#(Temperature at station)
#Abundance of copepodite stages at station:
# 8.CI, 9.CII, 10.CIII, 11.CIV, 12.CV, 13. CVI

stages<-c("CI","CII","CIII","CIV","CV") #Copepodite stages
trans<-c("CI-CII","CII-CIII","CIII-CIV","CIV-CV") #Copepodite stage pairs

#Coefficients to estimate development time per stage (Corkett, 1986)
aI<- 6419;  aII<-8014;  aIII<-9816;  aIV<-11601;  aV<-13526;  aVI<-17477;
alfa<-10.6;  b<-(-2.05)

#Estimate stage-specific ages from day-of-spawning based on temperature
#Age of stage i = midpoint between the age of entry until stage i and i+1
for (i in c(1:dim(dat)[1])){
  dat$Age.CI[i]<-
median(seq(aI*(dat$Temp[i]+alfa)^b,aII*(dat$Temp[i]+alfa)^b,length.out =
10))
  dat$Age.CII[i]<-
median(seq(aII*(dat$Temp[i]+alfa)^b,aIII*(dat$Temp[i]+alfa)^b,length.out
= 10))
  dat$Age.CIII[i]<-
median(seq(aIII*(dat$Temp[i]+alfa)^b,aIV*(dat$Temp[i]+alfa)^b,length.out
= 10))
  dat$Age.CIV[i]<-
median(seq(aIV*(dat$Temp[i]+alfa)^b,aV*(dat$Temp[i]+alfa)^b,length.out =
10))
  dat$Age.CV[i]<-
median(seq(aV*(dat$Temp[i]+alfa)^b,aVI*(dat$Temp[i]+alfa)^b,length.out =
10))
}

#Estimate stage-specific day-of-spawning
dat$Spd.CI<-dat$Day-dat$Age.CI;
dat$Spd.CII<-dat$Day-dat$Age.CII;
dat$Spd.CIII<-dat$Day-dat$Age.CIII;
dat$Spd.CIV<-dat$Day-dat$Age.CIV;
dat$Spd.CV<-dat$Day-dat$Age.CV;

#Estimate stage-durations from stage i to i+1
dat$Duration.CI<-aII*(dat$Temp+alfa)^b    -aI*(dat$Temp+alfa)^b;
```

```
dat$Duration.CII<-aIII*(dat$Temp+alfa)^b  -aII*(dat$Temp+alfa)^b;
dat$Duration.CIII<-aIV*(dat$Temp+alfa)^b  -aIII*(dat$Temp+alfa)^b;
dat$Duration.CIV<-aV*(dat$Temp+alfa)^b    -aIV*(dat$Temp+alfa)^b;
dat$Duration.CV<-aVI*(dat$Temp+alfa)^b    -aV*(dat$Temp+alfa)^b;

#Matrix to store mortality estimates per stage-pair
mortalities<-matrix(NA,ncol=length(trans))
colnames(mortalities)<-trans

#Estimate mortality per stage pair
for (i in 1:length(trans)) {
  #Create data-frame of to successive stages, i and i+1
  combined.abundance<-data.frame(cbind(dat[,stages[i]],dat[,stages[i+1]]))
  combined.ages<-
data.frame(cbind(dat[,paste0("Age.",stages[i])],dat[,paste0("Age.",stages
[i+1])]))
  combined.spds<-
data.frame(cbind(dat[,paste0("Spd.",stages[i])],dat[,paste0("Spd.",stages
[i+1])]))
  combined.duration<-
data.frame(cbind(dat[,paste0("Duration.",stages[i])],dat[,paste0("Duratio
n.",stages[i+1])]))
  Data<-data.frame(cbind(rep(dat$Year,2), #Repeat common variables for
the two stages observed in the same station
                         rep(dat$Day,2),
                         rep(dat$Lon,2),
                         rep(dat$Lat,2),
                   stack(combined.abundance)[1],#Add information for stage
i and i+1 in the same column
                   stack(combined.ages)[1],
                   stack(combined.spds)[1]),
                   stack(combined.duration)[1])
  colnames(Data)<-
c("Year","Day","Lon","Lat","Abundance","Age","Spd","Dur")
  Data<-Data[!is.na(Data$Abundance) & Data$Abundance>0,] #Remove samples
with zero abundance or missing values
  Data$Year<-as.factor(Data$Year) #Make sure year is a factor
  Data$Abundance<-Data$Abundance/Data$Dur #Scale abundance by stage
duration
  Data$Age<-scale(Data$Age,center=TRUE,scale=FALSE)  #Center the age
variable around zero
  Data$logAbundance<-log(Data$Abundance) #Log transform abundance
  m <-
gam(Data$logAbundance~s(Spd)+te(Lon,Lat,k=5)+s(Year,bs="re")+Age+s(Year,b
s="re",by=Age),data=Data) #SRA model
  mortalities[i]<- -coef(m)[2] #The negative of the age-coefficient gives
mortality
}
```